GEM TN-93-274

Korean Delegation Meeting - SSCL

January 18-19, 1993

Abstract:

Agenda and presentations of the Korean Delegation Meeting held at the SSC Laboratory on January 18-19, 1993.

Agenda
Korean Delegation
Directorate Conference #2 (by Library)

January 18-19, 1992

Monday, January 18

8:30	Greeting from SSCL Director	Roy Schwitters
8:35	Overview of the SSCL	Raph Kasper
9:00	GEM Muon System + Discussion	Marx/Taylor
10:30	Break	
11:00	Texas Test Rig (TTR)	Gena Mitselmakher
11:15	Visit to TTR	Gena Mitselmakher
11:30	Lunch	Upstairs Directorate
1:00	GEM Project	Gary Sanders
1:30	Tracker	Kate Morgan
2:00	Electronics/DAQ	Dan Marlow
2:30	Coffee Break	
3:00	Physics/Simulation/Computing	Ken McFarlane Frank Paige
4:30	Meeting (Schwitters, Gilman, Sanders, Jewan Kim, Wonyong Lee–Schwitters office)	
5:00	Discussion	
7:00	Dinner (Hosted by Dick Briggs) Invited guests are all speakers, Fred Gilman, Bob Sheldon, Greg Haas and Korean guests)	L' Ancestral

Tuesday, January 19

9:00-11:00	Calorimetry + Discussion	Howard Gordon
4:30	Discussion on Korean Participation in GEM	Willis

Overview of the SSCL

Raph Kasper

What are things made of?

How do they work?

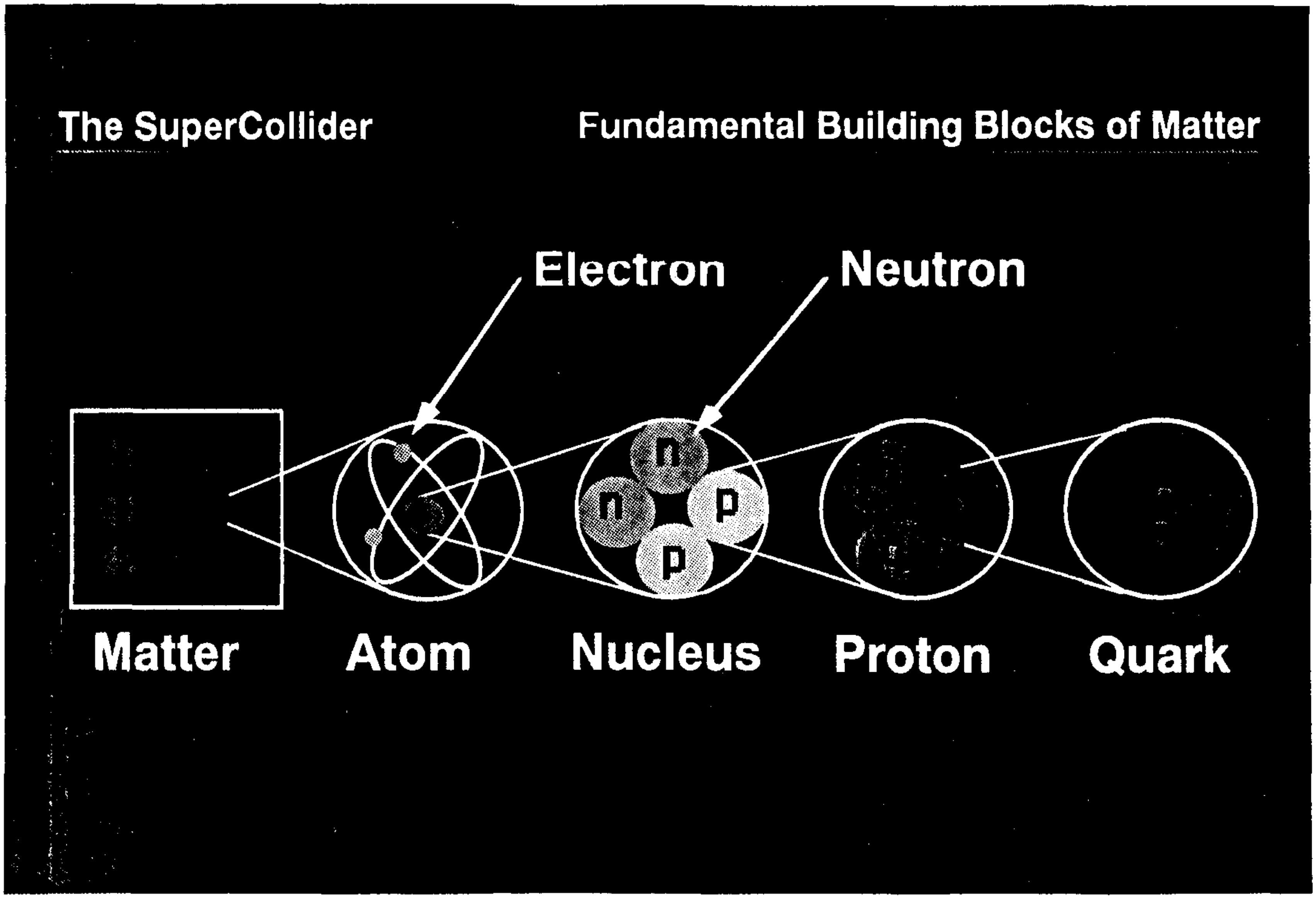

The SuperCollider
Fundamental Building Blocks of Matter
Electron
Neutron
n
n
p
p
Matter
Atom
Nucleus
Proton
Quark

The Standard Model

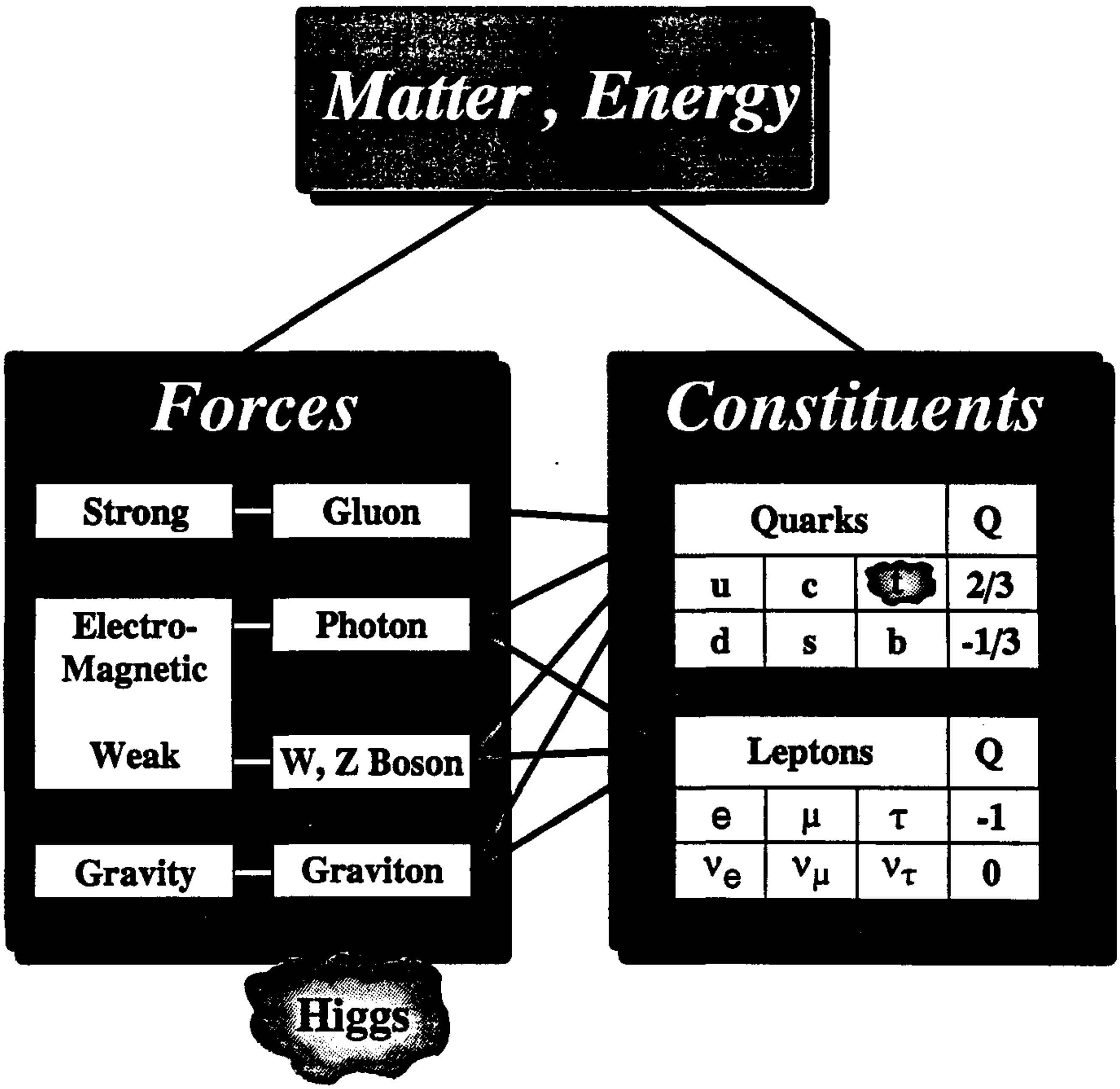

TIP-01740

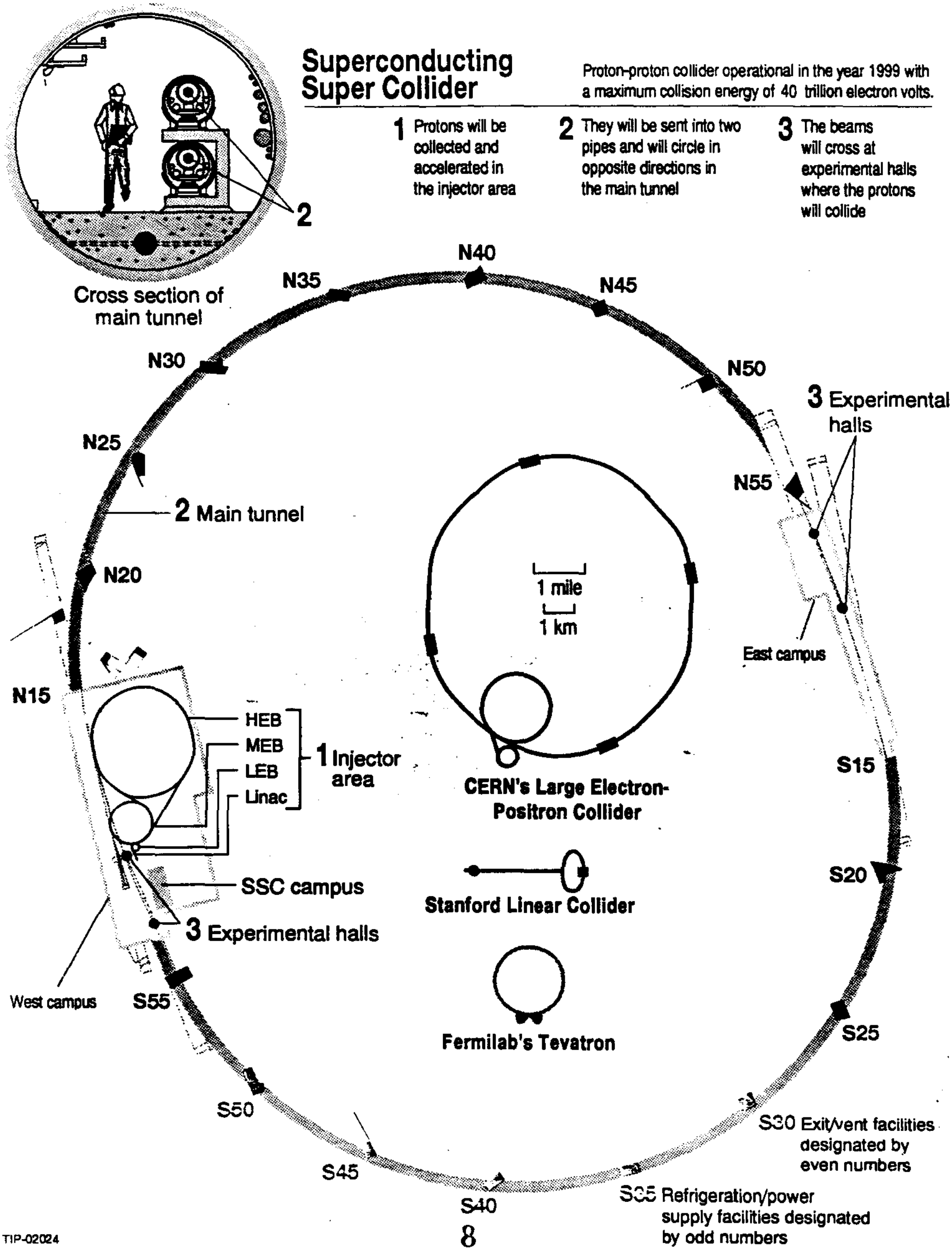
Superconducting Super Collider
Proton-proton collider operational in the year 1999 with a maximum collision energy of 40 trillion electron volts.
1 Protons will be collected and accelerated in the injector area
2 They will be sent into two pipes and will circle in opposite directions in the main tunnel
3 The beams will cross at experimental halls where the protons will collide
2
Cross section of main tunnel
N40
N35
N45
N30
N50
3 Experimental halls
N25
N55
2 Main tunnel
N20
1 mile
1 km
East campus
N15
HEB
MEB
LEB
Linac
1 Injector area
S15
CERN's Large Electron-Positron Collider
S20
SSC campus
Stanford Linear Collider
3 Experimental halls
West campus
S55
S25
Fermilab's Tevatron
S50
S30 Exit/vent facilities designated by even numbers
S45
S35 Refrigeration/power supply facilities designated by odd numbers
S40

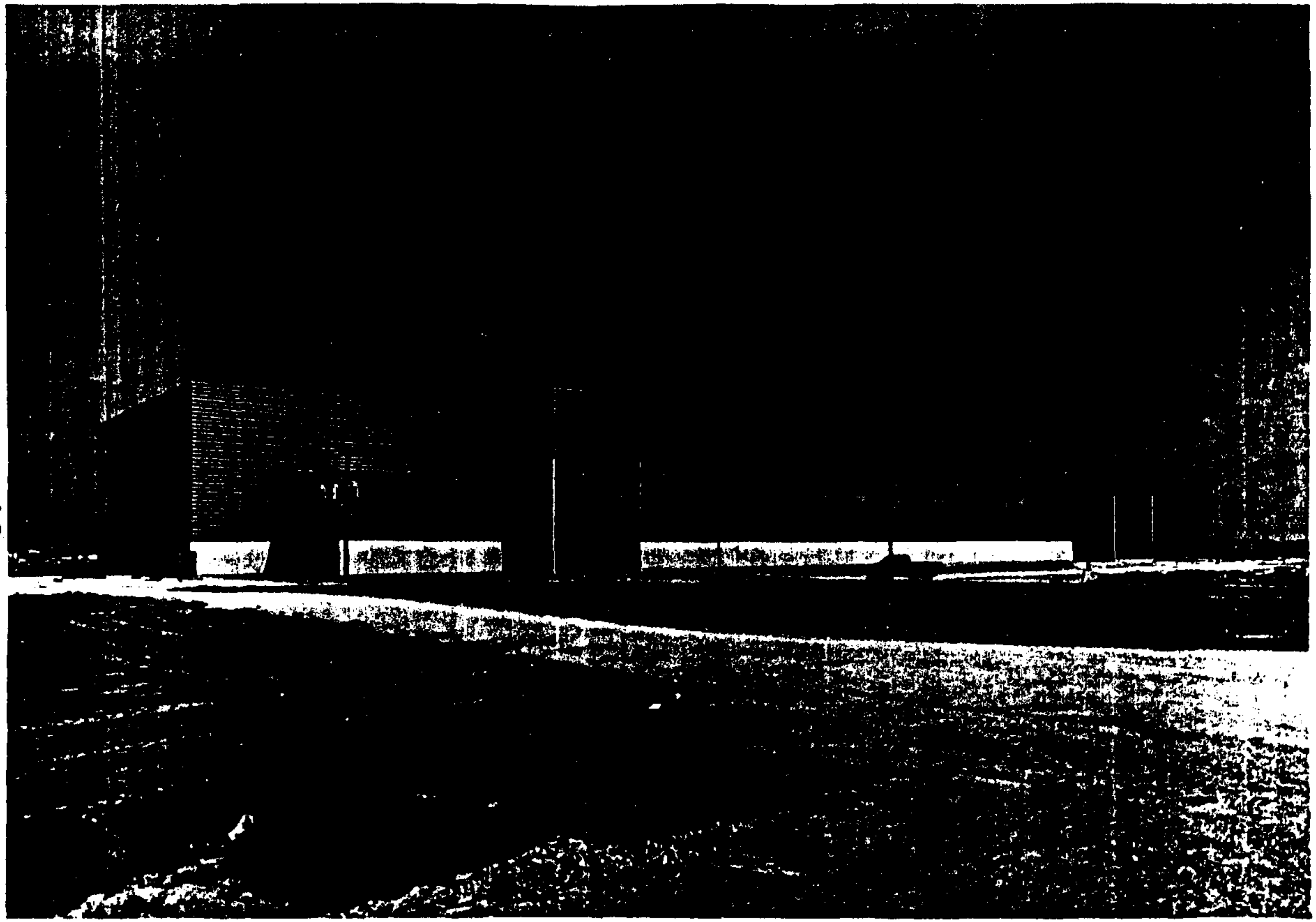

Magnet Development Laboratory
October 1991

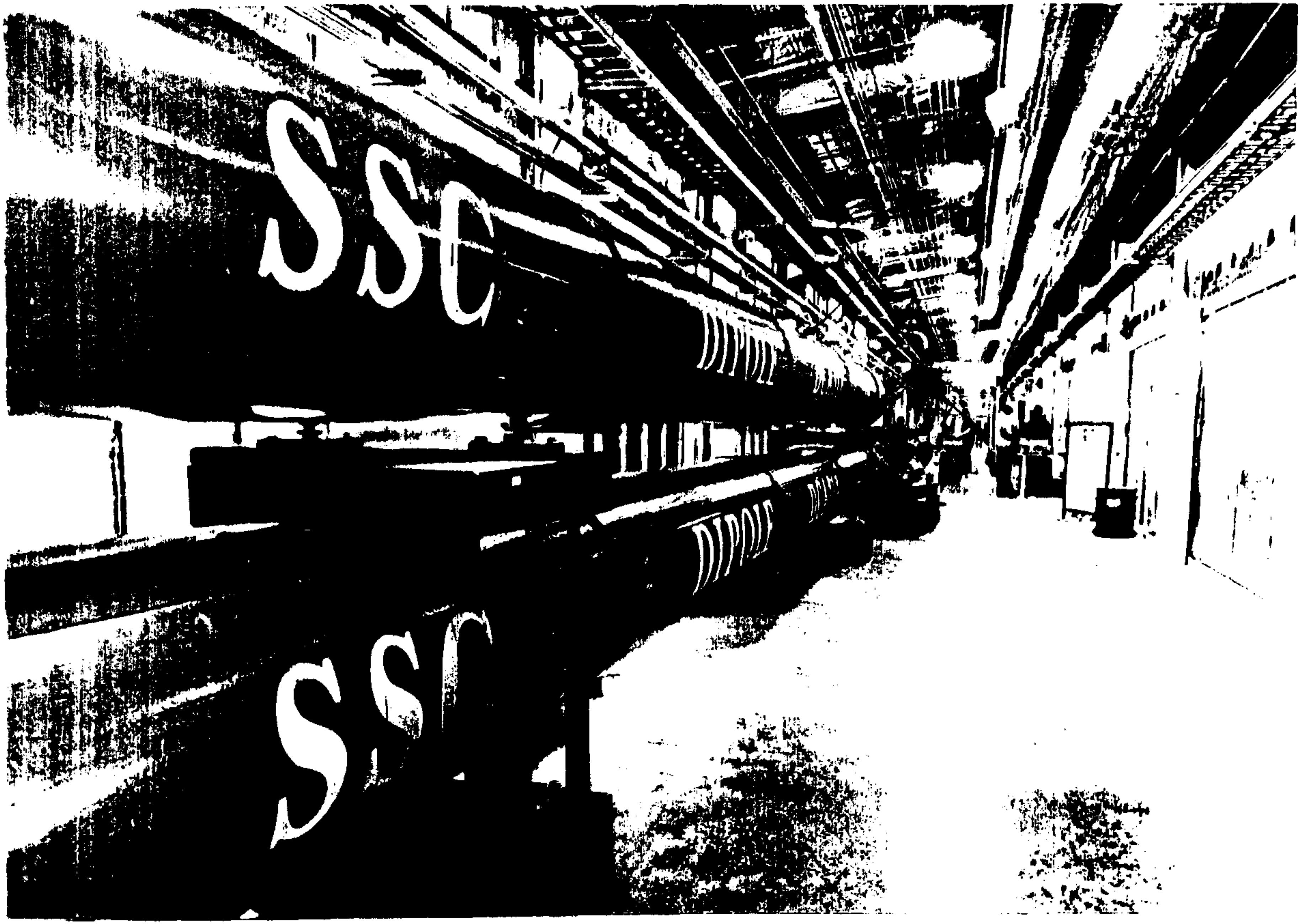

Accelerator Systems String Test Facility
String Enclosure

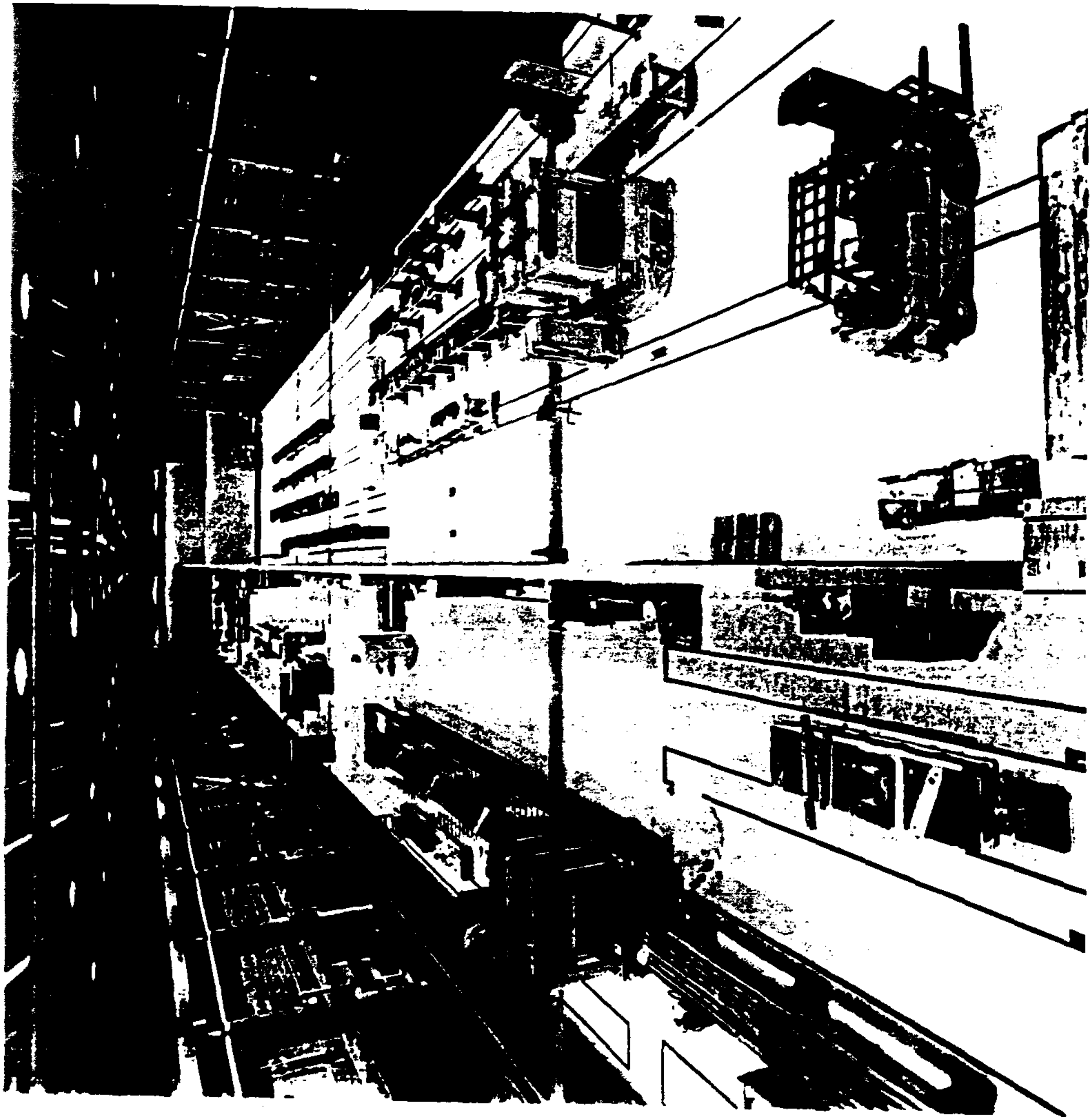

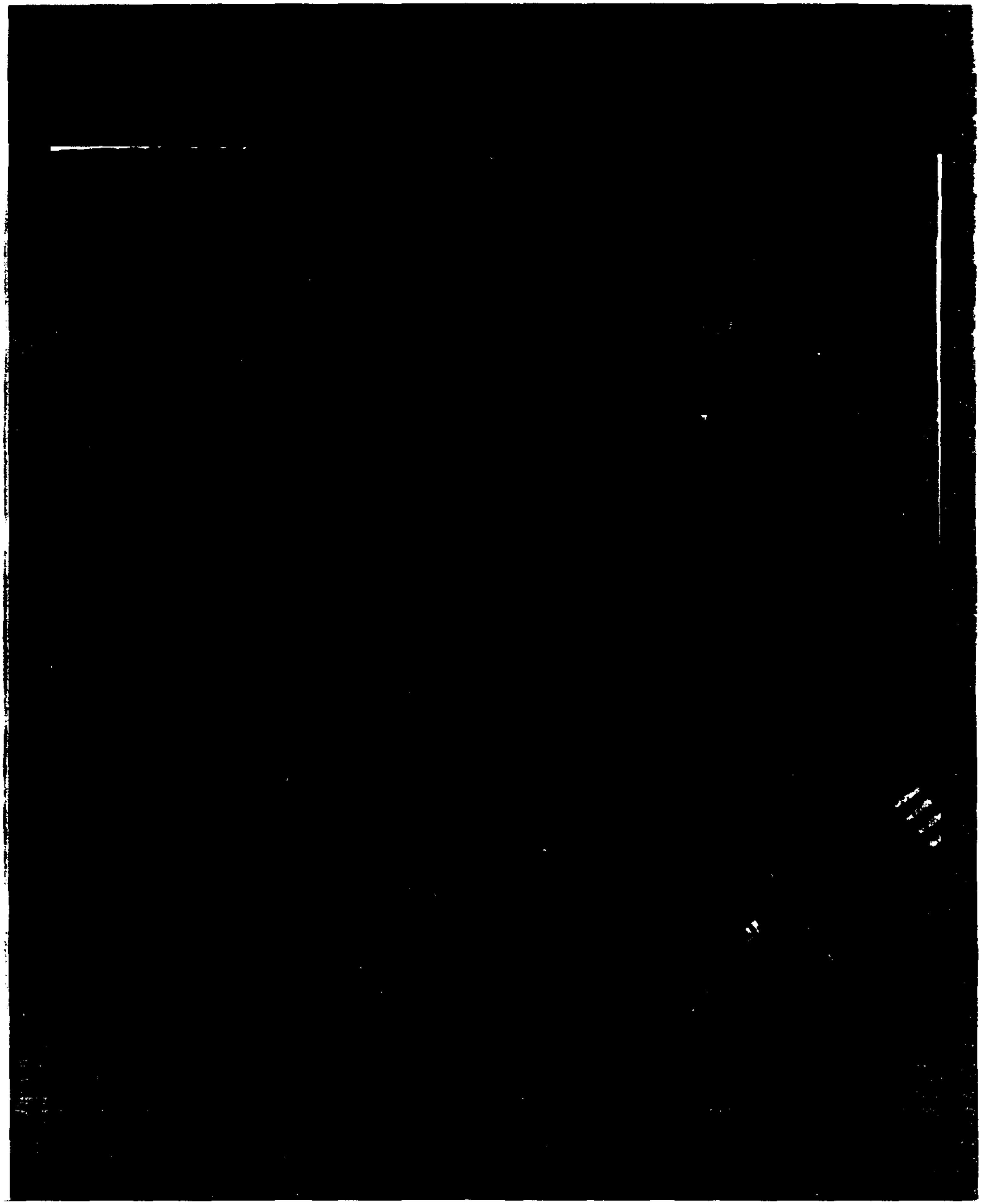

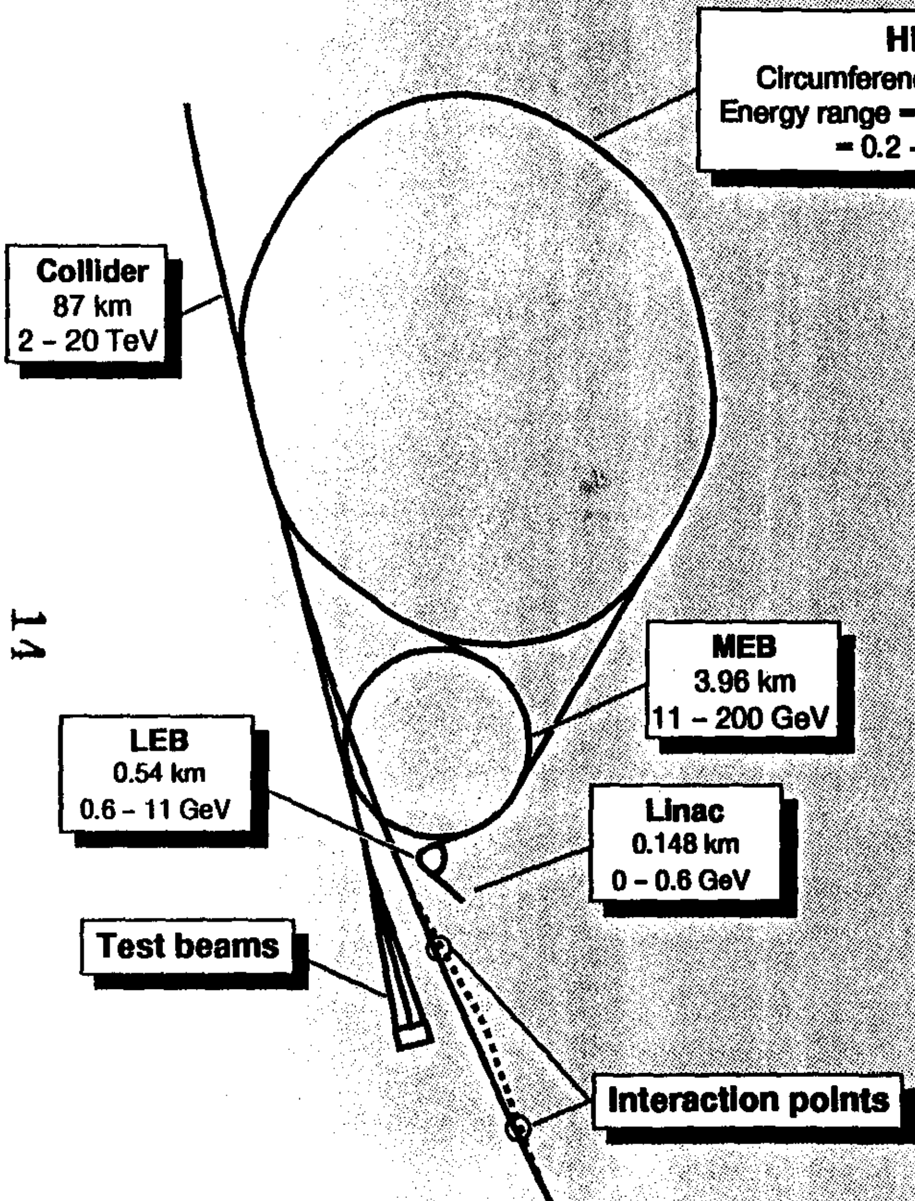

	Speed*	Mass**
Linac	0.792 C	1.64 M_p
LEB	0.996 C	12.83 M_p
MEB	0.99998 C	214.15 M_p
HEB	0.9999998 C	2132.51 M_p
Collider	0.9999999998 C	21316.14 M_p

*C = speed of light = 3×10^8 m/s

**M_p = rest mass of proton = 938.3 MeV

Schematic layout of the injector complex, a portion of the collider ring, and test beam area. The dashed path indicates a future beam bypass. Table shows maximum particle speed and mass in terms of the speed of light and proton rest mass respectively.

TIP-02795

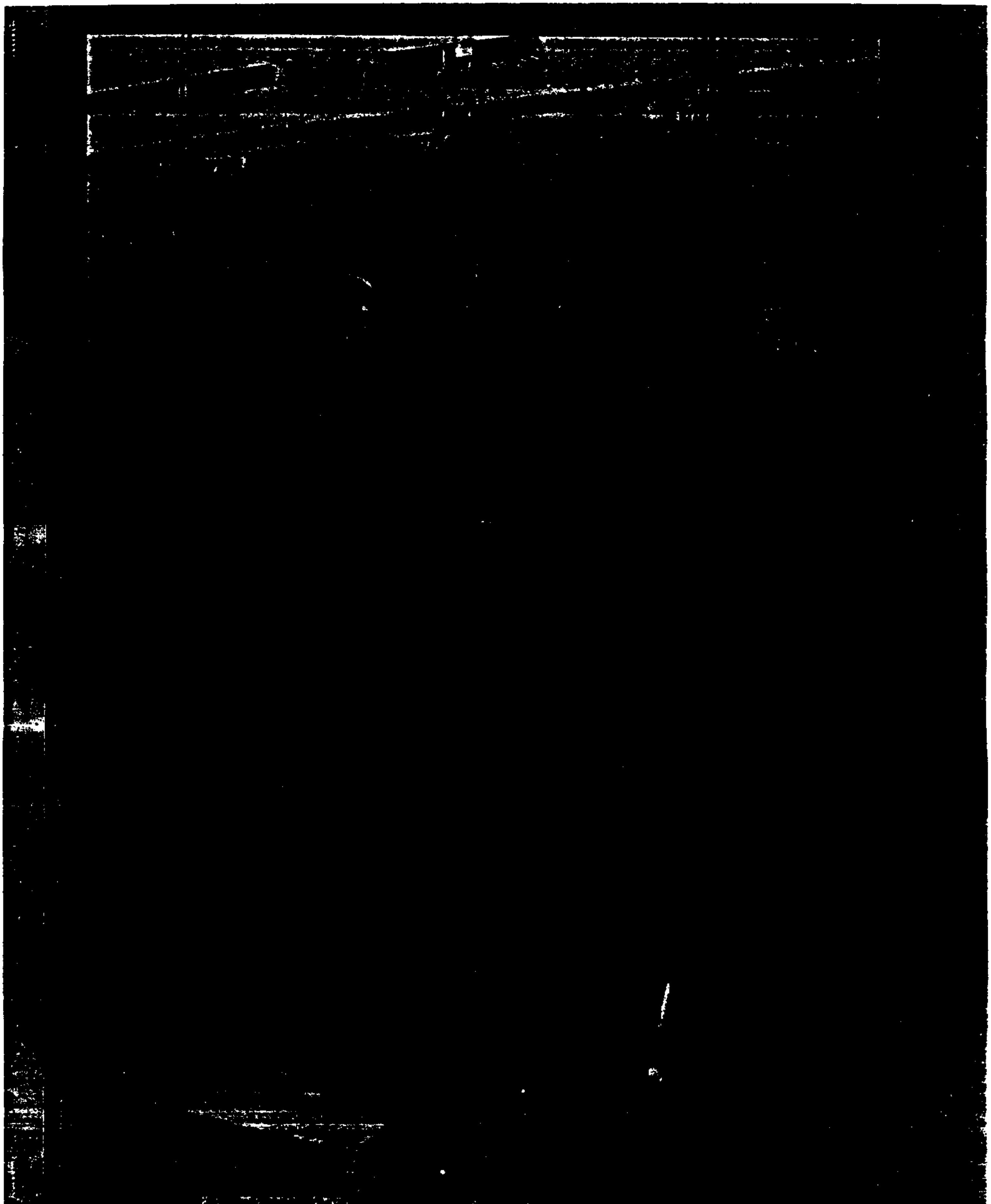

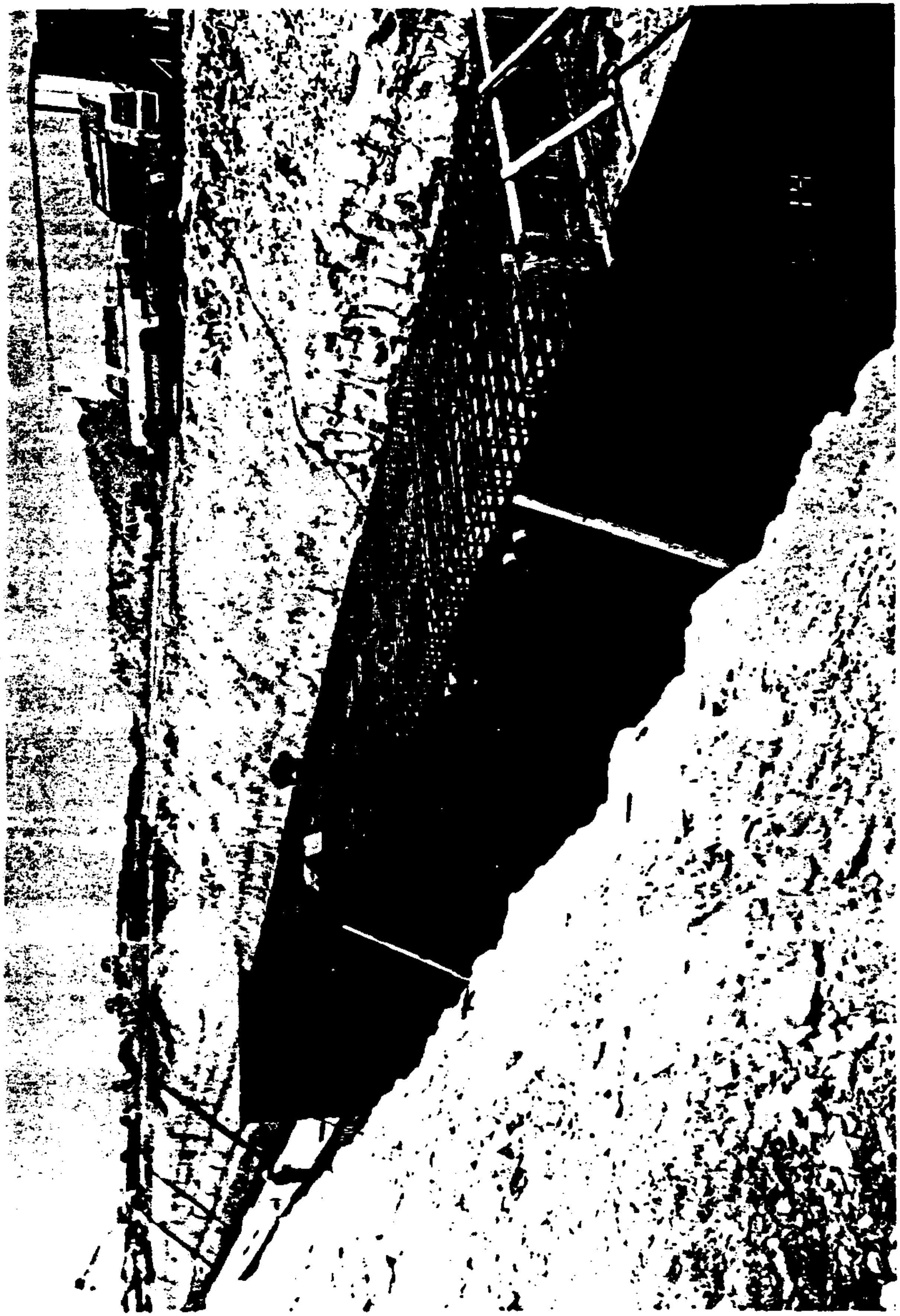

Schematic Location of SSC Facilities

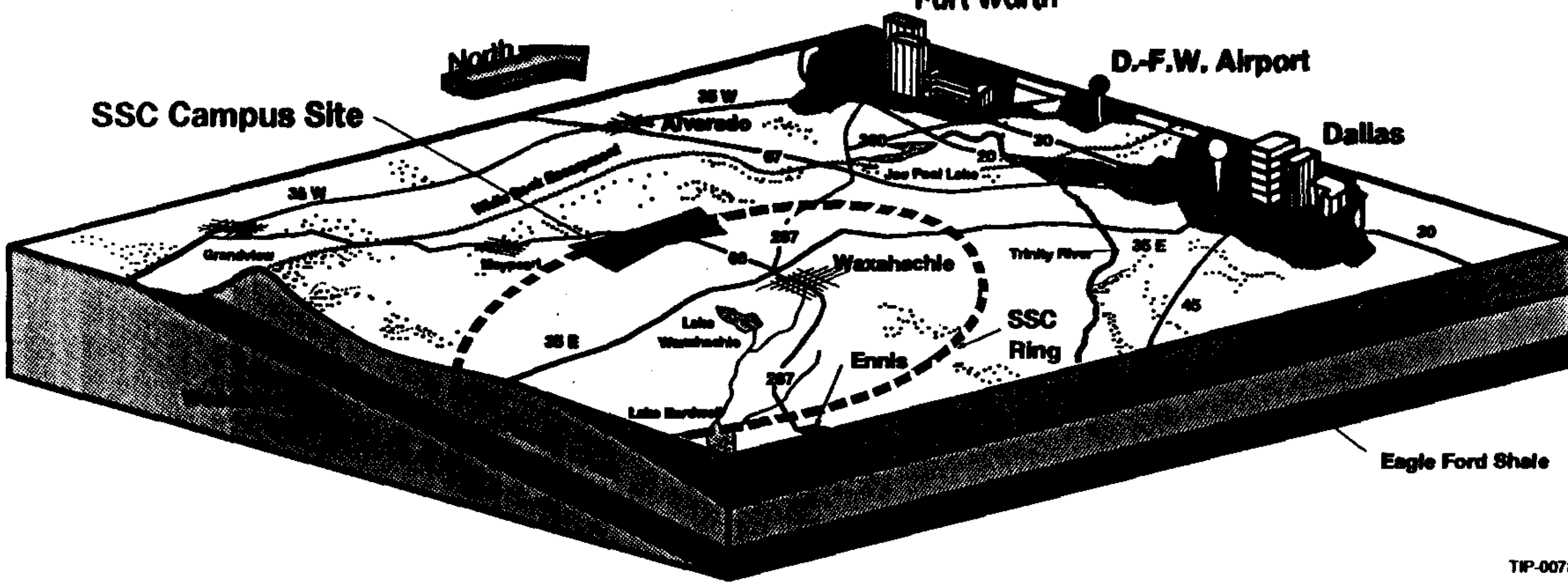

TIP-00783

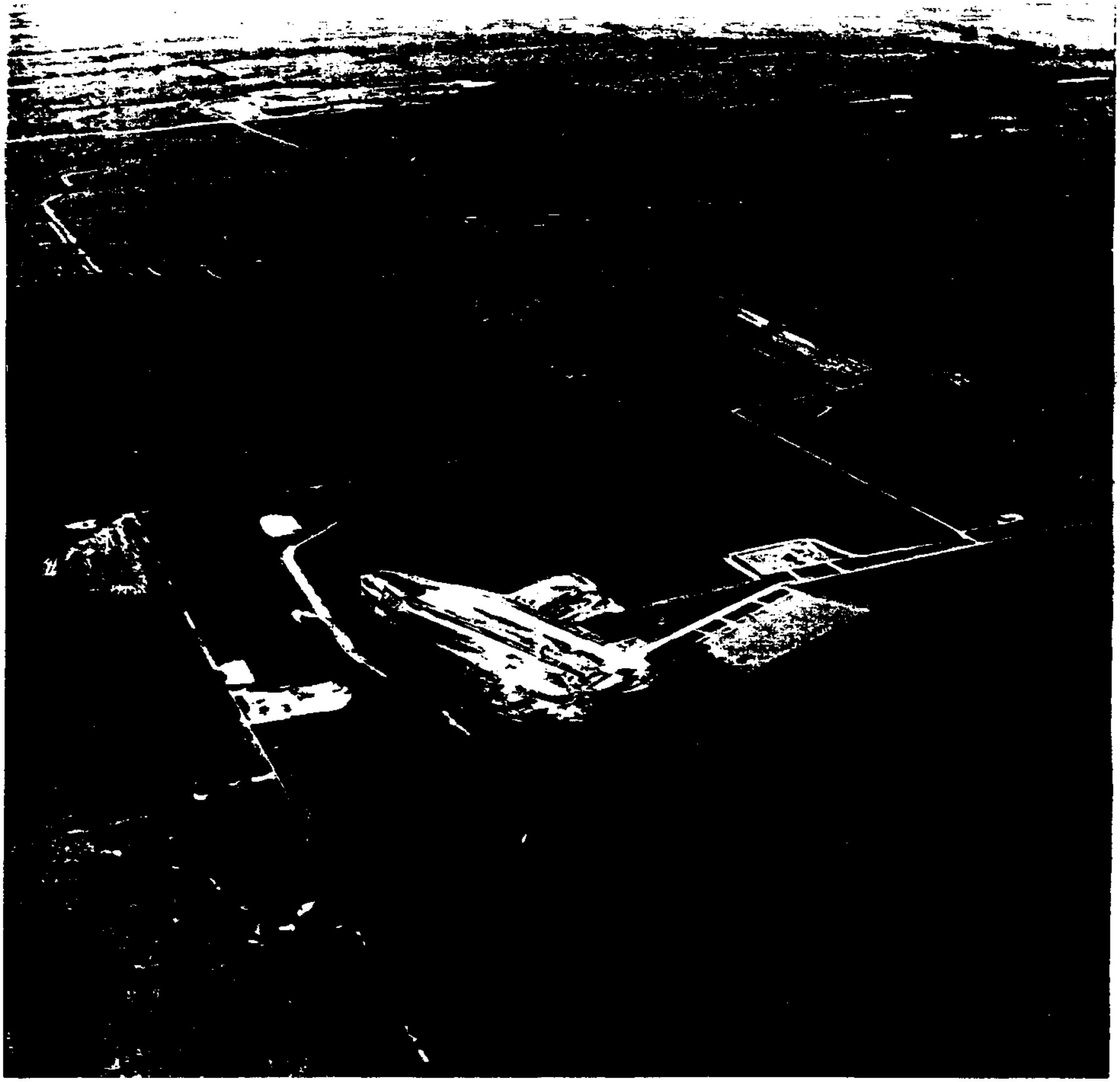

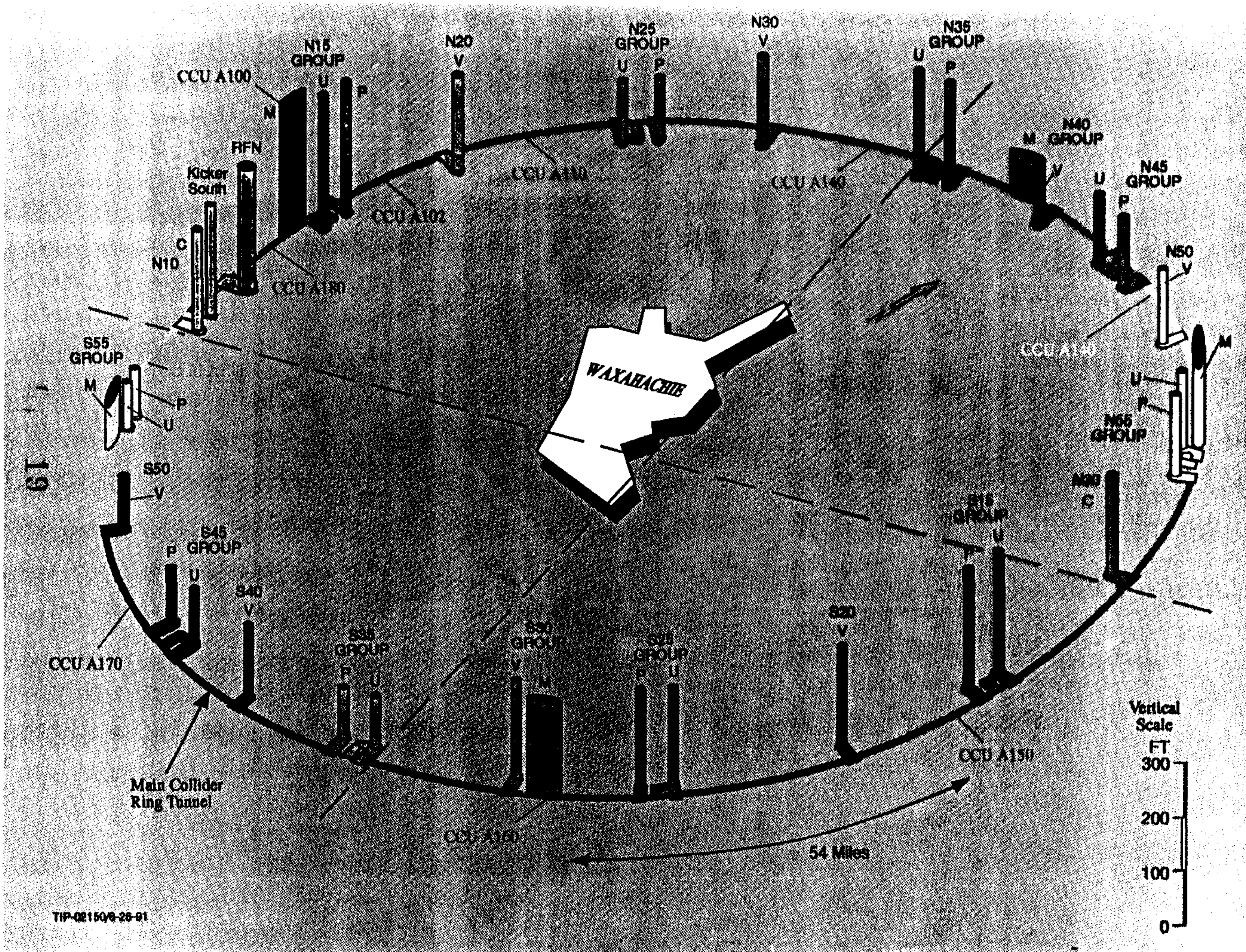
N15 GROUP
CCU A100
M
U
P
N20
V
N25 GROUP
U
P
N30
V
N35 GROUP
U
P
N40 GROUP
M
V
N45 GROUP
U
P
N50
V
N55 GROUP
M
U
P
N60
C
RFN
Kicker South
C
N10
CCU A102
CCU A180
CCU A110
CCU A140
WAXAHACHIE
S55 GROUP
M
P
U
S50
V
S45 GROUP
P
U
S40
V
S35 GROUP
P
U
S30 GROUP
V
M
S25 GROUP
P
U
S20
V
S15 GROUP
P
U
CCU A170
CCU A160
CCU A150
Main Collider Ring Tunnel
54 Miles
Vertical Scale
FT
300
200
100
0
TIP-02150/6-26-91

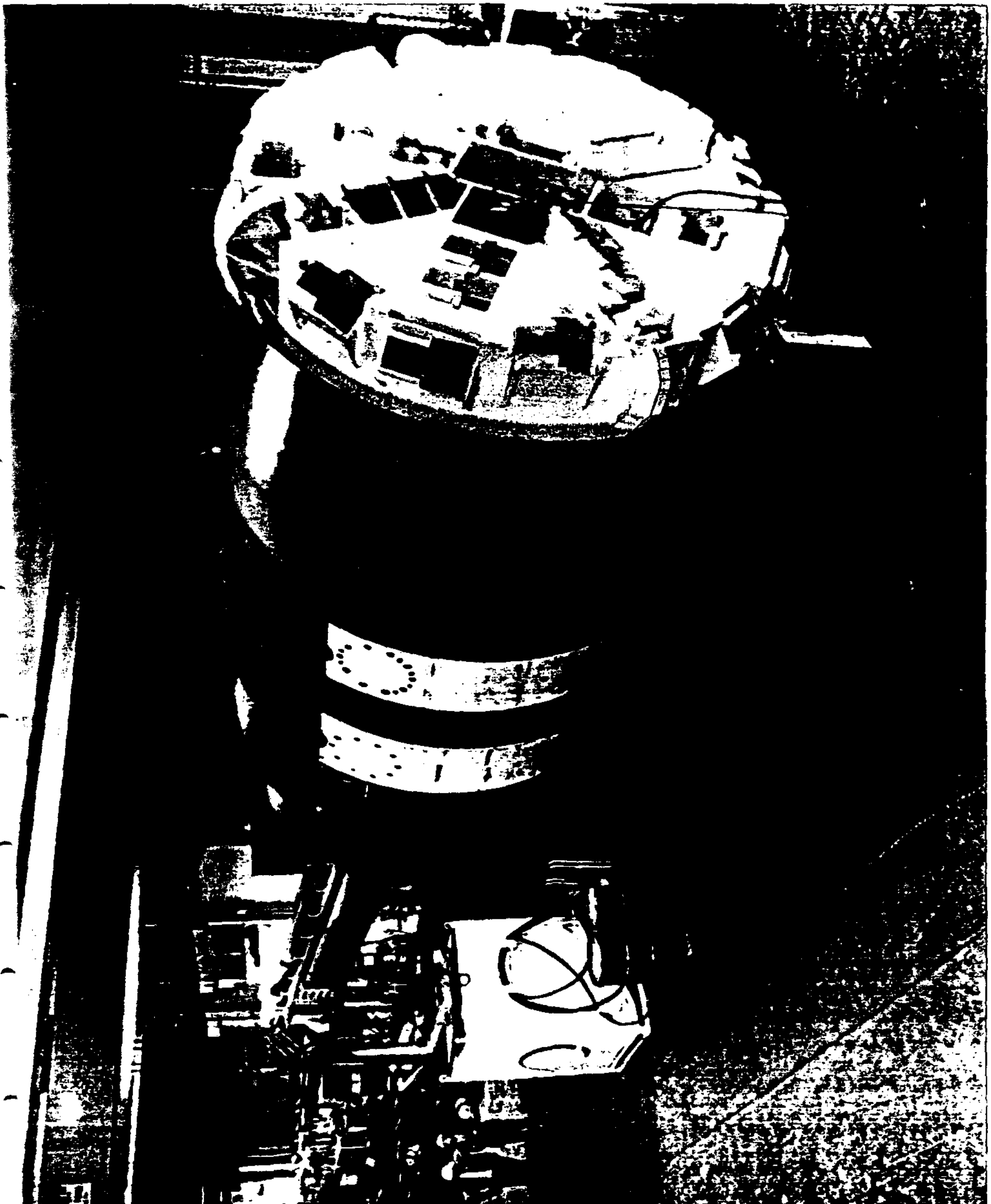

Initial Scientific Program

Proposal Driven — First Expressions of Interest June, 1990
20 EoI's received

2 Major, complementary detectors
- Formal proposal review – 1992
- SDC, GEM } ~ 700 U.S. physicists, major foreign participation

Smaller experiments
- Reserve capital funds
- Workshops, new calls for proposals : 1992-93

Detector R&D program

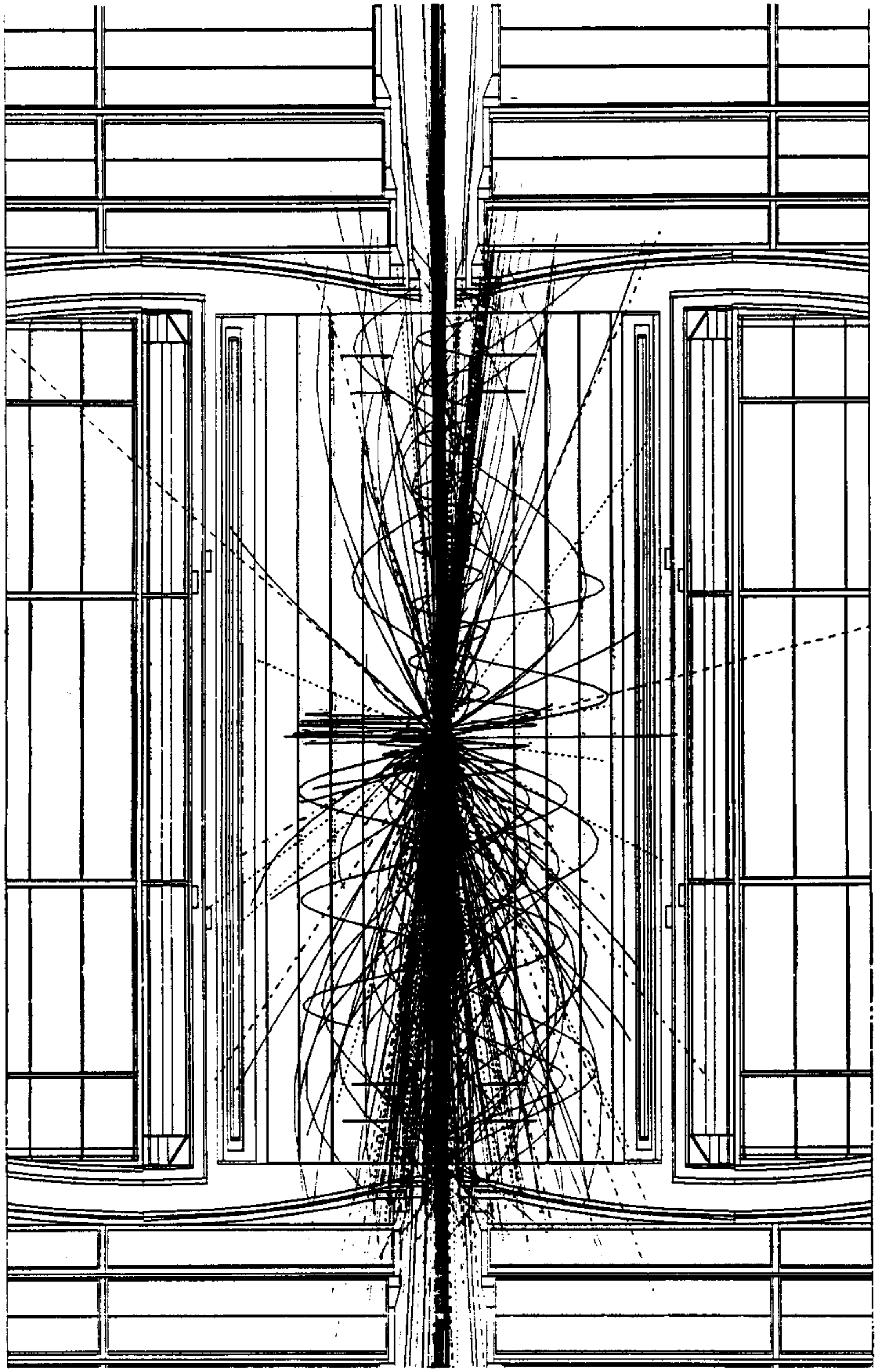

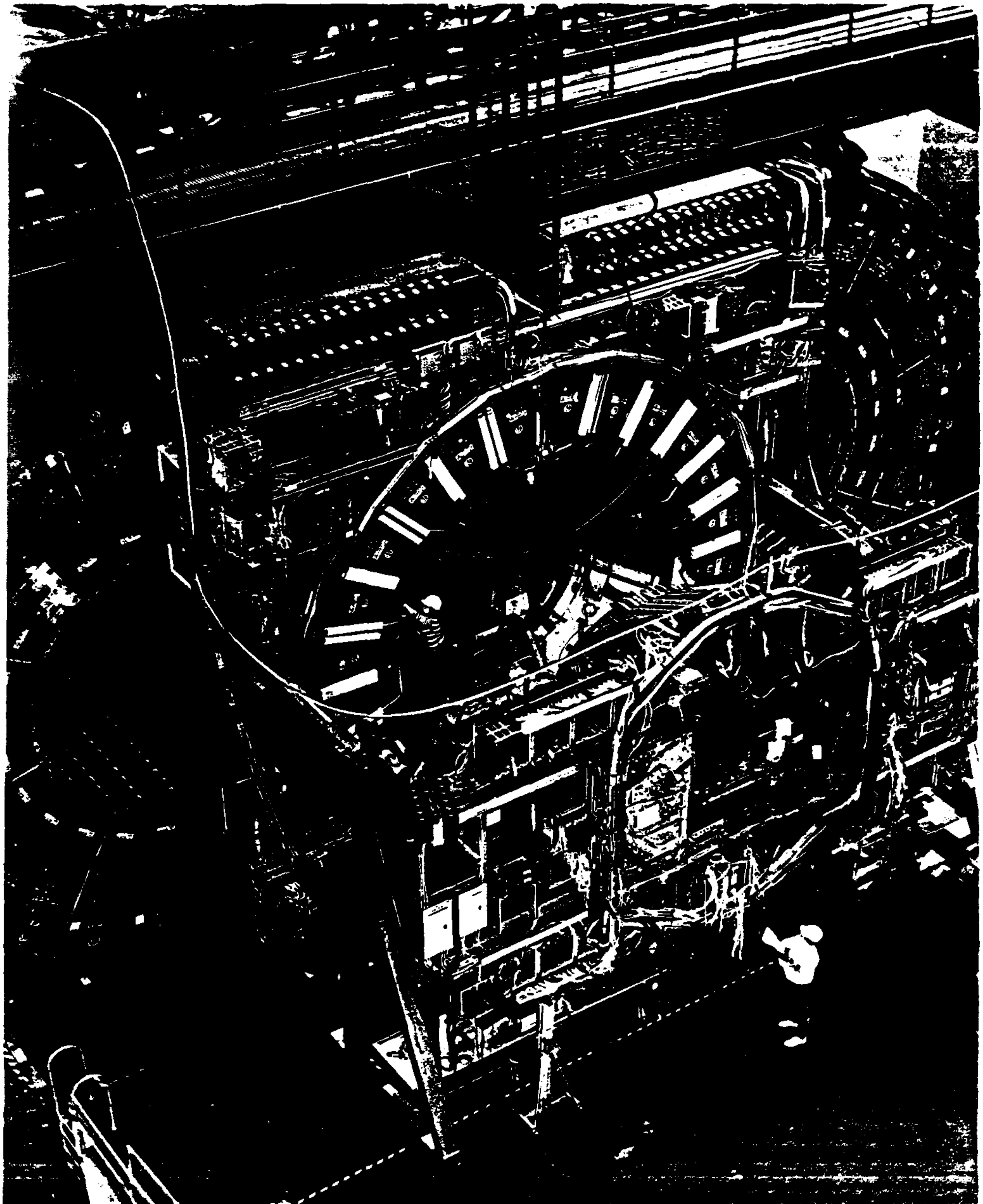

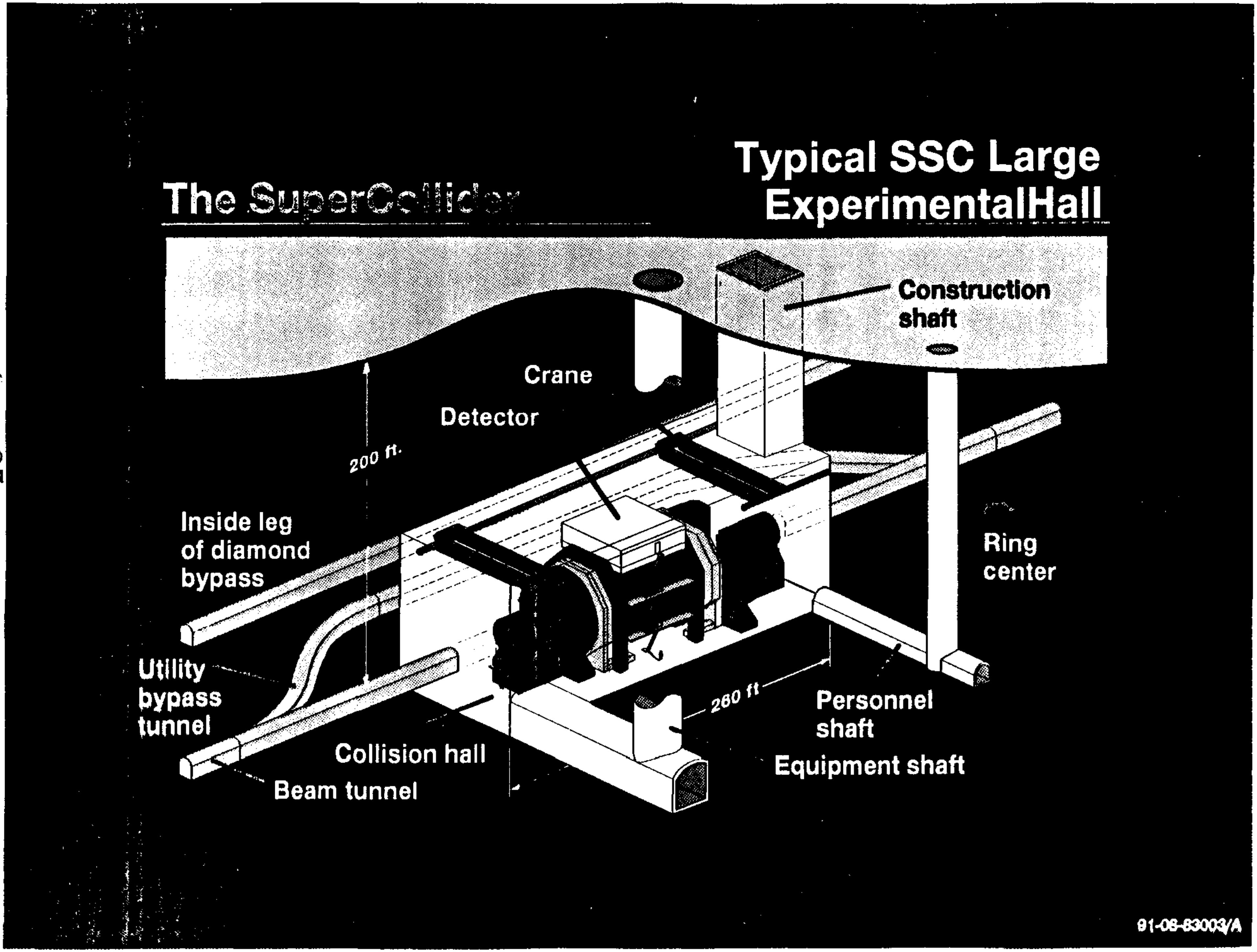
The SuperCollider
Typical SSC Large
ExperimentalHall
Construction
shaft
Crane
Detector
200 ft.
Inside leg
of diamond
bypass
Ring
center
Utility
bypass
tunnel
260 ft
Personnel
shaft
Equipment shaft
Collision hall
Beam tunnel
91-08-63003/A

GEM Muon System + Discussion

Mike Marx/Frank Taylor

Process:

(I) Muon Review SSCL 10/6/92

Input:

- Proponent Reports
- Engineering Assessment
- Panel of Experts
- Muon Steering Committee
- Chamber Tests at TTR

Conclusions - barrel system only:

Stepping stones

- LSDT with stand-alone trigger (no RPC ~~needed~~) looked most attractive for barrel application.
- PDT operated in LS mode and LSDT with RPC trigger same. (The PDT became the "RDT".).
- RPC with low resistivity plastic attractive (high rate possible).
- No rating of CSC barrel application.

GEM Muon Support Structures

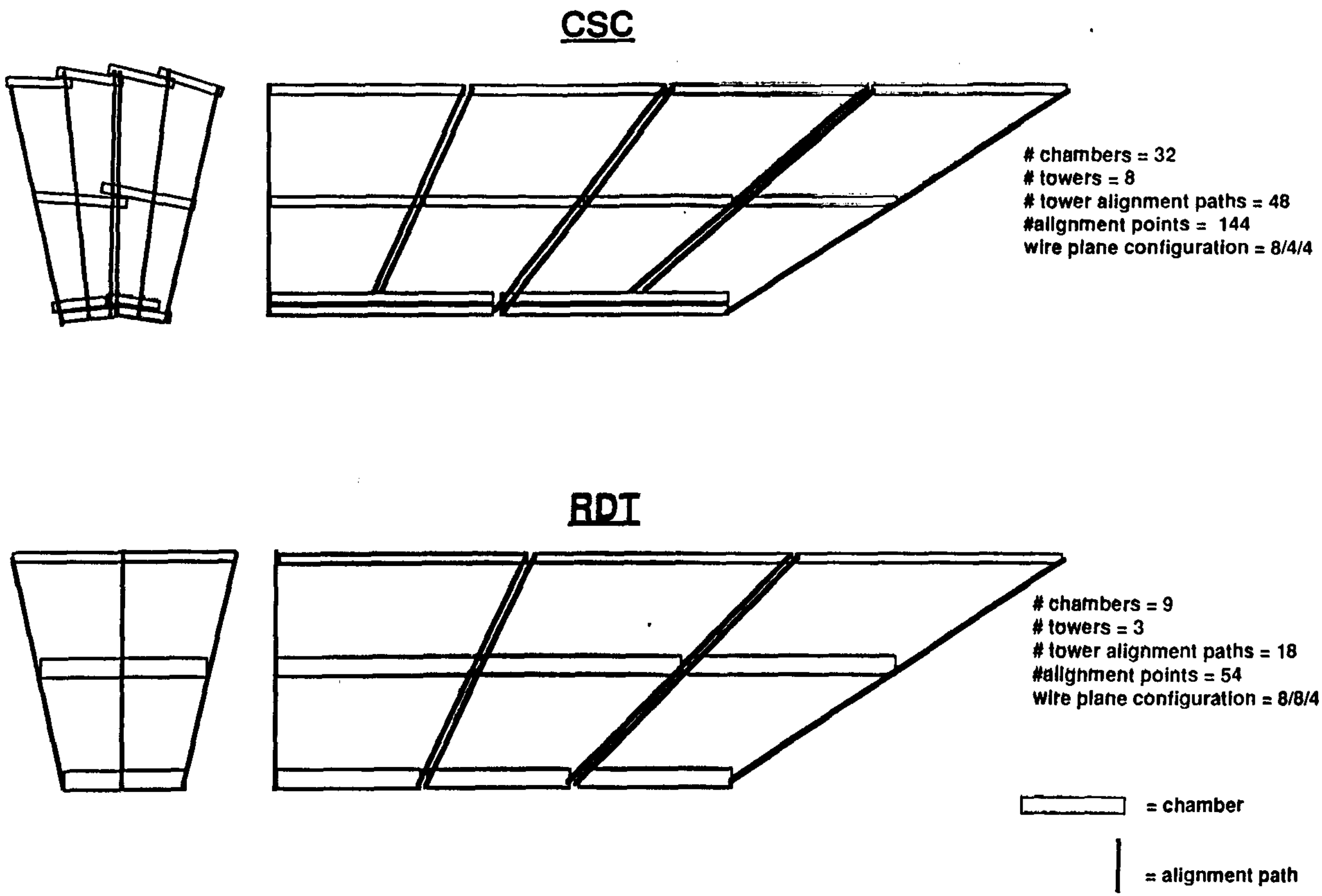

Figure 3. Local alignment schemes for muon barrel

F.E. Taylor -MIT
C.U. 12/18/92

GEM Muon System

- Design Philosophy
- Performance Goals
- Introduction to Chamber Technologies
- R&D and Construction Plans

GEM Case 600: revised baseline, Nov 18, 1992

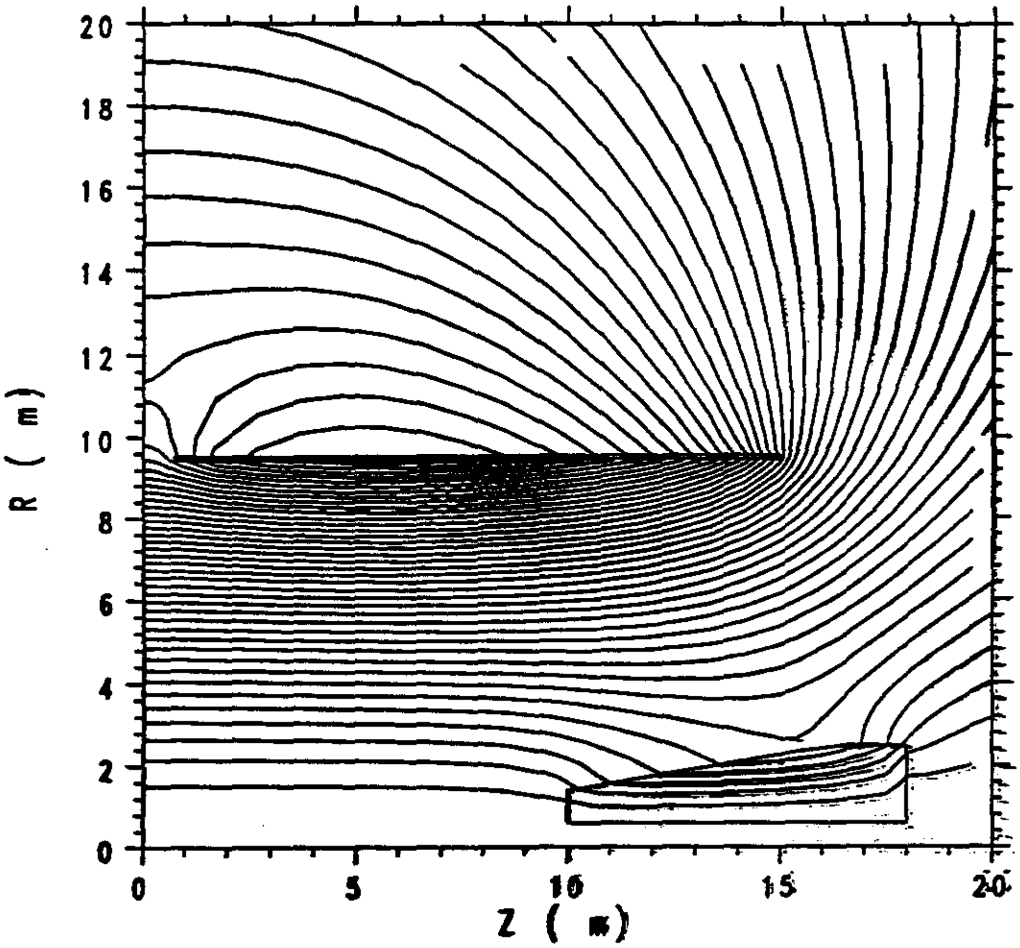

GEM Case 600: revised baseline, Nov 18, 1992

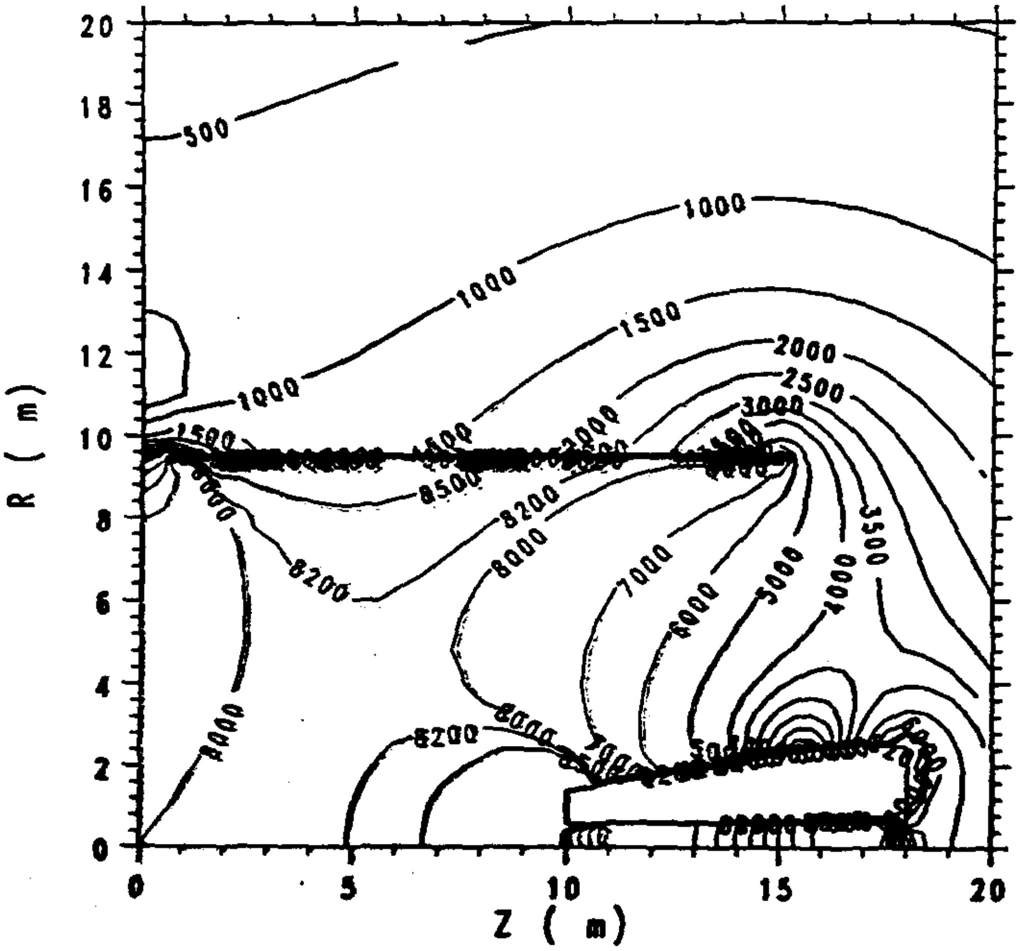

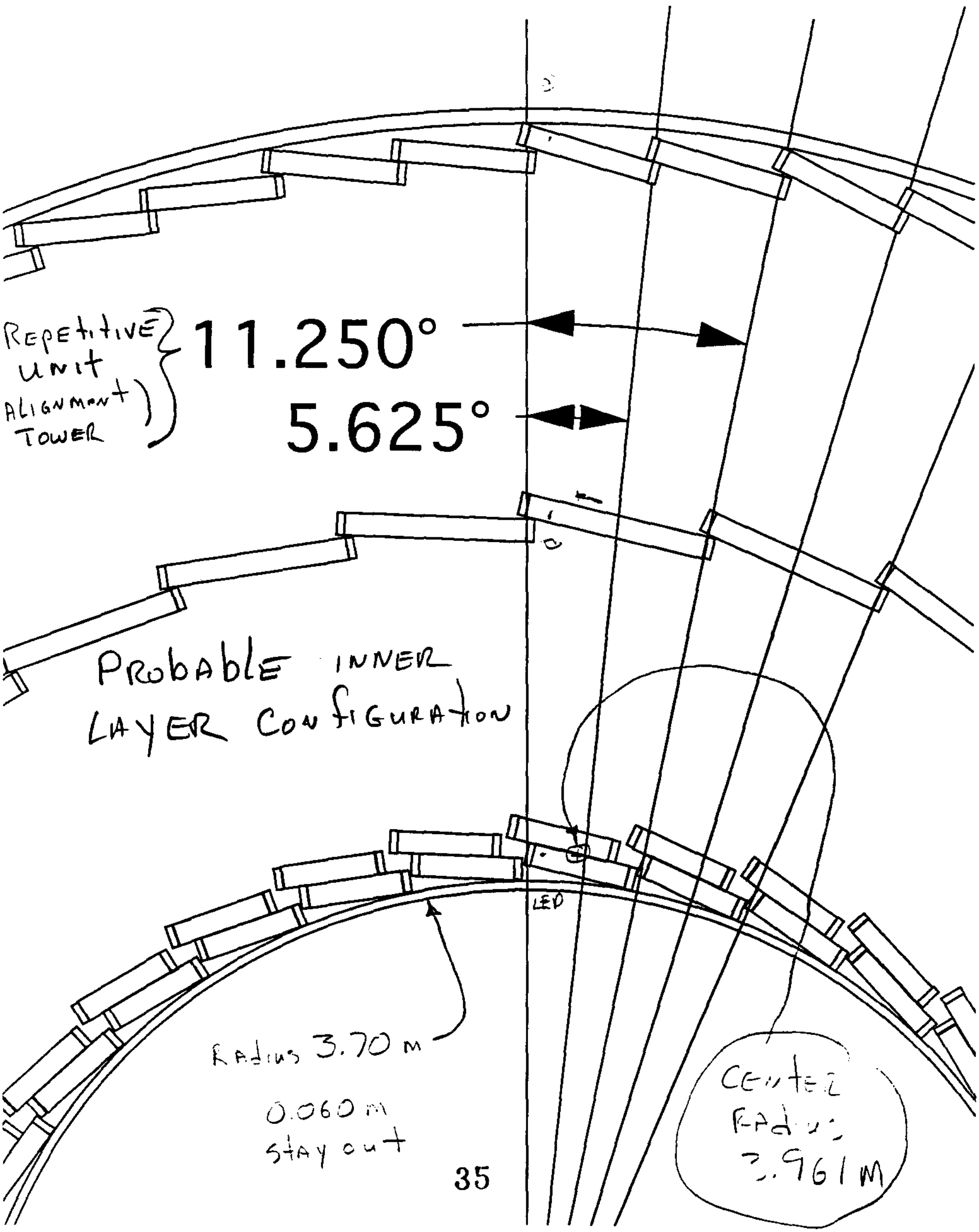
Repetitive unit alignment tower
11.250°
5.625°
Probable inner layer configuration
LED
Radius 3.70 m
0.060 m stay out
Center Radius 3.961 M

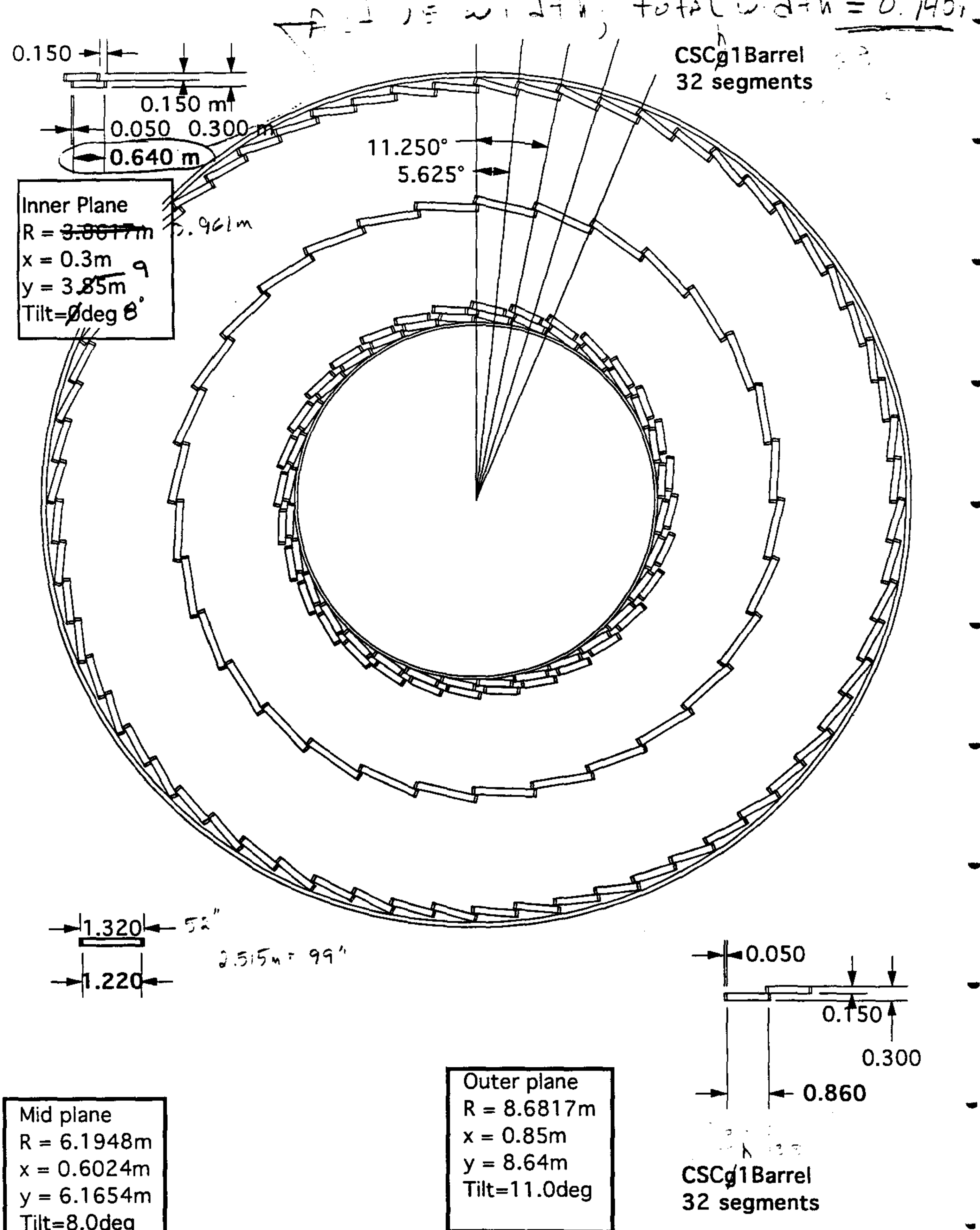

total width = 0.740
CSCg1Barrel
32 segments
0.150
0.150 m
0.050 0.300 m
0.640 m
11.250°
5.625°
Inner Plane
R = 3.8617m
x = 0.3m
y = 3.85m
Tilt=0deg
1.320
1.220
0.050
0.150
0.300
0.860
Outer plane
R = 8.6817m
x = 0.85m
y = 8.64m
Tilt=11.0deg
CSCg1Barrel
32 segments
Mid plane
R = 6.1948m
x = 0.6024m
y = 6.1654m
Tilt=8.0deg

GEM Muon Group

List of Personnel at Institutions:

Boston University:
Bing Zhou, Alex Marin, Steve Ahlen, Jianguo Xu, Robert Chivas, Scott Whitaker, J. Shank, E. Hazen, G. Varner, F.S.U. visitor
contact person: Scott Whitaker

Brookhaven National Laboratory:
Michael J. Murtagh, M. Atiya, V. Polychronakos, V. Radeka
contact person: M. J. Murtagh

Brown University:
Mildred Widgoff
contact person: Mildred Widgoff

BSU-MINSK
N.Shumeiko, M.Baturitsky, V.Shuliak, .Dvornikov, V.Stepanets, S.Degtiarev, V.Mikhailov, I.Emelianchik
contact person:Nikolai Shumeiko

Draper Laboratory:
Howard Baker, Frank Nimblett, Joe Paradiso, Martin Furry, Richard Gustavson
contact person: H. Baker

IHEP-Beijing
Yigang Xie, Yuanbo Chen, Ya-nan Guo
contact person: Yigang Xie

ITEP-Moscow
V. Akimov, V. Balagura, S. Bojarinov, M. Danilov, A. Droutskoi, V. Gavrilov, A. Golutvin, I. Korolko, S. Kuleshov, L. Laptin, P. Murat, V. Nagovitsin, A. Nepejpivo, A. Ostapchuk, P. Pakhlov, V. Popov, F. Ratnikov, V. Shibaev, V. Stolin, I. Tikhohirov, V. Tchistilin,-Z. Zhokin
contact person: M. Danilov

JINR-Dubna
I. Golutvin, Yu. Kiryushin, A. Makhankov, I. Melnichenko, V .Kalagin, V. Lysiakov, V.Rashevsky, A.Dergunov, Yu.Viktorov, V.Khabarov, Yu.Ershov L.Smirnov, V.Peshekhov, V.Zhiltsov, A.Vishnevsky, D.Smolin, S.Sergeev, V.Kondrashev, V.Perelygin, N.Gorbunov, S.Movchan, I.Ivanov, T.Preda, G.Alexeev, N.Khovansky, Z.Krumstein, G.Chelkov, A.Volodko, E.Ladygin, V.Obudovsky, D.Pose,V.Karzhavin, S.Khabarov, S.Sefunin, A.Lyubin, D.Belosludtsev
contact person:Igor Golutvin

Lawerance Livermore National Laboratory:
Craig Wuest, Orrin Fackler, Richard Bionta, Dan Makowiecki, Torre Wenaus, Rick Sawicki, Coleman Johnson, Allen House, Elden Ables, Joe Mauger, Owen Alford, Harlan Olson, Otis Clamp, Kerry Miller, Curt Cochran, Rich Coombs, Phil Ramsey, Mark McKernan, Max Haro, Karl Van Bibber
contact person: Craig Wuest

LeCroy Corporation:
R. Sumner
contact person: R. Sumner

Louisana State University:
Roger McNeil, C. Lydon, Graduate Student
contact person: Roger McNeil

Massachusetts Institute of Technology:
J. Kelsey, D. McCurry, A. Korytov, L. S. Osborne, L. Rosenson, D. Ross, J. Sullivan, F.E. Taylor, I. Pless, E.S. Hafen, P. Haridas
contact person: L.S. Osborne

Michigan State University:
M. Abolins, R. Brock, C. Bromberg, J. Huston, J. Linnemann, R. Miller, D. Owen, B. Pope, H. Weerts, D. Edmunds, S. Gross, P. Laurens, S. Joy, E. Skup, R. Richards, B. Tigner, 4 Research Associates, 10 Graduate Students, 40,000 Undergraduate Students.
contact person: C. Bromberg

Moscow State University
Yu. Fissiak, N. Sotnikova, V. Zhukov
contact person: Yu. Fissiak

Oak Rige National Laboratory:
R. A. Todd, engl
contact person: R. A. Todd

PNPI - St. Petersburg:
A. Krivshich, G. Gavrilov, Maleev, O. Prokofiev, V. Grachev, N. Bondar, V. Mylnikov, S. Patrichev, O. Kiselev, V. Andreev, A. Smirnov, P. Levchenko, An. Vorobyov, L. Lapina, O. Kiselev, A. Tsaregorodzev, A. Dobrovolsky, V. Grachev, A. Khanzadeev, G. Velichko, G. Korolev, N. Sagidova, I. Tkach, N. Abrosimov, G. Ryabov
contact person: A. Vorobyov

Superconducting Super Collider Laboratory:
G. Mitselmakher, M. Marx, G. Yost, K. McFarlane, C. Milner, Yu. Bonushkin, F. Stoker, M. Harris, P. Dingus, R. Shypit, L. Villasenor, V. Glebov, J. Fier-Amory, C. Johnson, E. Zimmer-Nixdorf, A. Gonzalez, M. Gamble, Yu. Fisyak, A. Vanyashin, + 6 guest scientists and engineers.
contact person: G. Mitselmakher

Stony Brook:
M. Mohammadi, A. Sanjari, M. Rijssenbeek, C. Yanagisawa
contact person: M. Mohammadi

Tsinghua University-Beijing:
Ni Weidou, Rencheng Shang, Keren Shi
contact person: Ni Weidou

University of Arizona:
K. Johns, J. Steinberg, L. Shaver
contact person: Ken Johns

University of Houston-SCARF:
K. Lau, B. Mayes, L. Pinsky, J. Pyrlik, R. Weinstein, D. Hungerford, D. Parks
contact person: K. Lau

Mike Marx joined muon system management

DEFINITION of GEM MUON SYSTEM

Functions:

- Muon Identification:
  Track identified outside 12 to 14 λ calorimeter
  (> 140 X0 of Cu)

- P_T trigger (P_T > 10 GeV/c typical):
  Segmentation: 1.3 cm - barrel
  5 mm - endcaps

  Output Rate: Level 1: < 3×10^3 Hz @ 10^{33}

- Beam Crossing Tag: (jitter τ < 5 ns.)

- Tracking:
  - P_T resolution:
    $\delta P_T/P_T \approx 5\ \%$
    for P_T= 500 GeV/c at $\eta \approx 0$ (90^0)
    $\delta P_T/P_T \approx 12\ \%$
    for P_T= 500 GeV/c at $\eta \approx 2.5$ (9.47^0)

  - Muon charge assignment:
    95 % confidence level
    for P_T < 2.8 TeV/c for $0 < \eta < 2.5$

GEM DETECTOR LAYOUT

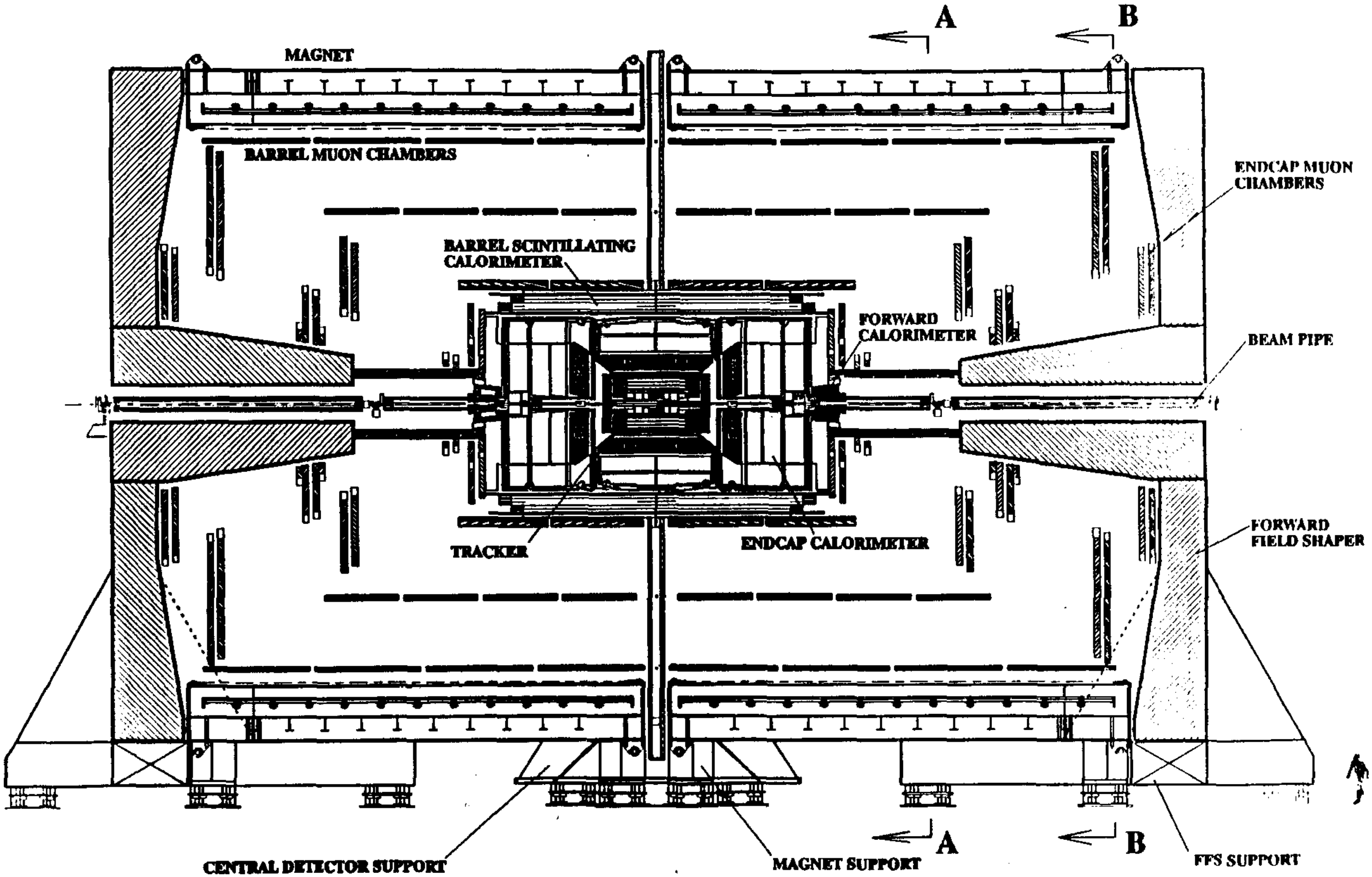

GEM DETECTOR PARAMETERS
BASELINE 2

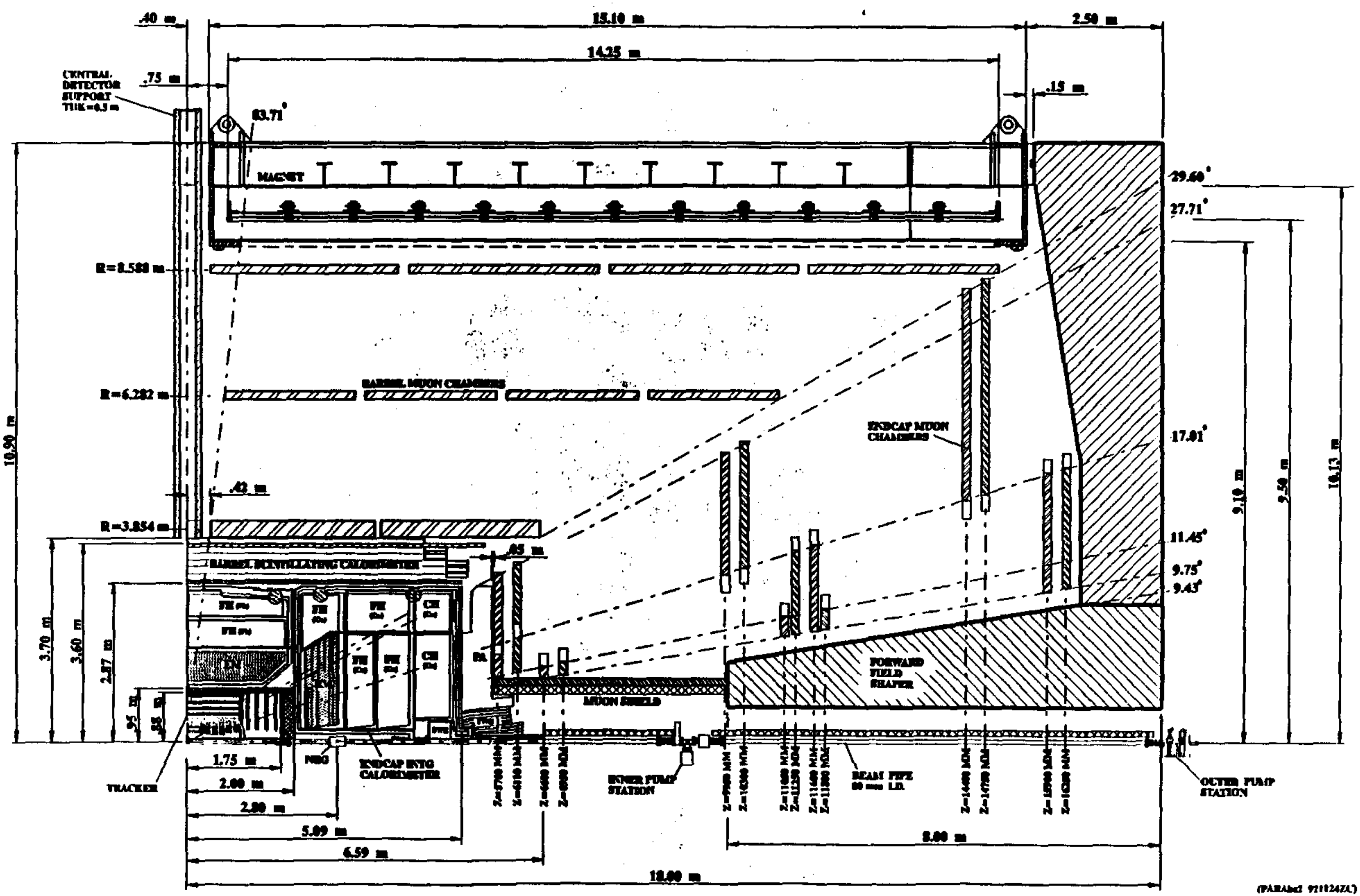

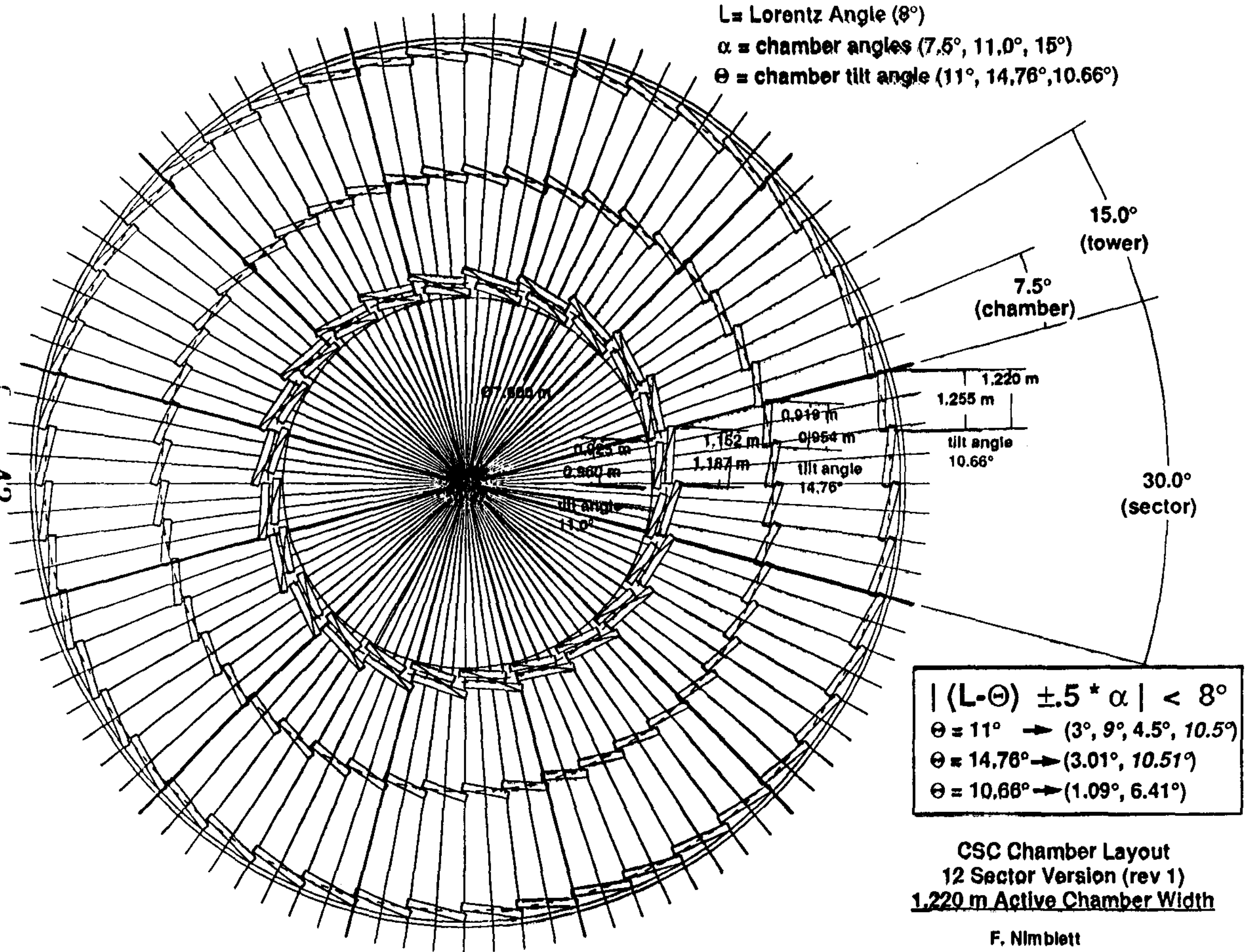

CSC Chamber Layout
12 Sector Version (rev 1)
1.220 m Active Chamber Width

F. Nimblett
16 December 1992

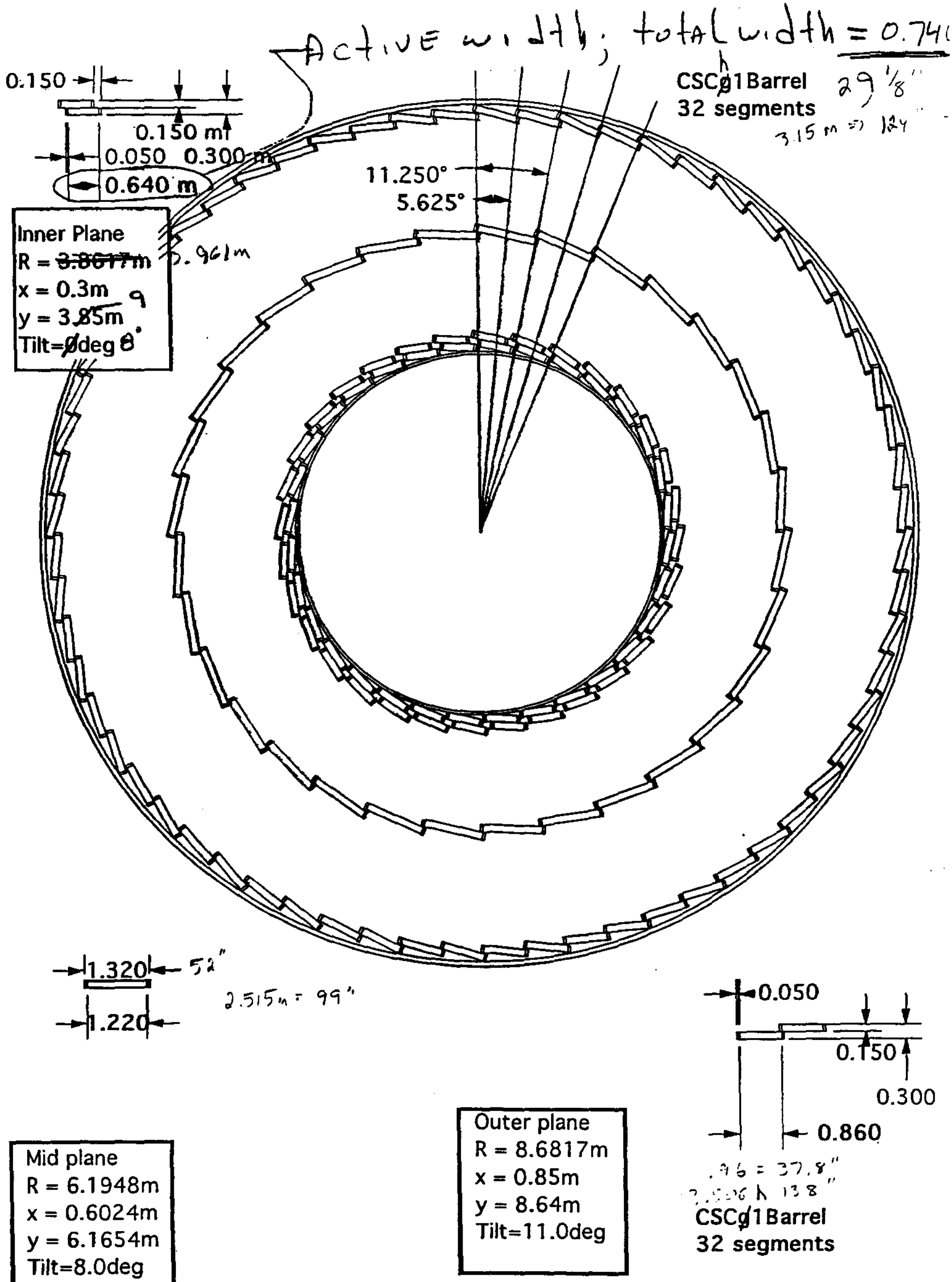
Active width; total width = 0.74
0.150
0.150 m
0.050 0.300 m
0.640 m
Inner Plane
R = 3.8617m 3.961m
x = 0.3m
y = 3.85m 9
Tilt=0deg 8°
11.250°
5.625°
CSCg1Barrel
32 segments
29 1/8"
3.15 m => 124"
1.320 52"
2.515m = 99"
1.220
Mid plane
R = 6.1948m
x = 0.6024m
y = 6.1654m
Tilt=8.0deg
Outer plane
R = 8.6817m
x = 0.85m
y = 8.64m
Tilt=11.0deg
0.050
0.150
0.300
0.860
CSCg1Barrel
32 segments

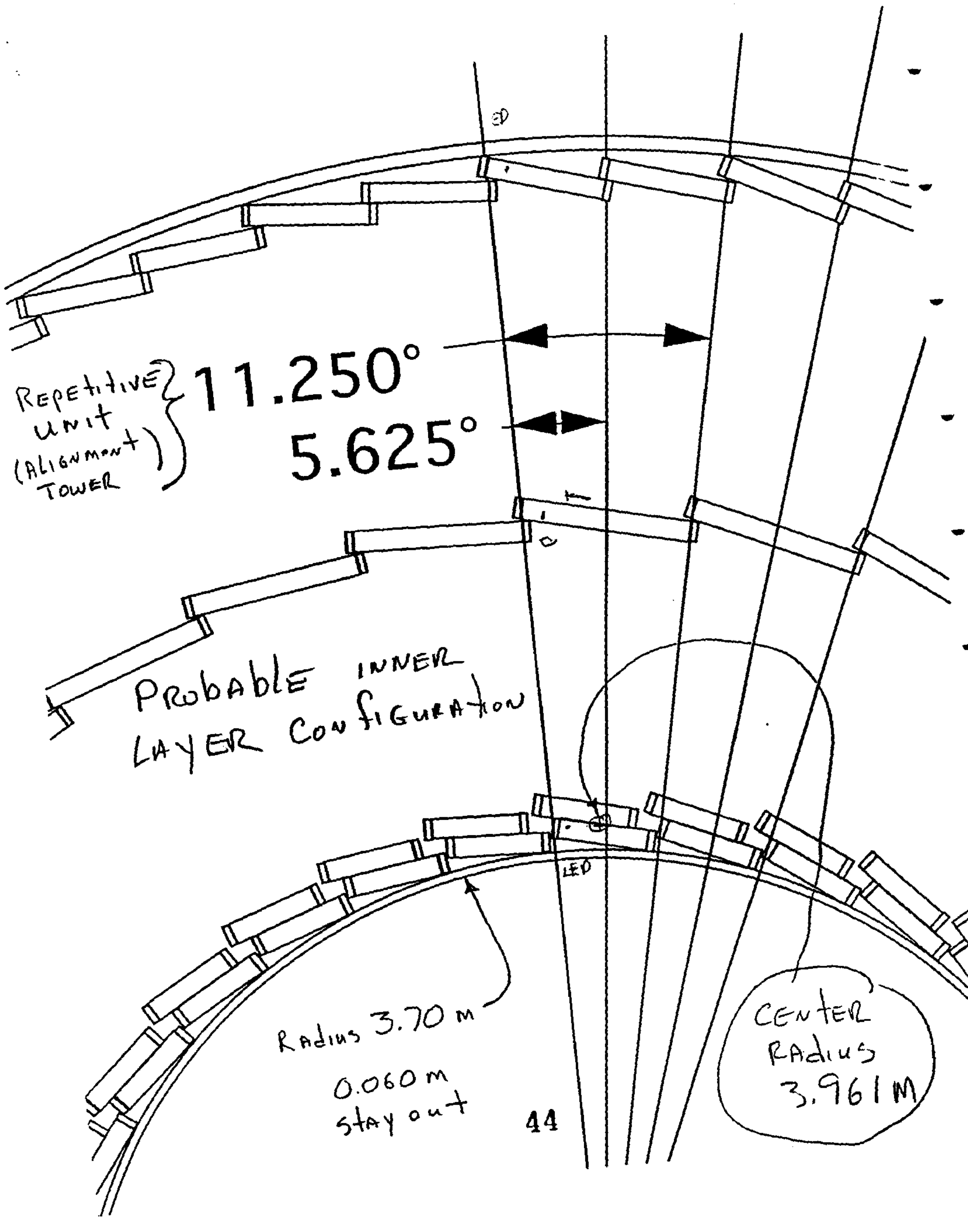

11.250°
5.625°
Repetitive unit (Alignment Tower)
Probable inner layer configuration
Radius 3.70 m
0.060 m stay out
Center Radius 3.961 M
LED

CSCf2crzBarrellayout

Lengths of active areas

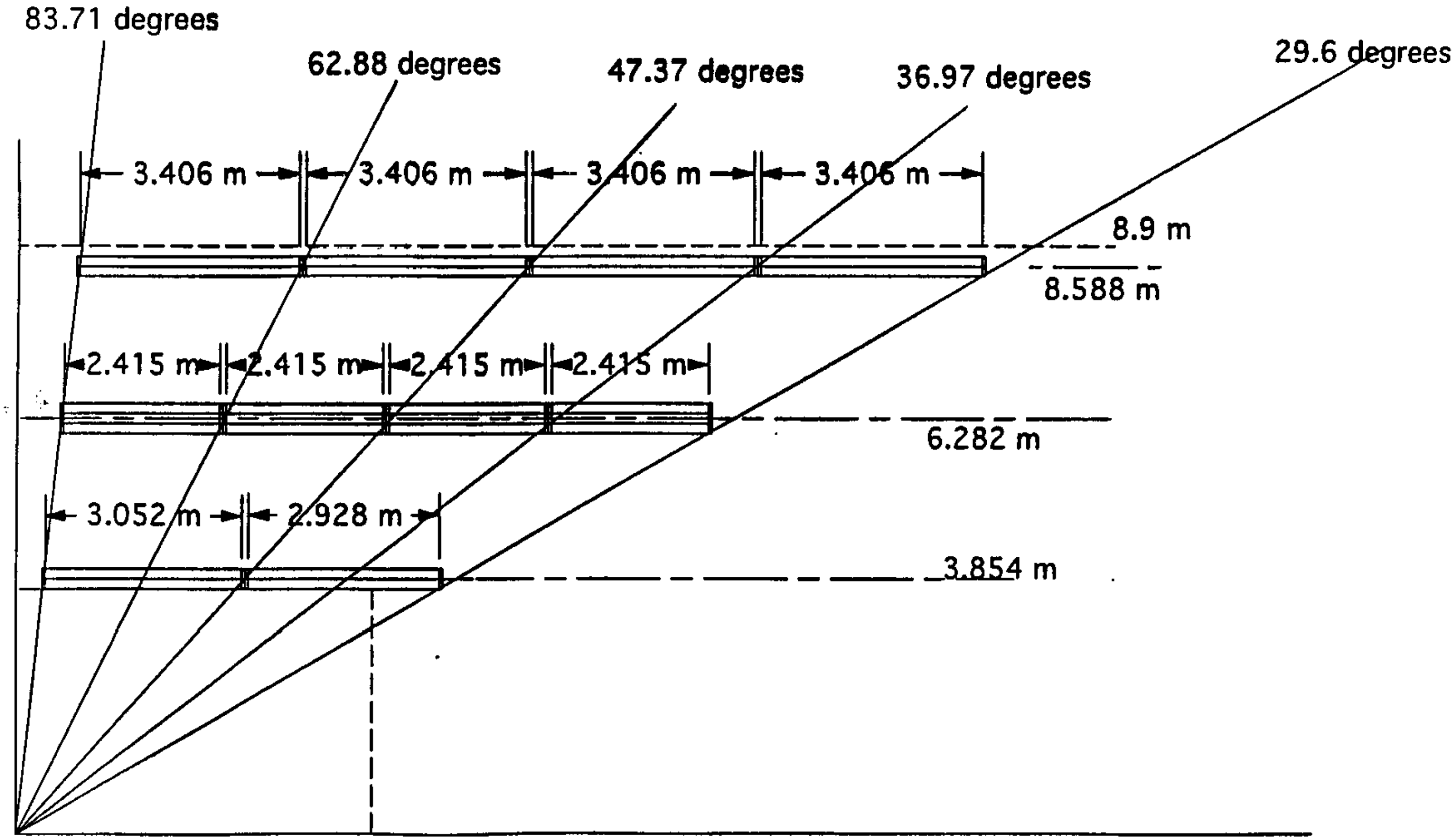

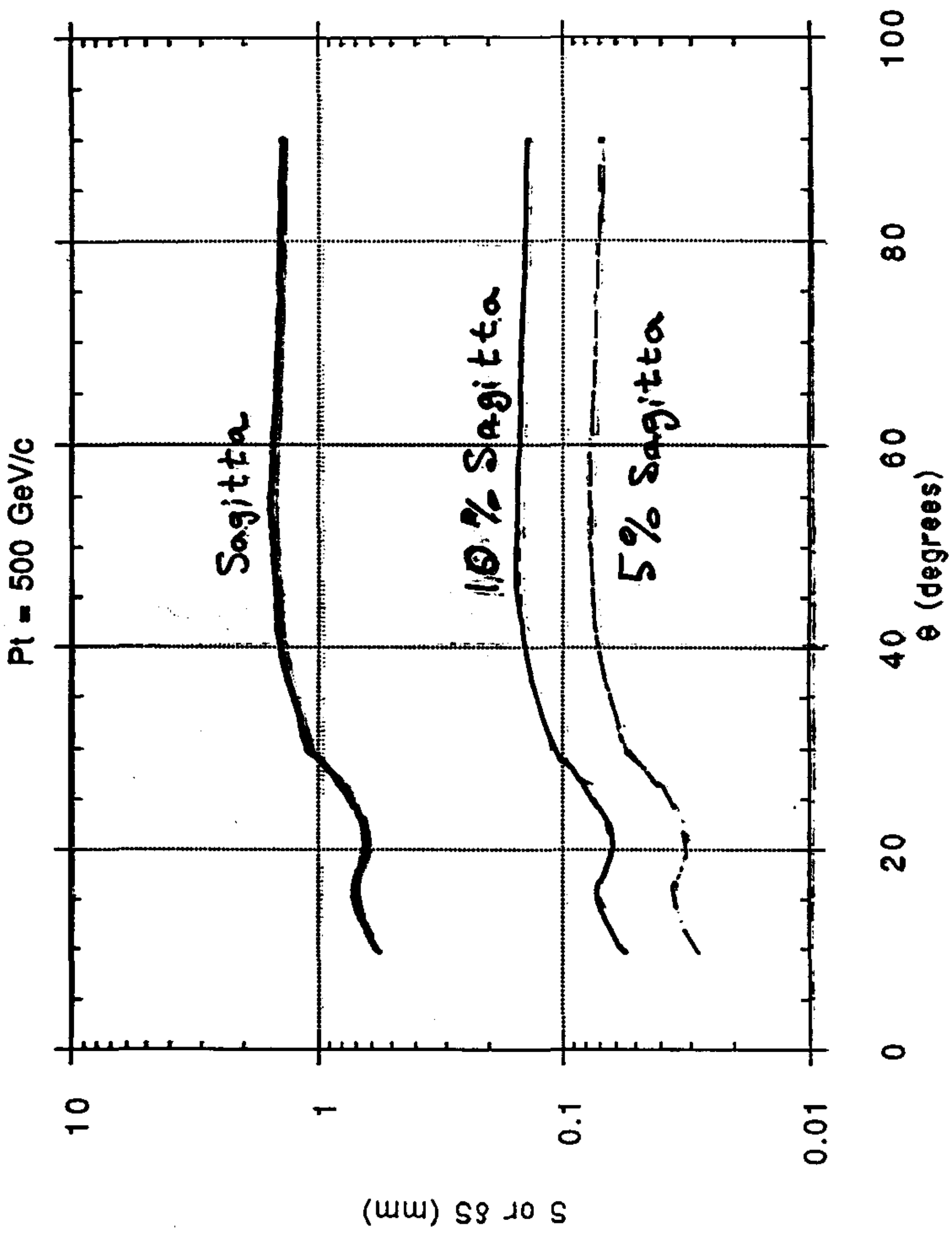

Pt = 500 GeV/c
Sagitta
10 % Sagitta
5% Sagitta
θ (degrees)
S or δS (mm)
0
20
40
60
80
100
10
1
0.1
0.01

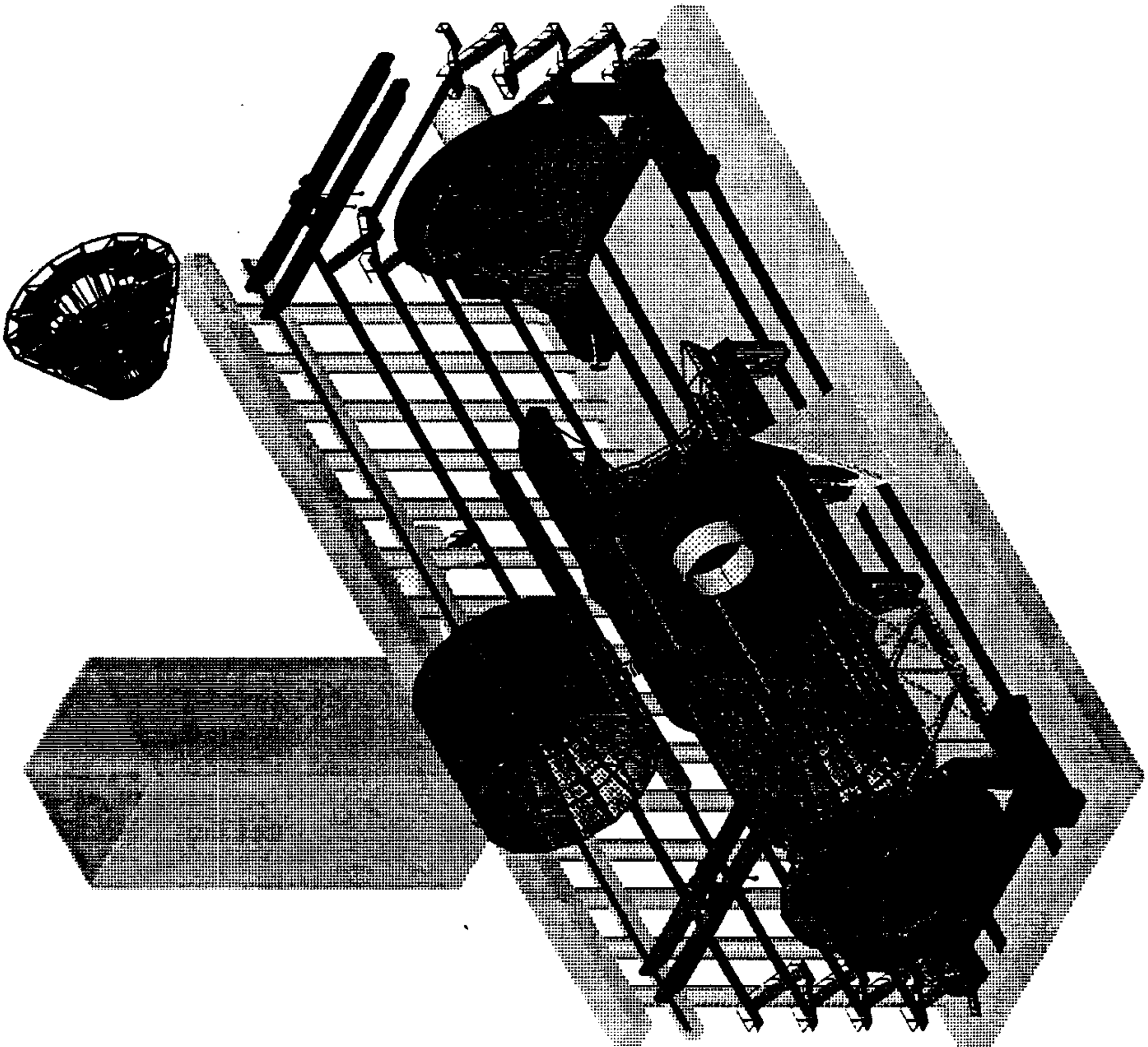

Chamber Support Structure

- Stable platform for chambers

  requirements:

  $\sigma \approx 25\ \mu m$ inter - superlayer alignment - systematic
  $\sigma \approx 50\ \mu m$ intra - superlayer alignment - random
  $\sigma \approx 75\ (100)\ \mu m$ single layer resolution - random

- Considered:

  performance (stability to vibrations)
  cost
  fabrication requirements
  schedule impact on GEM construction

- Propose to build:

  sectors (1/16) tied together as a monolith
  good vibration characteristics
  ease of construction in small parts
  prototype testing possible

Chamber Technologies

- Baseline:

CSC = Cathode Strip Chambers (anolog readout)

- Backup Technologies for Baseline:

RDT = Round Drift Tubes (time readout)

RPC = Resistive Plate Counter

Considered, but rejected:

LSDT = Limited Streamer Drift Tubes

- Chamber Testing Program:

TTR = Texas Test Rig (Cosmic ray muon laboratory at SSCL)

Prototype Cathode Strip Chamber

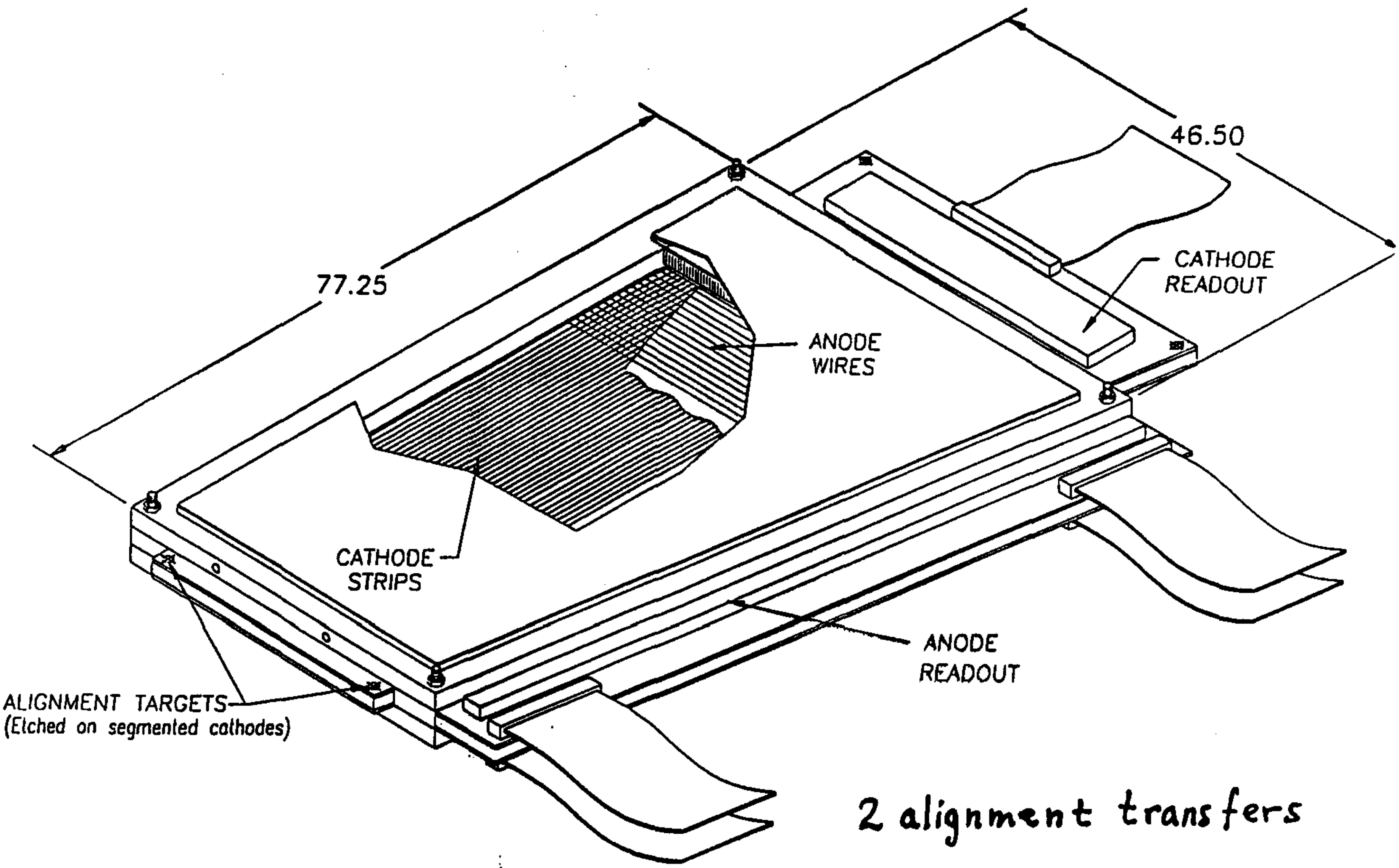

2 alignment transfers

Cathode Strip Chamber

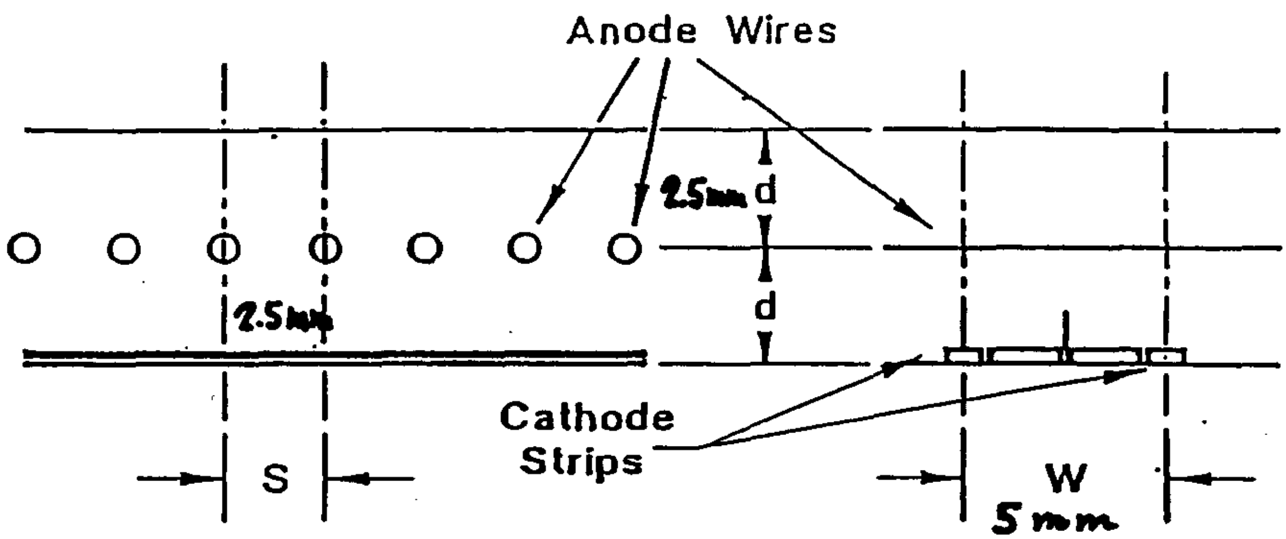

Figure 1: Geometry of the basic cell of the CSC

Run#: 666 Events on File: 45442 groups on file: 2
Event#: 4200 Fri, Oct 23, 1992 17:45

UH prototype

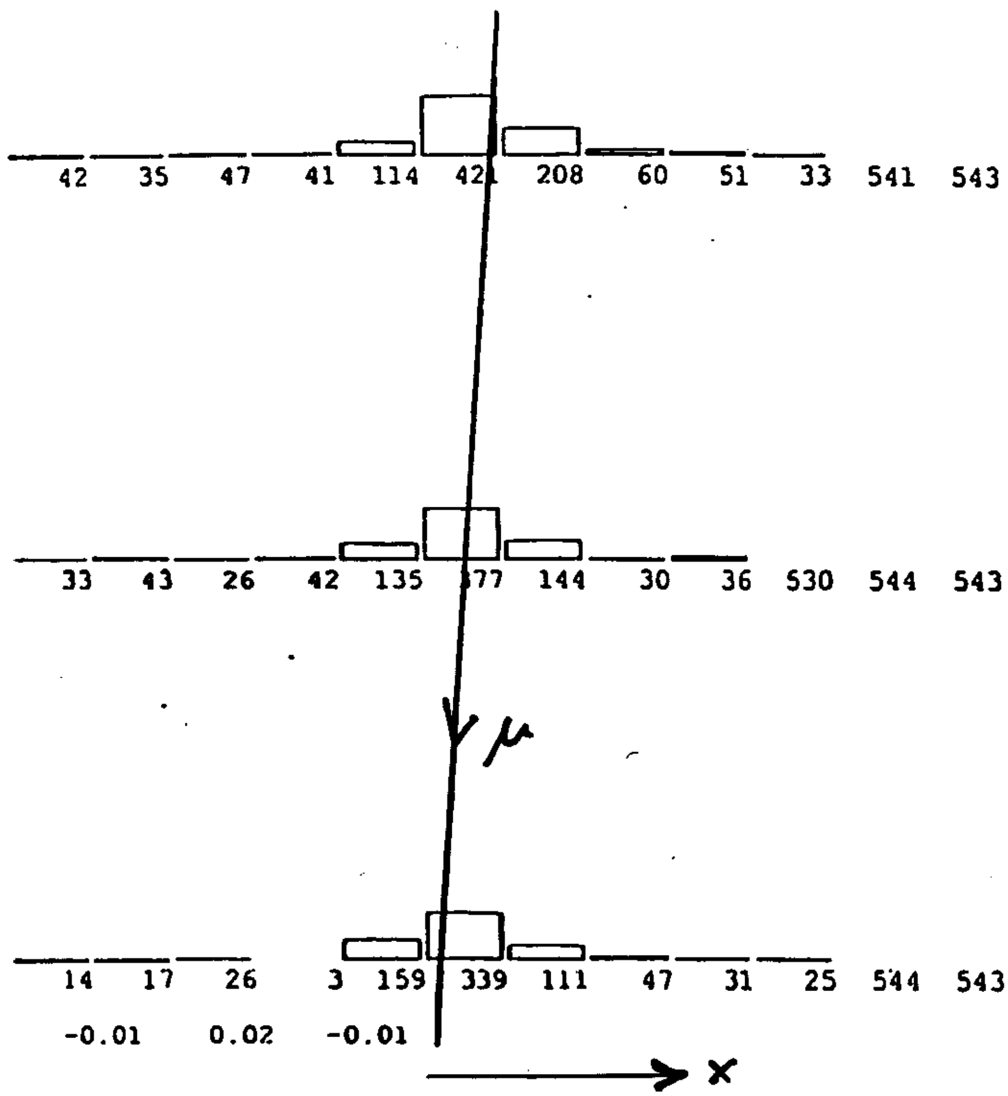

position: $x_{cg} = \frac{\sum x_i q_i}{\sum q_i}$ $\qquad x_i = (i)\ell_a$

resolution: $\sigma_{cg} \simeq \ell_a \frac{\sigma_{noise}}{Q}\sqrt{2}$ $\qquad$ for 3 strips

Round Drift Tube

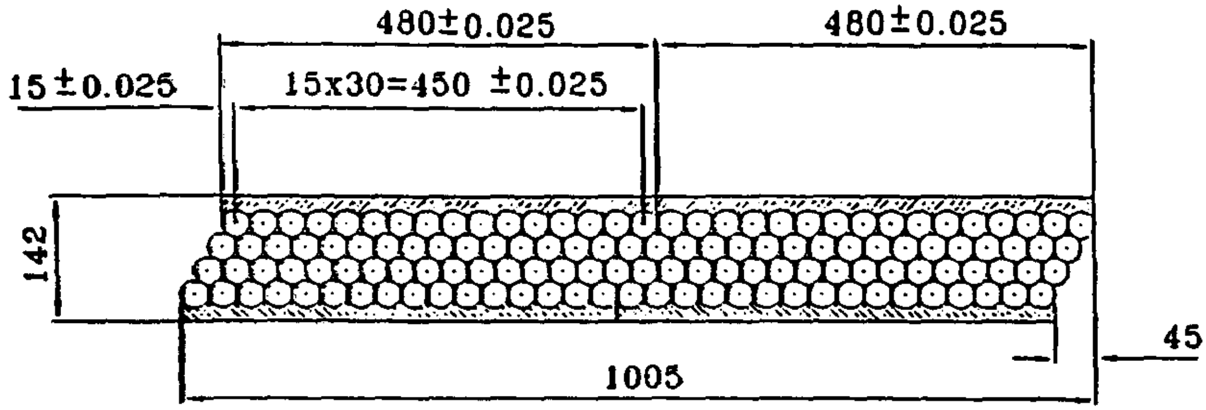

DUBNA PDT PROTOTYPE

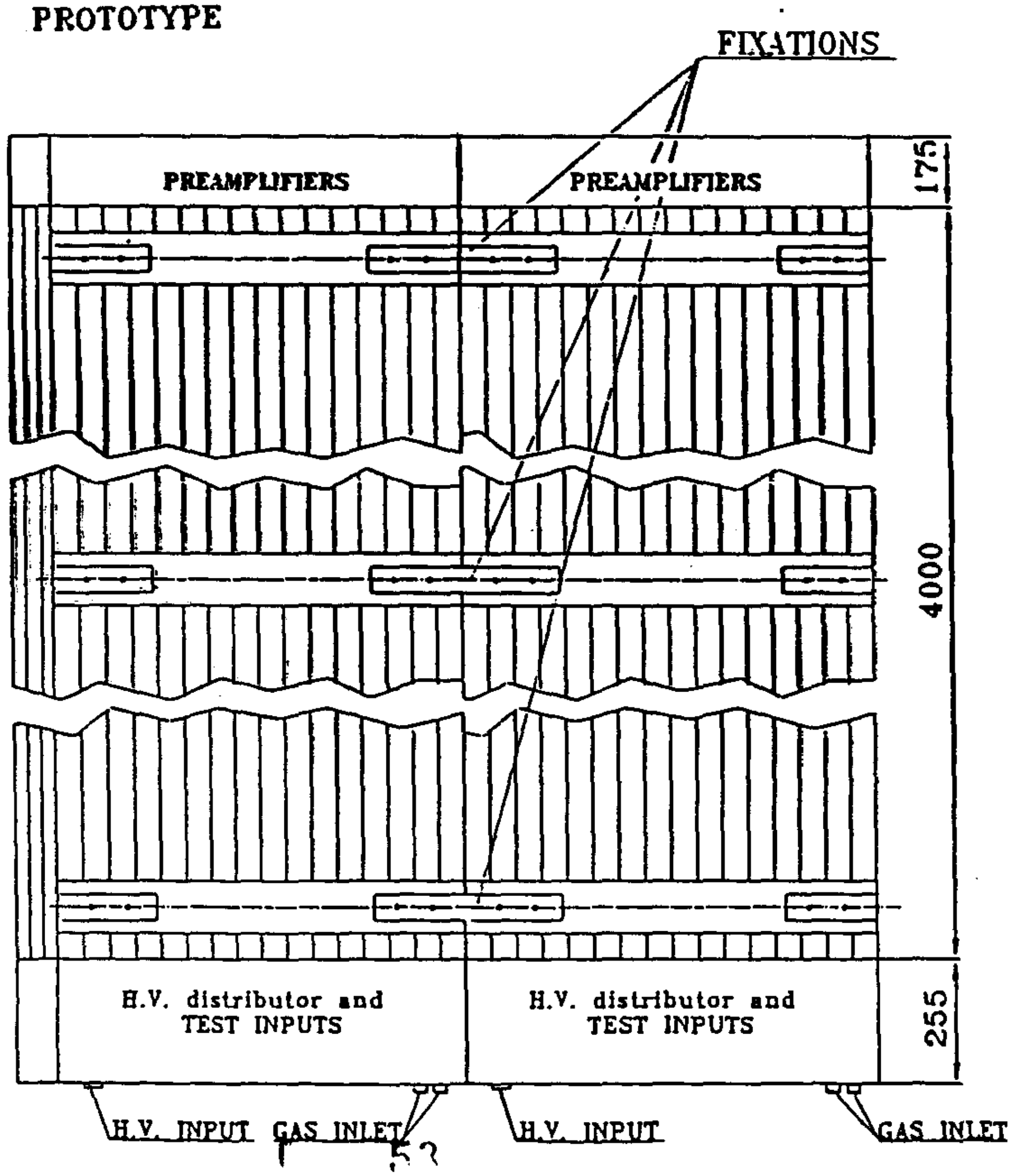

Resistive Plate Counter

Bakelite RPC

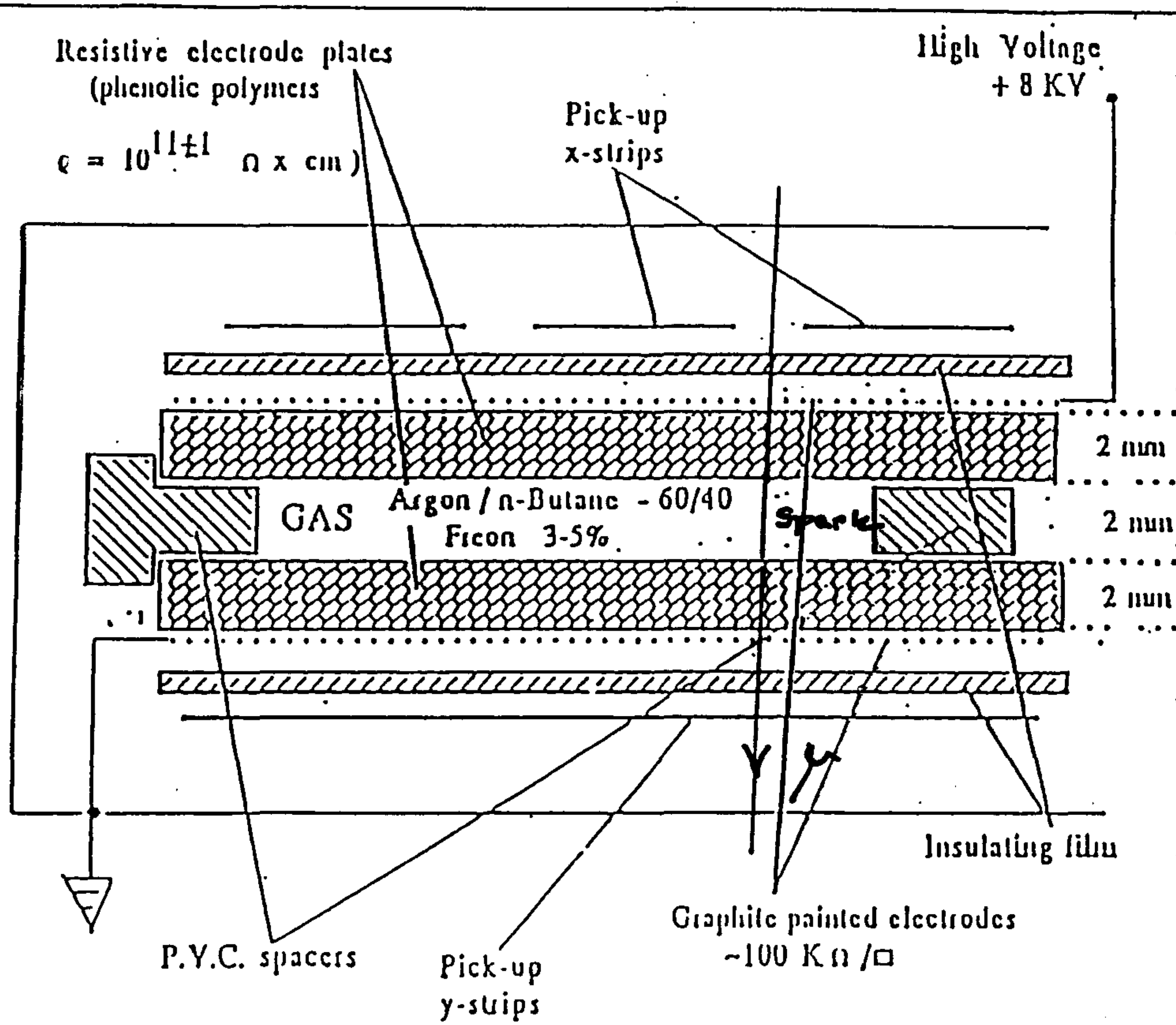

Bakelite RPC

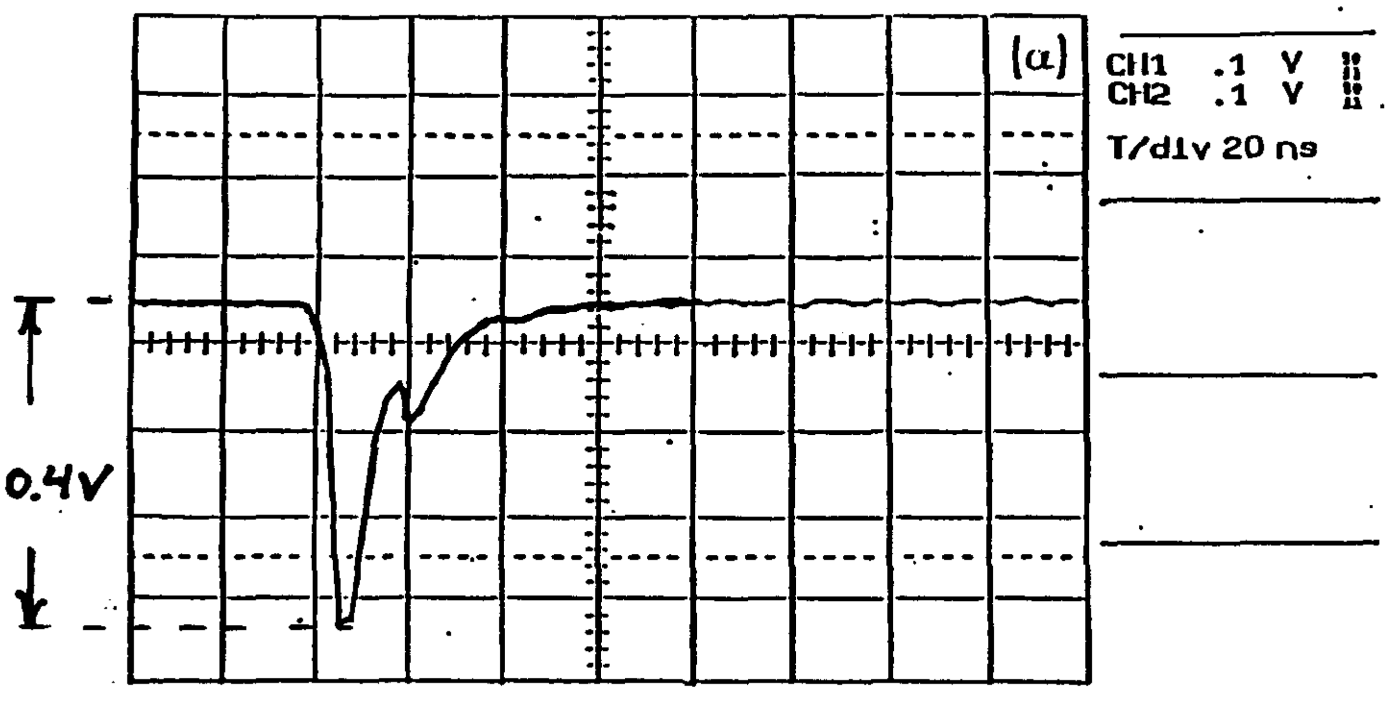

jitter $\lesssim$ 1.5 ns

r $\leq$ 50 Hz/cm^2 Bakelite (needs to be better)

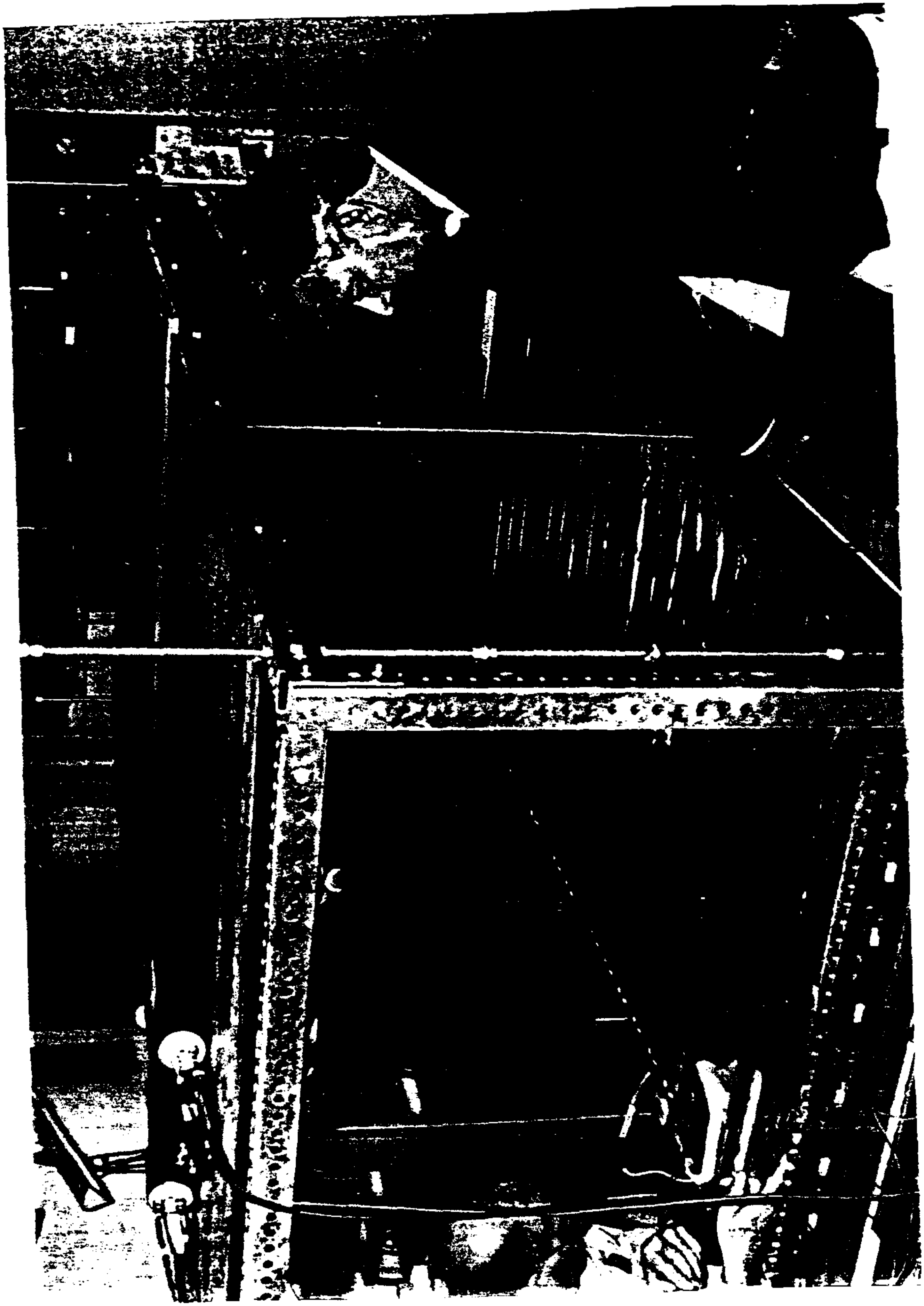

DUBNA PDT PROTOTYPE

TTR TEST SETUP

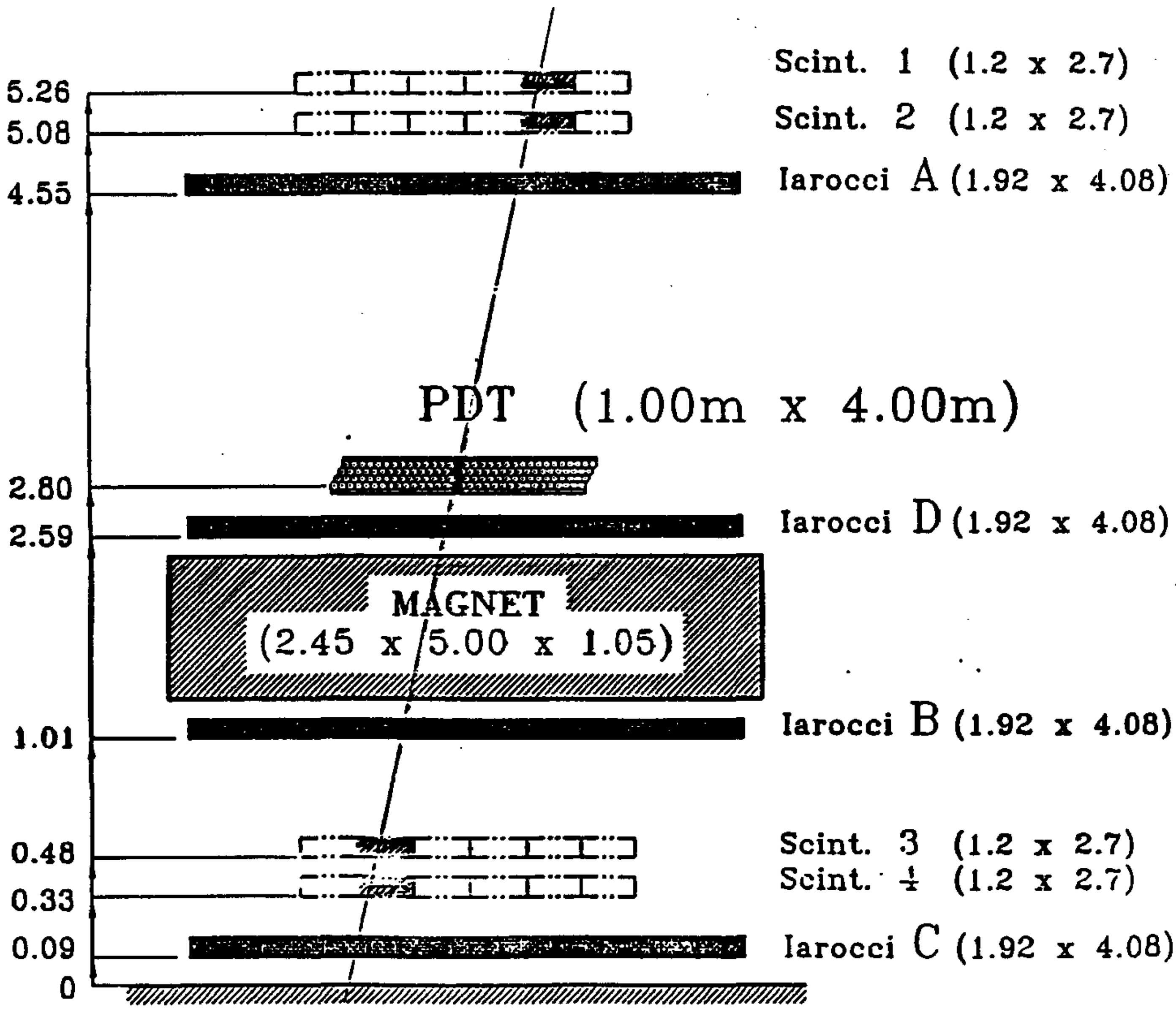

All dimensions in m


EAST

Chambers of R&D92 Program

Technology	Chamber size	TTR delivery date
RDT-JINR	1 m x 4 m x 8 layers	7/28/92 (delivered)
RDT-MSU	1.3 m x 3.8 m x 4 layers	9/29/92 (delivered)
LSDT	1 m x 4 m x 4 layers	9/22/92 (delivered)
LSDT	1 m x 4 m x 4 layers	10/23/92 (delivered) 10/28/92 (sent back)
RPC-INFN	1 m x 2 m x 2 layers	9/29/92 (delivered)
CSC-BU	0.3 m x 0.4 m x (2x2) layers	RD5-CERN (delivered)
CSC-BNL	0.5 m x 0.5 m x (2x2) layers	10/20/92(delivered)
CSC-BNL	1 m x 1.8 m x 4 layers	(under construction)
CSC-UH	0.5 m x 1 m x 3 layers	9/92 (delivered)
CSC-JINR	1.2 m x 1.5 m x 2 layers	10/10/92 (delivered)

BASELINE - 2 Parameters

Cathode Strip Chambers

Parameter*	Barrel value	Endcap value	Total
Bend-plane segment width	5 mm	5 mm (in middle)	
Bend-plane channel count	754,000	294,000	1,048,000
Nonbend-plane segment width	10 cm	5 cm	
Nonbend-plane channel count	124,000	35,000	159,000
Number of chambers (4-gap)	1024	352	1376
Number of wires	3.6 M	0.7 M	4.3 M
Number of alignment paths	1536	384 approx.	1920 approx.

* All values preliminary and not optimized.

Possible Areas of Collaboration

(1) Construction of chambers

In USA:
- Participate in R&D of chamber design

In PRC:
- Fabricate and test parts for chamber
- Assemble into complete chamber
- Test chambers with cosmic rays
- Ship to SSCL for installation

(2) Support Structure

In USA:
- Participate in design of structure
- Help assemble structure at SSCL

In PRC:
- Fabricate and test parts of structure
- (Pre assembly tests)

(3) Alignment

In USA:
- Participate in R&D
- Help assembly of parts
- Participate in commissioning at SSCL

In PRC:
- Fabricate parts and test
- Develop data system

(4) Slow Monitoring System

In USA:

Determine specifications for system
Participate in design
Commission system at SSCL

In PRC:

Final design of system (Gas, HV, LV, T, P monitoring)
Fabricate parts and test

Memorandum on the Mass-production of a Fraction of GEM Muon detectors at IHEP of China

10, 29,1992

Under the suggestion by GEM spokesmwn and the heads of GEM muon group well as the efforts of IHEP muon group, IHEP would like to raise the ıdertaken amount of mass-production for muon detectors to a significant ount (40-50%) of barrel part as the main contribution to GEM. This tention has been expressed in the recent letter from director of IHEP ipeng Zheng dated Oct.8 to spokesmen B.Barish and W. Willis.

In last two months Both parties(sides) have been pushing forward the llaboration in this field actively and effectively. Members of IHEP have troduced their background experiences (shown in GEM Note TN-92-178) and have en investigatig into the detector candidates for barrel part (LSDT, CSC, PDT d RPC) with respect to their characteristics, technologies, fabrication ocedures and some cost evaluations of mass production (shown in GEM Note -92-221).

In " GEM Muon R&D Program for FY-93 "drafted by muon steering committee, EP of China has been involved in the item "Task 2. develop chamber factory" d defined as one of the three leader institutions in this item,in which it anticipated that several prototype chambers with full-size will be nstructed, and the fabrication facilities will be developed and prepared. EP would like to get work started with the sub-items, i.e. prepare relevant rkshop and some of the facilities as the commitment of IHEP to FY-93 plan.

In order to realize the task mentioned in 3, the budget of FY-93 will be on broken down to institutions including IHEP of China. IHEP muon group s applied 140 k$ for the use of some preparation of workshop and facilities eparation described in the letter of IHEP group to GEM muon steering committee ted Sept.30. Once the budget being allocated, IHEP will get started 93-FY sk in time. An available amount from the budget is considered to be located to IHEP.

IHEP would like to participate in the "Task 1.develop chamber technology(s)" ncluding full-size chamber design for the necessity of mass-production.

Exchanging physicists and engineers will be improved. For this purpose an ditional physicist and several engineers could be supported by SSC in the ming year.

IHEP China

Frank E. Taylor
MIT

Xie Yigang
谢一冈

SSC/SUNY

Y. Guo 过雅南

11/5/92

10/23/92

GEM MUON SYSTEM MASTER SCHEDULE

FY 93

- PROTOTYPE CHAMBERS FOR R & D
- PRE-PRODUCTION STARTS FROM FACTORY
- INTEGRATION OF MUON SYSTEM
- ALIGNMENT

FY 94

- FABRICATION OF CHAMBERS
- PROTOTYPE OF SS, ALIGNMENT, CHAMBERS
- DEVELOP ASS'Y, INSTALLATION PROC @ SSCL

FY 95

- FABRICATION CHAMBERS, PARTS FOR SS, & TOOLING
- FULL SYSTEM CHECK
- START ASS'Y OF CHAMBERS IN SS

FY 96

- ASS'Y CHAMBERS IN SS
- CHAMBER CONSTRUCTION FINISHED

FY 97

- ASS'Y OF CHAMBERS IN SS

FY 98

- INSTALLATION OF BARREL/ENDCAP INTO GEM

FY 99

- FINAL COMMISSIONING

Agenda:

(1) Support Structure and Alignment
Frank Nimblett - Draper Lab.

(2) Cathode Strip Chambers
Vinnie Polychronakos - BNL

(3) Round Drift Tubes
Carl Bromberg - MSU

(4) Resistive Plate Counter Trigger
Irwin Pless - MIT

(5) Discussion
Frank Taylor et al.

Texas Test Rig (TTR)

Gena Mitselmakher

Rotation of layers

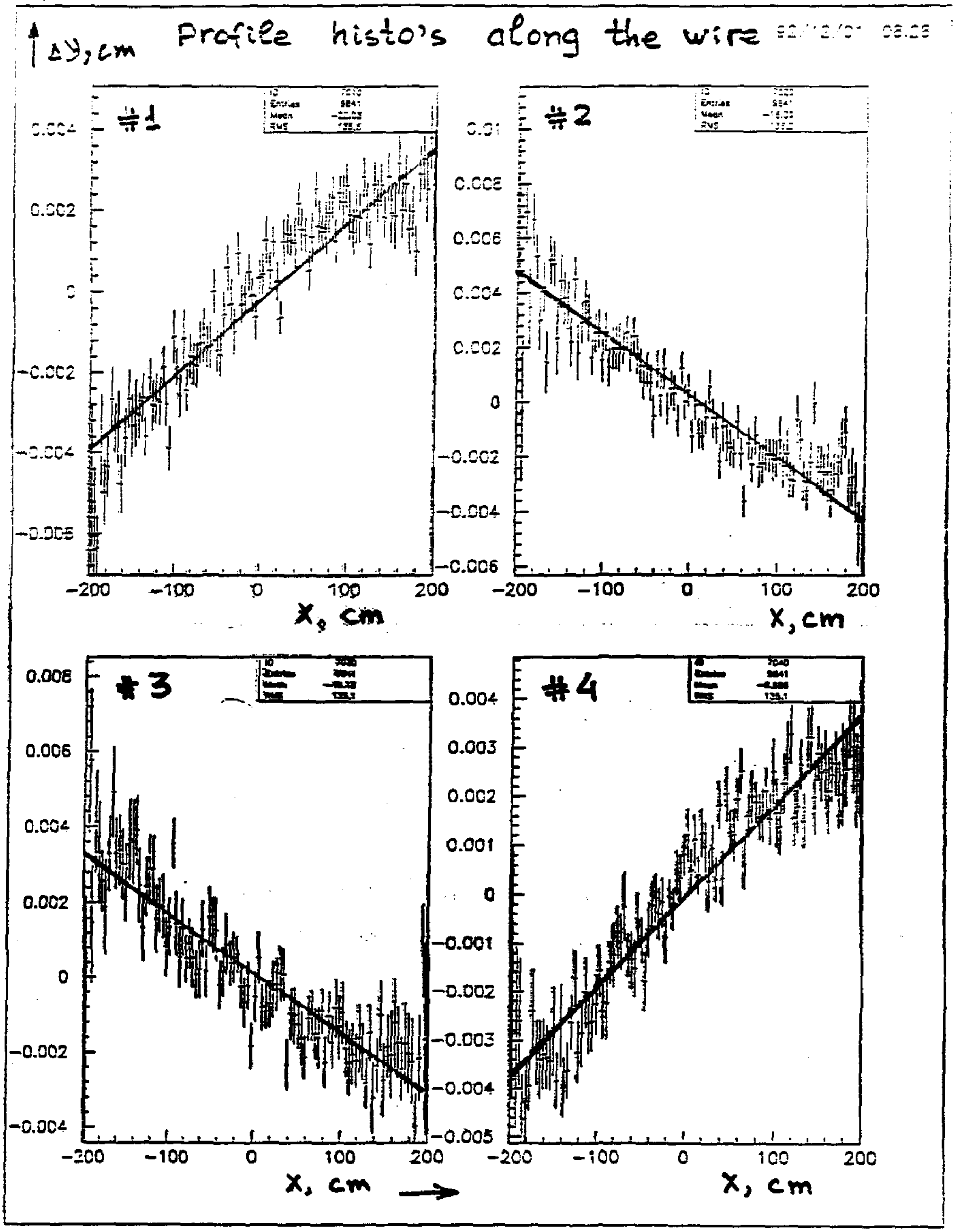

-26-

RESIDUALS vs TUBE NUMBER

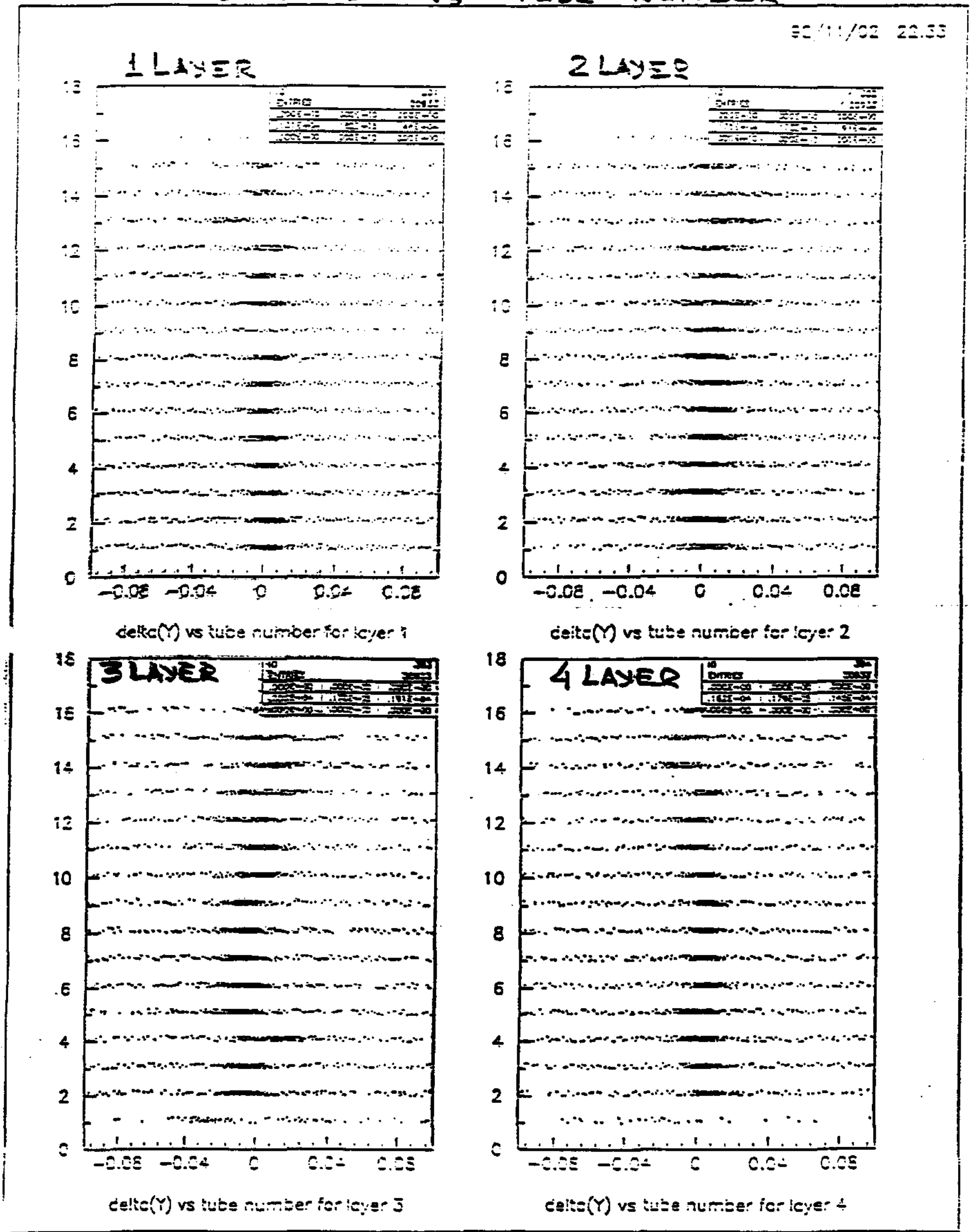

Resolution as a function of pressure

$Ar-C_2H_6$ (50/50)

(Resolution at averaged drift distances can be well approximated by $\sqrt{P}$)

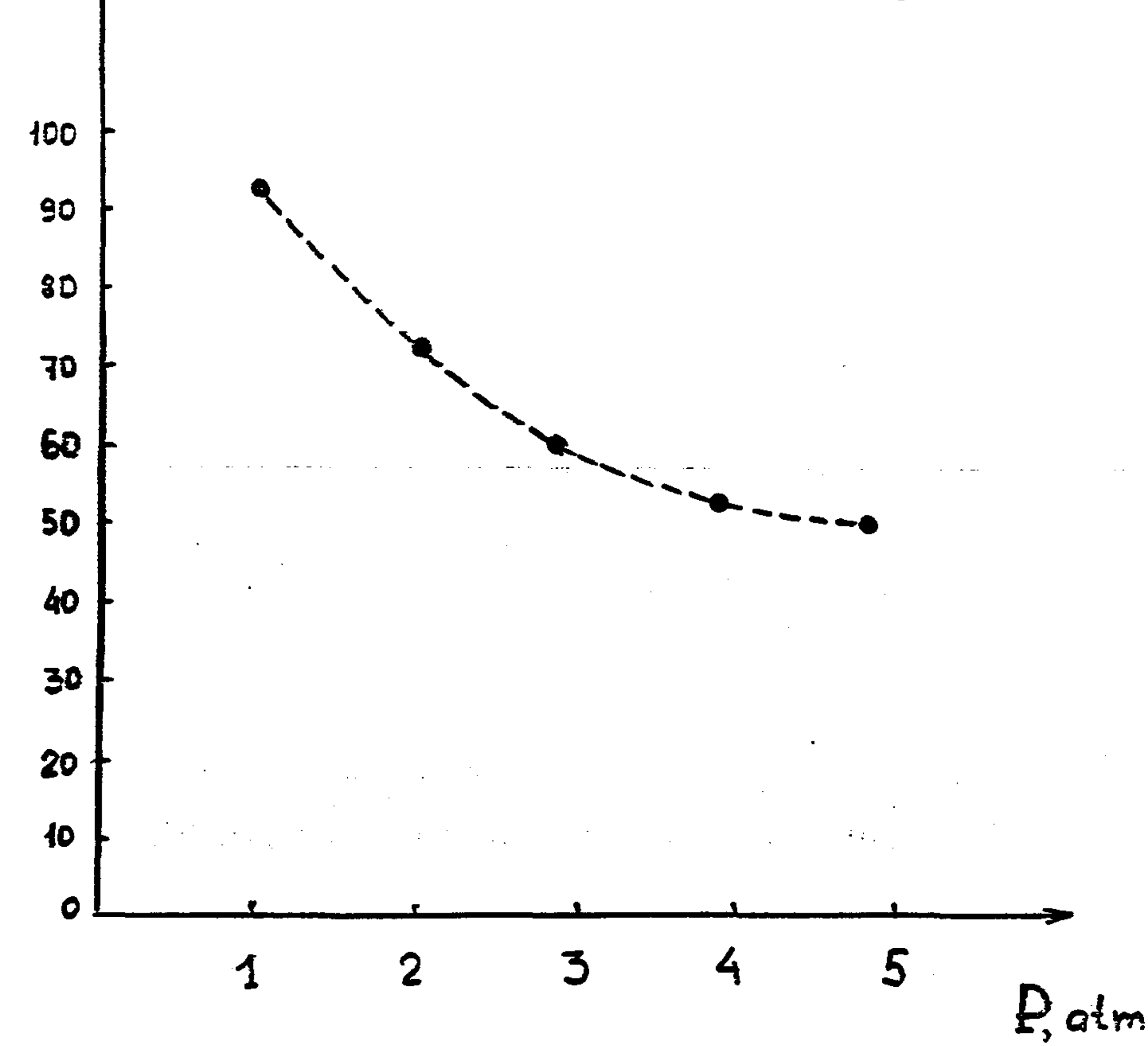

$Ar-C_4H_{10}$ (25/75) at 1 atm

$\langle\sigma\rangle_{layer} = 67\mu$! Unfortunately flammable gas

RESIDUALS FROM THE TRACK

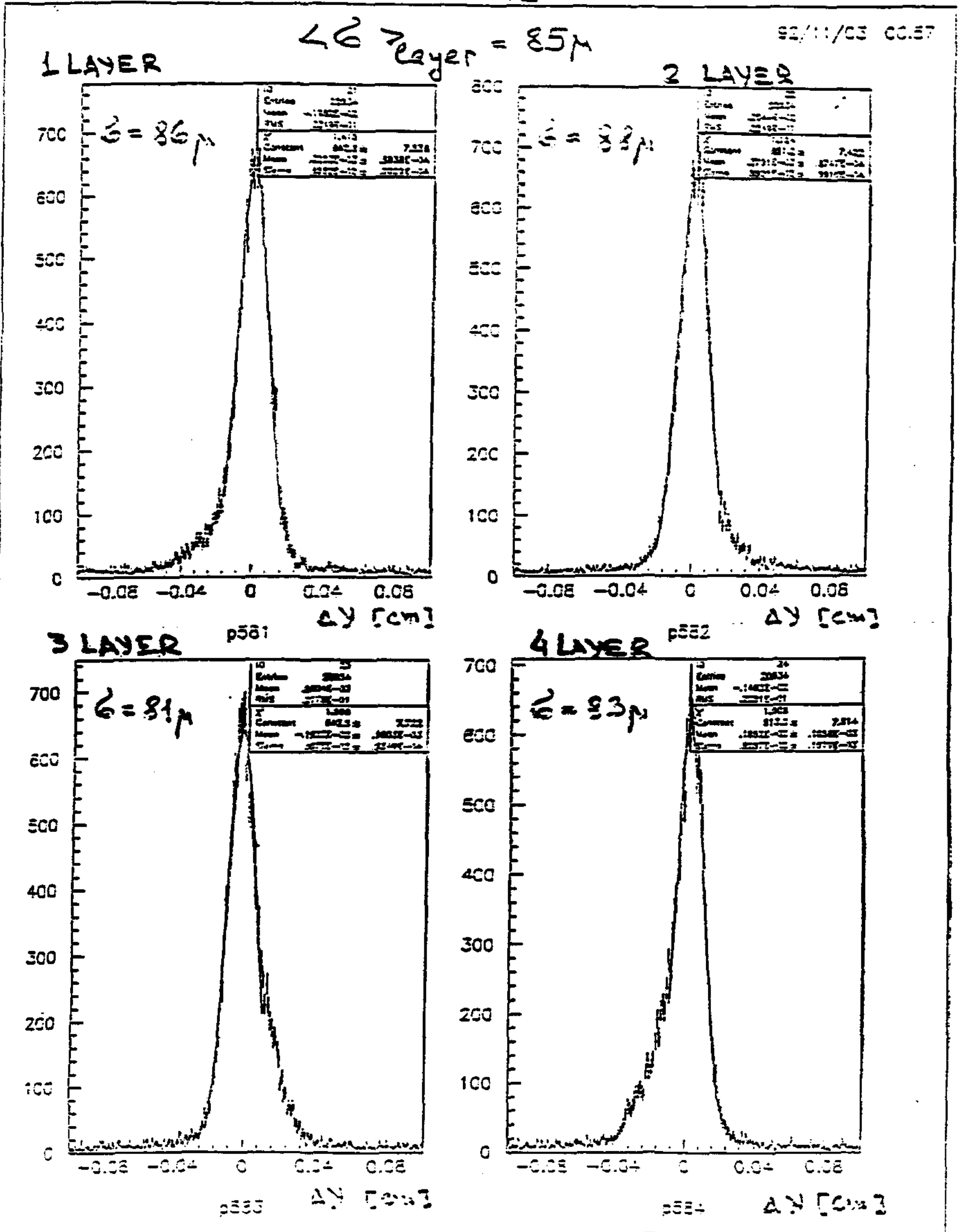

$Ar-C_2H_6$ (50/50) at 4.8 atm

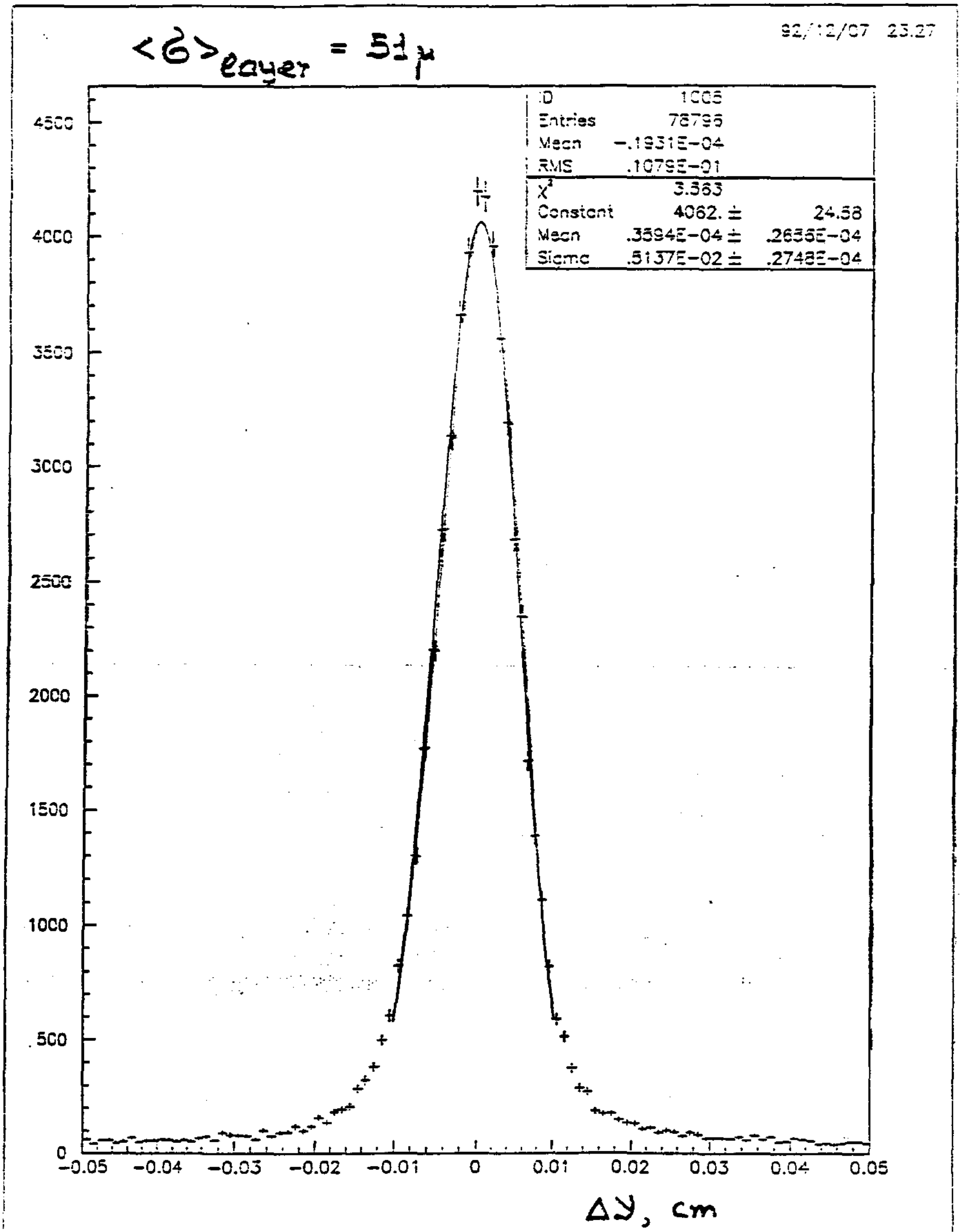

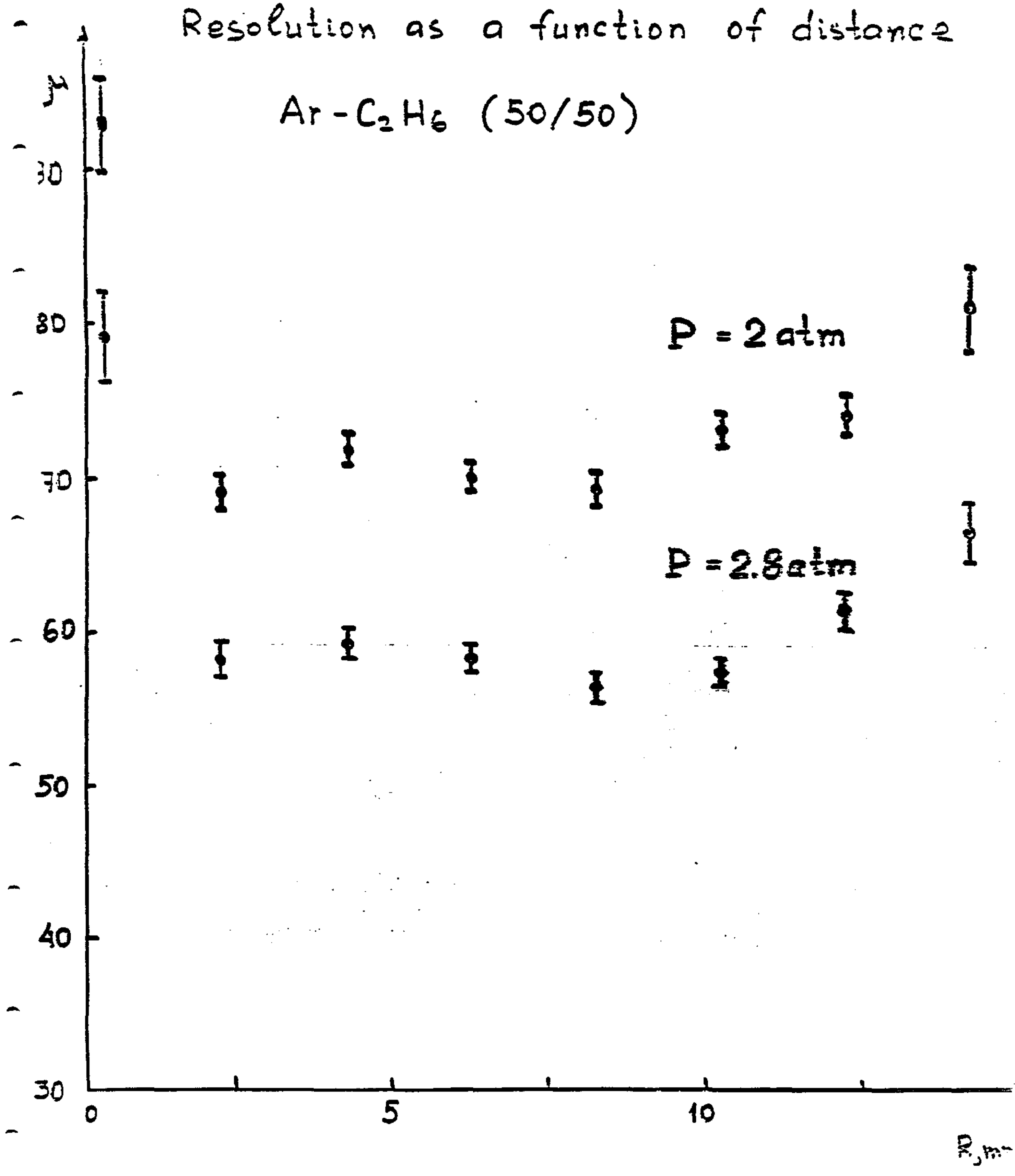
Resolution as a function of distance
Ar - C2H6 (50/50)
μ
P = 2 atm
P = 2.8 atm
30
40
50
60
70
80
0
5
10
R, m

DUBNA CSC PROTOTYPE

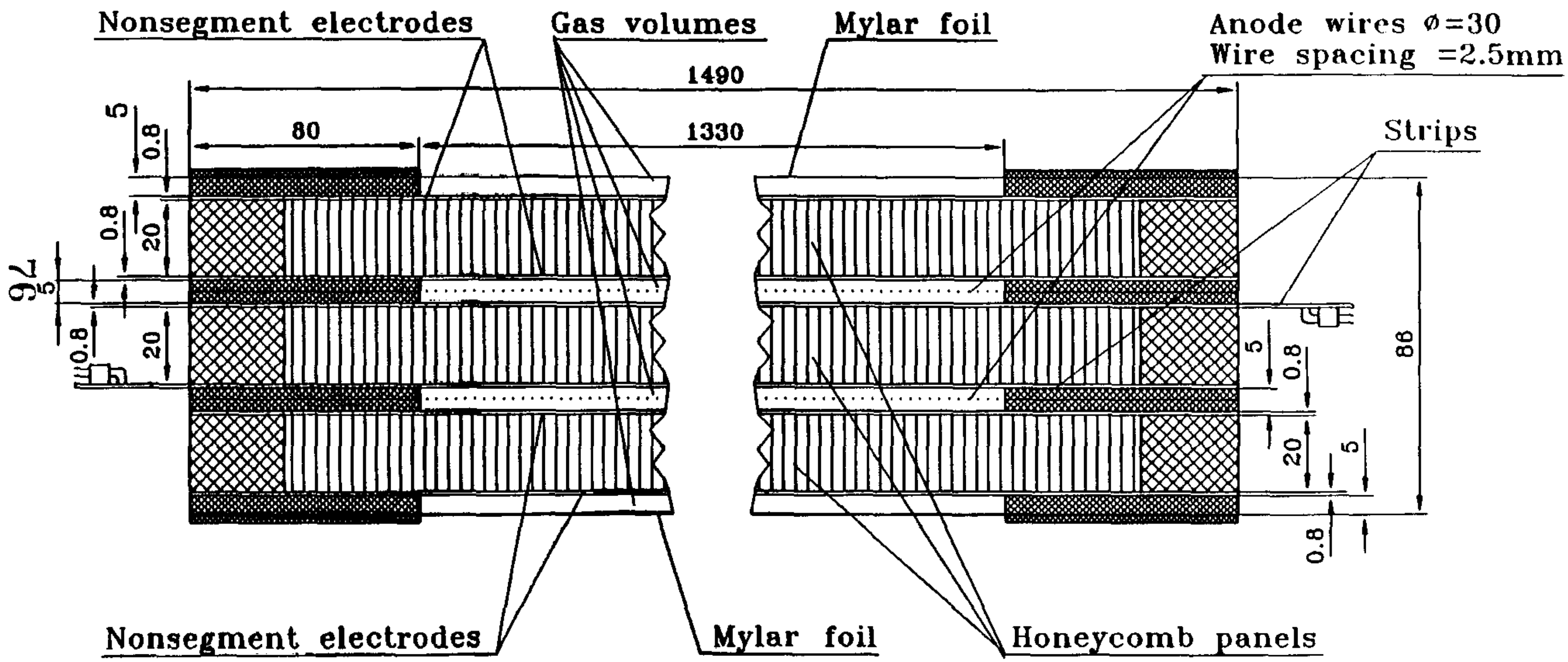

Cross–section of MWPC perpendicular to the wires

(All dimensions in mm)

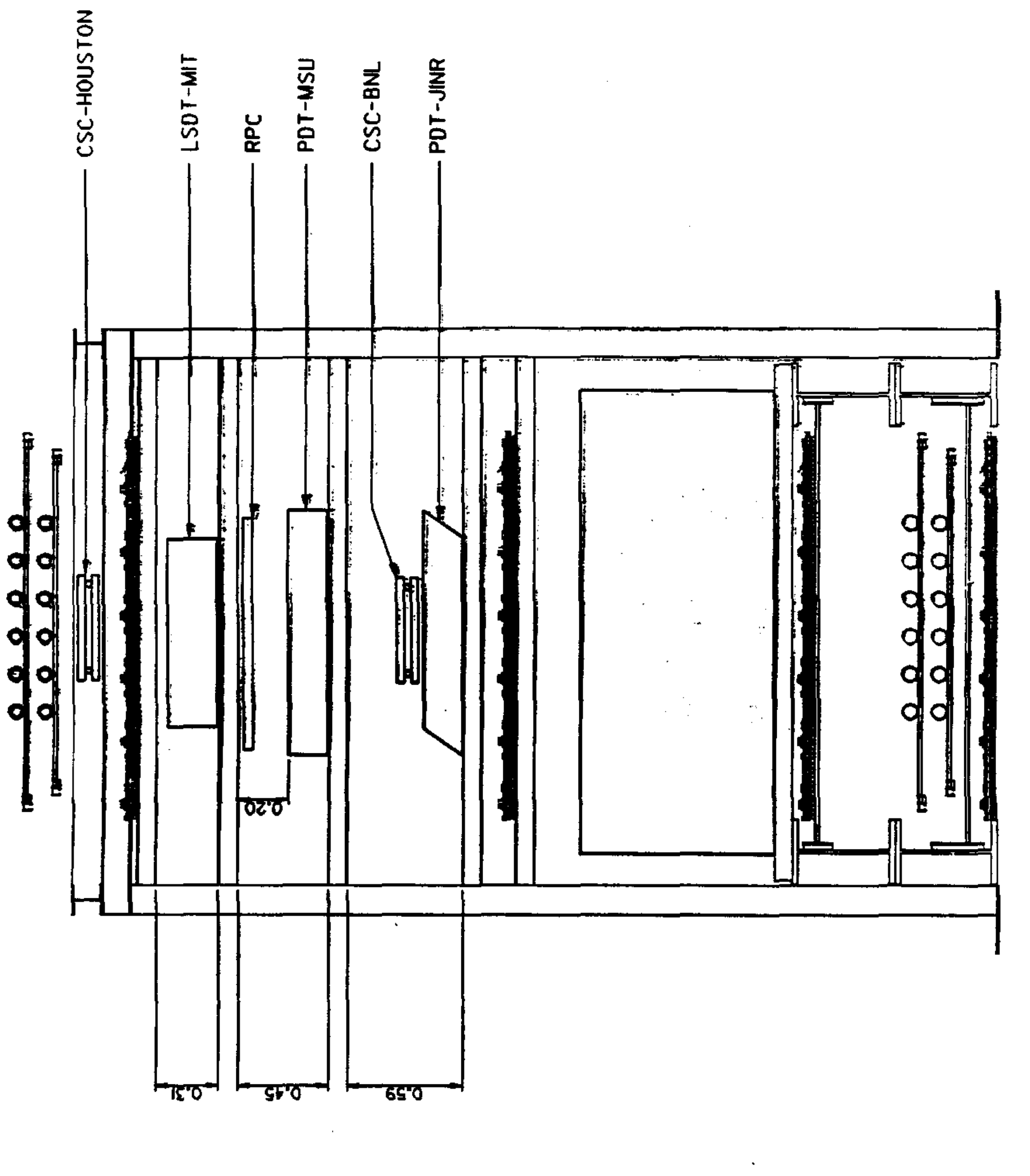

INSTALLATION IN TTR - EAST FACE

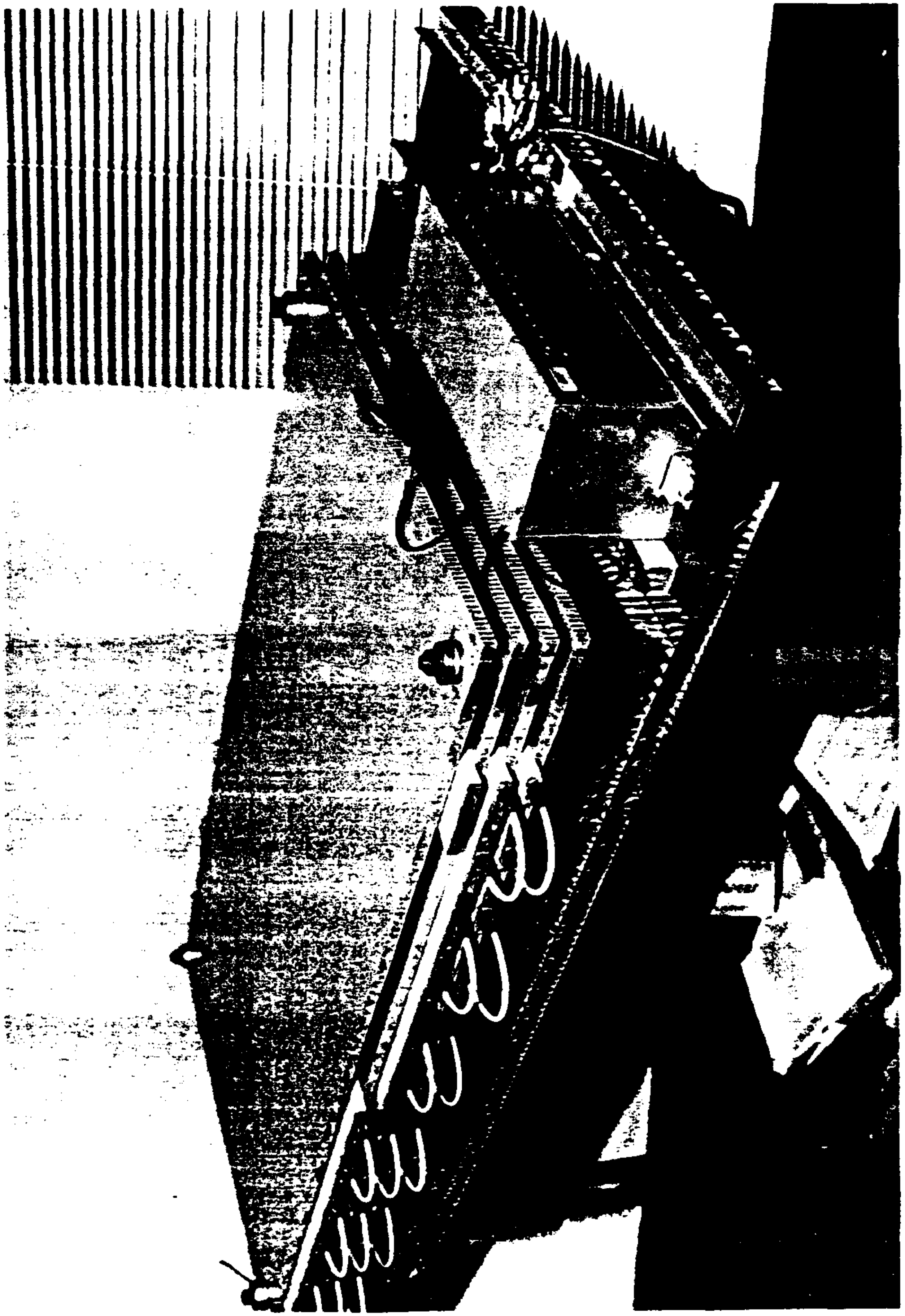

Run#: 666 Events on File: 45442 groups on file: 2
Event#: 4200 Fri, Oct 23, 1992 17:45

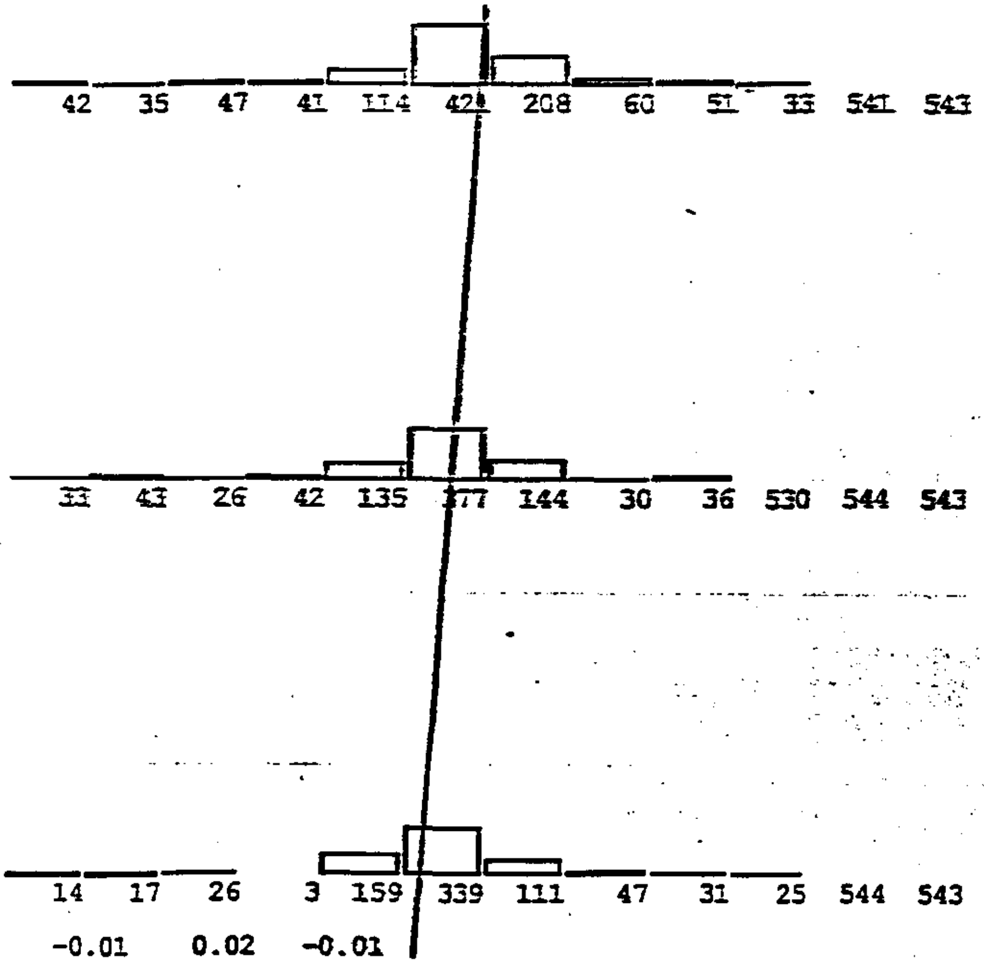

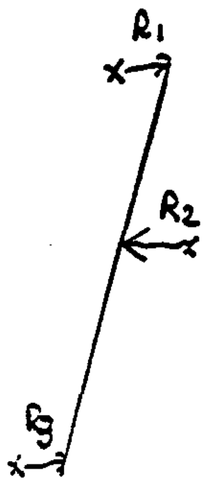

$R_1 = R_3 = -\frac{1}{2}R_2$

$\sigma = \sqrt{6}\, R_1$

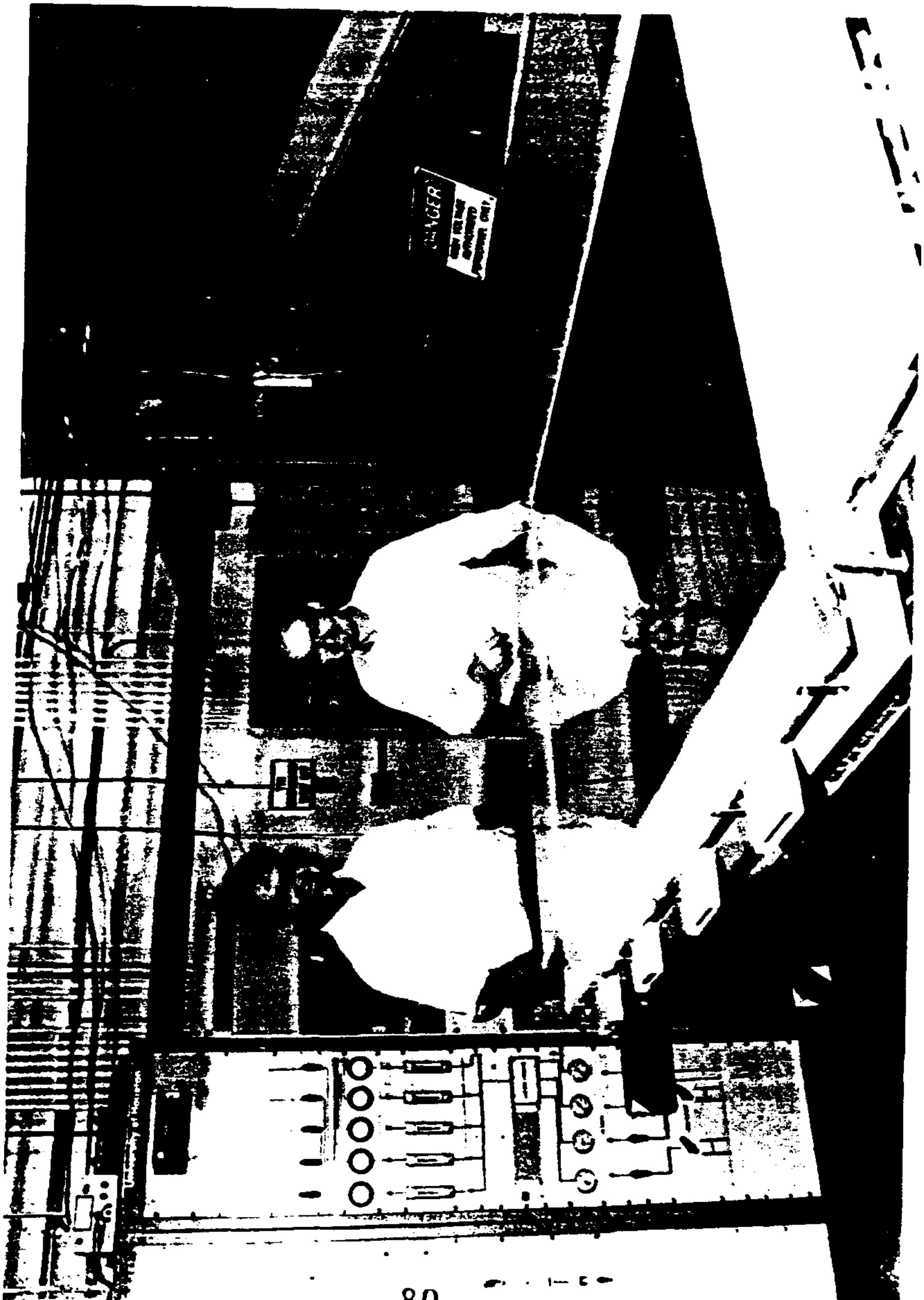
DANGER

BNL-CSC

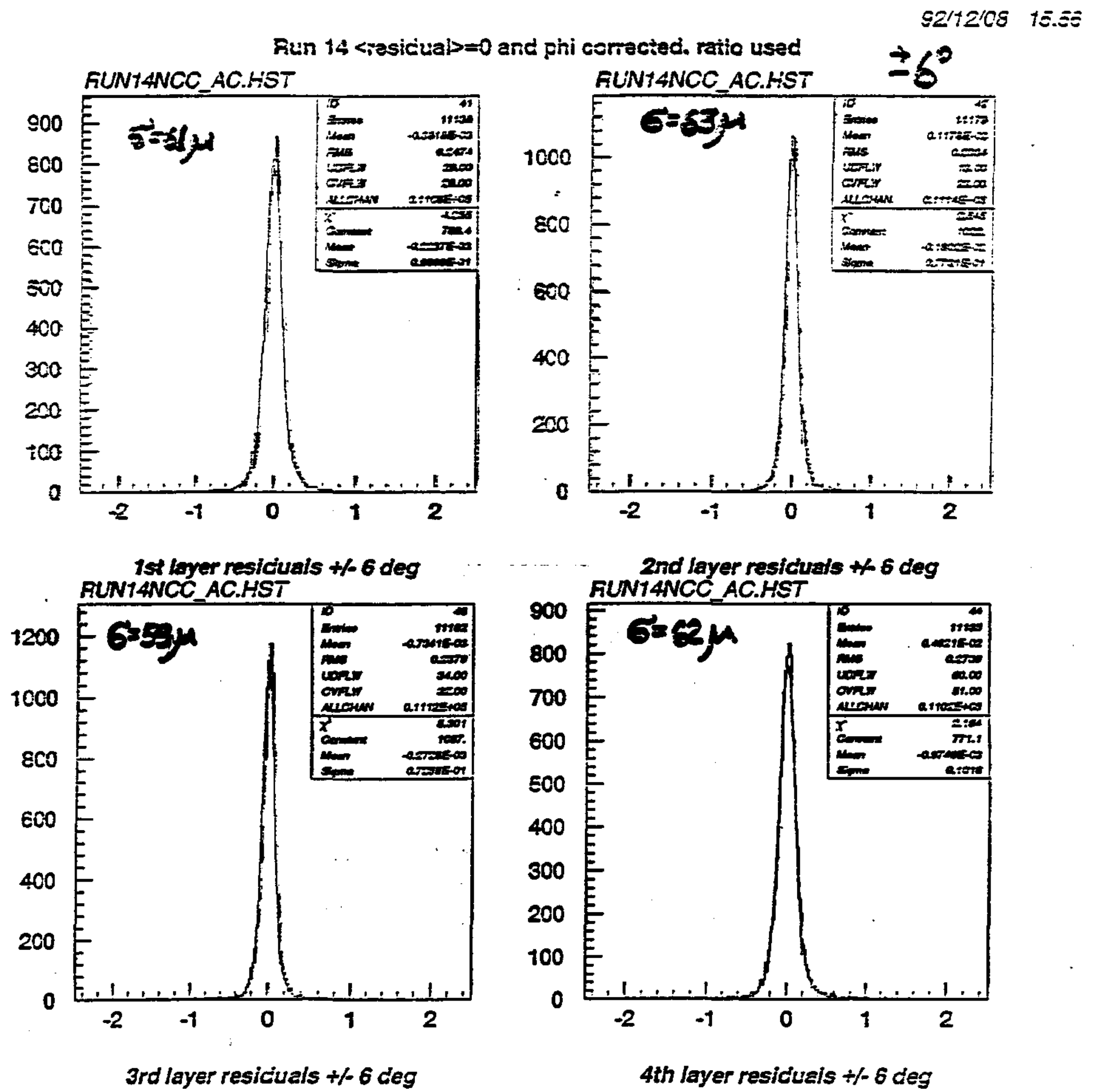

92/12/08 15:55
Run 14 <residual>=0 and phi corrected. ratio used
±6°
RUN14NCC_AC.HST
RUN14NCC_AC.HST
RUN14NCC_AC.HST
RUN14NCC_AC.HST
σ=61μ
σ=63μ
σ=58μ
σ=62μ
1st layer residuals +/- 6 deg
2nd layer residuals +/- 6 deg
3rd layer residuals +/- 6 deg
4th layer residuals +/- 6 deg

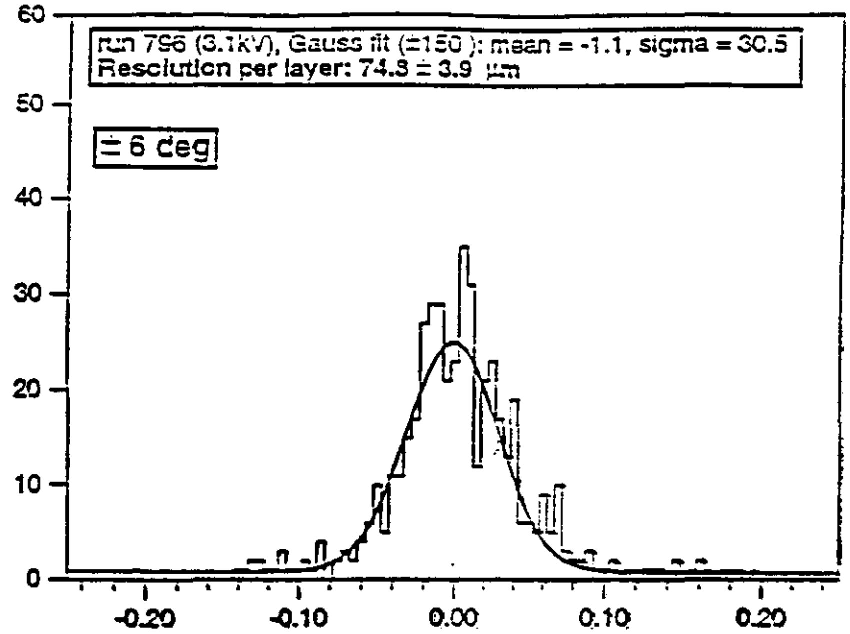
run 796 (3.1kV), Gauss fit (±150): mean = -1.1, sigma = 30.5
Resolution per layer: 74.8 ± 3.9 µm
± 6 deg
60
50
40
30
20
10
0
-0.20
-0.10
0.00
0.10
0.20

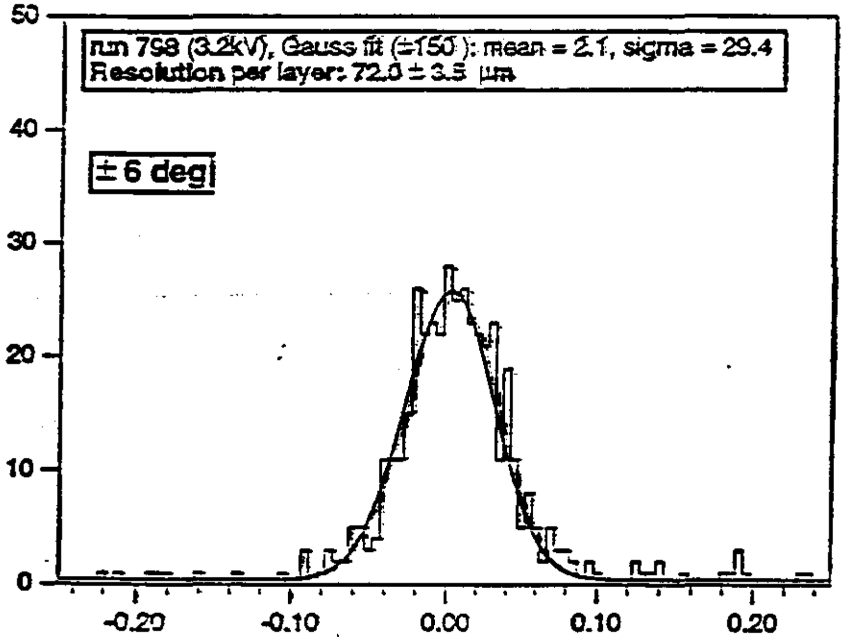
run 798 (3.2kV), Gauss fit (±150): mean = 2.1, sigma = 29.4
Resolution per layer: 72.0 ± 3.5 µm
± 6 deg
50
40
30
20
10
0
-0.20
-0.10
0.00
0.10
0.20

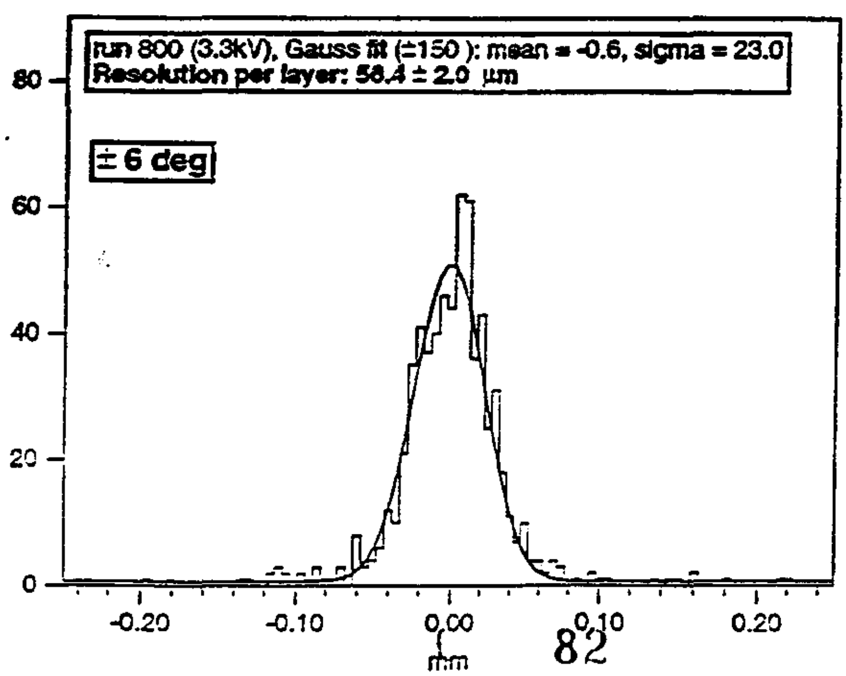
run 800 (3.3kV), Gauss fit (±150): mean = -0.6, sigma = 23.0
Resolution per layer: 56.4 ± 2.0 µm
± 6 deg
80
60
40
20
0
-0.20
-0.10
0.00
0.10
0.20
mm

GEM Project

Gary Sanders

GEM Collaboration

- **Collaborators** **710**

  U.S. **340**
  Non-U.S. **370**

- **Institutions** **93**

  U.S. **49**
  Non-U.S. **44**

- **Countries** **15**

Belarus, Brazil, China, Ecuador, Georgia, Germany, India, Israel, Japan, Korea, Mexico, Romania, Russia, Taiwan, U.S.A.

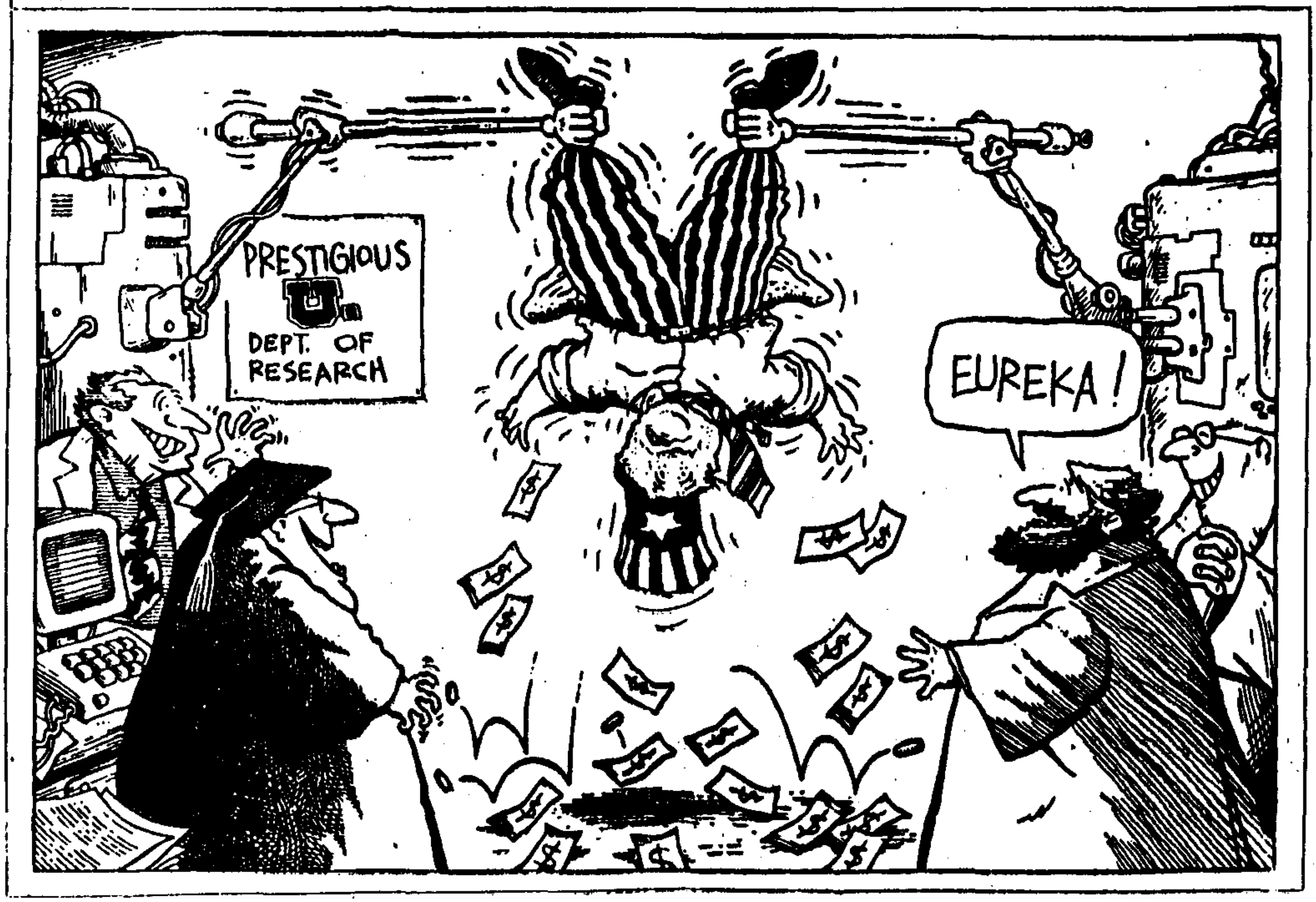

Tony Auth
The Philadelphia Inquirer
Universal Press Syndicate

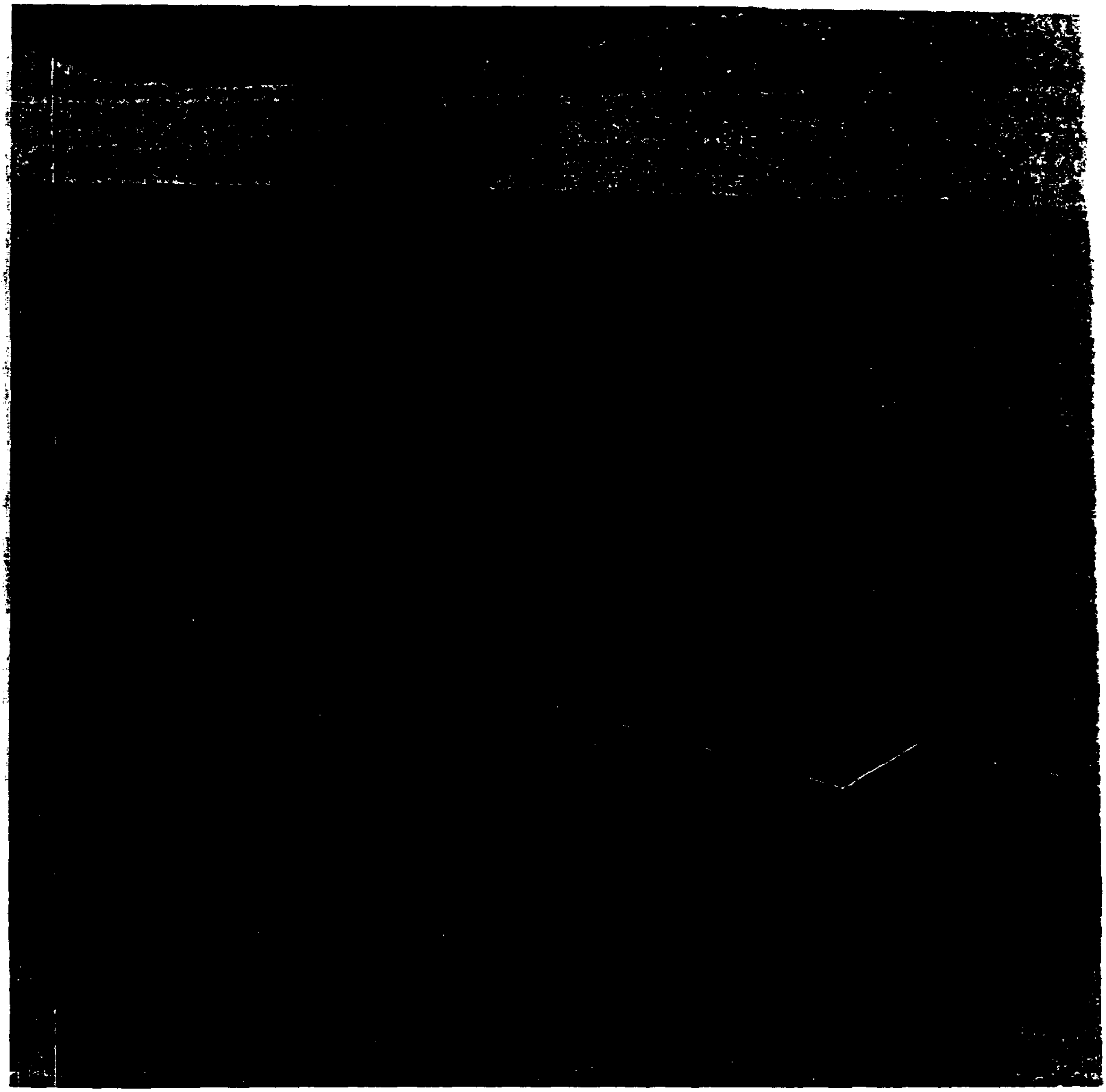

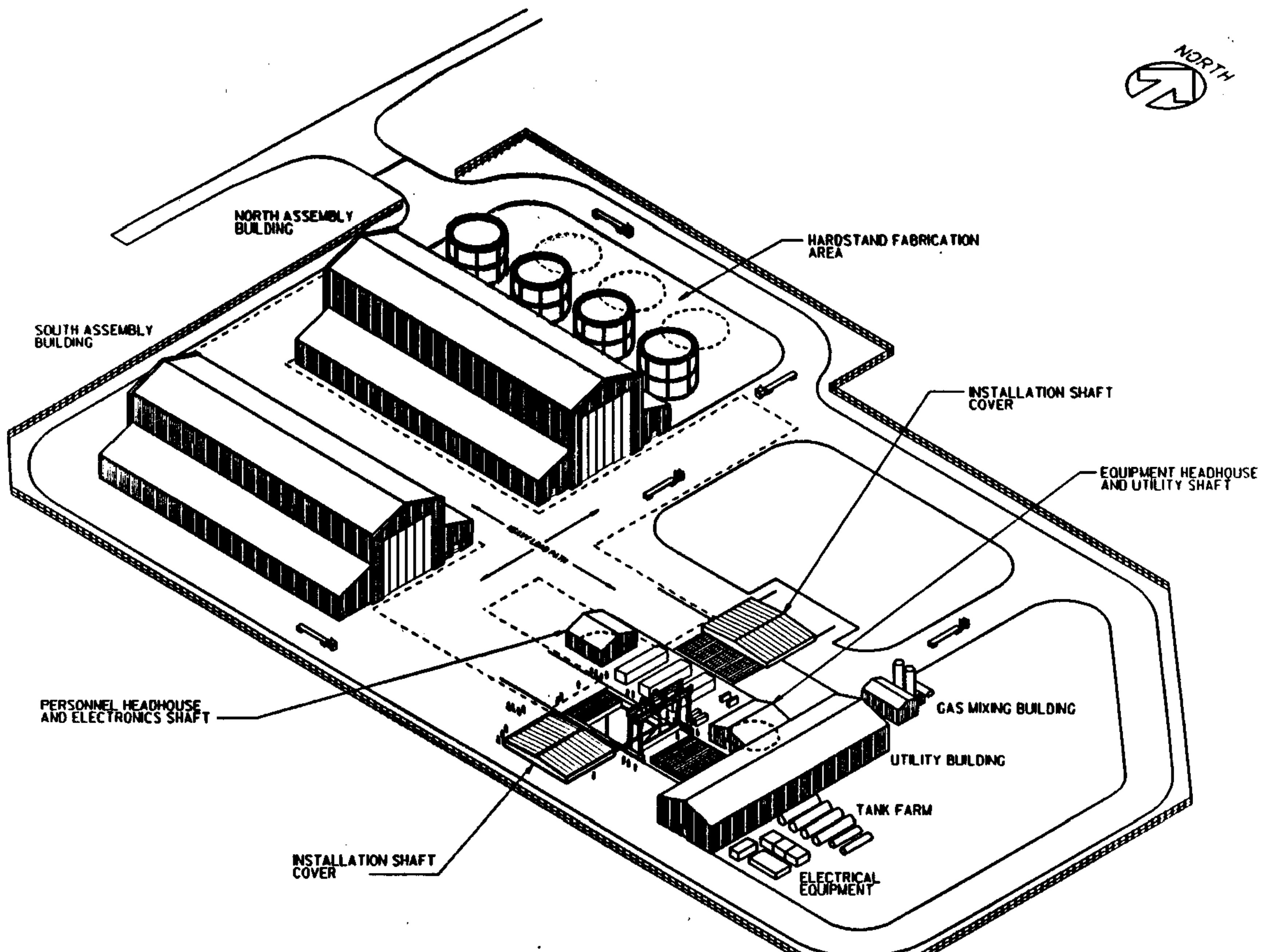

IR-5 SITE

TVP/kh - 17 AUG 1992 - GCD-000157.003

GEM Milestones

July 1991	Expression of Interest
Nov 1991	Letter of Intent
Dec 1991	Approval to Proceed to Technical Design Report
Apr 1992	GEM Detector Baseline I Established
Jul 1992	Program Advisory Committee Review of GEM and GEM Magnet
Dec 1992	GEM Magnet Contract Offered
May 1993	Technical Design Report Review Period

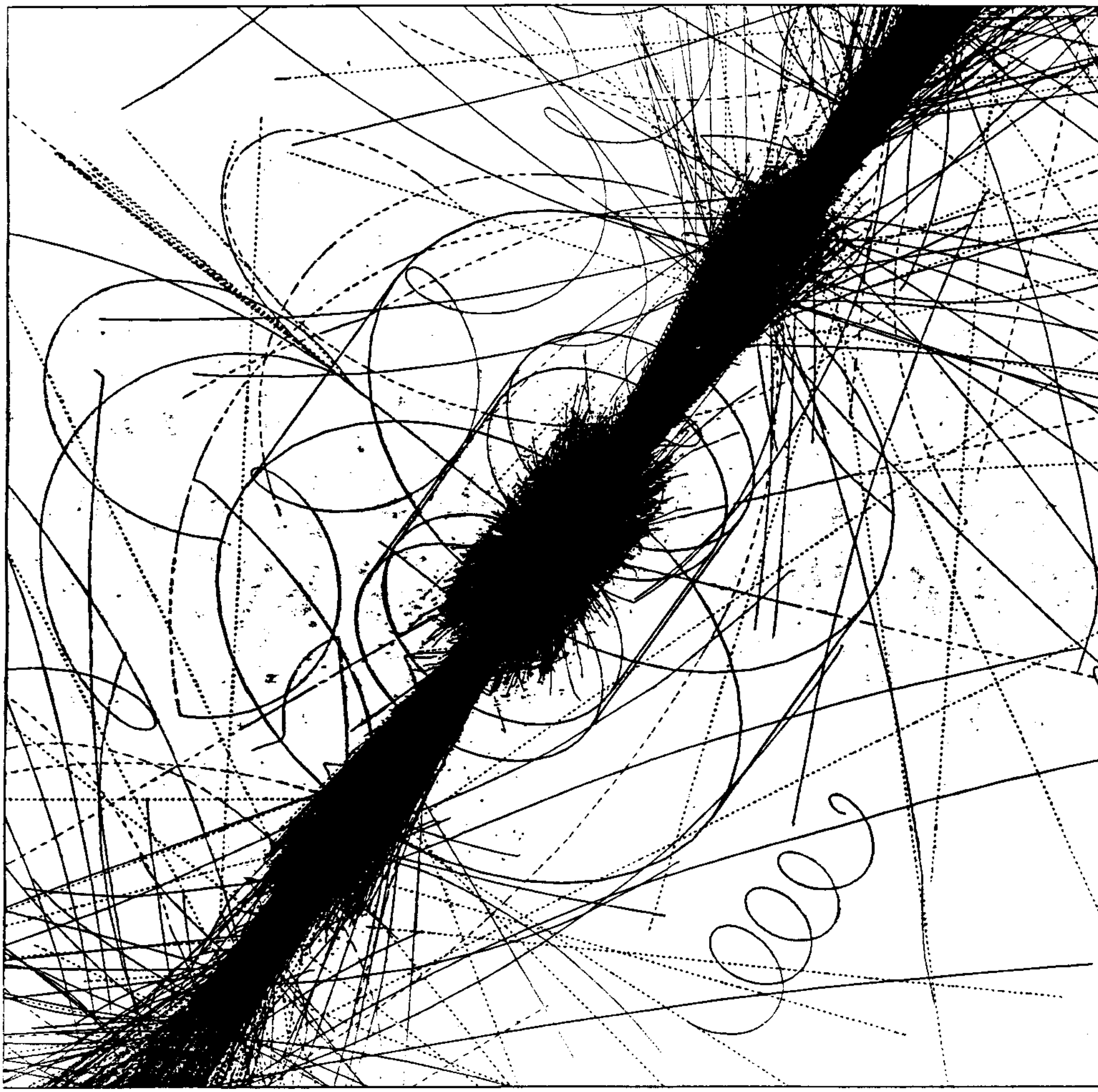

EMPHASIS IN GEM

- Very precise measurement of muon momenta using only the outer muon spectrometer in an open magnetic volume
- Very precise measurement of electron and photon energies using a precision electromagnetic calorimeter with no coil in front of the calorimeter
- Hermetic calorimetry and good jet resolution
- Central tracker emphasis on ensuring clean measurement of physics signals without requiring full pattern recognition
- High luminosity

Liquid Argon Calorimeter

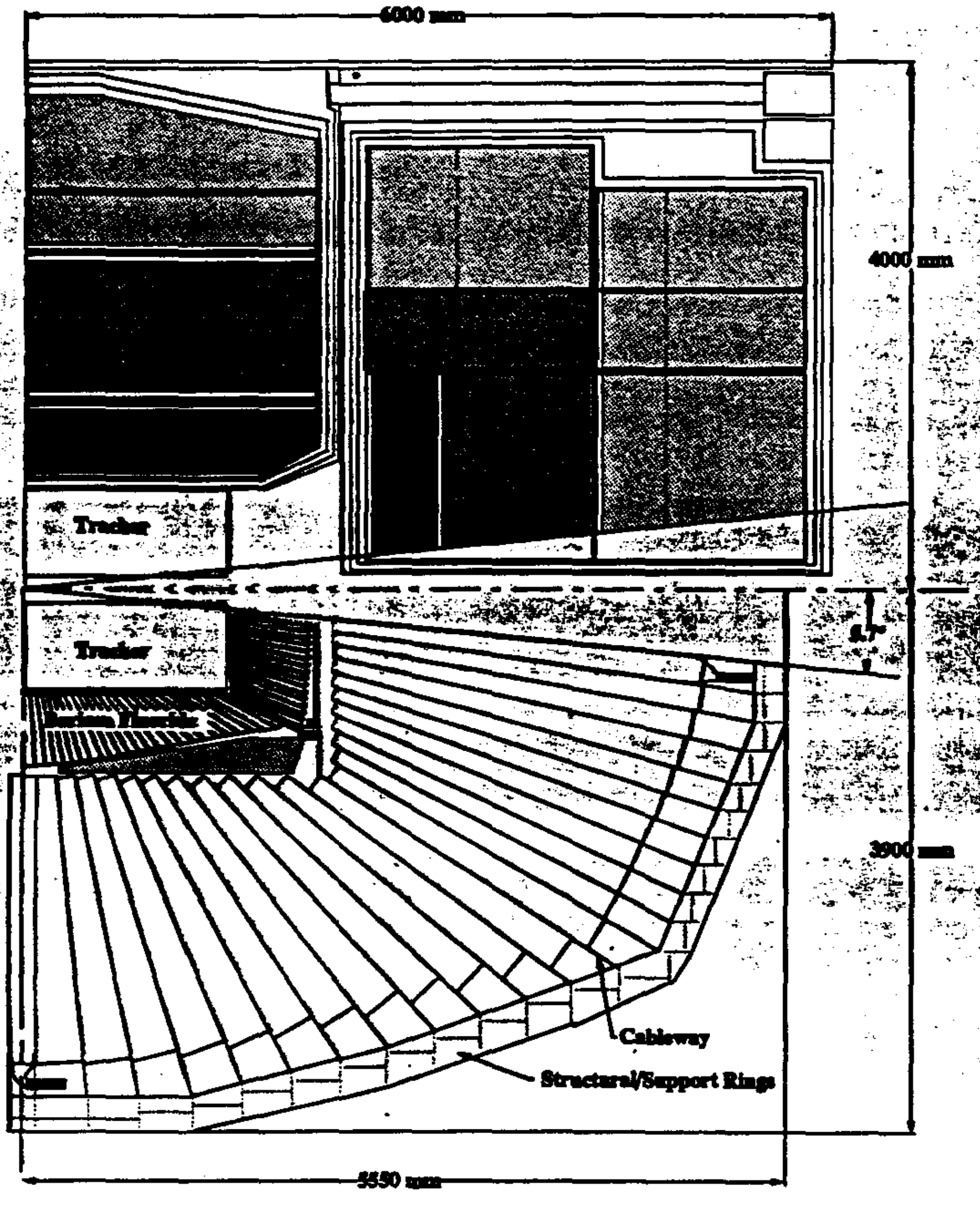

BaF2 EM with Scintillating Fiber Hadron Calorimeter

GEM Calorimeter

	Weight	Volume
Barrel Calorimeter	= 433 Mg	24135 L. LKr
2 Endcap Total	= 759 Mg	38475 L. LAr
Scint. Cal. & St. St.	= 1228 Mg	
2 Endcap PA Total	= 196 Mg	
2 FWH Total	= 30 Mg	
	2646 Mg	

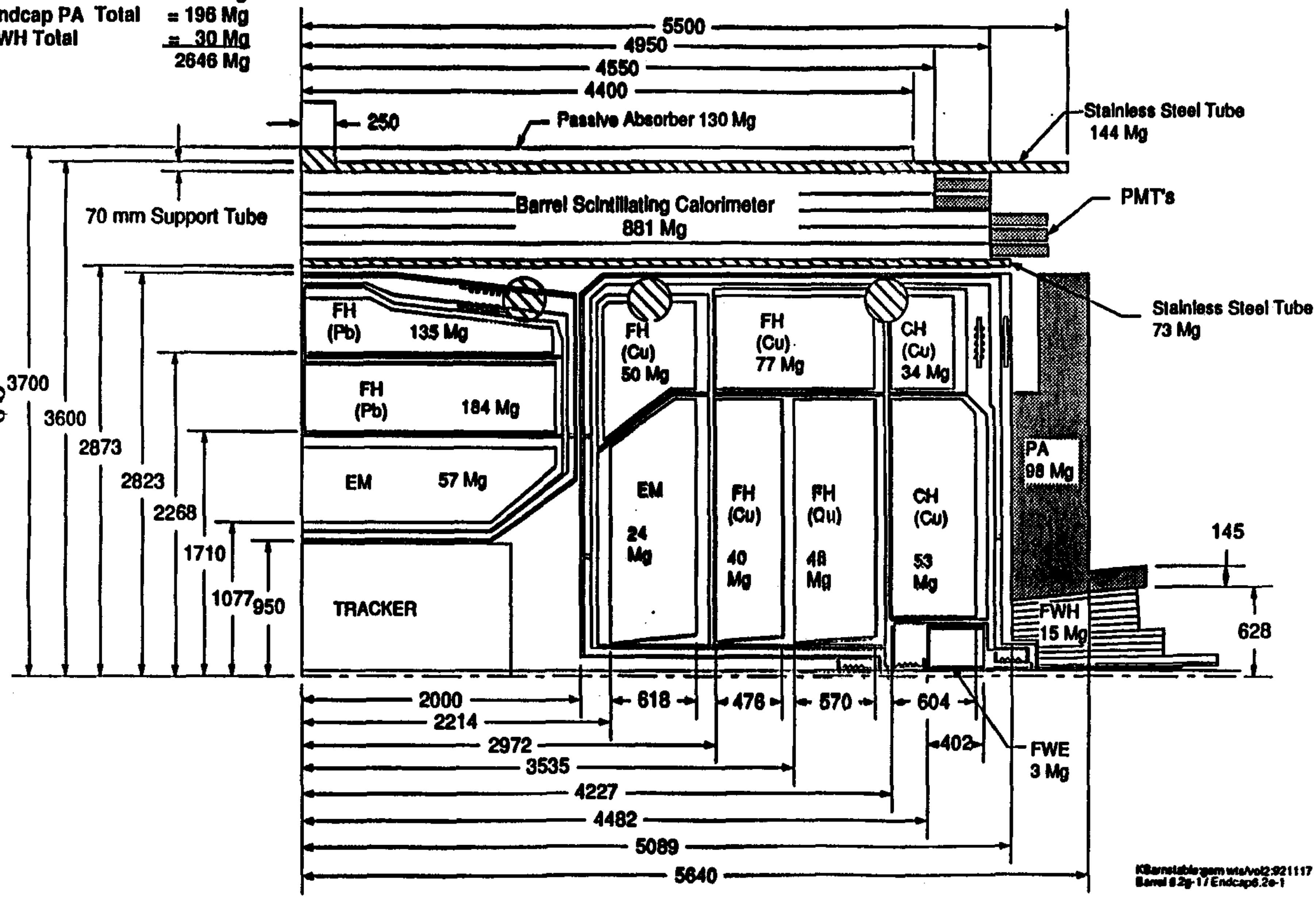

Tracker

Kate Morgan

GEM Central Tracker

Kate Morgan
SSCL

January 18, 1993

The Central Tracking Group

Academia Sinica, Taiwan, R.O.C.
A. Antos, Y.C. Chen, T.L. Chu, M. Huang, S.C. Lee, A. Sumarokov, P.K. Teng, M.J. Wang, P. Yeh

Brookhaven
P.O'Connor, V. Radeka, G. Smith, B. Yu

Indiana University
C. Bower, M. Gebhard, R. Heinz, S. Mufson, J. Musser, J. Pitts

Los Alamos
R. Barber, J.G. Boissevain, M. Brooks, D. Brown, M. Cafferty, B. Cooke, K. Fuller,, S.F. Hahn, C. Johnson, J. Kapustinsky, W.W. Kinnison, D.M. Lee, G.B. Mills, D. Neeper, R. Prael, G.H. Sanders, W.E. Sondheim, T. Thompson, J. VanAnne, L. Waters, B. Weinstein,

Moscow State University
G. Bashindzhagyan, Y. Fisyak, D. Karmanov, E. Kuznetsov, A. Larichev, M. Merkin, A. Savin, A. Voronin, V. Zhukov

Nanjing University
E. Chen, D. Gao, M. Qi, D.X. Xie, N.G. Yao, Z.W. Zhang

Rutgers University
P. Jacques, M. Kalelkar, R.J. Plano, P. Stamer, G.B. Word

SSCL
K. Morgan, I. Sheer, J. Thomas

University of Albany
M.S. Alam, I.J. Kim, B. Neman, J. O'Neill, H. Severini, C.R. Sun, L. Zhichao

University of Michigan
D Kouba, D. Levin, S. McKee, G. Tarle

University of Oregon
A. Arodzero, J. Brau, R. Frey, K. Furuno, D. Strom

Yale University
C. Baltay, R. Ben-David, D. Dong, W. Emmet, S. Manly, S. Sen, John Sinnott, J. Turk, E. Wolin

Central Tracker Steering Committee

C. Baltay, J. Brau, D. Lee, K. Morgan, J. Musser

Chairman: C. Baltay

GEM Central Tracker Performance Goals

Primary Goals:

- Primary vertex determination
- Separate e's from γ's
- Track information for e, μ or γ isolation cuts
- e/π separation by comparing p and energy
- background rejection by matching p in tracker with p in muons
- Electron sign up to 400 GeV/c.

Secondary Goals:

- Full reconstruction of the charged tracks
- Secondary vertex finding
- Tracking at low momenta with good resolution

KM

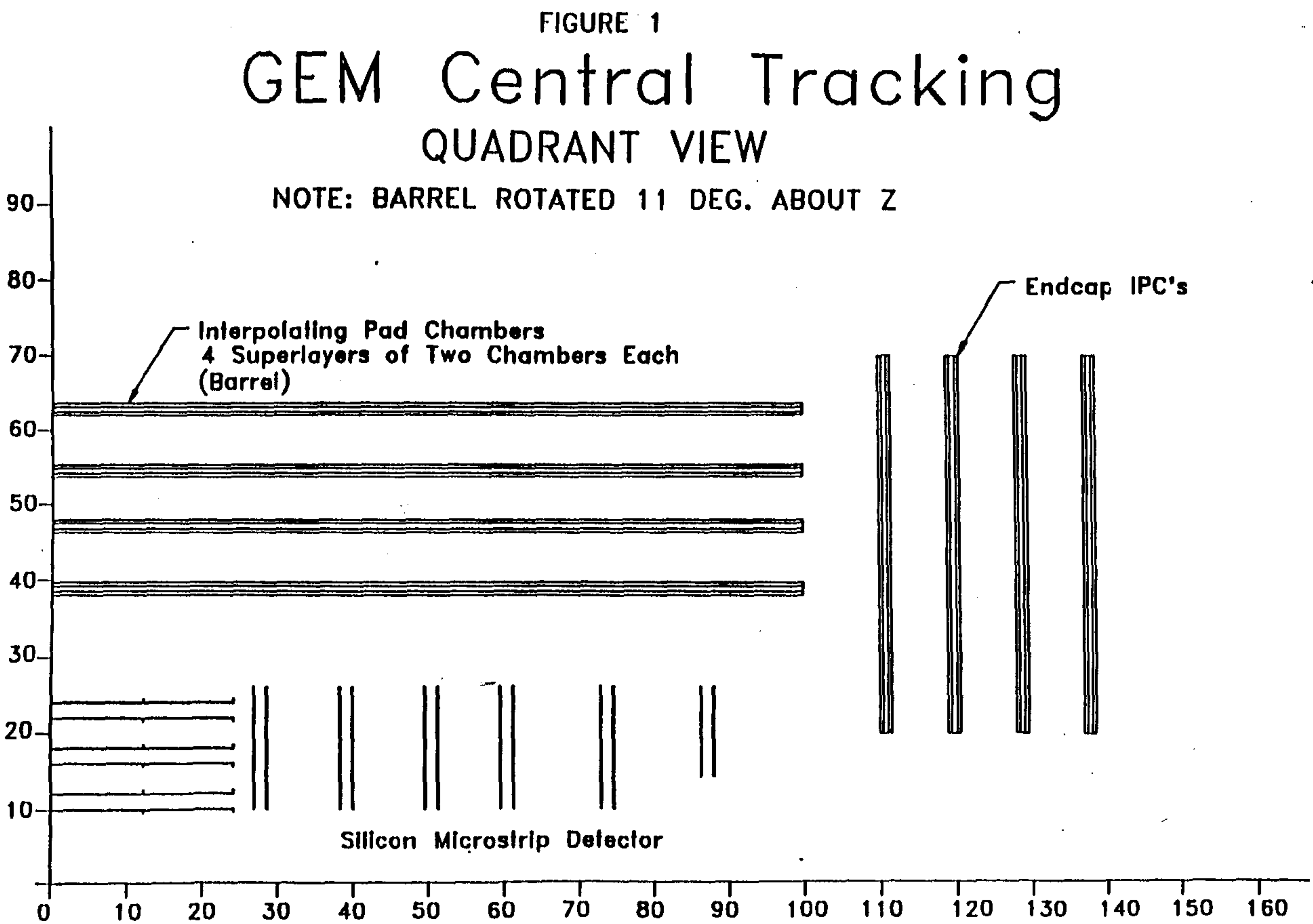
FIGURE 1
GEM Central Tracking
QUADRANT VIEW
NOTE: BARREL ROTATED 11 DEG. ABOUT Z
Interpolating Pad Chambers
4 Superlayers of Two Chambers Each
(Barrel)
Endcap IPC's
Silicon Microstrip Detector
90
80
70
60
50
40
30
20
10
0
10
20
30
40
50
60
70
80
90
100
110
120
130
140
150
160

Figure 1.1a

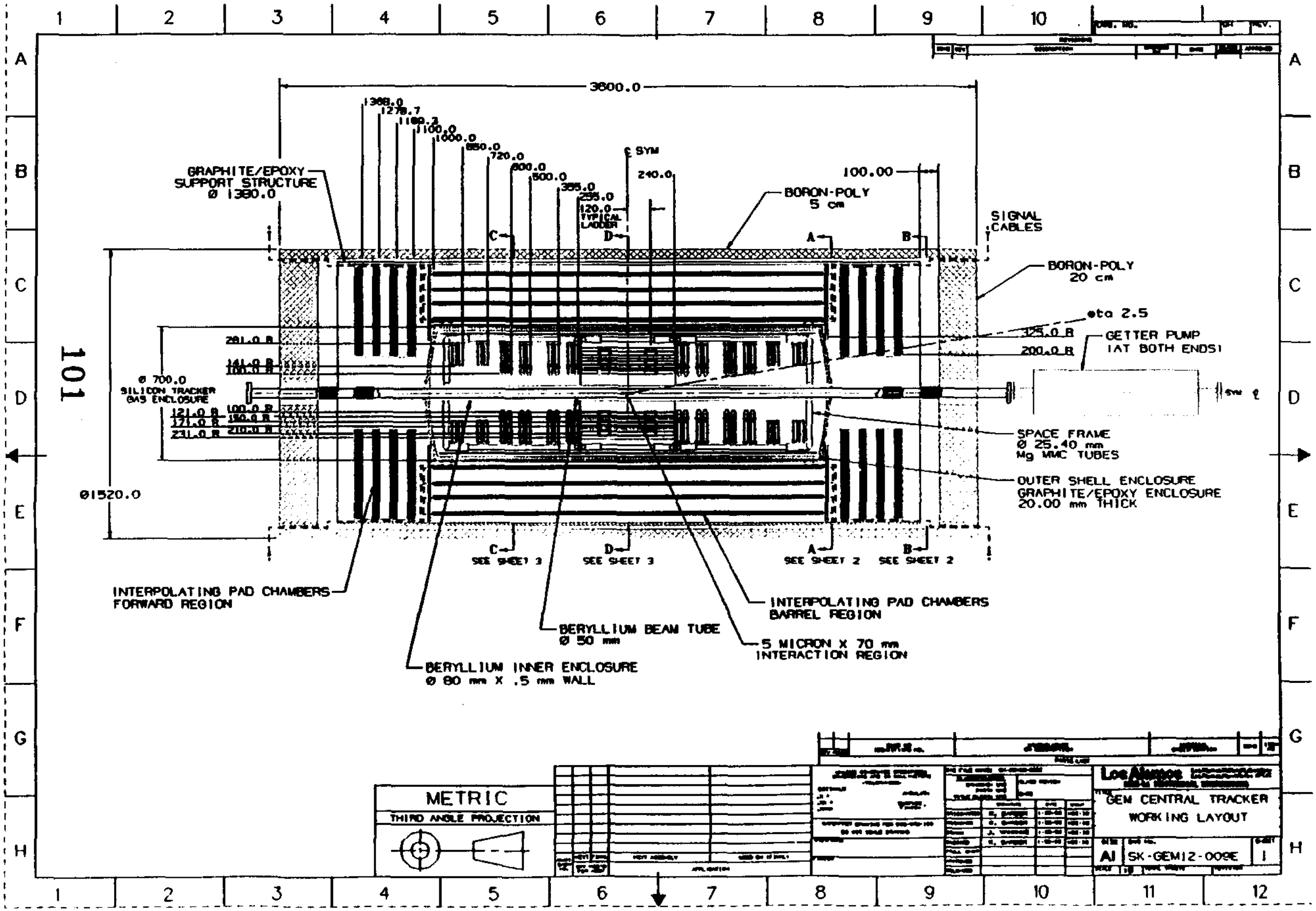

3800.0
1308.0
1278.7
1189.3
1100.0
1000.0
850.0
720.0
600.0
500.0
355.0
255.0
120.0 TYPICAL LADDER
240.0
℄ SYM
100.00
GRAPHITE/EPOXY SUPPORT STRUCTURE Ø 1380.0
BORON-POLY 5 cm
SIGNAL CABLES
BORON-POLY 20 cm
eta 2.5
125.0 R
200.0 R
GETTER PUMP (AT BOTH ENDS)
281.0 R
141.0 R
100.0 R
Ø 700.0 SILICON TRACKER GAS ENCLOSURE
100.0 R
121.0 R
171.0 R
150.0 R
231.0 R
210.0 R
Ø1520.0
SPACE FRAME Ø 25.40 mm Mg MMC TUBES
OUTER SHELL ENCLOSURE GRAPHITE/EPOXY ENCLOSURE 20.00 mm THICK
C SEE SHEET 3
D SEE SHEET 3
A SEE SHEET 2
B SEE SHEET 2
INTERPOLATING PAD CHAMBERS FORWARD REGION
INTERPOLATING PAD CHAMBERS BARREL REGION
BERYLLIUM BEAM TUBE Ø 50 mm
5 MICRON X 70 mm INTERACTION REGION
BERYLLIUM INNER ENCLOSURE Ø 80 mm X .5 mm WALL
METRIC
THIRD ANGLE PROJECTION
Los Alamos
GEM CENTRAL TRACKER WORKING LAYOUT
A1
SK-GEM12-009E
1

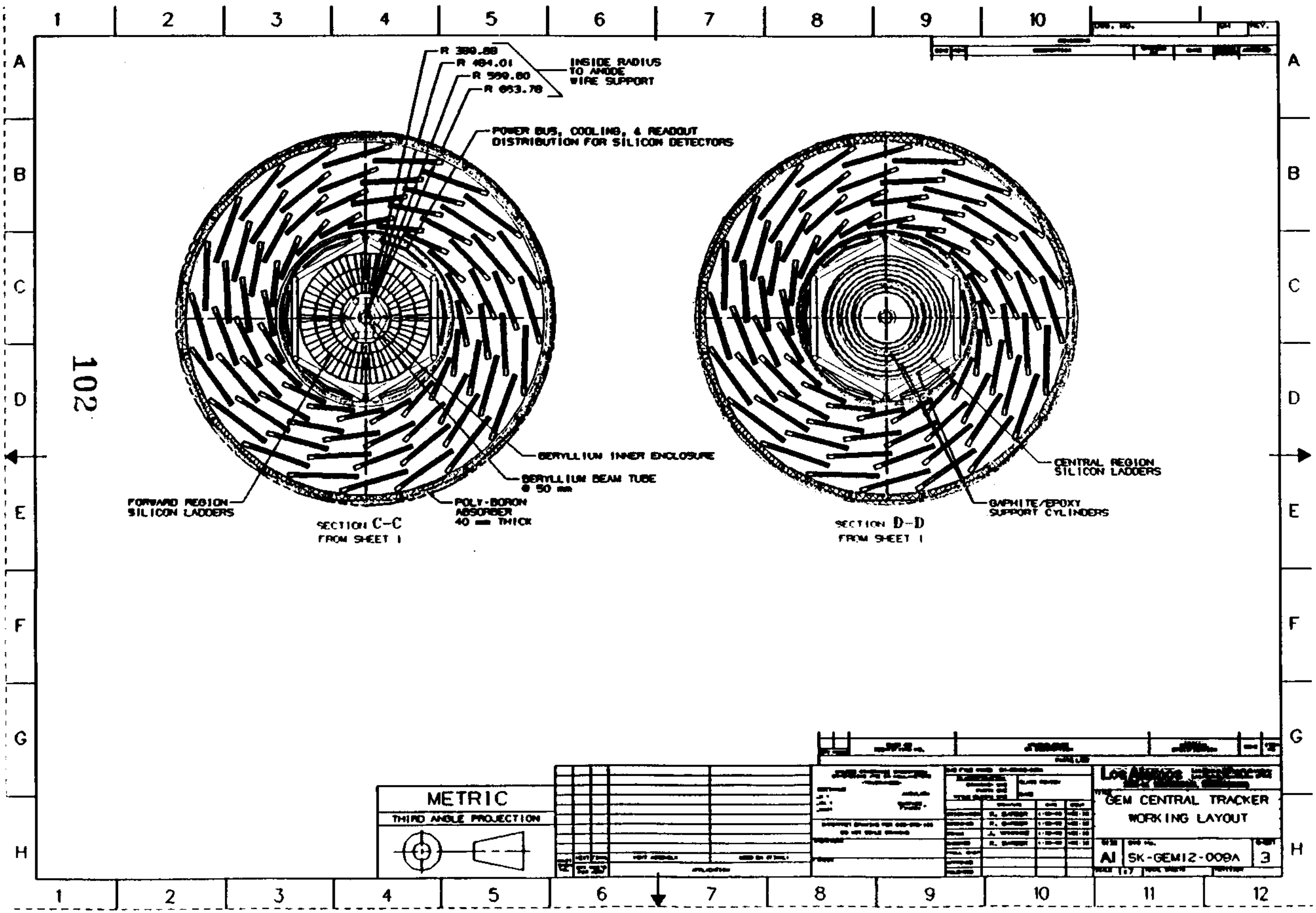
R 380.00
R 484.01
R 590.80
R 693.70
INSIDE RADIUS TO ANODE WIRE SUPPORT
POWER BUS, COOLING, & READOUT DISTRIBUTION FOR SILICON DETECTORS
BERYLLIUM INNER ENCLOSURE
BERYLLIUM BEAM TUBE Ø 50 mm
FORWARD REGION SILICON LADDERS
POLY-BORON ABSORBER 40 mm THICK
SECTION C-C FROM SHEET 1
CENTRAL REGION SILICON LADDERS
GAPHITE/EPOXY SUPPORT CYLINDERS
SECTION D-D FROM SHEET 1
METRIC
THIRD ANGLE PROJECTION
GEM CENTRAL TRACKER WORKING LAYOUT
A1
SK-GEM12-009A
3

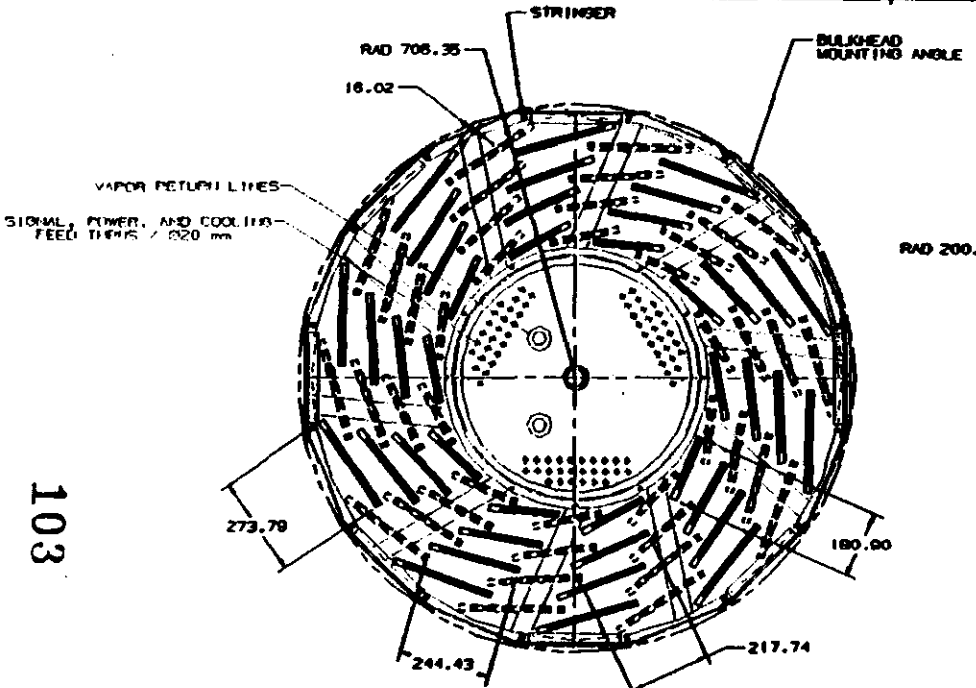

SECTION A–A
FROM SHEET 1

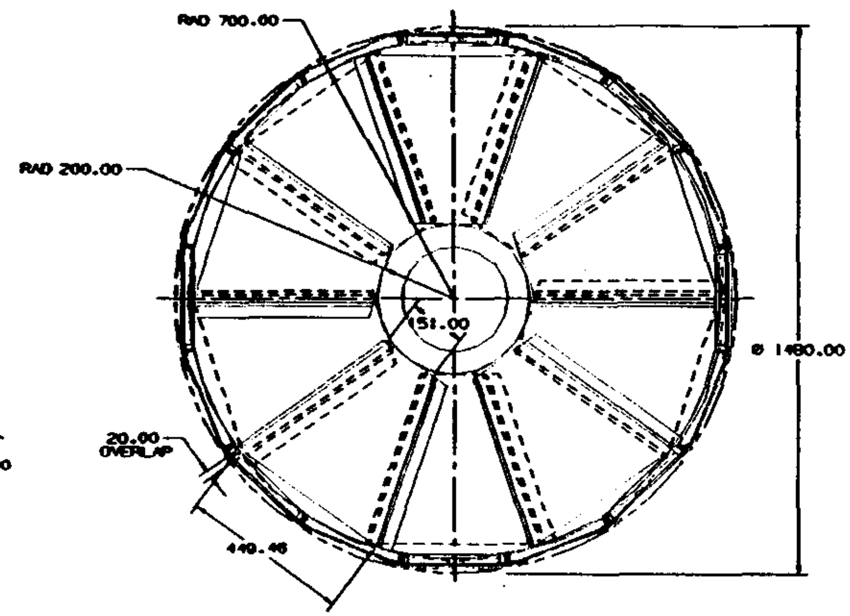

SECTION B–B
FROM SHEET 1

NOTE: EACH LEVEL OF 10 SECTORS ROTATED 9 DEGREES RELATIVE TO ADJACENT LEVELS (4 LEVELS IN TOTAL)

INTERPOLATING PAD CHAMBERS (BARREL REGION)
20 SECTORS OF 4 SUPERLAYERS EACH LORENZ ANGLE OF 12 DEGREES EACH LEVEL ROTATED 4.5° RELATIVE TO ADJACENT LEVELS 2 LAYERS PER SUPERLAYER DIMENSIONS FOR CHAMBERS ARE FOR ACTIVE WIDTHS(ADD 5 CM FOR OVERALL WIDTHS)

METRIC
THIRD ANGLE PROJECTION

Los Alamos
GEM CENTRAL TRACKER
WORKING LAYOUT

A1 SK-GEM12-009A 2

Lorenz angle 12°

barrel 20 sectors in ϕ
end cap 10 sectors

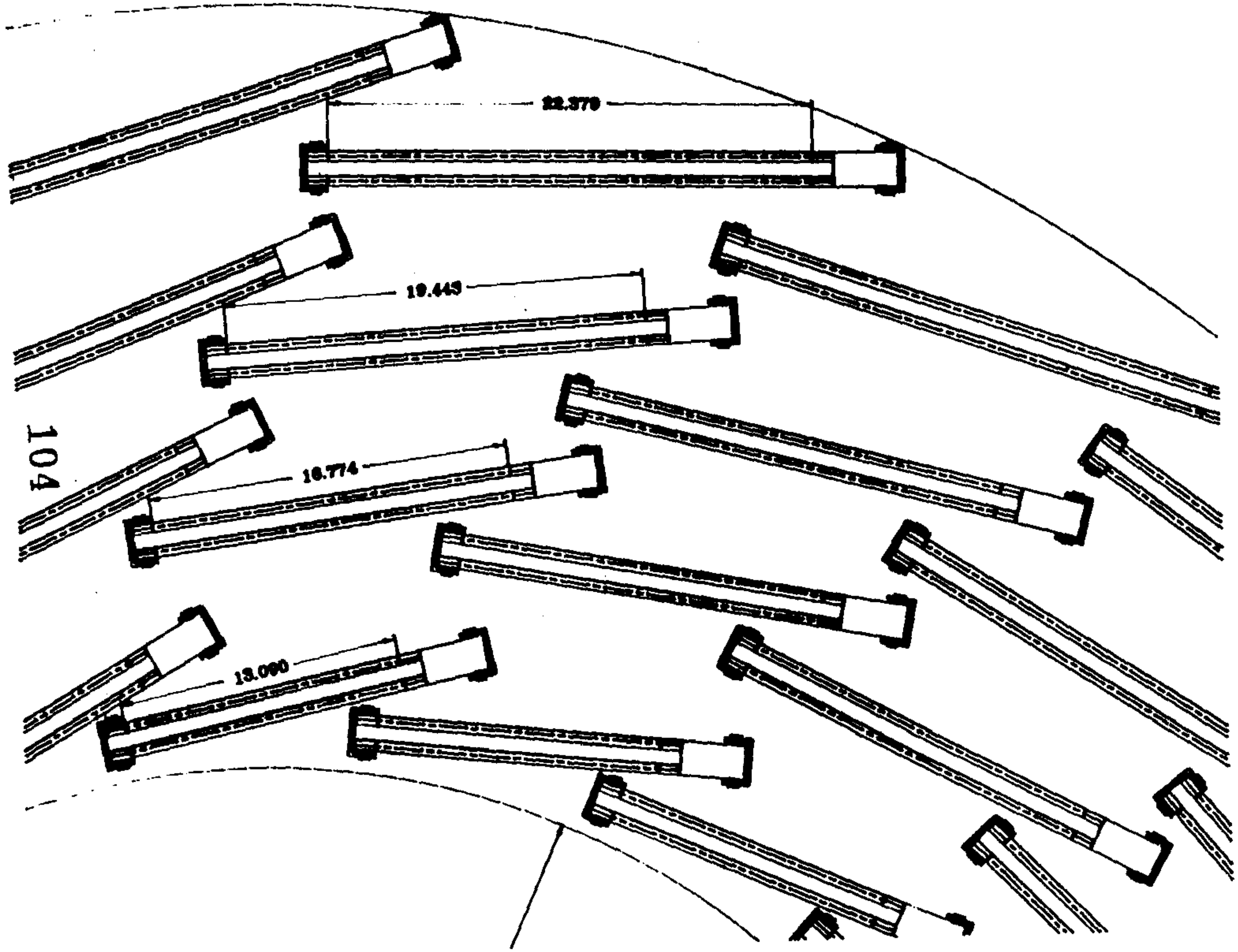

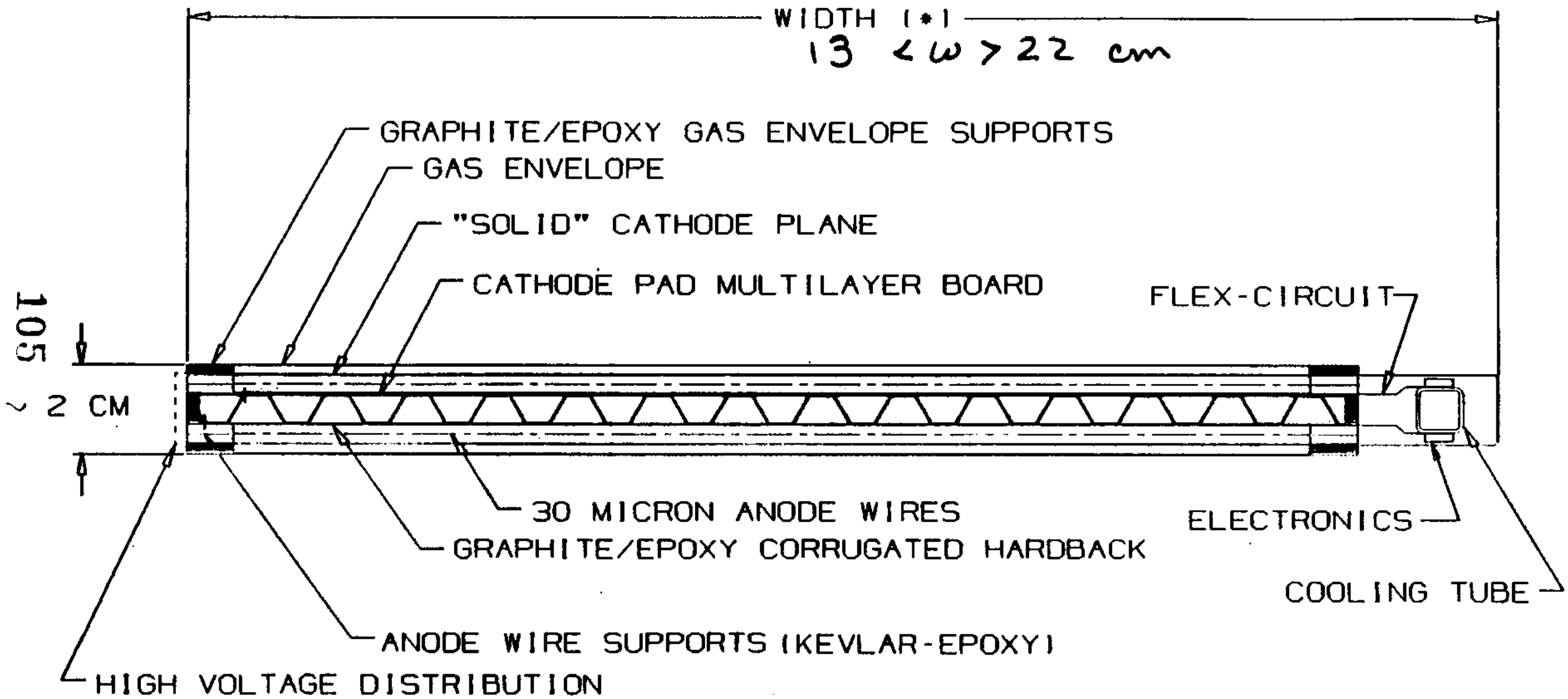

GEM TRACKING IPC SUPERLAYER

SECTIONAL OF TYPICAL BARREL MODULE

*NOTE: LEVEL I = 18 CM
LEVEL II = 21.8 CM
LEVEL III = 24.5 CM
LEVEL IV = 27.4 CM
(SUBTRACT 5 CM FOR ACTIVE WIDTH)

W. EMMET
YALE PPG 22-JAN-1992

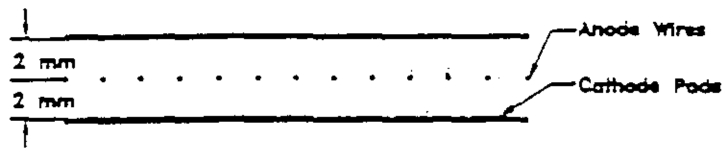

a) Cell Geometry Viewed Along the Anode Wires

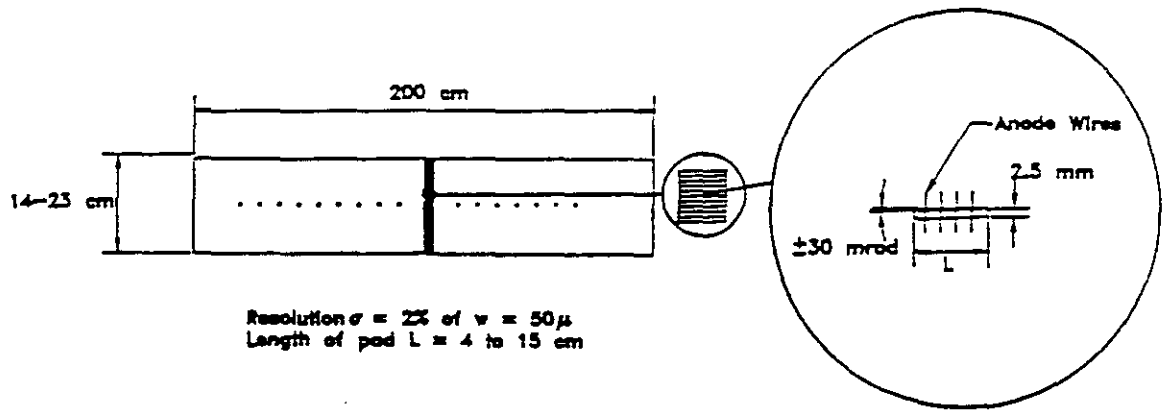

b) Pad Arrangement in the Barrel Chambers

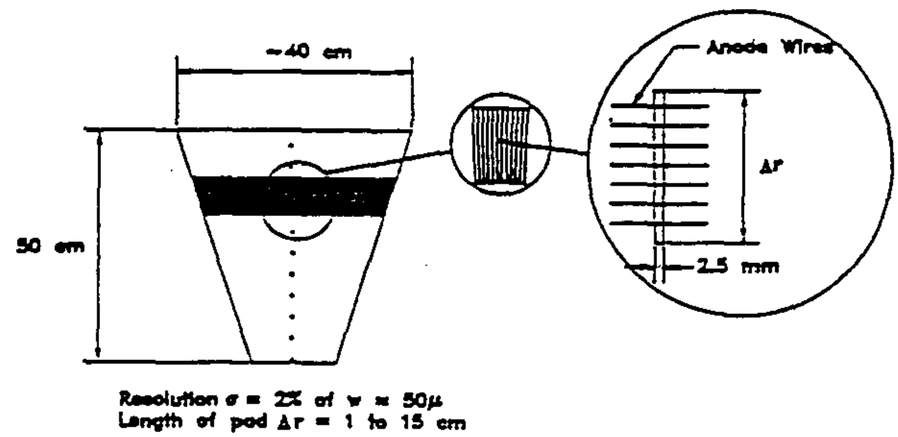

c) Pad Arrangement in the End Cap Chambers

GEOMETRY OF THE INTERPOLATING PAD CHAMBERS

Fig. 1.3

GEM IPC TRACKER

IPC MODULE ASSEMBLY

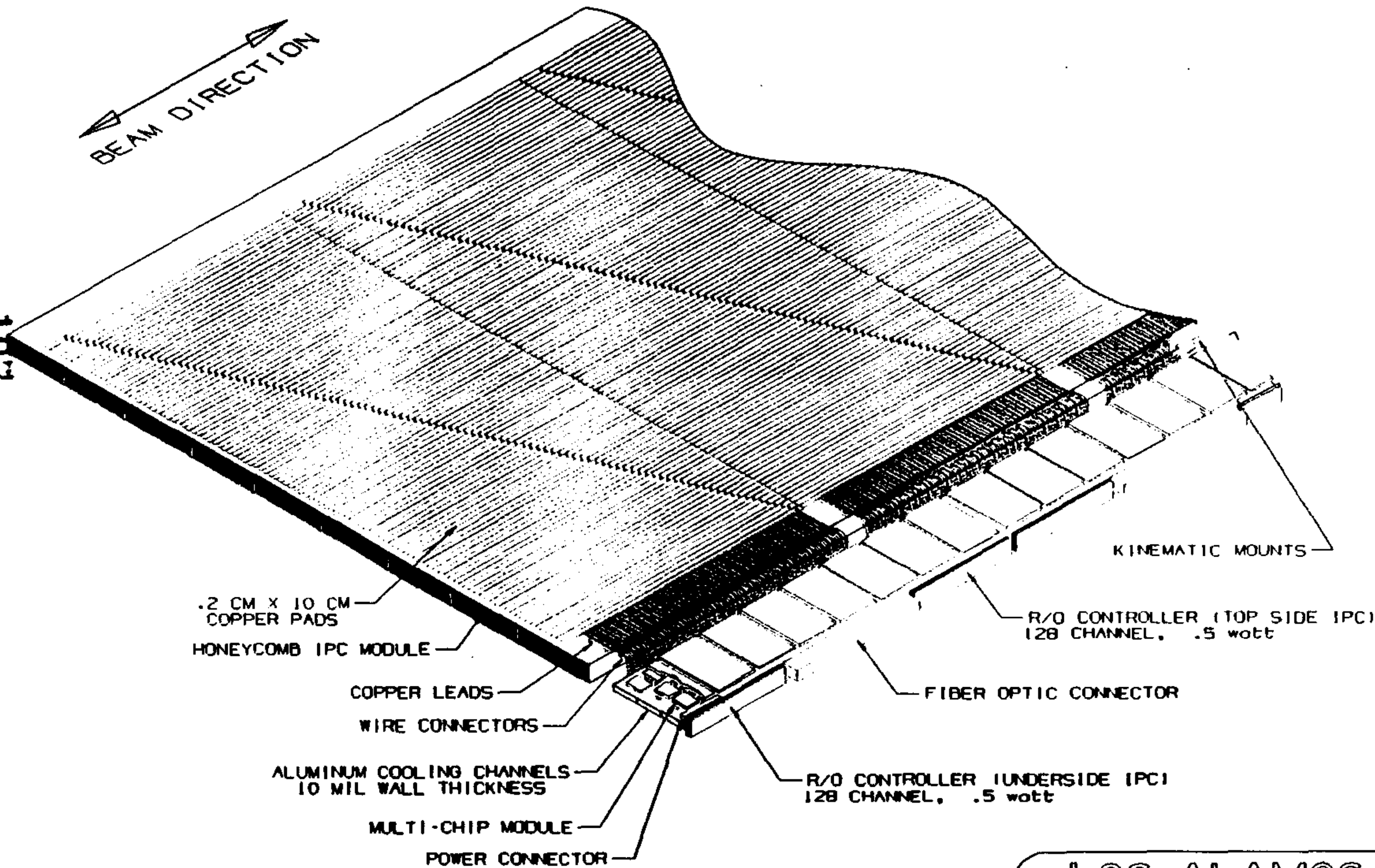

ALL DIMENSIONS ARE IN mm

LOS ALAMOS

MEE-12
MECHANICAL AND ELECTRONIC
ENGINEERING DIVISION

JRVCOOLASSY 8-31-92

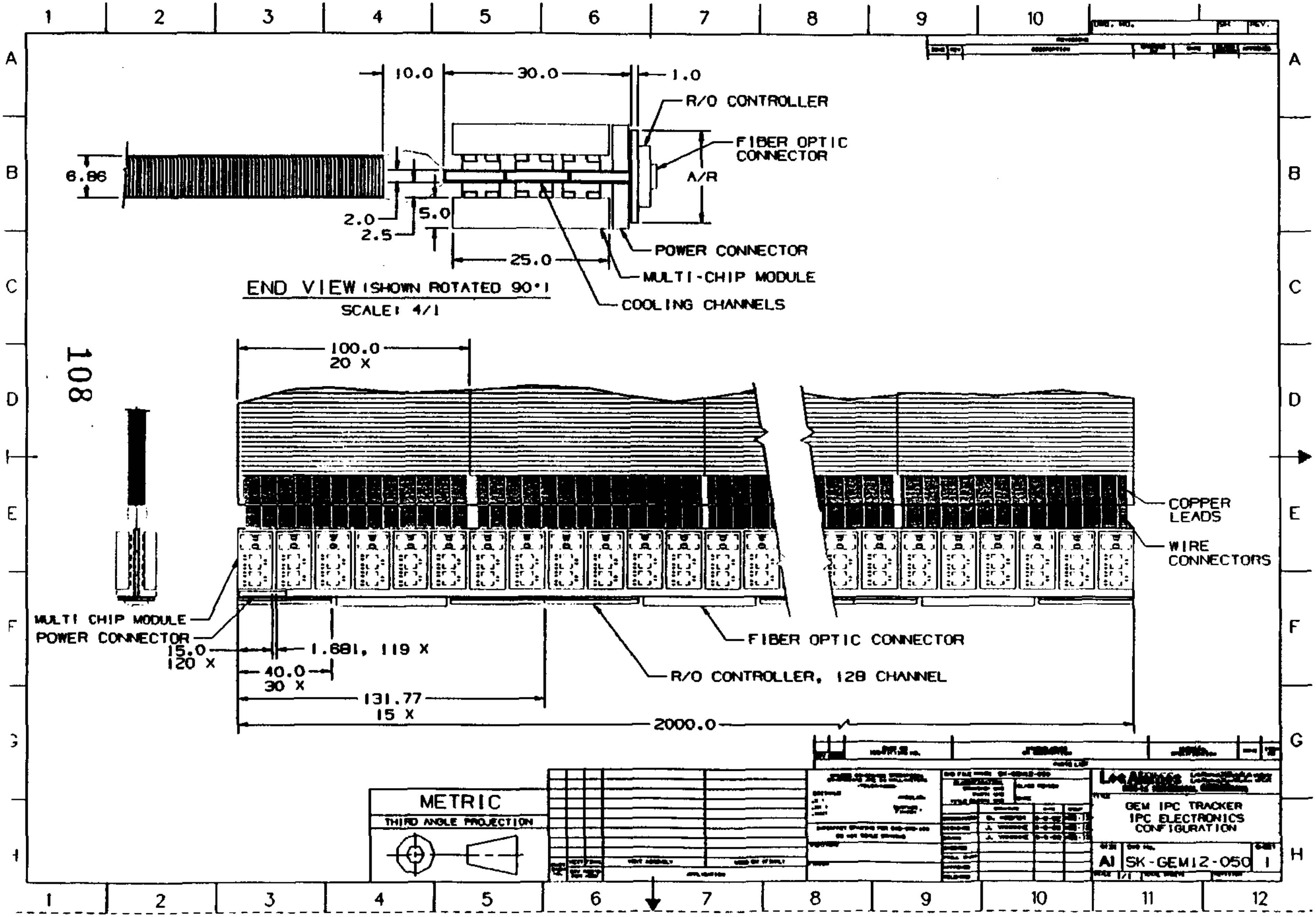

10.0
30.0
1.0
R/O CONTROLLER
FIBER OPTIC CONNECTOR
A/R
6.86
2.0
2.5
5.0
25.0
POWER CONNECTOR
MULTI-CHIP MODULE
COOLING CHANNELS
END VIEW (SHOWN ROTATED 90°)
SCALE: 4/1
100.0 20 X
COPPER LEADS
WIRE CONNECTORS
MULTI CHIP MODULE
POWER CONNECTOR
15.0 120 X
1.681, 119 X
40.0 30 X
131.77 15 X
2000.0
FIBER OPTIC CONNECTOR
R/O CONTROLLER, 128 CHANNEL
METRIC
THIRD ANGLE PROJECTION
GEM IPC TRACKER
IPC ELECTRONICS
CONFIGURATION
A1
SK-GEM12-050
1

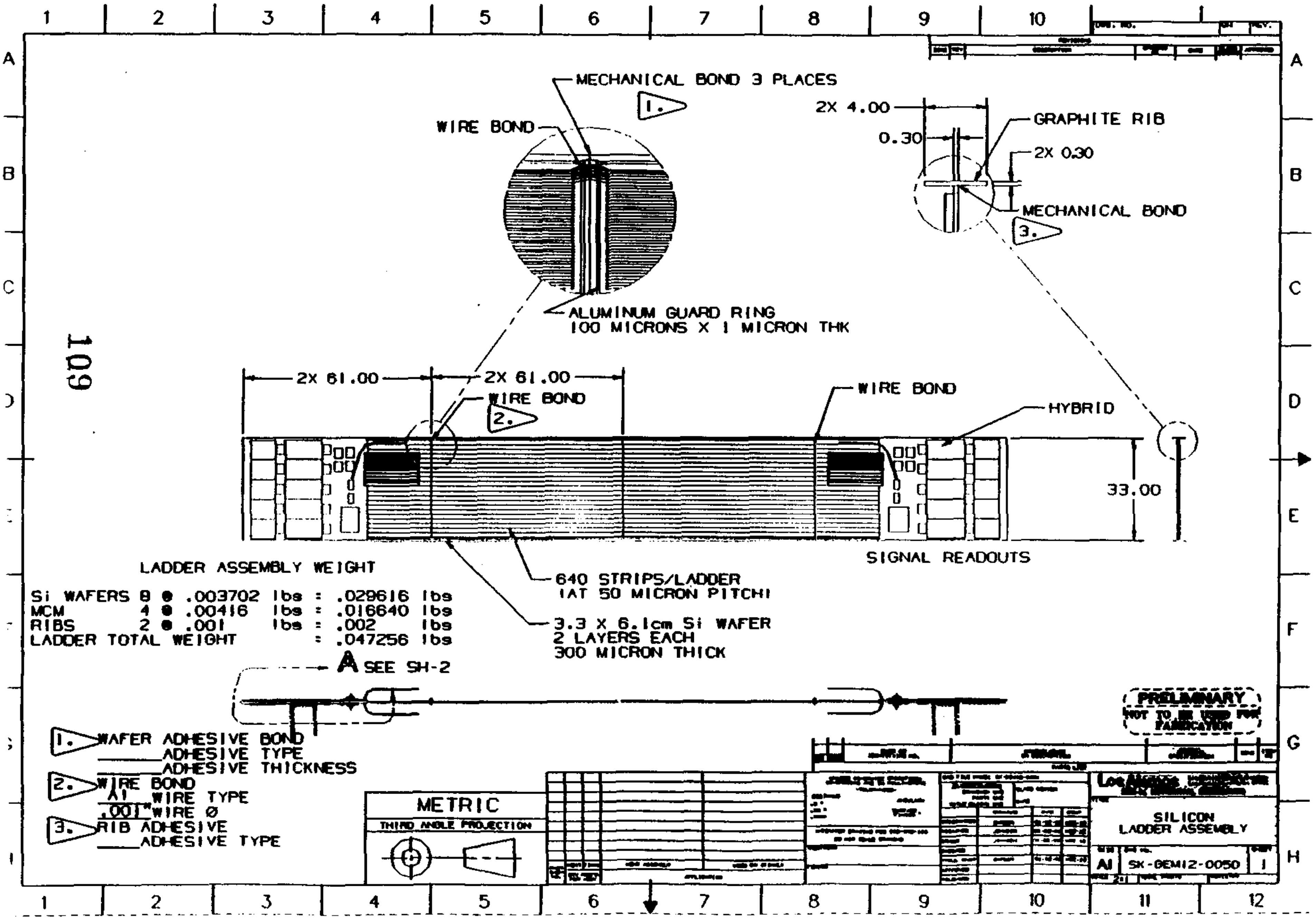

MECHANICAL BOND 3 PLACES
1.
WIRE BOND
ALUMINUM GUARD RING
100 MICRONS X 1 MICRON THK
2X 4.00
0.30
GRAPHITE RIB
2X 0.30
MECHANICAL BOND
3.
2X 61.00
2X 61.00
WIRE BOND
2.
WIRE BOND
HYBRID
33.00
SIGNAL READOUTS
640 STRIPS/LADDER
(AT 50 MICRON PITCH)
3.3 X 6.1cm Si WAFER
2 LAYERS EACH
300 MICRON THICK
LADDER ASSEMBLY WEIGHT
Si WAFERS 8 @ .003702 lbs : .029616 lbs
MCM 4 @ .00416 lbs : .016640 lbs
RIBS 2 @ .001 lbs : .002 lbs
LADDER TOTAL WEIGHT : .047256 lbs
A SEE SH-2
1. WAFER ADHESIVE BOND
______ ADHESIVE TYPE
______ ADHESIVE THICKNESS
2. WIRE BOND
Al WIRE TYPE
.001" WIRE Ø
3. RIB ADHESIVE
______ ADHESIVE TYPE
PRELIMINARY
NOT TO BE USED FOR FABRICATION
METRIC
THIRD ANGLE PROJECTION
SILICON
LADDER ASSEMBLY
A1
SK-8EM12-0050
1

110

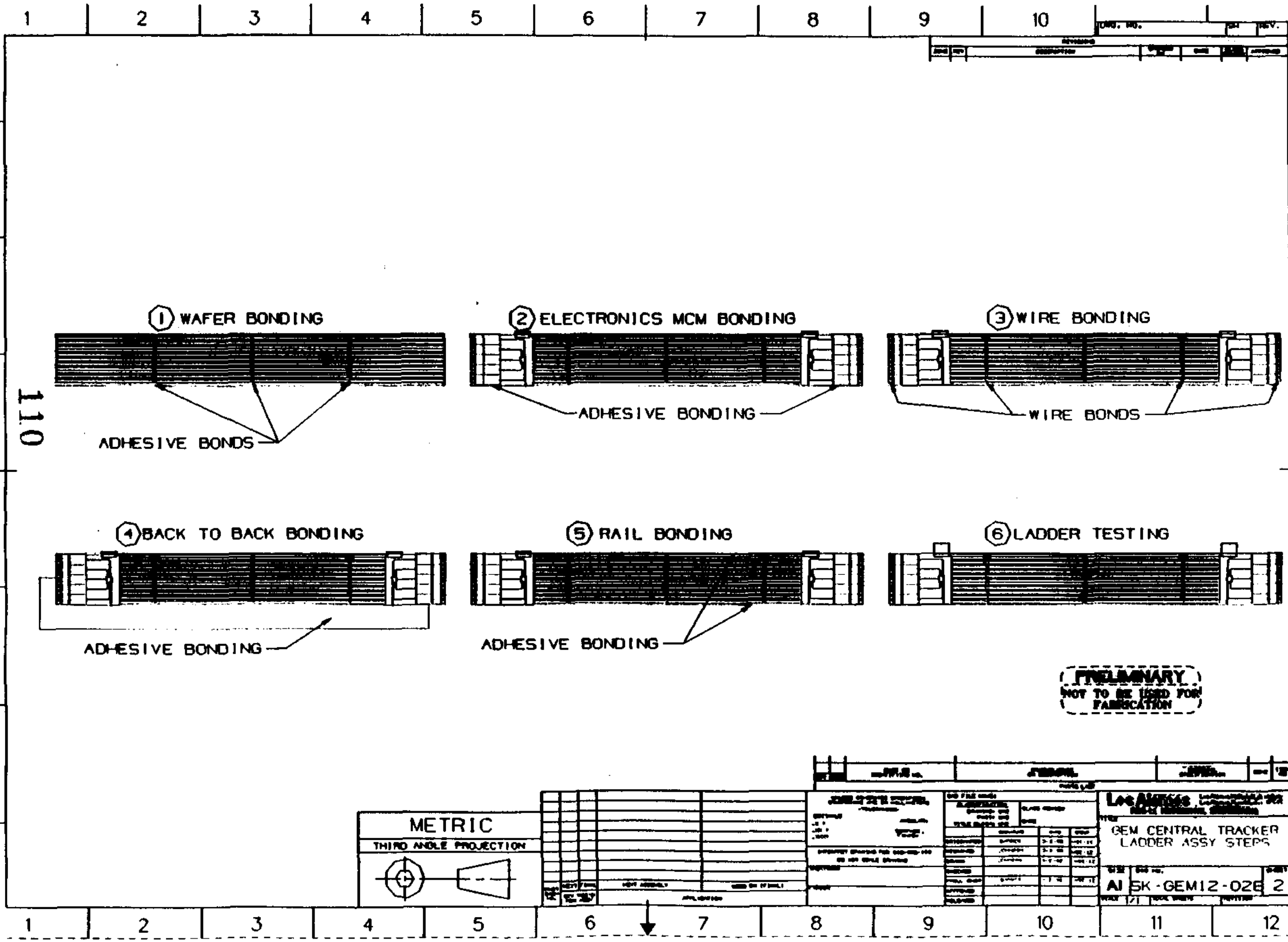

1 WAFER BONDING
ADHESIVE BONDS
2 ELECTRONICS MCM BONDING
ADHESIVE BONDING
3 WIRE BONDING
WIRE BONDS
4 BACK TO BACK BONDING
ADHESIVE BONDING
5 RAIL BONDING
ADHESIVE BONDING
6 LADDER TESTING
PRELIMINARY
NOT TO BE USED FOR FABRICATION
METRIC
THIRD ANGLE PROJECTION
Los Alamos
GEM CENTRAL TRACKER
LADDER ASSY STEPS
A1
SK-GEM12-026
2

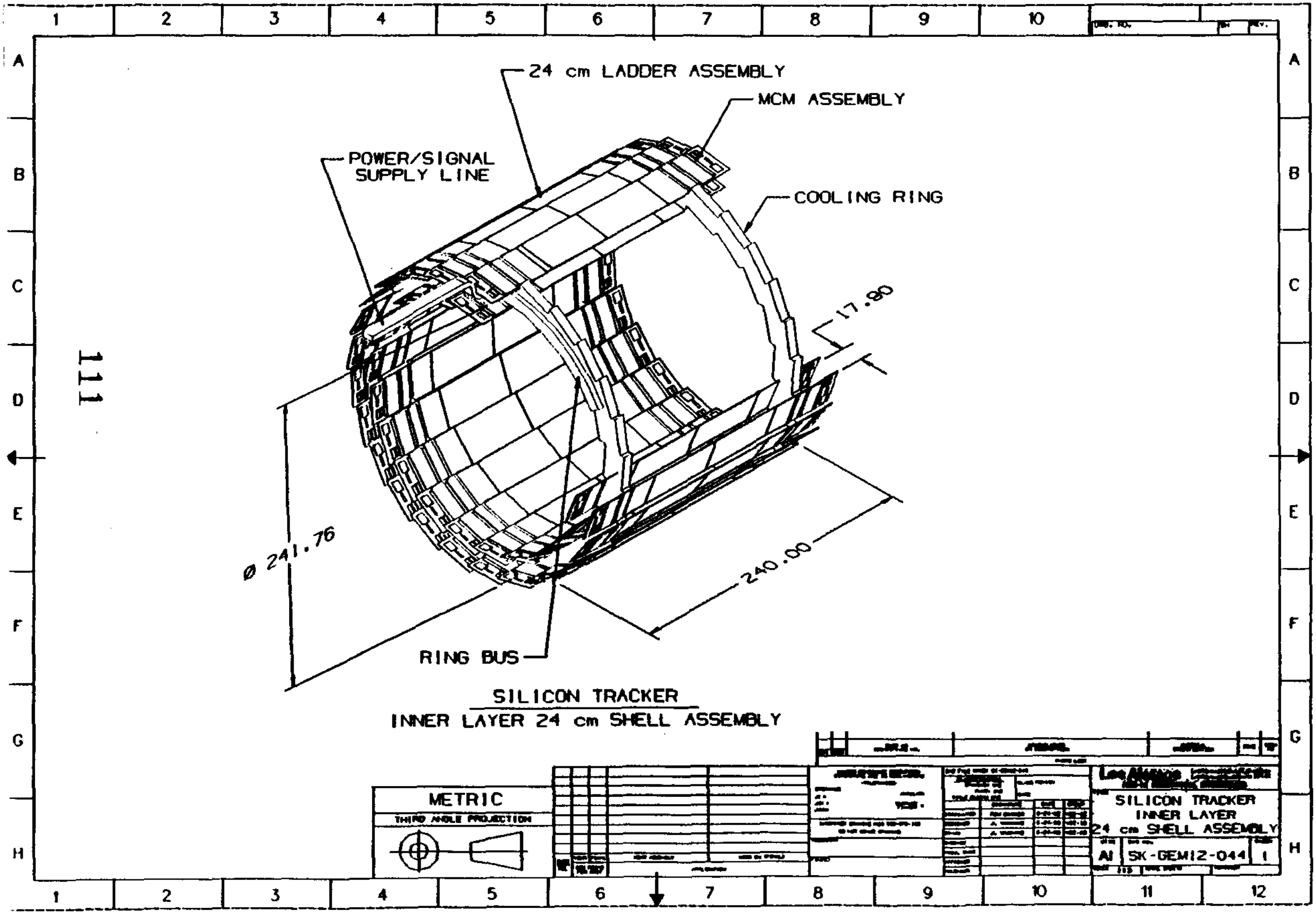
24 cm LADDER ASSEMBLY
MCM ASSEMBLY
POWER/SIGNAL SUPPLY LINE
COOLING RING
17.80
Ø 241.76
240.00
RING BUS
SILICON TRACKER
INNER LAYER 24 cm SHELL ASSEMBLY
METRIC
THIRD ANGLE PROJECTION
Los Alamos
SILICON TRACKER
INNER LAYER
24 cm SHELL ASSEMBLY
A1
SK-GEM12-044
1

112

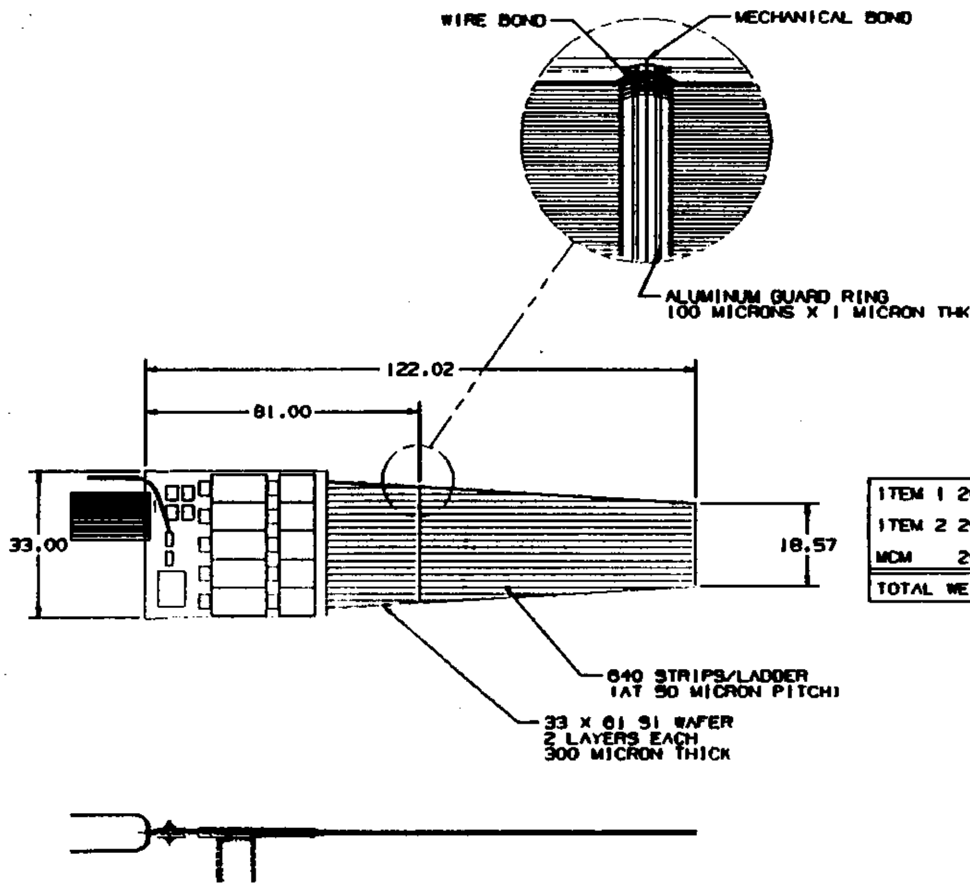

ITEM 1 2@	1.243g(.0027 lbs)	2.486g(.0054 lbs)
ITEM 2 2@	.915g (.002 lbs)	1.83g (.004 lbs)
MCM 2@	.932g (.0021 lbs)	1.864g(.0041 lbs)
TOTAL WEIGHT PER LADDER		6.18g (.0135 lbs)

PRELIMINARY
NOT TO BE USED FOR FABRICATION

METRIC
THIRD ANGLE PROJECTION

Los Alamos

GEM SILICON TRACKER
FORWARD LADDER ASSEMBLY
DETAIL

A1 SK-GEM12-030C 1

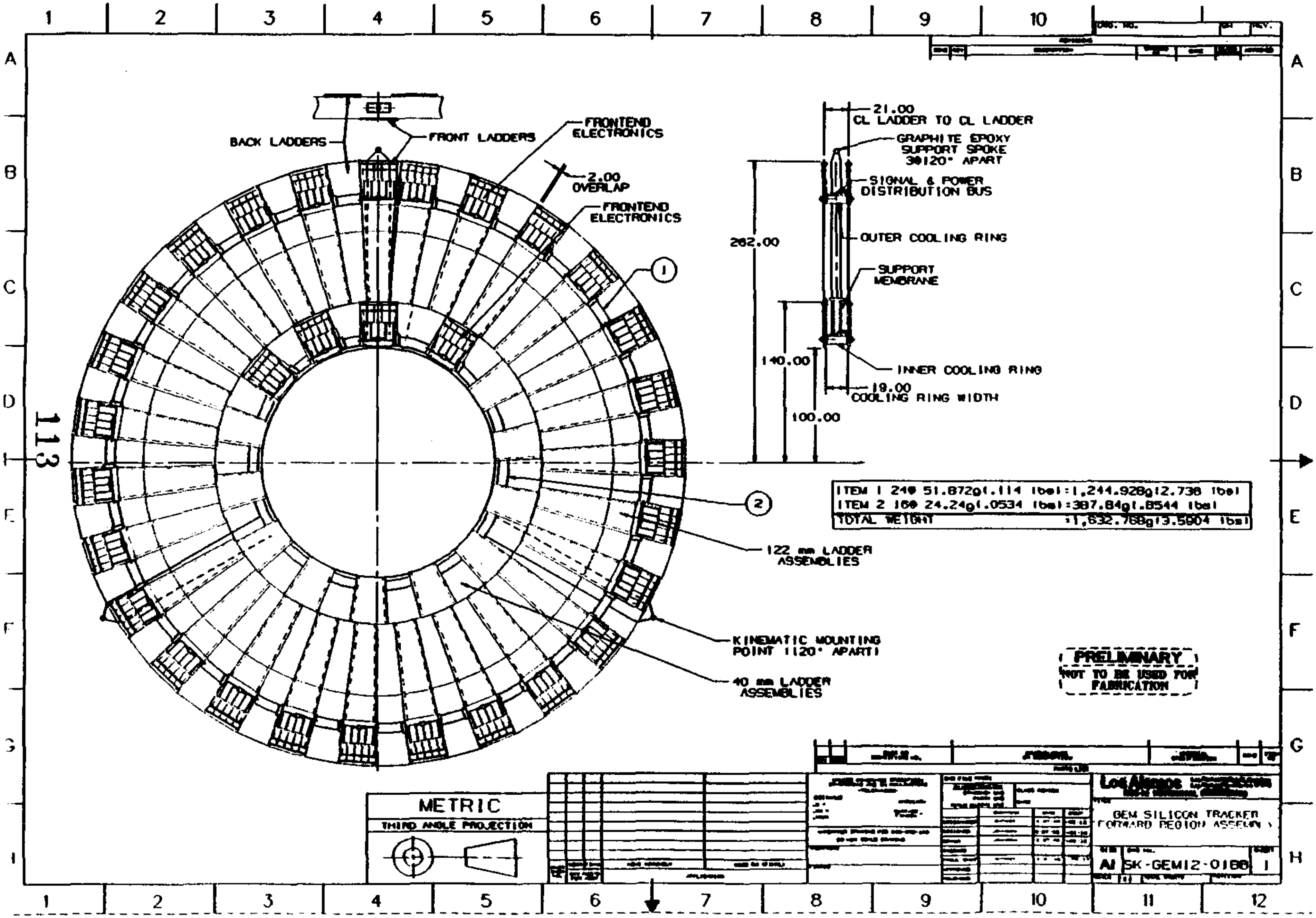
BACK LADDERS
FRONT LADDERS
FRONTEND ELECTRONICS
2.00 OVERLAP
FRONTEND ELECTRONICS
1
2
21.00 CL LADDER TO CL LADDER
GRAPHITE EPOXY SUPPORT SPOKE 3@120° APART
SIGNAL & POWER DISTRIBUTION BUS
OUTER COOLING RING
SUPPORT MEMBRANE
INNER COOLING RING
19.00 COOLING RING WIDTH
262.00
140.00
100.00
ITEM 1 24@ 51.872g(.114 lbs):1,244.928g(2.738 lbs)
ITEM 2 16@ 24.24g(.0534 lbs):387.84g(.8544 lbs)
TOTAL WEIGHT :1,632.768g(3.5904 lbs)
122 mm LADDER ASSEMBLIES
KINEMATIC MOUNTING POINT (120° APART)
40 mm LADDER ASSEMBLIES
PRELIMINARY
NOT TO BE USED FOR FABRICATION
METRIC
THIRD ANGLE PROJECTION
Los Alamos
GEM SILICON TRACKER
FORWARD REGION ASSEMBLY
A1 SK-GEM12-0188 1

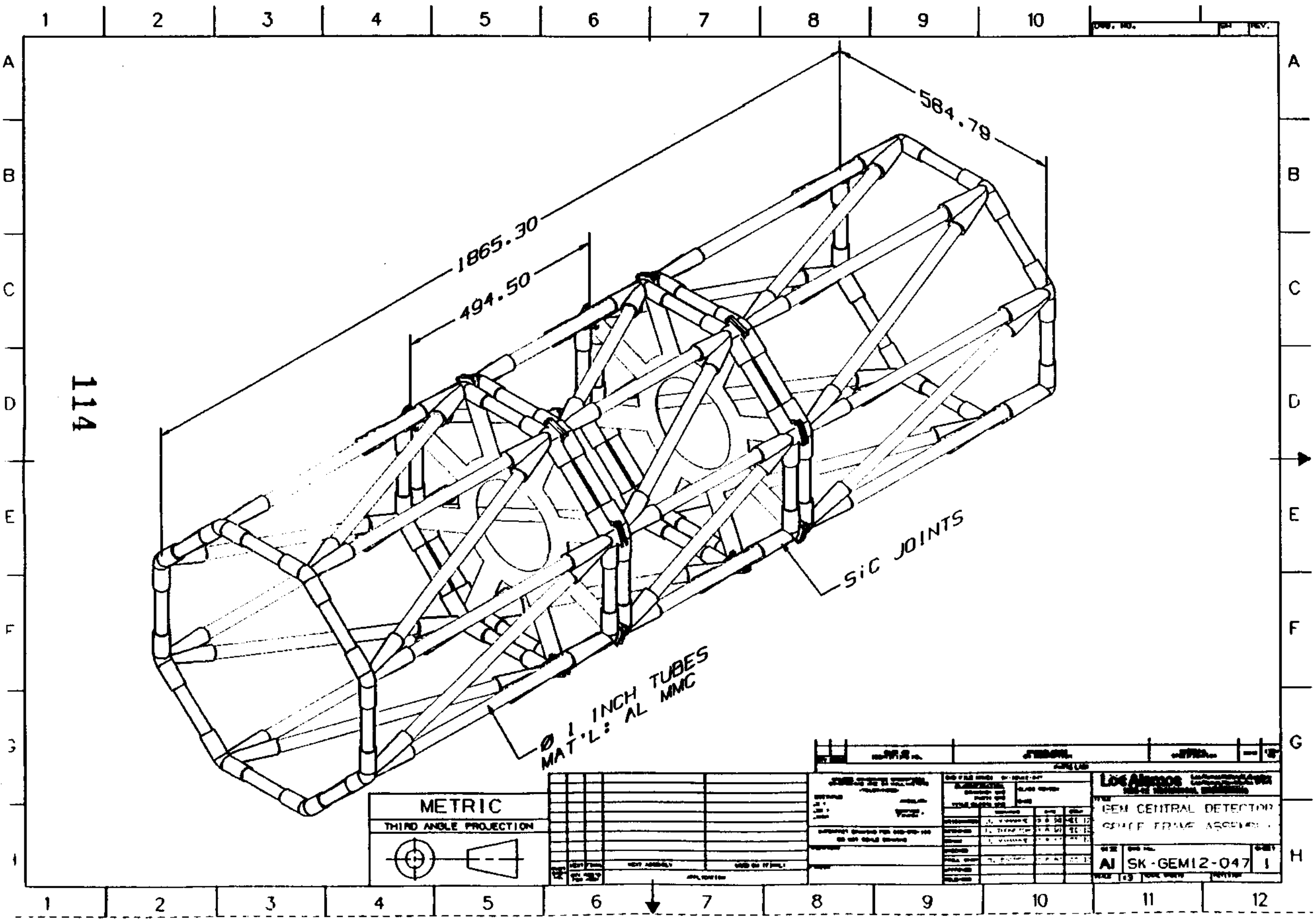
1865.30
494.50
584.79
SiC JOINTS
Ø 1 INCH TUBES
MAT'L: AL MMC
METRIC
THIRD ANGLE PROJECTION
GEM CENTRAL DETECTOR
SPACE FRAME ASSEMBLY
A1
SK-GEM12-047
1

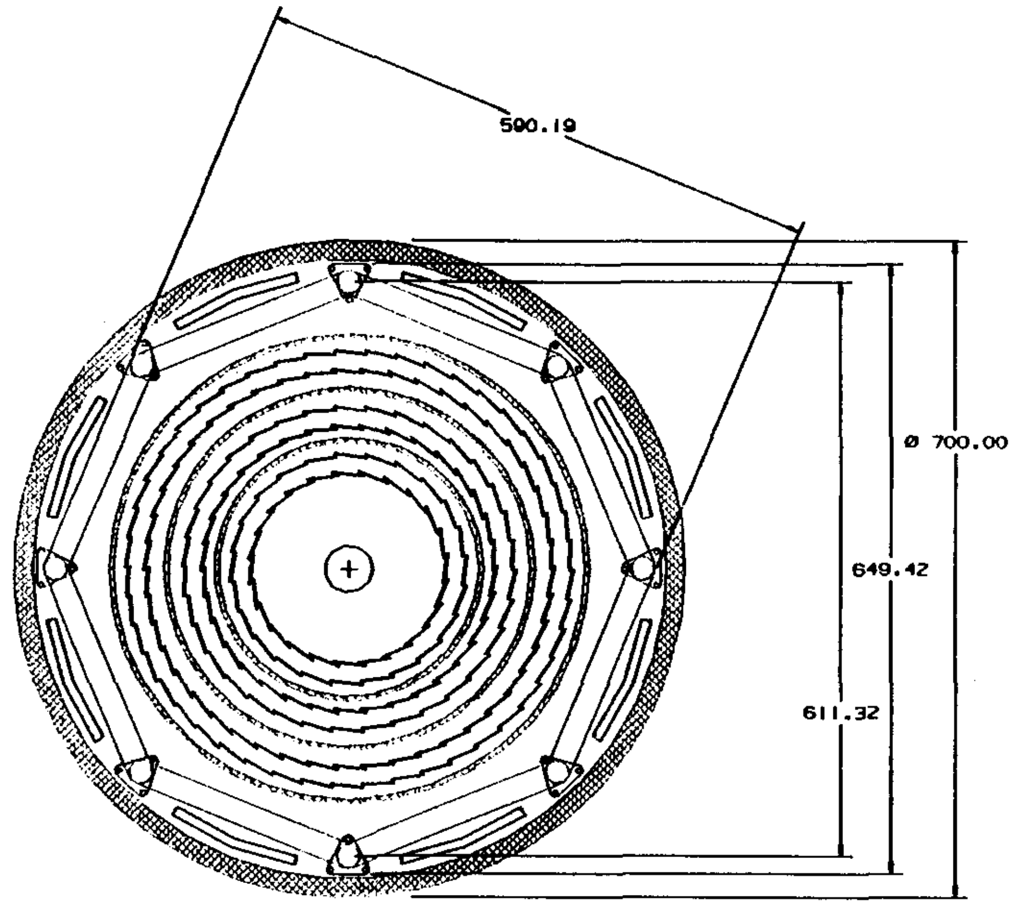

SECTION THRU BARREL REGION

METRIC

THIRD ANGLE PROJECTION

Los Alamos

GEM CENTRAL DETECTOR

A1 GEMVG-047-JV 1

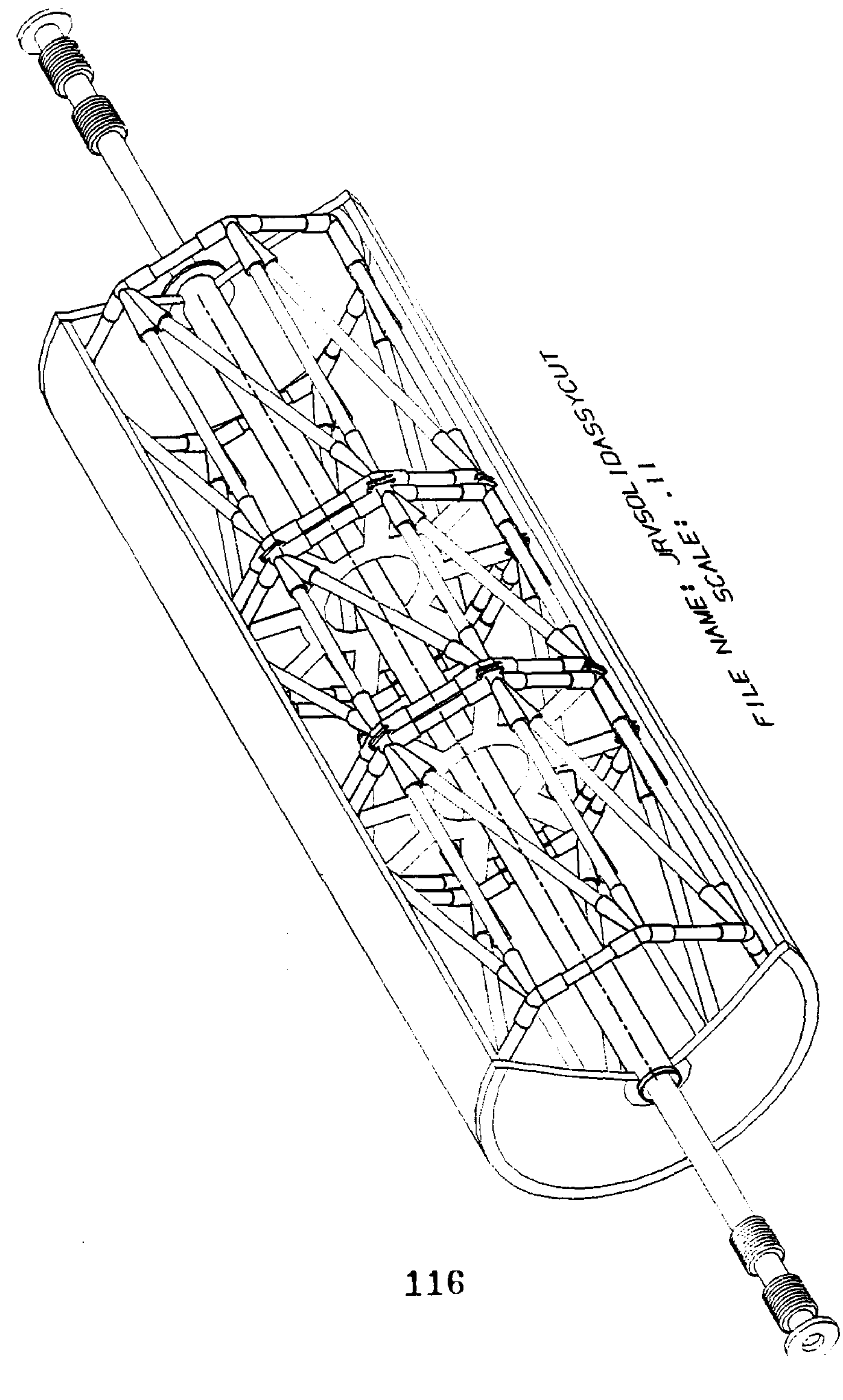
FILE NAME: JRVSOL IDASSYCUT
SCALE: .11

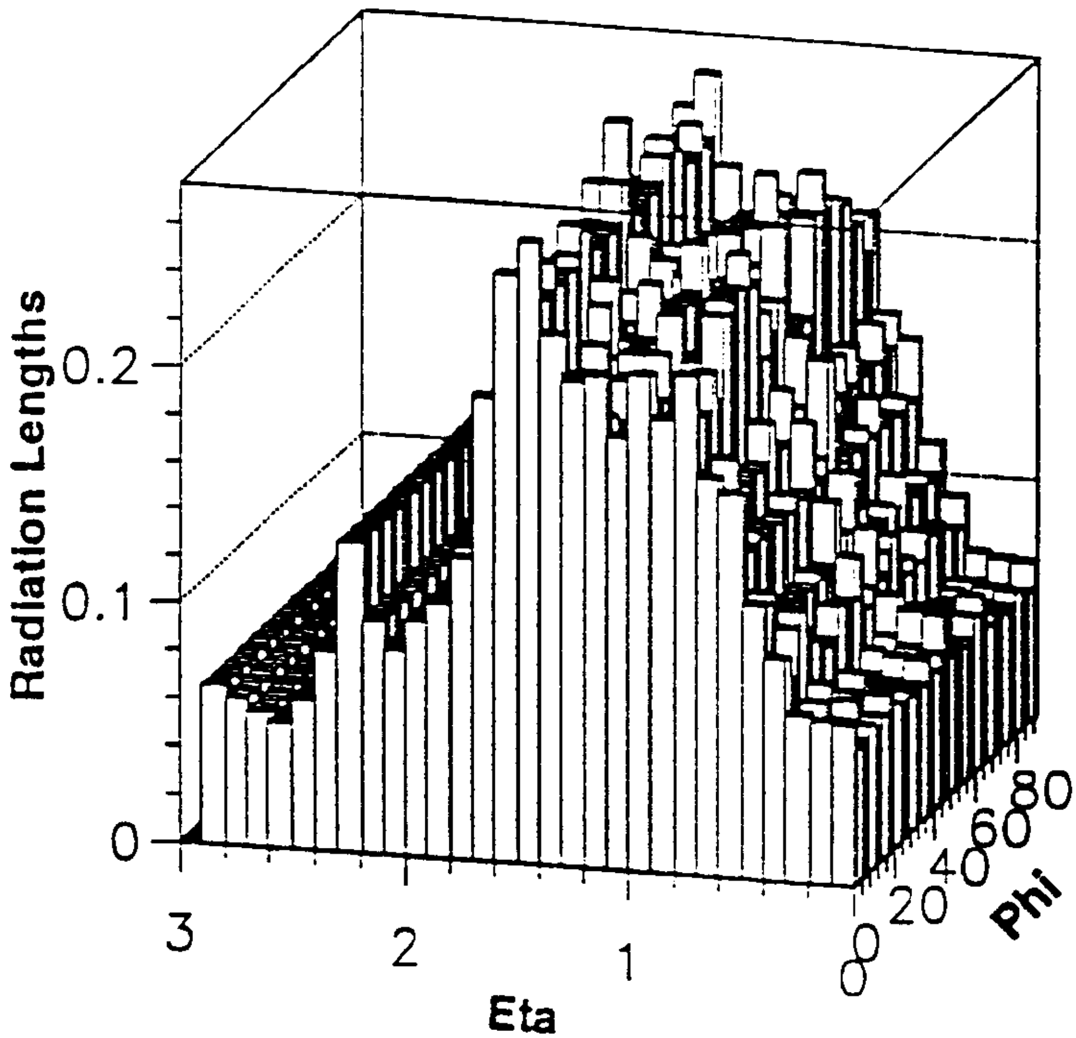

Figure 6.2-2 The radiation lengths of material in the silicon tracker vs. eta and phi. Included are all non-silicon volumes as well as the silicon detectors.

H mass and luminosity.

To check the dependence of this result on the isolation requirement described above a full run was made with a cut that was twice as tough in the ϕ direction: $\Delta\phi) < 0.04$. Nearly identical results were obtained.

Conclusions

Given the kinematics of H^0 production it is relatively simple to tag the Higgs vertex using high-P_T isolated charged tracks Such tracks should be observable in the tracker with near perfect efficiency yielding a vertex tagging efficiency of 80-90% at nominal luminosity and 50-60% at

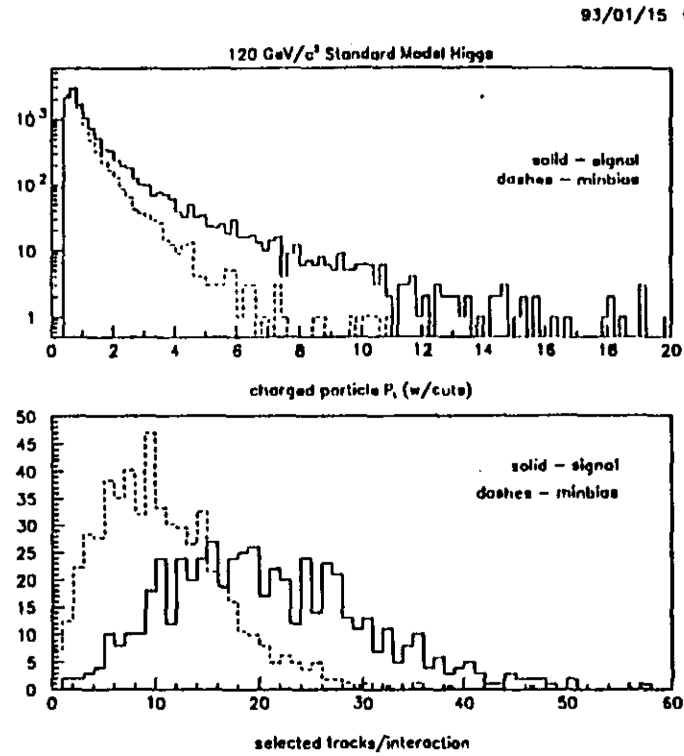

Figure 6.2-29

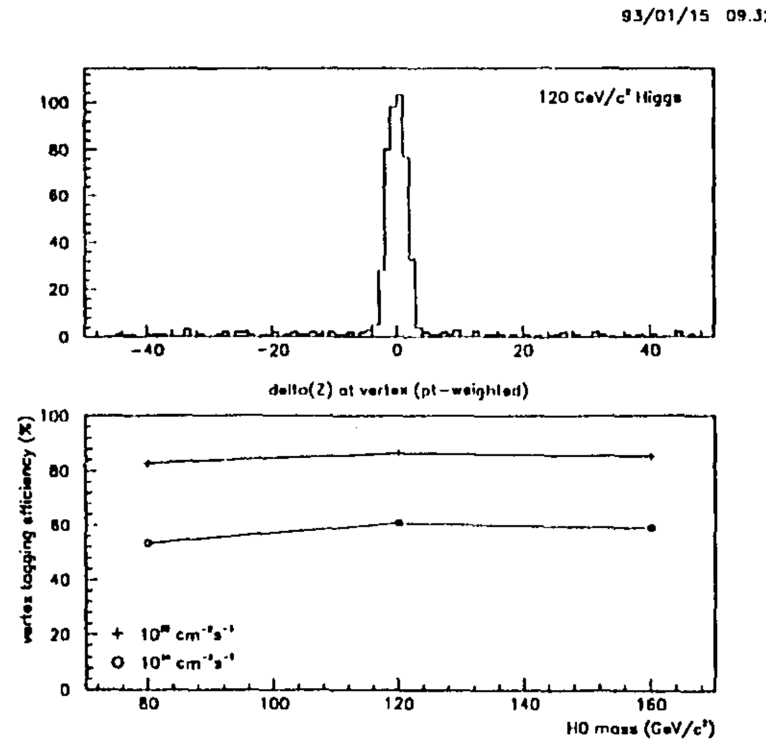

Figure 6.2-28

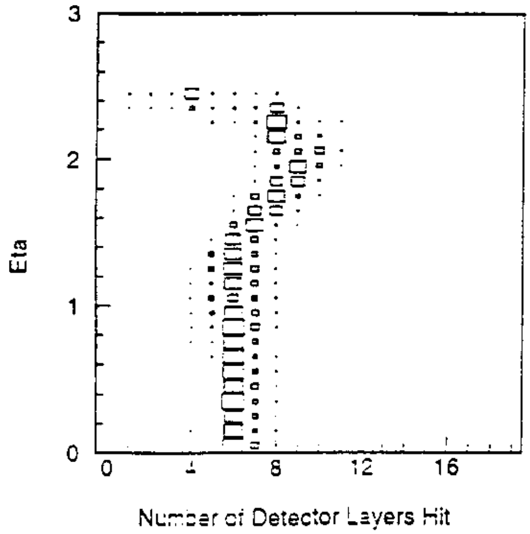

Figure 6.2-10 The number of silicon tracker layers that are hit by straight tracks vs. eta.

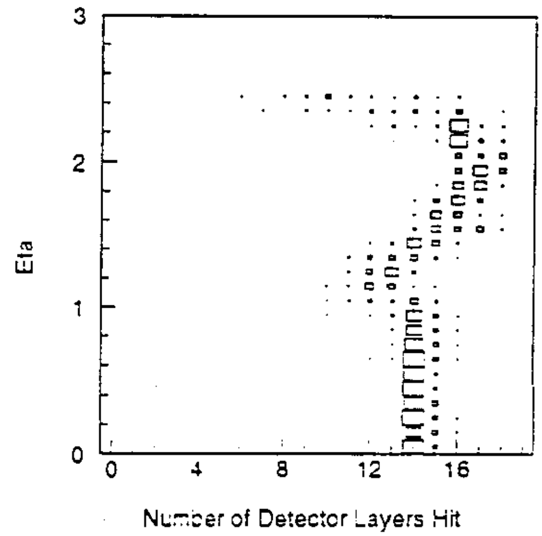

Figure 6.2-12 The number of silicon and pad tracker layers that are hit by straight tracks vs. eta.

We have also begun to look at track finding efficiencies in a typical physics event, which we have defined to be a Higgs event (m_{Higgs} = 300 GeV, $H^0 \to l^+l^-l^+l^-$) with a random number of minimum bias events (Poisson distribution with mean 1.6) as background. When we calculate the efficiency for finding all tracks above 5 GeV/c, we find that in the silicon portion of the tracker approximately 96% of all tracks are found (figure 6.2-9). The efficiency is approximately flat over eta (figure 6.2-11), begins to decrease at approximately 10 GeV/c, and decrease dramatically below approximately 1 GeV/c (figure 6.2-13).

The efficiencies for all tracks in the silicon plus pads are not as good (see figure 6.2-14???)

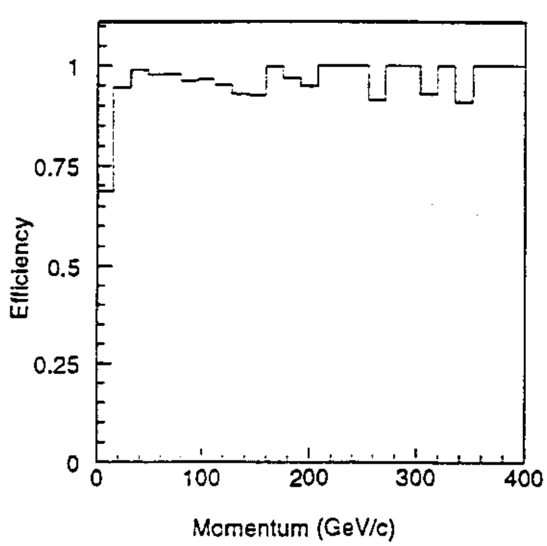

Figure 6.2-9 The efficiency for finding all tracks in the silicon trcker vs. momentum for Higgs plus 10^{33} minimum bias background events.

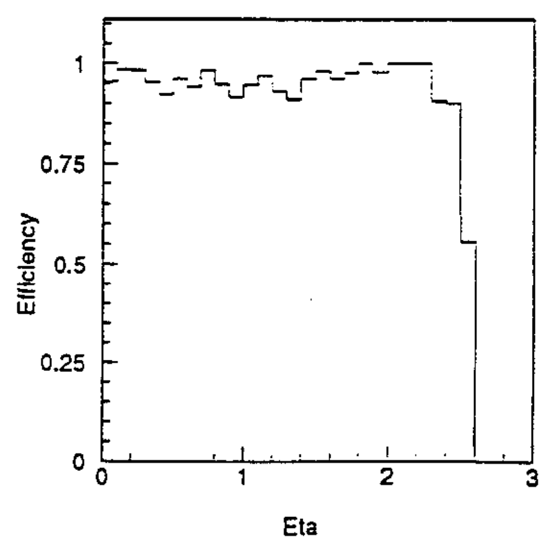

Figure 6.2-11 The efficiency for finding all tracks above 5 GeV/c in the silicon tracker vs. eta for Higgs plus 10^{33} minimum bias background events.

Electron sign determination

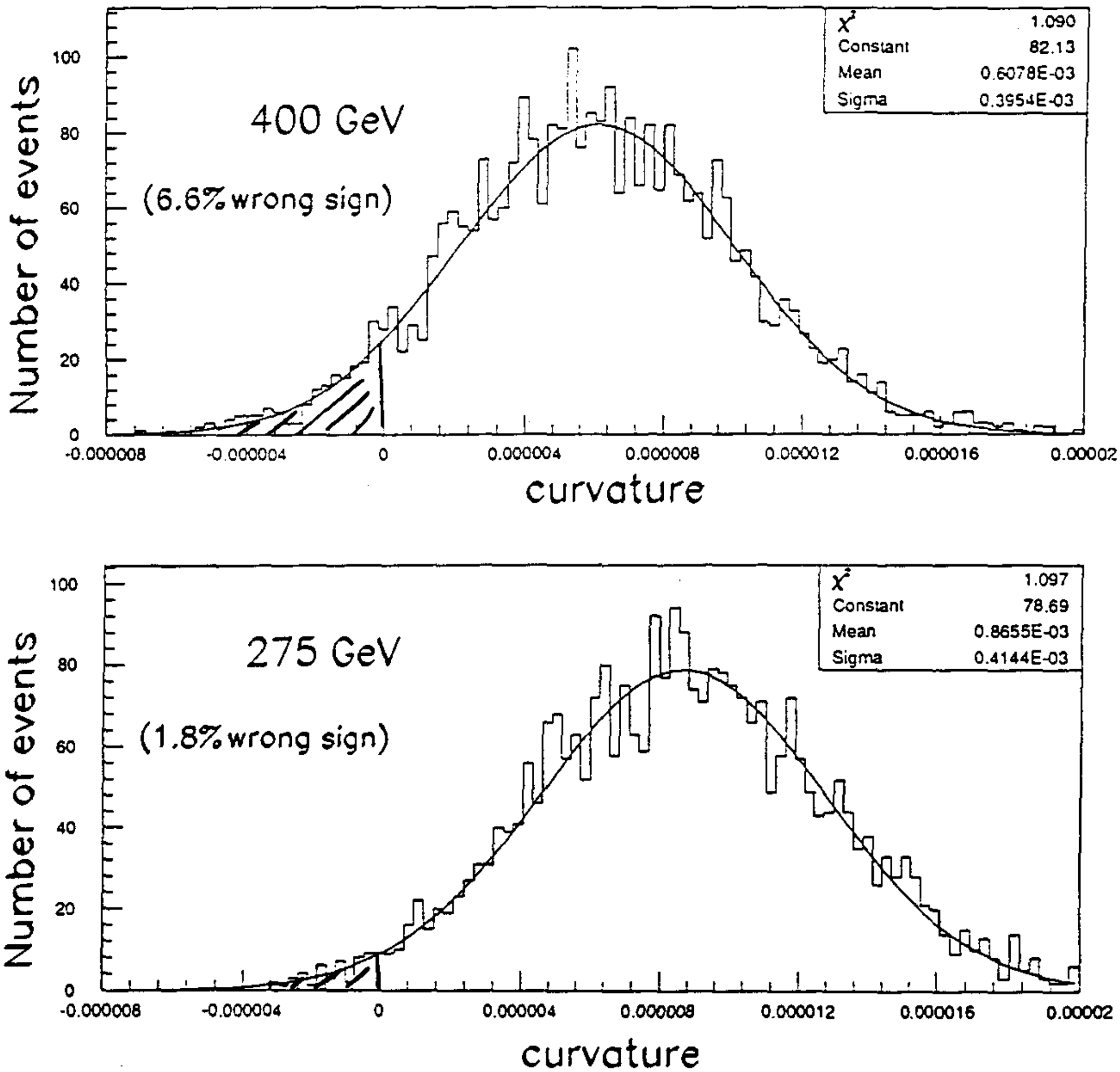

Figure 4: Measured curvature

GEM TN-92-65
J. Thomas
E. Wang

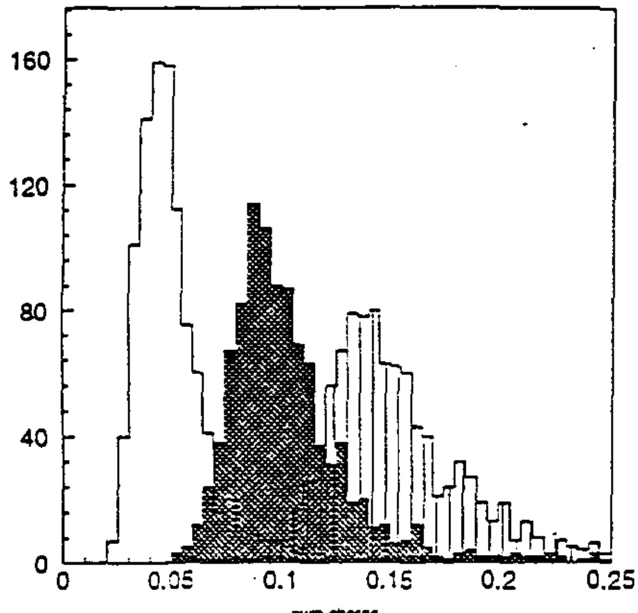

Figure 18. Total charge for a single IPC layer for 1, 2 and 3 tracks (in pC).

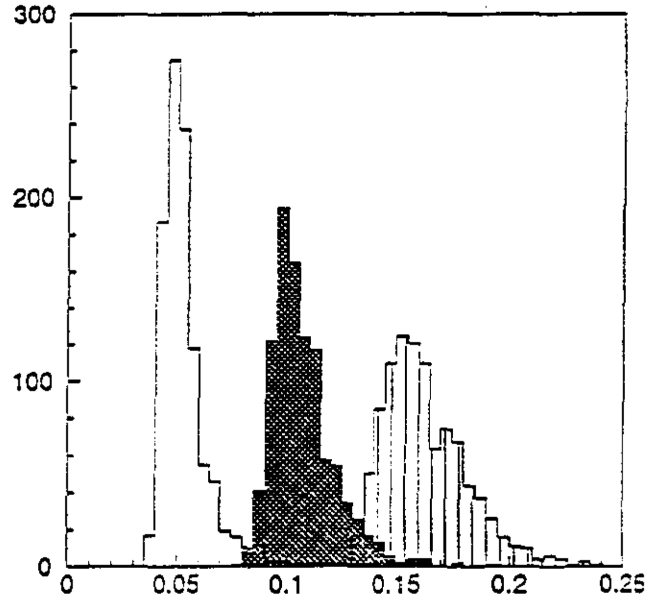

Figure 19. Average charge over 8 layers for 1, 2 and 3 tracks (in pC).

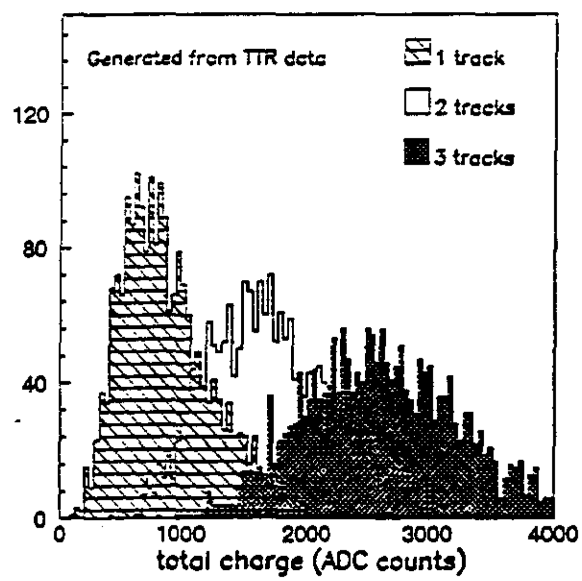

Figure 18a. Total charge for 1, 2 and 3 tracks generated from a Landau distribtuion for 1 track from the TTR.

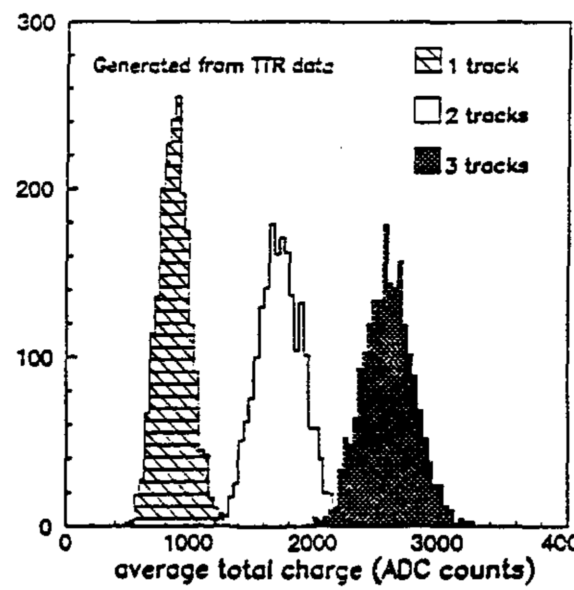

Figure 19a. Average integrated charge for 1, 2 and 3 tracks generated from TTR data.

bution has larger tails. A potential source of degredation is when low momentum tracks cross the tracks of interest. These tracks will be more bendy and will only contribute to one or two layers . This is easy to simulate and with two layers having the charge from two tracks deposited in them for *every* track, the resulting overlap in average charge between one and two tracks changes from 2% to 6%.

When it has been determined that there are indeed two tracks close together, it is necessary to fit to two Gaussians of known width (σ_{PRF}) whose total normalization (total charge) is also known. This results in a three parameter fit of three points and a normalization. The results are shown in Figure 20 for two tracks separated by 0.4 pad widths. The widths and the displacements for several different separations are summarized in Figures 21 and 22. The limit of the two track resolution is reached at

Superconducting Super Collider Laboratory
2550 Beckleymeade Avenue, Mail Stop 2000
Dallas TX 75237-3946
(214) 708–6027
Fax: (214) 708-6354
EMail: MORGAN@SSCVX1
Physics Research Division

Memorandum

To: **A. Carroll, D. Dayton**

CC: **George Yost**

From: K. Morgan, Spokesperson, Central Tracker Test Beam Team

Subject: Letter of Intent to use the AGS Test Beam B2

Date: January 7, 1993

The Central Tracker Team of the GEM Collaboration requests the use of the AGS B2 test beam at the earliest possible date in 1993, which we understand is the beginning of June. Our tests will include determination of the intrinsic resolution of prototype Interpolating Pad Chambers (IPC's), uniformity scans, and efficiency measurements in a high counting rate environment. To minimize multiple scattering, we request the highest energy beam available, 9 GeV, and as clean a beam as is possible. Ideally, the beam intensity should be on the order of $8*10^6$/spill. We can also run with lower intensities for some of our studies. We believe our needs can be met with the following beam times:

100 hours	setup
150 hours	data taking at low intensity
150 hours	data taking at high intensity
400 hours	total

We can run parasitically during set-up and debugging, however, we will require priority control of the beam for approximately 7 shifts late in our data taking time. We would like to be located first in the beam line. In addition to a minimum of three chambers, we expect to install a Silicon telescope and plastic scintillator trigger counters. We plan to arrive approximately one week before beam start up.

We require 3 meters of length along the beam line and 2 meters in the transverse direction. We may have one crate located in the beam enclosure. We will use a precision transport system for scanning the chambers through the beam. Outside the beam enclosure we will require space for two electronics racks, one desk, one storage cabinet, one gas system (exact dimensions presently unknown), and two terminals. Our power requirements will not exceed 240 Amps, 110 Volts, single phase. (Three Camac crates, 1 VME Crate, 1 Fastbus Crate, two NIM crates, 1 oscilloscope, two terminals, PM Tube power supplies, IPC power and low voltage, Silicon power and low voltage.) The IPC gas is CO2::CF4 in a 50::50 ratio at atmospheric pressure, and is not flammable. Drawings are included with dimensions of the components. No other hazardous or toxic materials will be present, except for a source. We would like to request your assistance with the provision of a source on site to eliminate the need to transport radioactive materials. We will use 106Ru and/or a 55Fe.

Item	Person Responsible	Date Required	Date Expected	Back up or Assistance
IPC System	**Basem Barakat**			
Prototype	Basem			
Electronics	Jim Musser			
Mech. support	Basem			Gary Word
HV and cables	Basem			
Gas System	(Dick Plano)			Musser/J. Thomas
Cooling	not req.			
Silicon Telescope	**Saj Alam**			Dave Lee
Detectors	Alam			
Electronics	Alam			
Mech. Support				
LV, cables, cooling	Alam			
Trigger System	**Jenny Thomas**			
Scint. + PMT's	Jenny			
Logic				
HV and cables				
Mech. supports				
DAQ	**Rick Shypit**			
Work Station	Rick			
Fastbus Interface	Gary			
On line program	Jenny/Rick			
On line diagnostics	Rick			
Off line analysis	~~Gary~~ Jenny			
Schedule, coord.	**Kate Morgan**			

Letter of Understanding

We, the National Science Council on behalf of the Academia Sinica, the Universities and the Industrial Technology Research Institute, and the Superconducting Super Collider, express definite intention to proceed in accordance with the Cooperative Agreement (as attached).

1. Upon the signing of this letter, the following will start immediately (with all terms defined in the attached document).

   a) A start of the scientific exchange program

   b) The startup of the strengthening of the research groups and their infrastructure in Taiwan

   c) A start of the R&D (Research and Development) program and the collaboration on the engineering design of the GEM Central Tracker

2. Formal agreement will be signed upon the completion of due review process and approval from the relevant agencies of both parties. We expect this completion should not be later than February 1993.

Executed by the parties this 6TH day of NOVEMBER, 1992.

For Superconducting Super Collider Laboratory

R. Schwitters

For National Science Council

Yii Der Chuang

Electronics/DAQ

Dan Marlow

CSC Muon Electronics the GEM Detector

Presented to the

Korean Delegation

at the SSCL Laboratory

Daniel R. Marlow

Princeton University

January 18, 1993

GEM CSC Readout Design Goals

- Equivalent noise charge ($\sim 3000\ e^-$) rms (for $\tau = 300$ ns)
- Dynamic Range
  - — 50 μm measurement for strip width $w = 5$ mm

$$\frac{\sigma_s}{w} \simeq \sqrt{2}\frac{\sigma_q}{Q} \Longrightarrow \frac{Q}{\sigma_q} \simeq \sqrt{2}\frac{w}{\sigma_s} = 140$$

$\Longrightarrow$ 7.1 bits

  - — Landau tail $\varepsilon \simeq 95\% \Longrightarrow 40 - 230\ e^-$

$\Longrightarrow$ 2.5 bits

  - — $\times 2$ Design margin $\Longrightarrow$ 1.0 bits
  - — Total $\Longrightarrow$ 10.6 bits
- $< 10\ \mu$s conversion time
- Time resolution $\sim$ BX (for rejection of neutron hits)
- Low cost ($\sim$ \$10. – \$20. per channel)
- Radiation hard? $F_n \simeq 10^{13}$ cm^{-2} 10 SSC-yr^{-1} ?

<u>Neutron Rates</u>

- Currently very uncertain
- Product of three factors

$$R = \varepsilon_n F_n A \equiv r_n A$$

where

$$\varepsilon_n = \text{detection efficiency}$$
$$F_n = \text{fluence}$$
$$A = \text{strip area}$$

The efficiency

calculated → measured

$$2 \times 10^{-4} < \varepsilon_n < 5 \times 10^{-3}$$

the fluence (TN 92-91)

z=235cm → z=575cm

$$10^3 < F_n < 10^5 \text{ cm}^{-2}\text{s}^{-1}$$

the area

$$A = \ell w \simeq 300 \times 0.5 = 150 \text{ cm}^2$$

yielding a rate per strip (assuming $\varepsilon_n = 0.5\%$ of

$$0.75 < R < 75 \text{ kHz}$$

note that the corresponding rates per unit area are

$$5 < r_n < 500 \ \ \text{cm}^{-2}\text{s}^{-1}$$

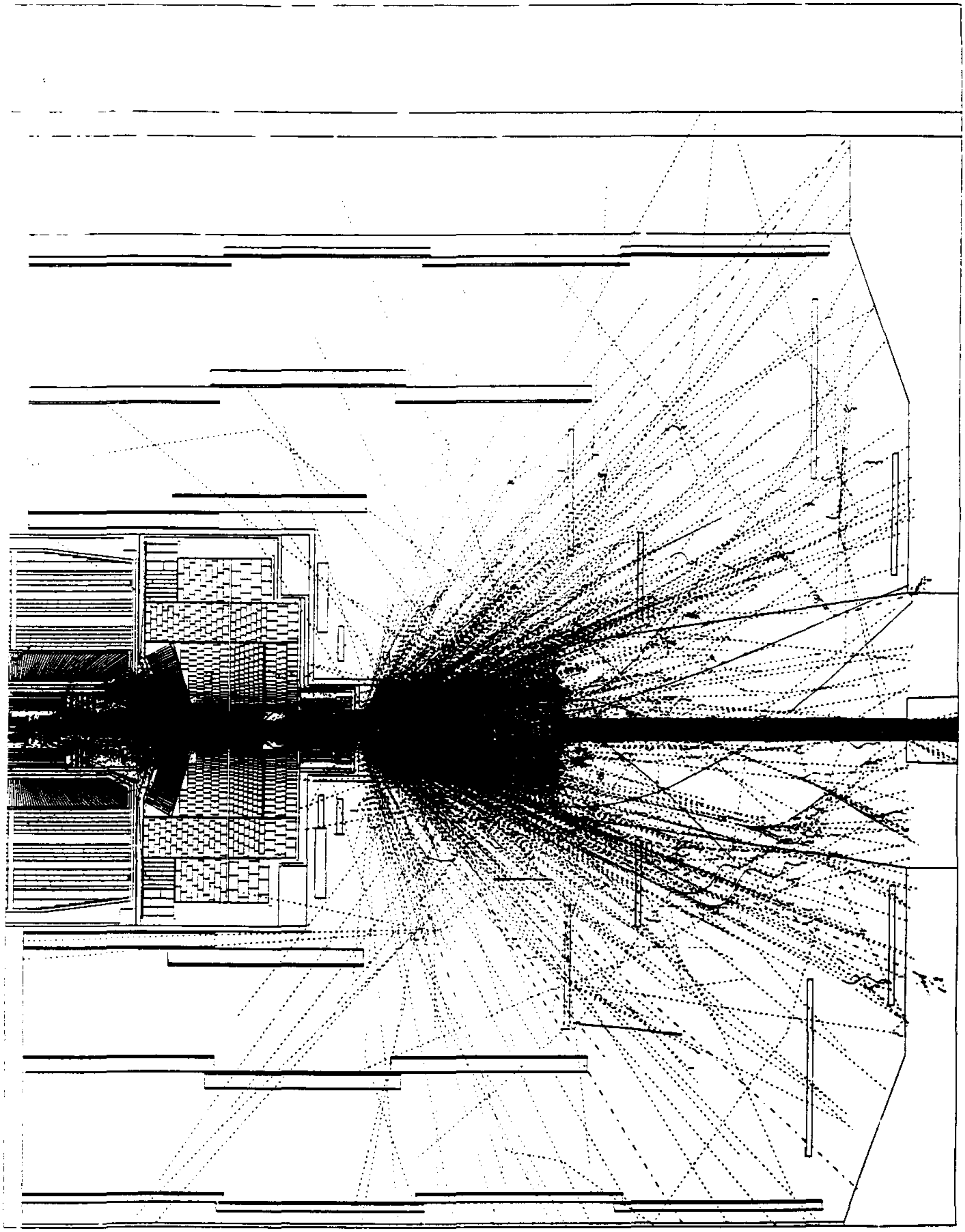

GEM Trigger/DAQ Design Goals				
Level	Rate In	Rate Out	Latency	Comments
1	60 MHz	10 kHz	2 μs	Synchronous, Pipelined
2	100 kHz	300 Hz	$\sim$ 100 μs	Asynchronous, Monotonic
3	3 kHz	10 Hz	—	CPU Ranch

Note: Design *goal* for rate out at each Level is 1/10'th the design *goal* for the input rate handling capacity of the subsequent Level.

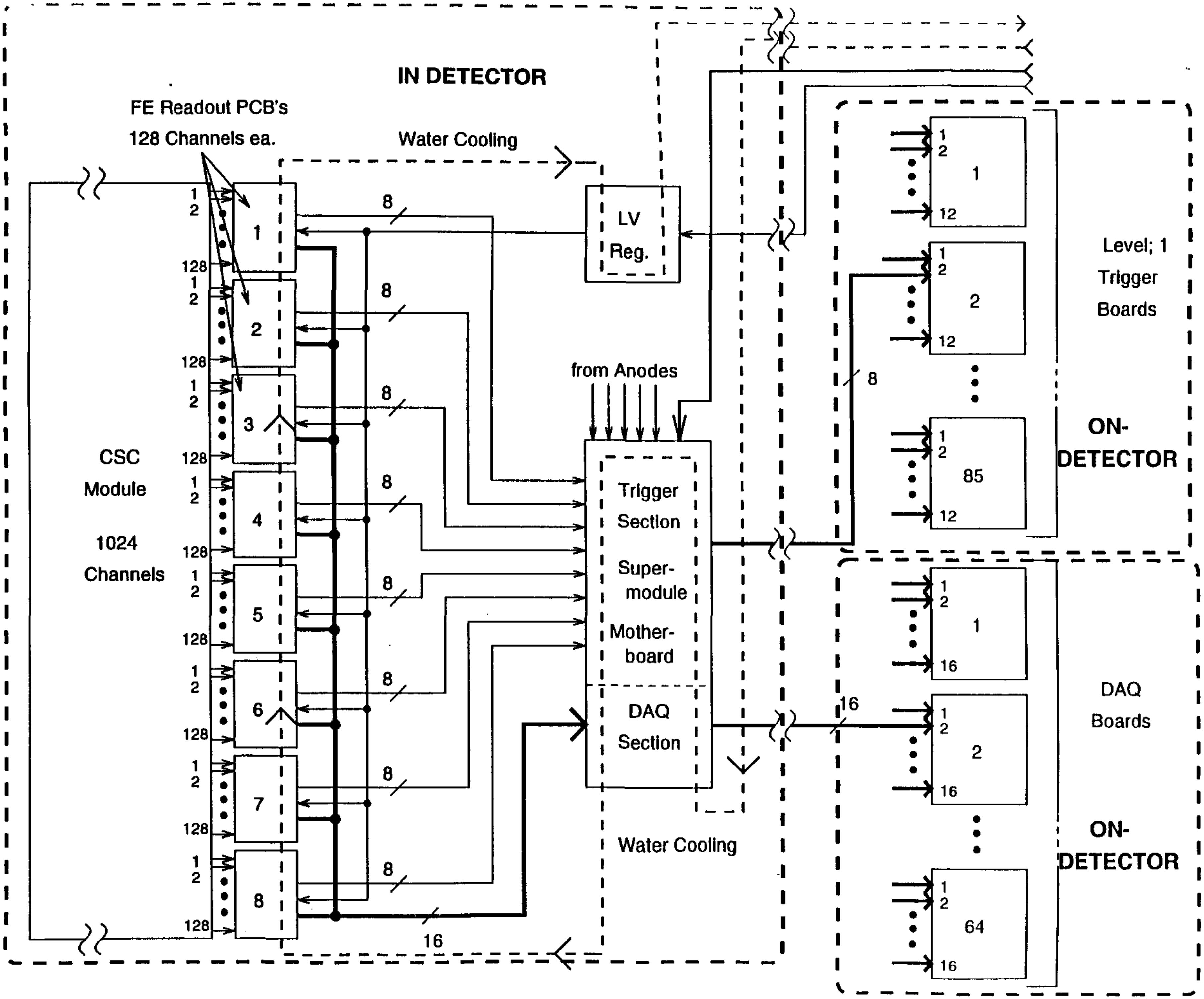
IN DETECTOR
FE Readout PCB's
128 Channels ea.
Water Cooling
LV
Reg.
CSC
Module
1024
Channels
from Anodes
Trigger
Section
Super-
module
Mother-
board
DAQ
Section
Water Cooling
Level; 1
Trigger
Boards
ON-
DETECTOR
DAQ
Boards
ON-
DETECTOR

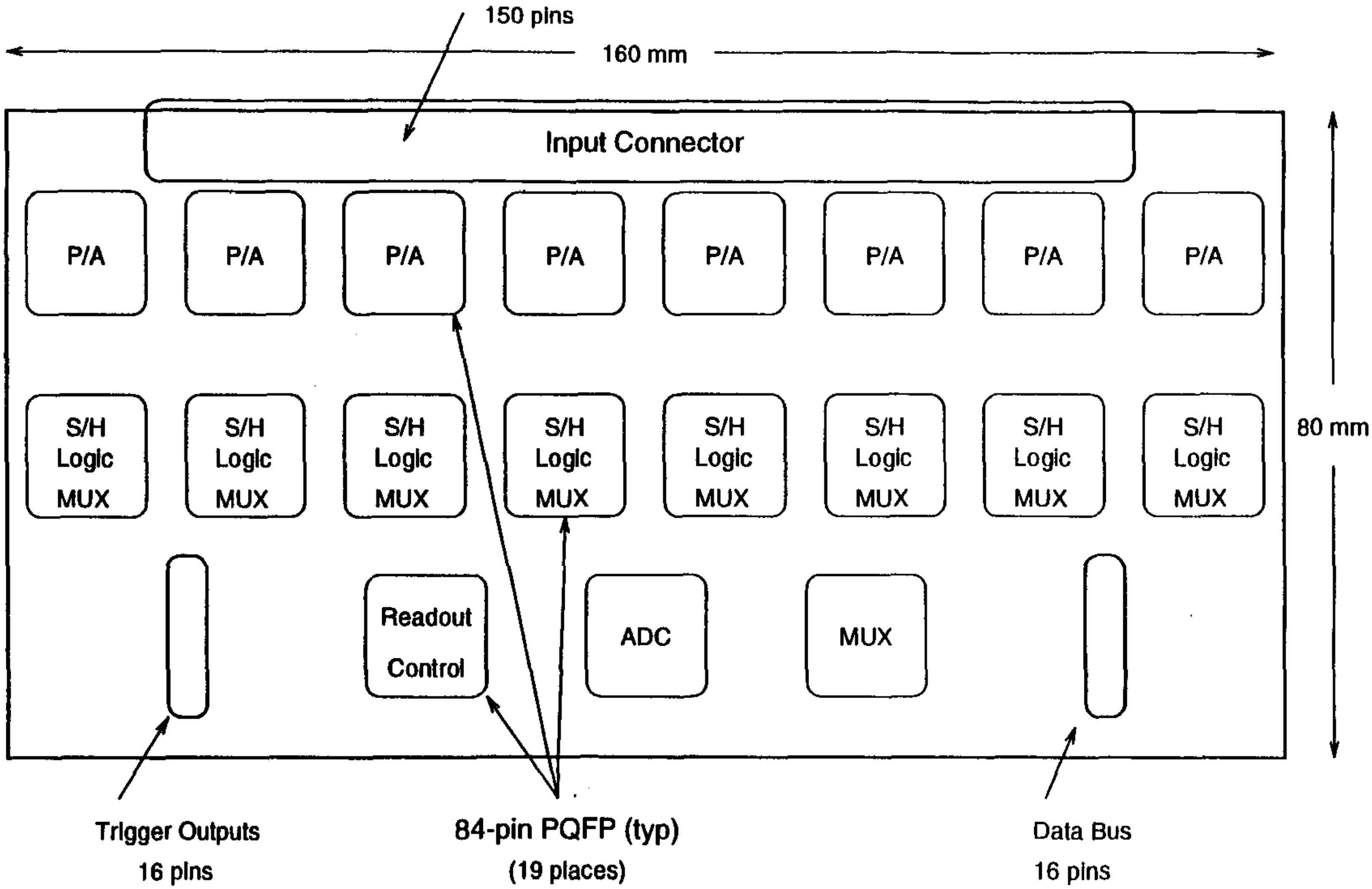

CSC Chamber Board Layout
128 Channel Version

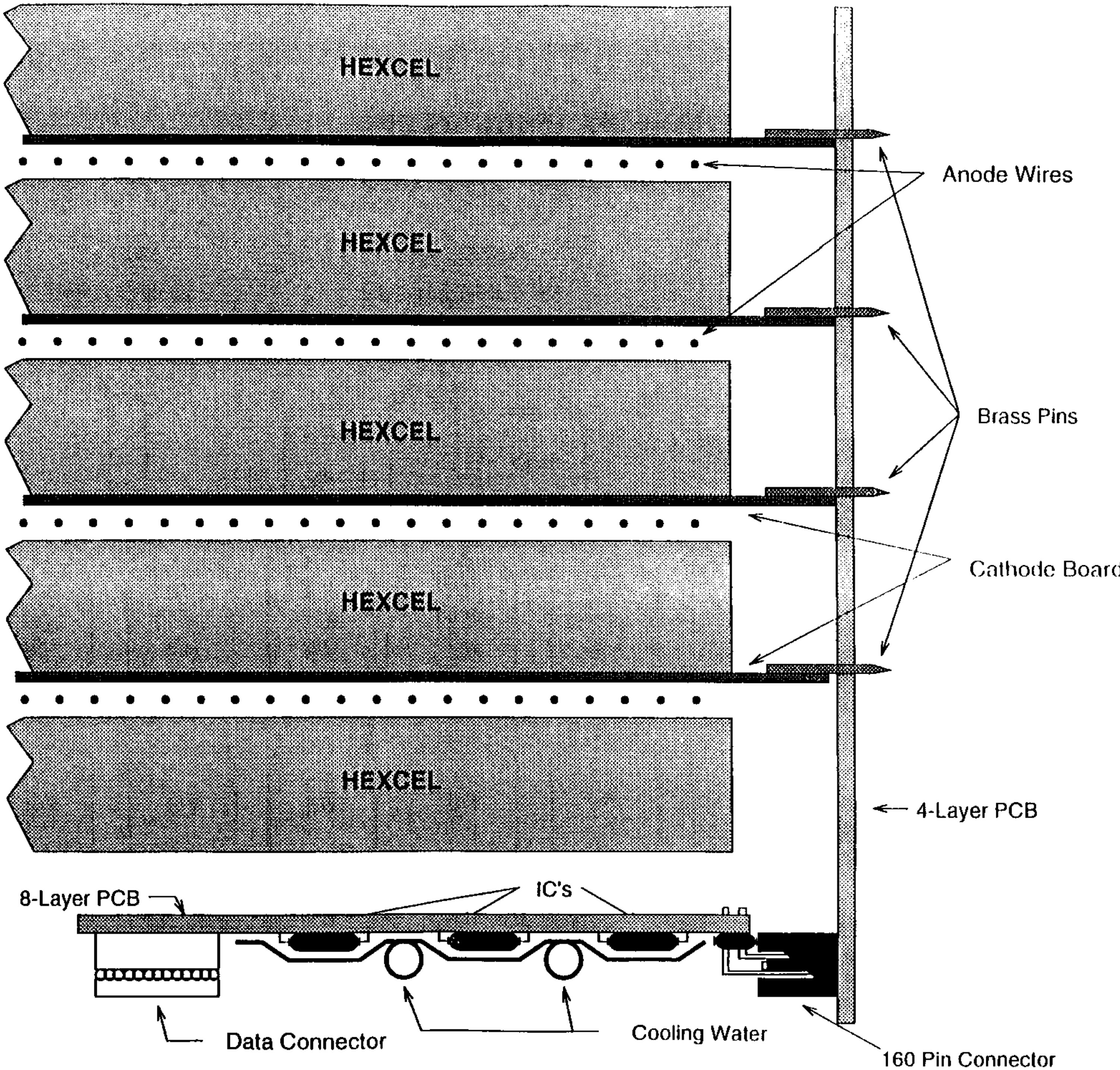
HEXCEL
HEXCEL
HEXCEL
HEXCEL
HEXCEL
Anode Wires
Brass Pins
Cathode Board
4-Layer PCB
8-Layer PCB
IC's
Data Connector
Cooling Water
160 Pin Connector

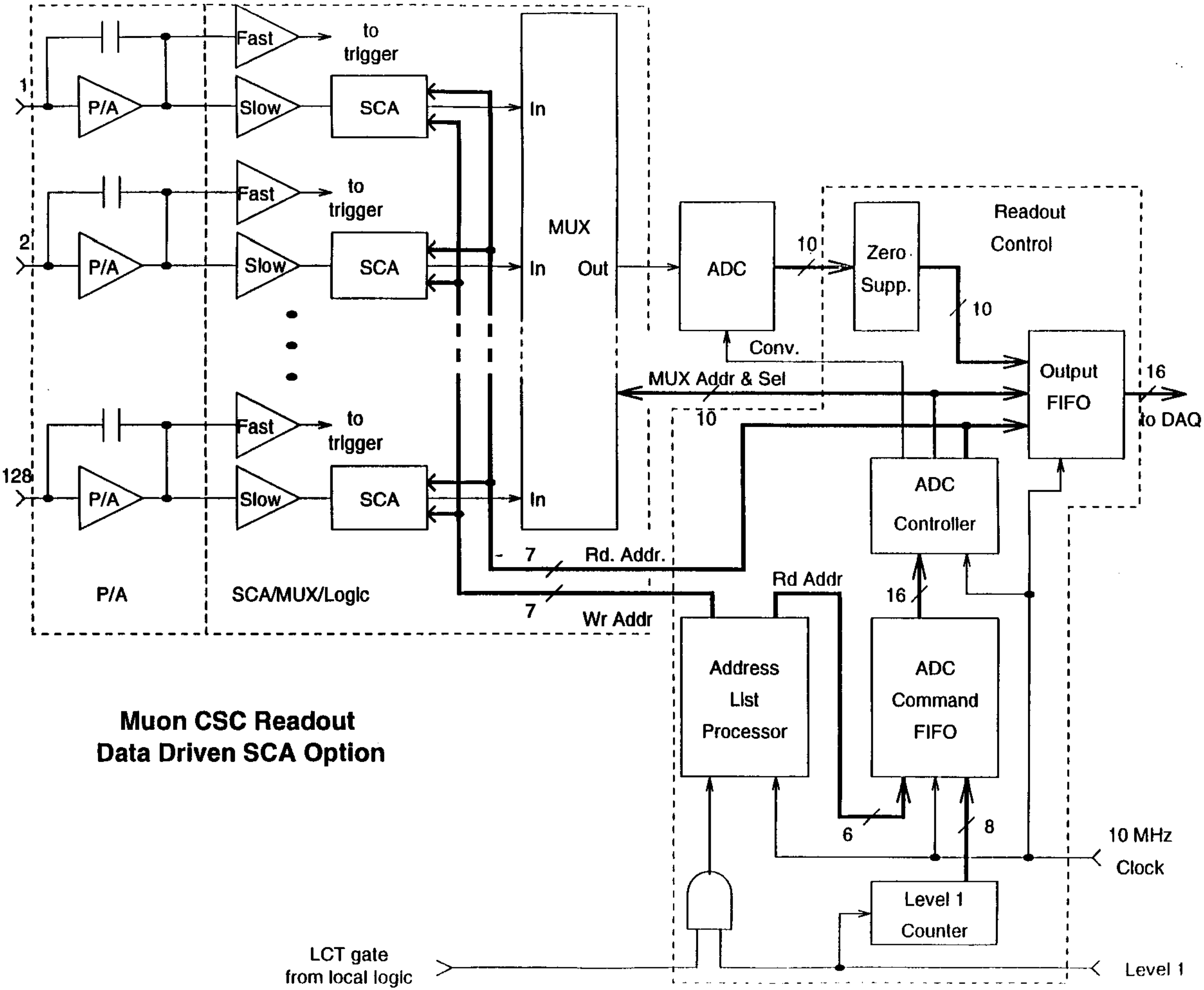

Muon CSC Readout
Data Driven SCA Option

Analog Pipeline (SCA) Option

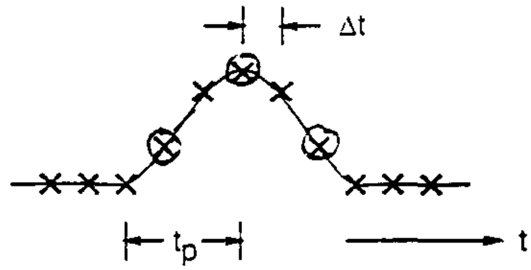

Assume

$$t_p = \text{pulse peaking time} = 300 \text{ ns}$$
$$\Delta t = \text{sample clock period} = 100 \text{ ns}$$

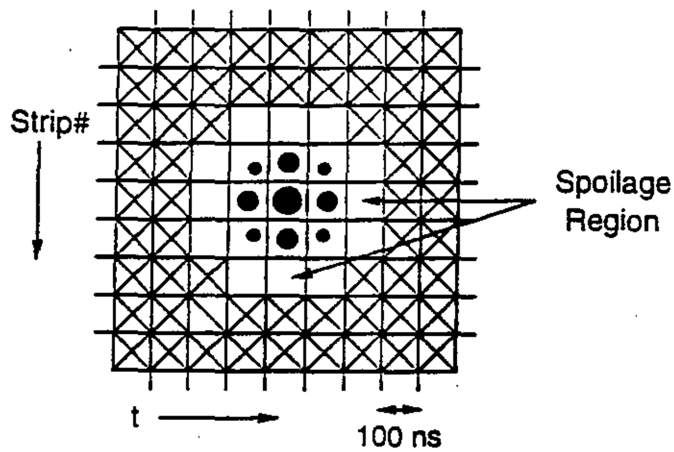

If accidental pulses falling within the indicated region in the space-time grid shown above are considered to spoil the signal pulse, the maximum unspoiled rate is given by

$$R_{\max} = \frac{p_{\max}}{21\Delta t} = \frac{0.1}{21 \times 10^{-7}} = 48 \text{ kHz}$$

(corresponding to $r = 320 \text{ cm}^{-2}\text{s}^{-1}$)

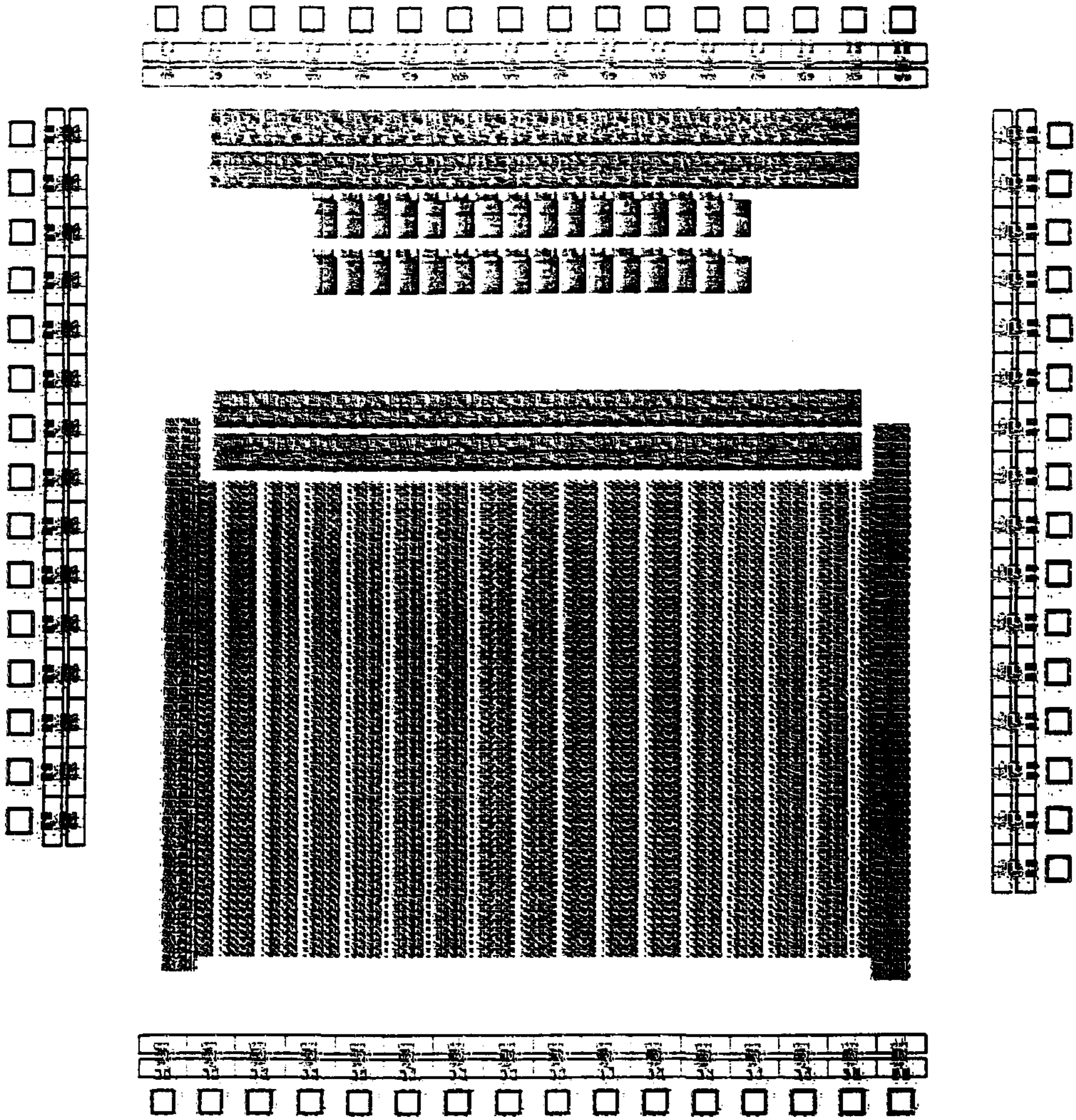

Advantages of SCA Readout

- Extracts maximum information from raw data
  - — Records "space-time" information
  - — Identifies BX on channel-by-channel basis
  - — Optimum identification and rejection of random hits
- Maximum clock frequency $\sim$ 10 MHz
- Conceptual simplicity
- Commonality with IPC & CAL readouts

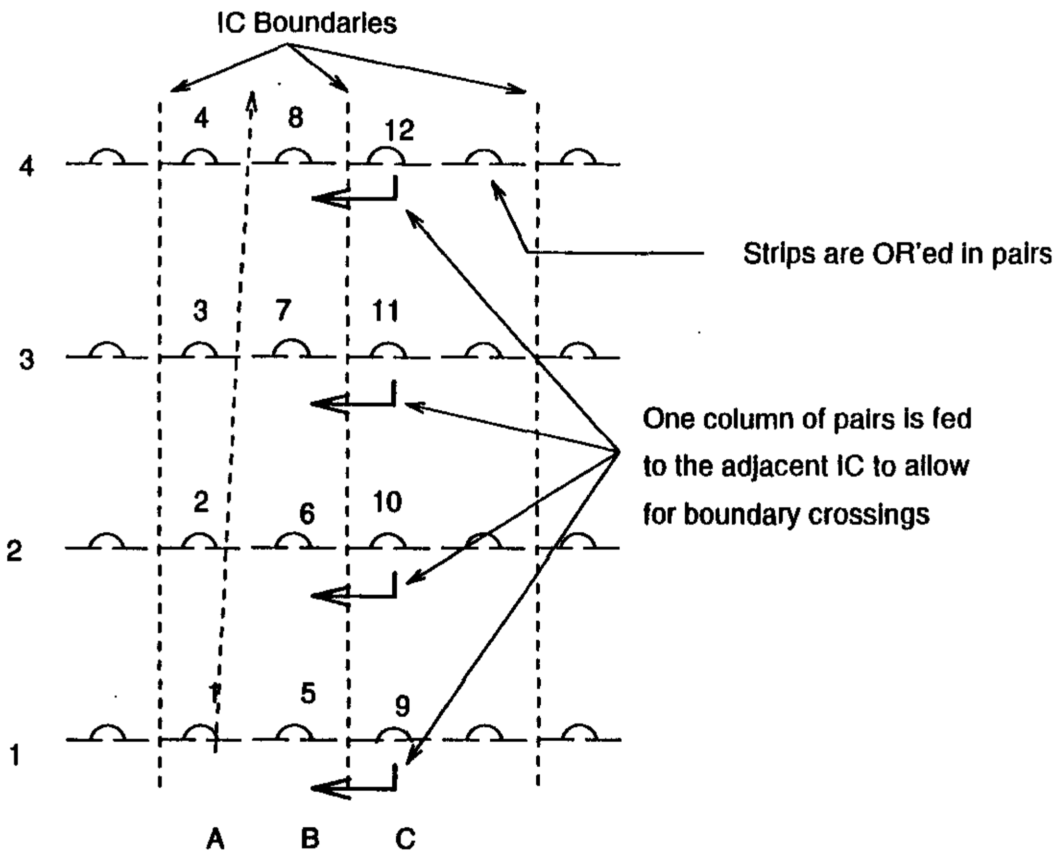

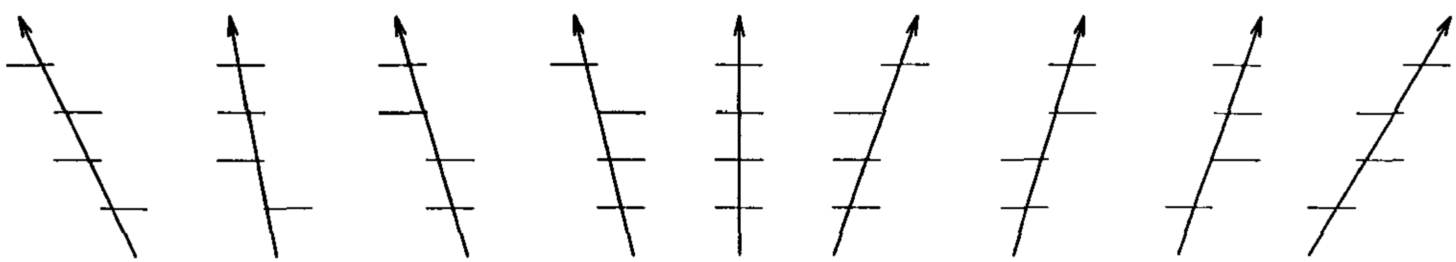

Possible Tower Combinations

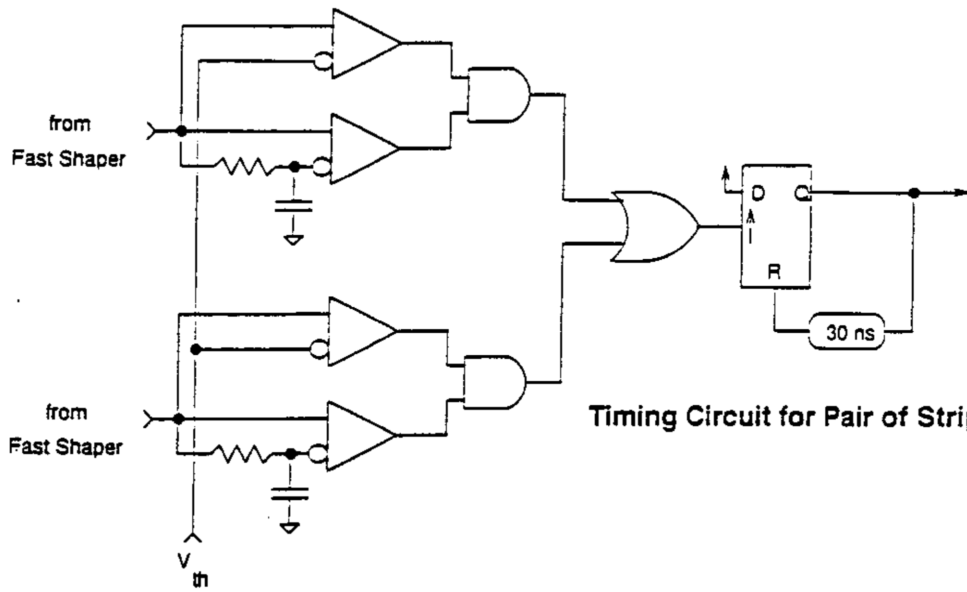

Timing Circuit for Pair of Strips

HIGH SPEED COMPARATOR

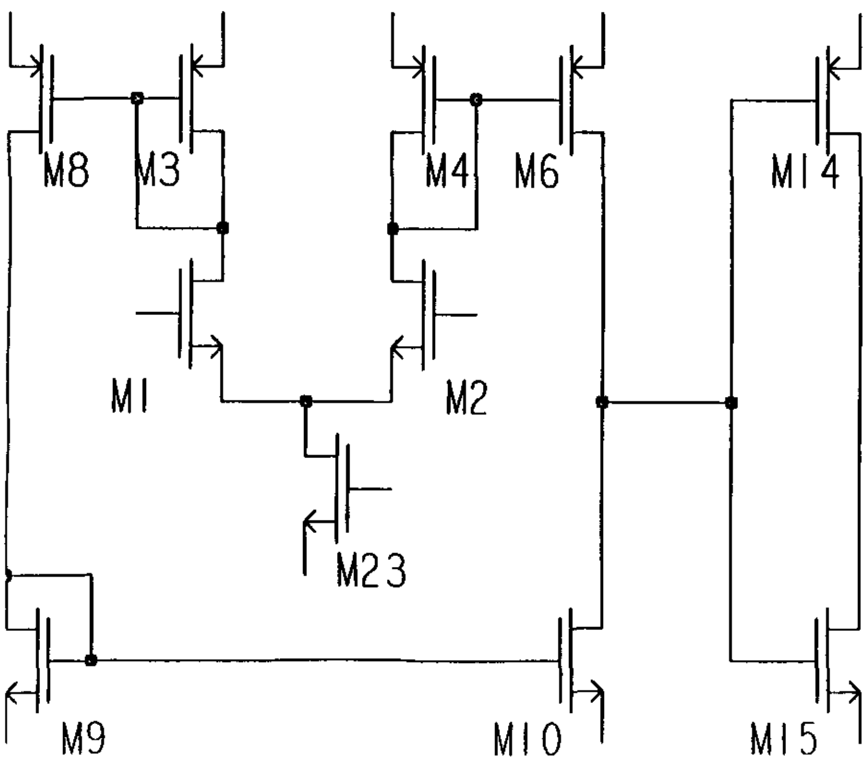

Ø.5V In

Fast Timer Circuit

Date/Time run: 01/03/93 18:34:41

Temperature: 25.0

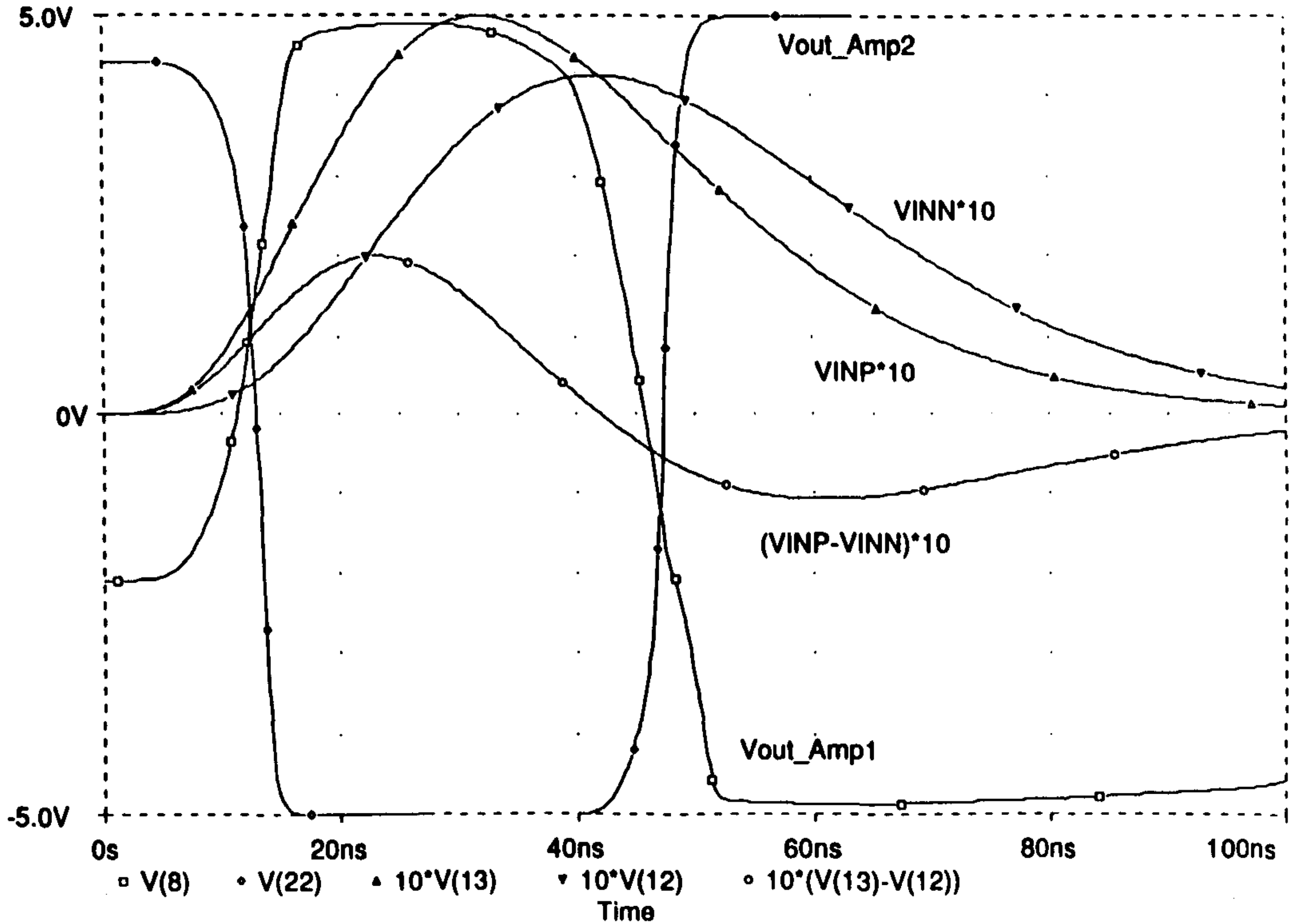

2.0V In

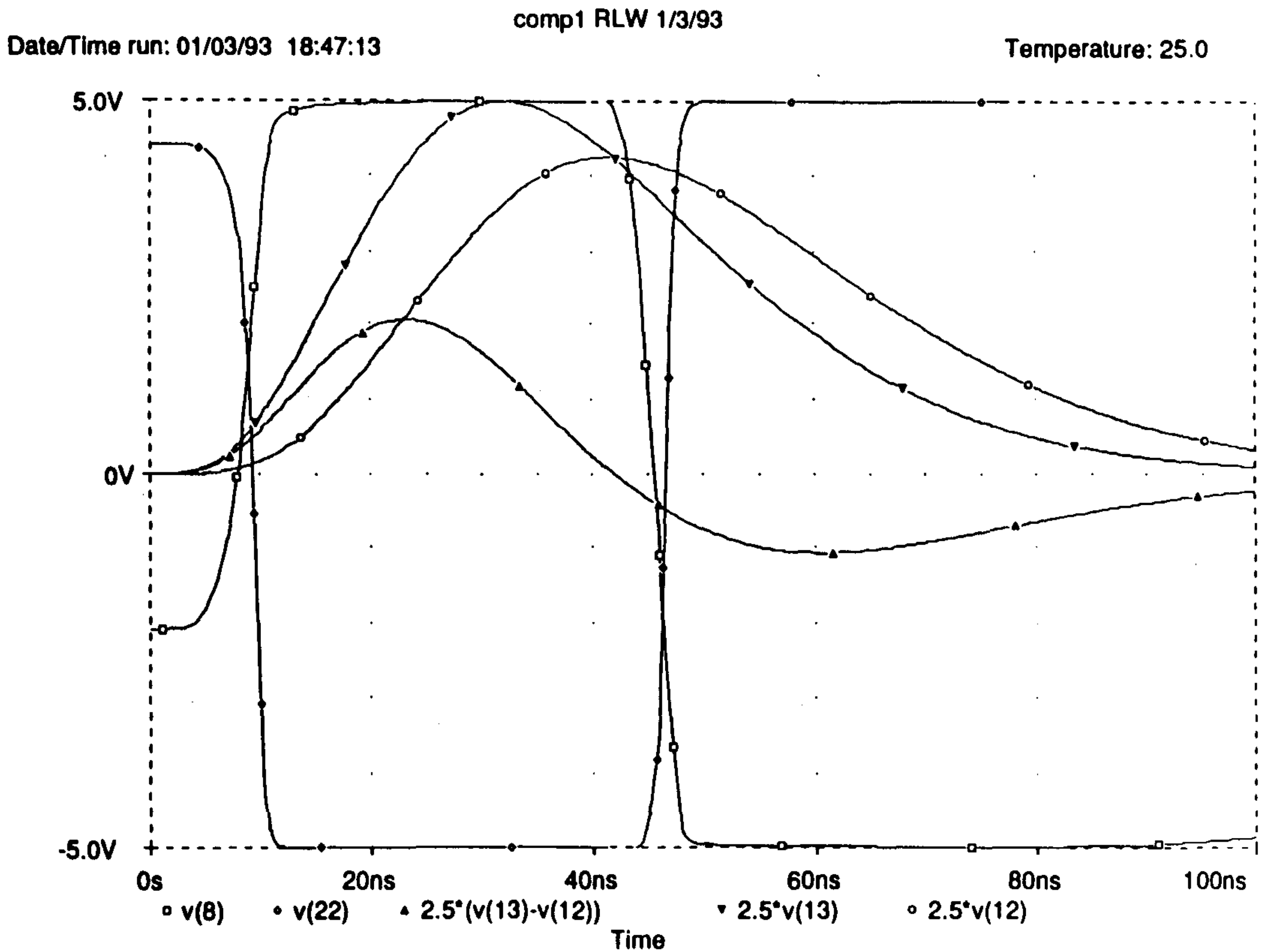

comp1 RLW 1/3/93
Date/Time run: 01/03/93 18:47:13
Temperature: 25.0
5.0V
0V
-5.0V
0s
20ns
40ns
60ns
80ns
100ns
v(8)
v(22)
2.5*(v(13)-v(12))
2.5*v(13)
2.5*v(12)
Time

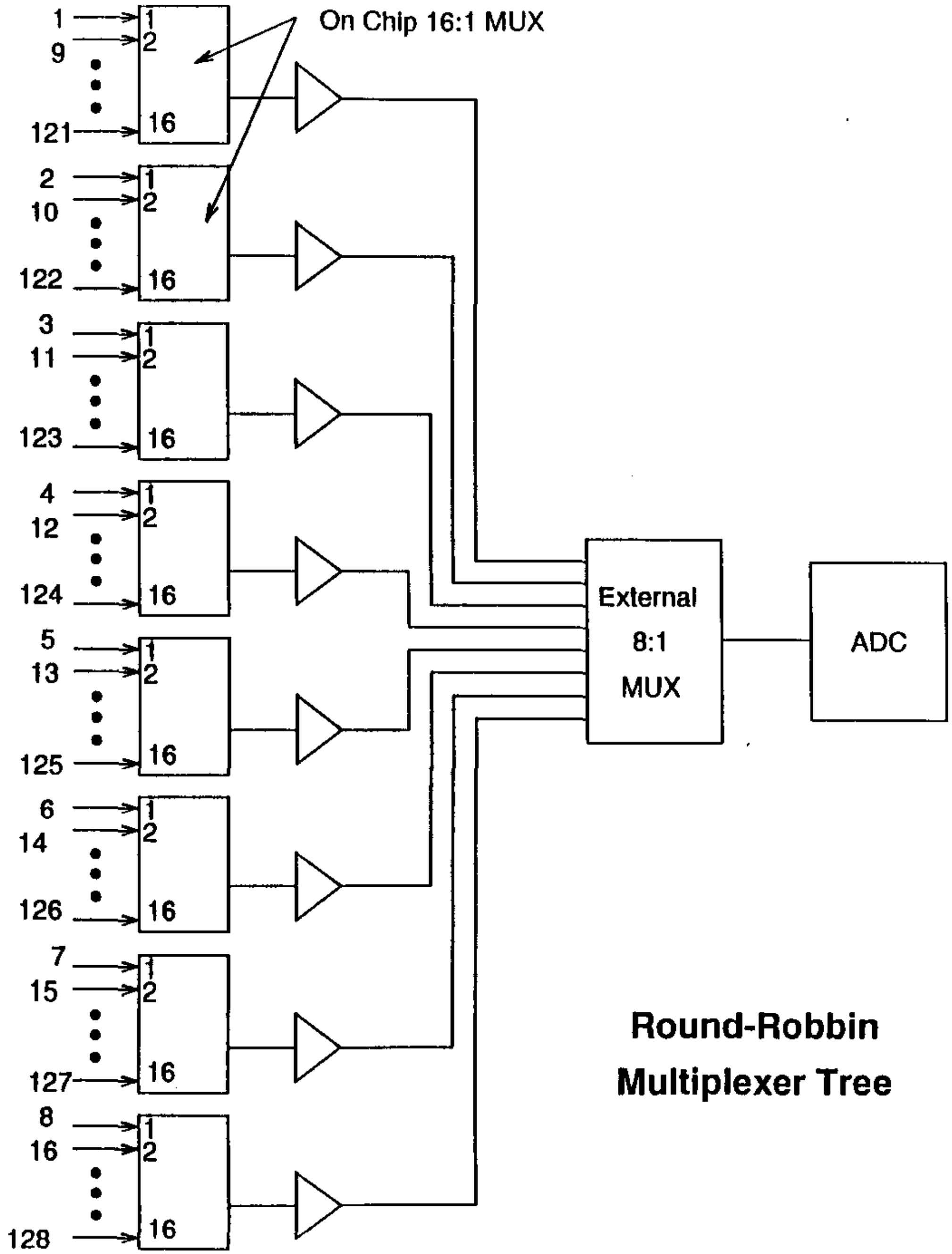

Round-Robbin Multiplexer Tree

SPT
SIGNAL PROCESSING TECHNOLOGIES

SPT7850*

10-BIT, 20 MSPS, 100 mW A/D CONVERTER

PRELIMINARY INFORMATION

EATURES

Monolithic 20 MSPS Converter
100 mW Power Dissipation
On-Chip Track-and-Hold
+5 V Power Supply Only
TTL Outputs
5 pF Input Capacitance
Low Cost
Tri-State Output Buffers
High ESD Protection: 6,000 V Minimum

APPLICATIONS

- All High-Speed Applications Where Low Power Dissipation Is Required
- Video Imaging
- Medical Imaging
- Radar Receivers
- IR Imaging
- Scanners
- Digital Communications

3ENERAL DESCRIPTION

he SPT7850 is a 10-bit monolithic, low cost, ultra-low power nalog-to-digital converter capable of word rates of a minimum f 20 MSPS. The on-chip track-and-hold function assures ery good dynamic performance without the need for external omponents. The input drive requirements are minimized due o the SPT7850's input capacitance of only 5 pF.

ower dissipation is extremely low at only 100 mW typical (150 W maximum) at 20 MSPS with a power supply of +5.0 V. The ower dissipation is further reduced to 70 mW typical (100 mW naximum) at a 10 MSPS sample rate.

The SPT7850 has incorporated proprietary circuit design and double-poly CMOS processing technologies to achieve its advanced performance. Inputs and outputs are TTL-compatible to interface with TTL-logic systems. Output data format is straight binary.

The SPT7850 is available in a 28-lead, cerdip package over the temperature range of 0 to 70 °C. For other package types, temperature ranges and /883 processing requirements, consult the factory.

3LOCK DIAGRAM

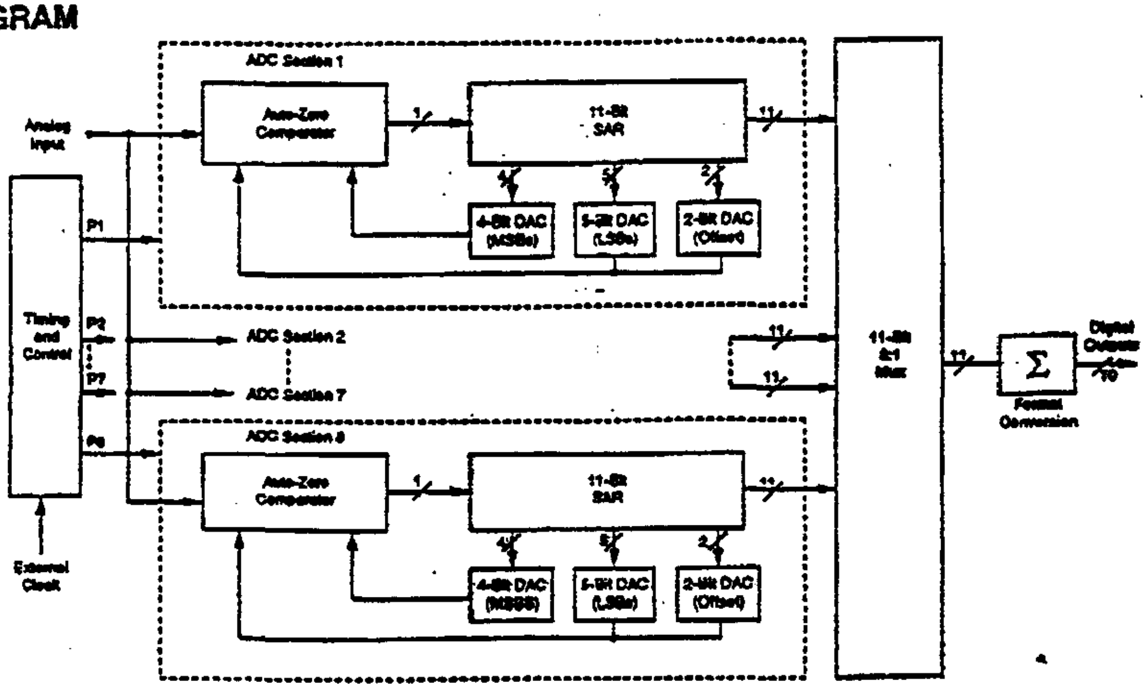

* Patent pending.

Signal Processing Technologies, Inc.
4755 Forge Road, Colorado Springs, Colorado 80907, USA
Phone: (719) 528-2300 FAX: (719) 528-2370

7.X GEM DATA ACQUISITION DRAFT - 1.2 OF January 8, 1993

7.x.1 Introduction

The Data Acquisition System is responsible for bringing the data for the relevant physics events to mass storage in an efficient way. It also provides the context in which the level 2 and level 3 triggers run and brings the data to these triggers.

A design goal specific to the GEM DAQ system is that all front-end chips are read after each level 1 trigger. This way no data has to be stored on the front-end chips during the level 2 decision. Only buffers of moderate size will be needed to de-randomize the level 1 trigger rate fluctuations. It also allows for level 2 implementations with large latency.

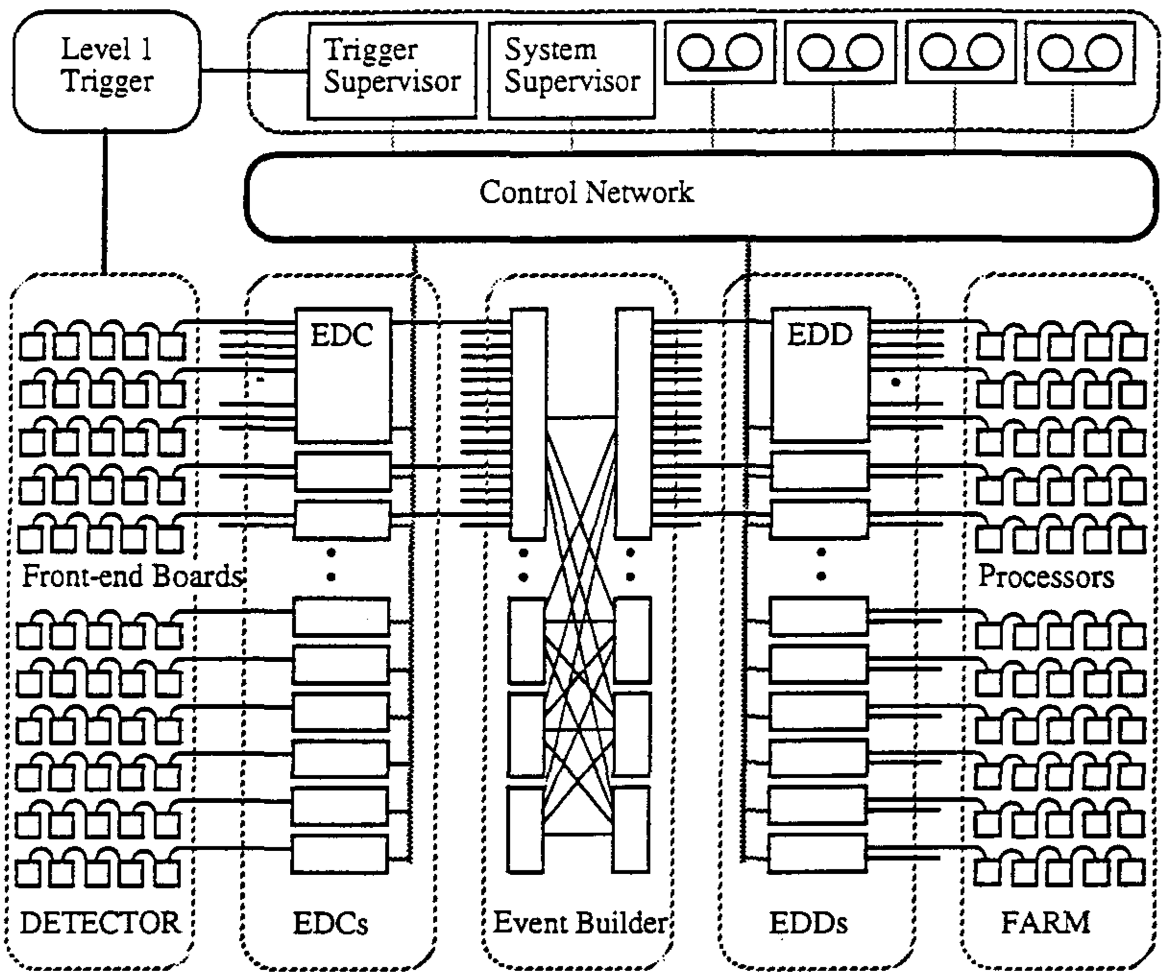

Figure 7.x-1. Overview of the GEM DAQ system

The level 2 and 3 algorithms will be executed in the general purpose processors of the on-line farm. Hence, the event data must be transported to the farm at rates up to the maximum specified level 1 trigger rate of 100 kHz. It also means that there are basically only two levels of triggering: a low latency trigger (level 1) and the combined level 2 & 3 that forms a high latency trigger. The latency for level 1 is fixed by the depth of the pipeline buffers on the front-end chips. The latency for level 2 & 3 is variable and limited by the cost of buffer memory.

We propose a readout (Figure 7.x-1.) where for each level 1 accept, the data from the front-end boards are read out via serial links of moderate speed. The data are stored in a number Event Data Collector modules (EDCs). These modules contain the large buffers where most event data remains during the level 2 execution. Data needed by level 2 & 3 are transported on high speed fibers to the processor farm via a switching network (Event Builder). They are received by Event Data Distributor modules (EDDs). Data for each event originate in different EDCs. Event data fragments are combined in the EDDs. The EDDs forward the data to the processors in the farm, again via moderate speed links.

Because front-end occupancies, trigger rates and trigger processing times are not yet well known, the initial design for the GEM data acquisition system places a large emphasis on scaling and flexibility. Below we describe the system in more detail.

7.x.2 Data Collection

The table below lists the major GEM subsystems with estimates of channel counts, number of front-end boards, number of bytes per events and data volume at a level 1 trigger rate of 100 kHz.

Table 7.x-1. Numbers of channles and Front-end boards for the GEM subsystems, number of bytes per event and data volume at a level 1 trigger rate of 100 kHz.

Subsystem	Channels	FE Boards	Bytes/event	Data Volume
Calorimeter	82 k	1640	50 kB	5 GBytes/s
IPC	446 k	1742	80 kB	8 GBytes/s
Silicon	3230 k	1262	20 kB	2 GBytes/s
Muon	518 k	518	40 kB	4 GBytes/s
Total	4276 k	5162	190 kB	19 GBytes/s

The estimate for initial level 1 trigger rates is 10 to 20 kHz. The data acquisition system should therefore provide a minimum capacity of 4 GBytes/s (190 kB/event * 20 kHz). To accommodate increases in trigger rates or data volumes, the design bandwidth must be scalable by a factor of five, preferably without replacement of any existing components. Load balancing is essential for economic use of the available bandwidth. It can be achieved by grouping of front-end modules so that the average data volume for any group of modules is equal. If the trigger rate or data compression mode changes significantly, the front-end modules must be regrouped. This is done most cheaply by re-cabling the front-end boards on the serial links.

All components in the data acquisition system are interconnected using point-to-point links which allow greater flexibility in system configuration and are generally more reliable. Standard backplanes are used only for power supply and auxiliary features, reducing the cost of the crates and software.

7.x.2.1 Data Format

A data packet (event fragment) is generated for every L1 Trigger Accept. If there is no data, only the packet header information is sent. A typical event fragment header might include a destination ID, event number, byte count and CRC followed by data. The data field may include a "data type" header and some source ID information. Consideration will be given to finding a common packet format which can be used in all low-speed links (both control and data).

7.x.2.2 Low bandwidth Data Links

A "low speed" bi-directional data link (approximately 100 Mbits/s) is needed for communication with front-end boards. The candidates which have been considered for this link standard include:

- AMD TAXI. This is the original 100 Mbits/s serial link. The user defines all protocol. Current cost would be approximately $150 for a bi-directional link.

- Transputer DS link. This is an very simple protocol, which will be implemented in the next generation Transputer and associated peripheral ICs, including a 32 port crossbar switch.

- IEEE P1394. P1394 is not yet well defined. It provides all the necessary protocol but may be more complicated than desired. The overhead seriously degrades performance for short data packets. The target cost is $50 for a bi-directional link. It is intended as a replacement for SCSI and general serial connections (keyboards, etc.).

- Fibre Channel, etc. Fibre channel, FDDI, and SONET protocols (and costs) are probably excessive for this application.

A standard link protocol is suggested because it allows use of commercial computers and software in testing of front-end boards. The current preferred "standard" is the Transputer DS link which can be implemented in user programmable logic. P1394 may be the eventual choice but it is dependent on availability of interface ICs and test of actual performance with small packets.

7.x.3 Event Data Collection modules

At the Event Data Collector, up to sixteen front-end serial data links are multiplexed to form a single 100 MByte/s data stream. This data is buffered in a large dual-port memory which serves two main functions; time-ordering of packets transmitted to the Event Builder (to eliminate blocking) and buffering of event fragments pending level 2 & 3 decisions. The EDCs send data to the Event Builder switch via 1 Gbits/s links.

7.x.4 Event Building

The Event Builder function is performed by a modular crossbar switch. Data flows through the switch in one direction only. If no more than 256 channels are needed, the switch can be assembled in 16 channel increments as a two stage design. In its simplest configuration, a N by N switch provides the equivalent of N**2 separate virtual data links, one from each Event Data Collector to each Event Data Distributor. Each of these virtual channels operates at a rate of 1/N Gbits/s. A 16 by 16 module implements 256 channels operating at 64 Mbits/s for a total bandwidth of 16 Gbits/s. A 256 by 256 switch has 65,536 virtual channels, each operating at 4 Mbits/s for a total of 256 Gbits/s.

If the switch is programmed to operate in a synchronous barrel-shift rotation, there are fewer external control requirements. This reduces the cost to about $500 per channel for the switch itself. However, it requires tight synchronization between the EDCs and the Switch. Data packets have to be ordered by the Event Data Collectors so that there is no blocking. Without the input queuing (time-slot interchange) function performed by the EDCs, a general-purpose switch would require three stages with an expanded intermediate stage. It would also require arbitration and feedback paths.

Commercial standards (such as Fibre Channel, SONET/ATM, SCI and HIPPI) have been examined for the high-speed data links and switching system. There is significant additional cost and overhead in using a general-purpose, bi-directional network but some of this cost is offset by the reduced development expense. Serial HIPPI appears to be the best choice among commercial standards.

7.x.5 Event Data Distribution modules

The Event Data Distributor receives packages from the switch through a high speed link. Switch packet boundaries need not coincide with event boundaries. The EDD reconfigures the data into event blocks that are then forwarded to the processors. Data is passed to the processors on 16 serial output links. The EDD also provides the path through which the processors write data to mass storage. If needed, data for many event can be grouped in large blocks before they are streamed to tape.

7.x.6 Level 2 Trigger

In the baseline design we assume that the level 2 decisions are taken in the farm. A single processor is allocated to each event and takes care of the complete level 2 & 3 trigger algorithms. The design is flexible and allows for different trigger strategies.

7.x.6.1 Alternative Event Building Strategies

There are several alternative trigger strategies. One can, for example, read out complete events or read data only as needed by the algorithms. For the first strategy one sends all data of an event to a processor, before the trigger algorithm decides on whether data is discarded or written to mass storage. There is no sharp distinction between level 2 and level 3 algorithms. This method involves a fairly simple control protocol since events can be send to the farm in the same order they were accepted by level 1.

The second strategy is currently the prefered one. The level 2 algorithm starts by reading the level 1 trigger output data. Based on the signature of the event, the algorithm retrieves only data needed by subsequent steps of the algorithms. For rejected events, data that are still in the Event Data Collectors are removed. For accepted events, all remaining data is brought into the processor and the level 3 algorithm is started. We no longer assume that the data stored in the Event Data Collectors is read out in monotonous order. This strategy may reduce the data traffic through the switch by a large factor, so that a smaller switch can be used.

The flexibility of the GEM DAQ design allows for more complex schemes as well. For example, it is possible to apply different levels of zero suppression on the data sets used by level 2 and level 3. It has been shown that the level 2 calorimeter algorithms perform well even if a 1 GeV threshold cut is made on the e.m. tower energies. The reduced data set for level 2 would be prepared in the EDCs and send to the farm. The much larger full data set would remain in the EDCs, and only be send to the farm for events accepted by level 2.

7.x.6.2 Execution times of level 2 algorithms

To estimate the contribution to the latency from the level 2 algorithms, we have run simple calorimeter trigger algorithms on a workstation. The algorithms perform rudimentary checking on the data, compute missing Et, build a lego plot and use it for jet and electron finding. Execution times depend strongly on the zero suppression level and will take several milliseconds on a 500 MIPS CPU. Execution times for tracking algorithms may be significantly larger. This indicates that the latency contribution from the algorithms themselves will be of the order of milliseconds. Hundreds of 500 MIPS CPUs will be needed to keep up with a level 1 rate of 100 kHz. As typical system latencies will be larger than a few milliseconds, each processor will be working on many events simultaneously. This will require extra processor memory, fast context switching and re-entrant code.

7.x.6.3 Level 2 Upgrade Path

An upgrade of the level 2 trigger may have different goals: reduced latency, smaller load on the processors, or reduced traffic through the switch. This can be done in many different ways. Special purpose coprocessors can be added to the farm or special purpose engines can be added to the Event Data Distributors. To reduce traffic through the switch, hardware must be inserted upstream from it. Special level 2 processors can be implemented for specific subsystems. For example, one can install a silicon tracker trigger in the silicon data flow path at the EDCs. The trigger would output lists of high Pt tracks to be used in the level 2 algorithms.

7.x.7 Level 3 Trigger and Mass Storage

Details on the farm and mass storage implementation are given in subsequent chapters. In essence, the level 3 trigger algorithms are executed in the processors connected to the Event Data Distributors. Events accepted by level 3 will be sent back to the EDDs to be stored on mass-storage devices. When processing power is available during and between runs, farm CPUs can execute off-line analysis of events just accepted by the level 3 trigger or stored during earlier runs. Processed events will be written back to designated storage devices. Obviously the farm can also be used for Monte Carlo studies.

7.x.8 Control Network

The most challenging aspect of this design is the control. Data flow must be regulated to use buffers and links in the most efficient way. Provisions must be made to download constants and software and to monitor the overall state of the DAQ system. Most of the control is done via a segmented Control Network. Event Data Collectors, Event Data Distributors and Tape Drives and connected with a medium speed data links. A general-purpose commercial network may be usable in this application. A Trigger Supervisor CPU is connected to the network to assign events to processors and a Supervisor CPU monitors the readout.

7.x.8.1 Front-end control

The bi-directional DS link is used to download and initialize each front-end board. During operation, the output channel is used for data transfer while the input channel is used to send asynchronous control information. For fast controls two lines are used. In addition to the crossing clock, there is a single coded synchronous line used to indicate a level 1 trigger Accept. It is also used to synchronize control messages received on the DS link. Synchronous control messages may include "reset", "start", "stop", "test", etc.

7.x.8.2 Event Data Collectors

Events are buffered in the Event Data Collectors. Control messages are used to request transmission to the Event Builder. As only part of the data used by level 2, only a fraction of the EDCs are asked to transmit it. For rejected events a control message is sent to request pending event data in the remaining EDCs. The required control network bandwidth for event data requests is estimated at 2 Gbits/s (100 kHz event rate * 256 buffers * 64 bits/message).

The Event Data Collector buffers hold the event data for the period of the level 2 decision, which is typically less than 100 milliseconds. This requires approximately 10 MBytes (100 MBytes/s * 100 milliseconds). A buffer size of 32 MBytes should provide adequate margin. If all data is transmitted following each level 1 trigger, smaller buffers of about 4 MBytes can be used.

7.x.8.3 Event Builder Synchronization

The EDCs, switch and EDDs operate from a common global clock, used for synchronization of data links and data packets. It should be relatively stable, to avoid drifts in the data link phase-locked-loops and should operate independently of the crossing clock.

7.x.8.4 Event Data Distributors

The data request messages from a processor to the EDCs pass through an EDD. By inspection of the messages, the EDD knows which EDCs have been requested to send data. The EDD waits until all requested data fragments have arrived, assembles the data and forwards them to the requesting processor.

7.x.8.5 Event allocation

Each processor in the farm provides buffer space for multiple events. As described below, the latency of the data collection network is large. A processor is has to ask for new events before it is done with all previous ones. To get a new event allocated to it, the processor sends an "event number request" message to the Trigger Supervisor CPU. This CPU sees the level 1 accept signals and knows how many events have gone to the EDCs. The Trigger Supervisor returns an "event number assignment" message to the processor that contains the event number for an event not yet allocated to any other processor. The processor then issues "send data" messages to the Event Data Collectors from which it needs data, specifying the event number and processor ID. While the event data is being transmitted, the processor continues to process one of the previous events in its buffers. The processor may request event data fragments in any order and may process part of the data before issuing additional requests. The processor must issue either a "send data" or "delete data" message to each Event Data Collector.

7.x.8.6 Data flow control

Each processor regulates its own data flow by requesting events only when it has a free buffer. This prevents buffer overflow in the processors. Processor efficiency is maintained by allocating multiple processes per processor. Each process has a buffer associated with it and deals with only one event. When no new event data are available for processing in the EDCs, the processor can allocate time to off-line processing.

The EDDs have very large buffers, calculated to avoid buffer overflows. If under exceptional circumstances buffers in an EDD starts to fill up, messages must be sent to the EDCs to limit data flow to that particular EDD. The Event Builder and high-speed data links are entirely synchronous, so no overflows are possible in these components. The Event Data Collectors avoid overflow by sending XON/XOFF type control messages to the individual front-end modules.

The net result is that the only components in the data acquisition system which are subject to overflow are the front-end modules. "Almost full" signals from each front-end module are ORed at the Trigger Supervisor or Gating Logic to inhibit triggers. The front-end module must either allow sufficient space for the remainder of the event which caused the almost full condition, or it can generate a data packet with an "incomplete data" type field for that event. In any case, the front-end module should send a packet for every event trigger.

7.x.8.7 *Data flow latency*

The time required to access a block of data in an Event Data Collector and transmit that data to an Event Data Distributor is a function of the block size and access method. For example, sending a 1 kB block at 1 Gbits/s takes 8 microseconds. However, in a N channel system, the Event Builder provides the required EDC-EDD connection only 1/N of the time. Hence, before retrieving a 1 kB block of data in a 256 channel system one must wait between zero and 2.5 milliseconds. However, under full load the derandomizing output buffers in the EDCs normally contain several events and one may have to wait several full cycles of the barrel switch. This adds order 10 milliseconds of latency to each set of event data requests to the EDCs. As a typical level 2 algorithm may require 4 to 6 sets of data before an event is rejected, leading to overall latencies of about 50 to 100 ms. This means that up to 10,000 events may have to be stored in an EDC. For strategies where all data are shipped to level 2, an important contribution to the latency comes from the time it takes to transmit complete events over the medium speed links to the processors and leads to latencies of about 30 ms.

7.x.8.8 *Error Detection and Recovery*

At a data link bit-error-rate of 10**-15, an error can be expected every 1000 seconds. When an error is detected, data from several thousand events may reside in Event Data Collector buffers. If the system is reset following each error, approximately 0.01% of the events are lost. This is acceptable if the reset is very fast. Detection of errors can be accomplished with a simple checksum or CRC on each data packet.

7.x.8.9 *Monitoring*

The System Supervisor consists of one or more workstations. They download embedded software and configuration data to the data acquisition system. During operation, various components of the data acquisition system transmit summary status information to the System Supervisor for monitor purposes. User control of the DAQ is sone via these CPUs.

7.x.9 Partitioning

Partitioning is the mechanism by which several users can independently read different parts of the detector. This mechanism is needed during commissioning, testing and calibration. In its most basic implementation one group of processors can read a given set of front-end boards, while another processor group reads a different set. To apply partitioning, one must control the different groups of front-end boards independently. They get independent level 1 trigger signals and may have independent dead times and event number sequences.

We propose to provide partitioning at the Event Data Collector level. All front-end boards connected to one EDC will always belong to the same partition. As different partitions share resources such as Control Network and switch, overall throughput may suffer in a partitioned system. This will happen, for example, in a simple partitioning scheme, where a group of 16 Event Data Collectors connected to a single 16 X 16 switch module, is read by a group of 16 Event Data Distributors, also connected to a single switch module. The throughput will decrease as only a limited number of physical links are available between the input and output switch modules. In a 256 X 256 switch the bandwidth will decrease by a factor 16. This can be avoided by using a different set of EDDs, namely 16 EDDs that are connected to the 16 different output switch modules.

7.x.10 Scalability

The design of the overall Data Acquisition System is done such that components can be used to implement smaller systems. This way one can provide data acquisition facilities that are needed for front-end electronics tests and detector prototype tests.

The smallest system with relatively few channels would be a single front-end group. One uses standard front-end boards to acquire the data. As a standard serial link is used to connect the front-end boards, any processor with an interface to that link can be used to handle the data.

For a larger setup, up to sixteen front-end groups can be hooked up to one Event Data Collector. If the data rate is low, the data could be transferred over the medium speed serial I/O link of the EDC that is normal used for control only. Again any processor with an interface to that link can be used to handle the data. If the data rate is high, the data could be shipped over the high bandwidth link to an Event Data Distributor.

The largest 'small system' would be of the detector sub component size. The Data Acquisition System for such a setup would use several Event Data Collectors and would be connected to several Event Data Distributors via a single 16X16 switch module. Additional processors would provide the Trigger Supervisor and Storage Supervisor functionality.

7.x.11 DAQ Software

The GEM-DAQ software covers all aspects of computing in any part of the data acquisition, except in the areas where physics code is executed. For example, The DAQ software is responsible for the proper generation of timing and control signals and the data manipulations in all stages of the readout. Trigger algorithms and non-critical applications such as slave monitors, some GUI's etc. can be handled by other project groups.

The main purpose of software in the GEM-DAQ is to provide flexibility, reliability and modularity in a complex environment. In most cases, deterministic behavior is required of hardware devices and software algorithms, running on a wide variety of processor platforms, linked together by different communication mechanisms.

Care has to be taken not to degrade the readout by using unsafe programs or by using software where a hardware implementation of a certain function could do the job equally well. We believe that a balance between hardware, supported by imbedded software, and software, running on a commercial hardware platform is of utmost importance for the success of the DAQ. As a consequence, all projects and tasks in the GEM-DAQ, whether hardware or software, have to follow a stringent design, test, implementation, and review process to enhance the chances of having a final product that meets specifications.

Requirements:

All software components of the GEM-DAQ have to be designed with the following requirements:

- Established need: Any component must have proven, well documented reasons for its existence before the implementation and integration of the component is carried out.

- Modularity: Any component has to execute its functions independent of the presence of other components. In other words, any component has to have some degree of data encapsulation and hiding, resulting in easier implementation of the requirements.

- Reliability: During the design of a component, the required reliability of the component has to be specified. On the architectural level, the impact of a component failure has to determined. The need for fire-walling and the level of redundancy has to be established. Where possible, security should be improved by using techniques such as data hiding or redundancy. Each component should be well documented.

- Testability: Every component has to be testable according to reliability assessments in isolation and together with other relevant components. For testing standard protocols will be used where available.

- Standard: Wherever possible, software standards, developed by industry backed international groups such as IEEE, OSF, POSIX etc. should be used. The acquired knowledge from software developers surpasses by far HEP internal capabilities. Where appropriate, members of GEM-DAQ will try to work in close collaboration with workers outside HEP.

- Portability: All components should be adaptable to changes in environment. Every component has to have a well defined, standard interface to the outside world. Where possible, the code and the structure within a component have to be transportable between computer architectures, languages and data formats.

- Expandability: Component functionality should be reusable. Components should allow for the addition, deletion and alteration of its functions. New components should be constructed from already existing ones (inheritance).

internal capabilities. Where appropriate, members of GEM-DAQ will try to work in close collaboration with workers outside HEP.

- Portability: All components should be adaptable to changes in environment. Every component has to have a well defined, standard interface to the outside world. Where possible, the code and the structure within a component have to be transportable between computer architectures, languages and data formats.

- Expandability: Component functionality should be reusable. Components should allow for the addition, deletion and alteration of its functions. New components should be constructed from already existing ones (inheritance).

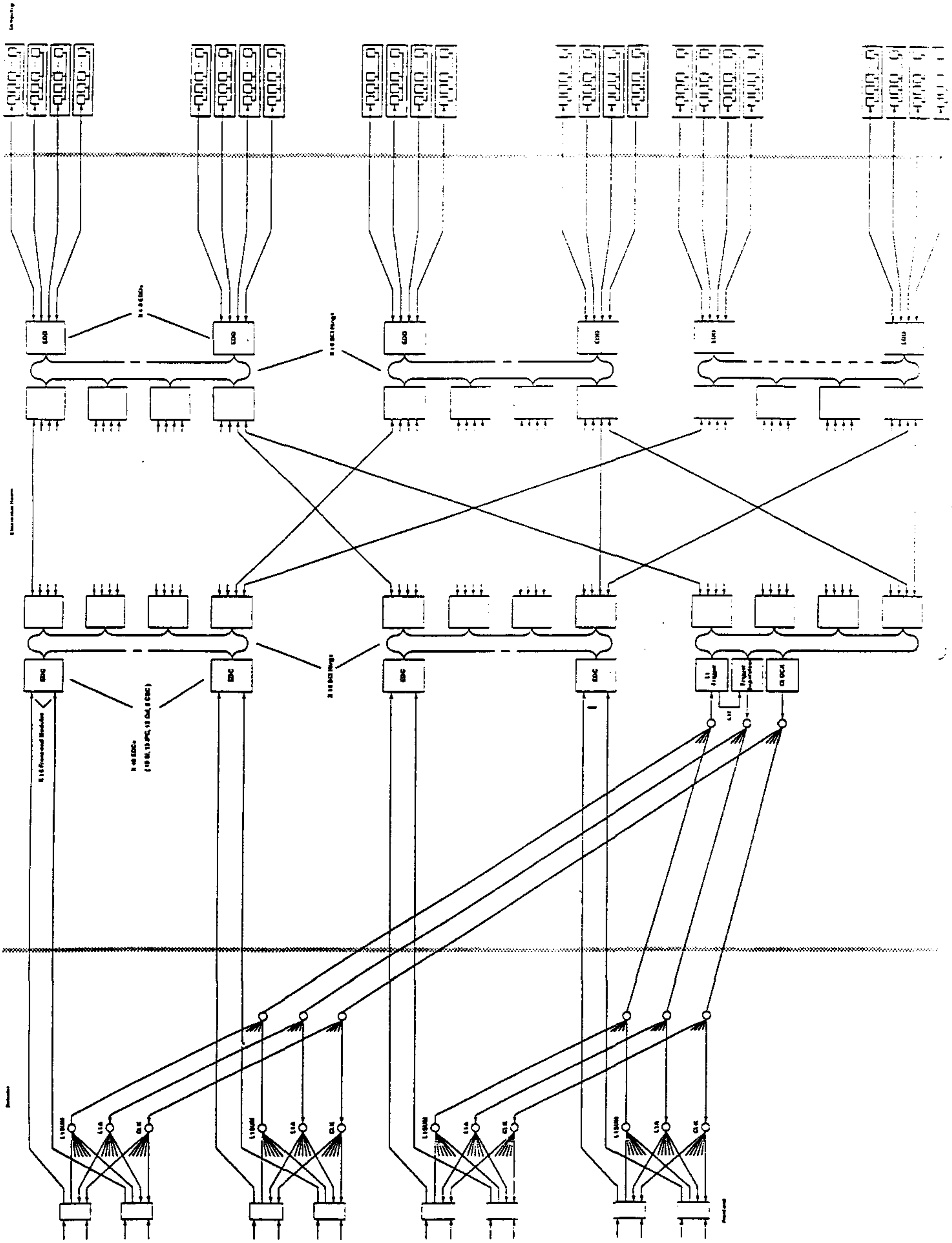

Advantages of SCA Readout

- Extracts maximum information from raw data
  - — Records "space-time" information
  - — Identifies BX on channel-by-channel basis
  - — Optimum identification and rejection of random hits
- Maximum clock frequency $\sim$ 10 MHz
- Conceptual simplicity
- Commonality with IPC & CAL readouts

Physics/Simulation/Computing

Ken McFarlane

GEM Computing (K. McFarlane)

Ensure that computing systems are in place to fulfil overall goals of GEM.

- Control Systems
- On-line Computing (Event Filters)
- Reconstruction
- Storage
- Analysis
- Simulation

Requirements/goals

- Assured quality
  - Easy correlation of data from different sources (events, monitor, calibration)
  - Tested software
  - filter design and testing
  - data definition/dictionary

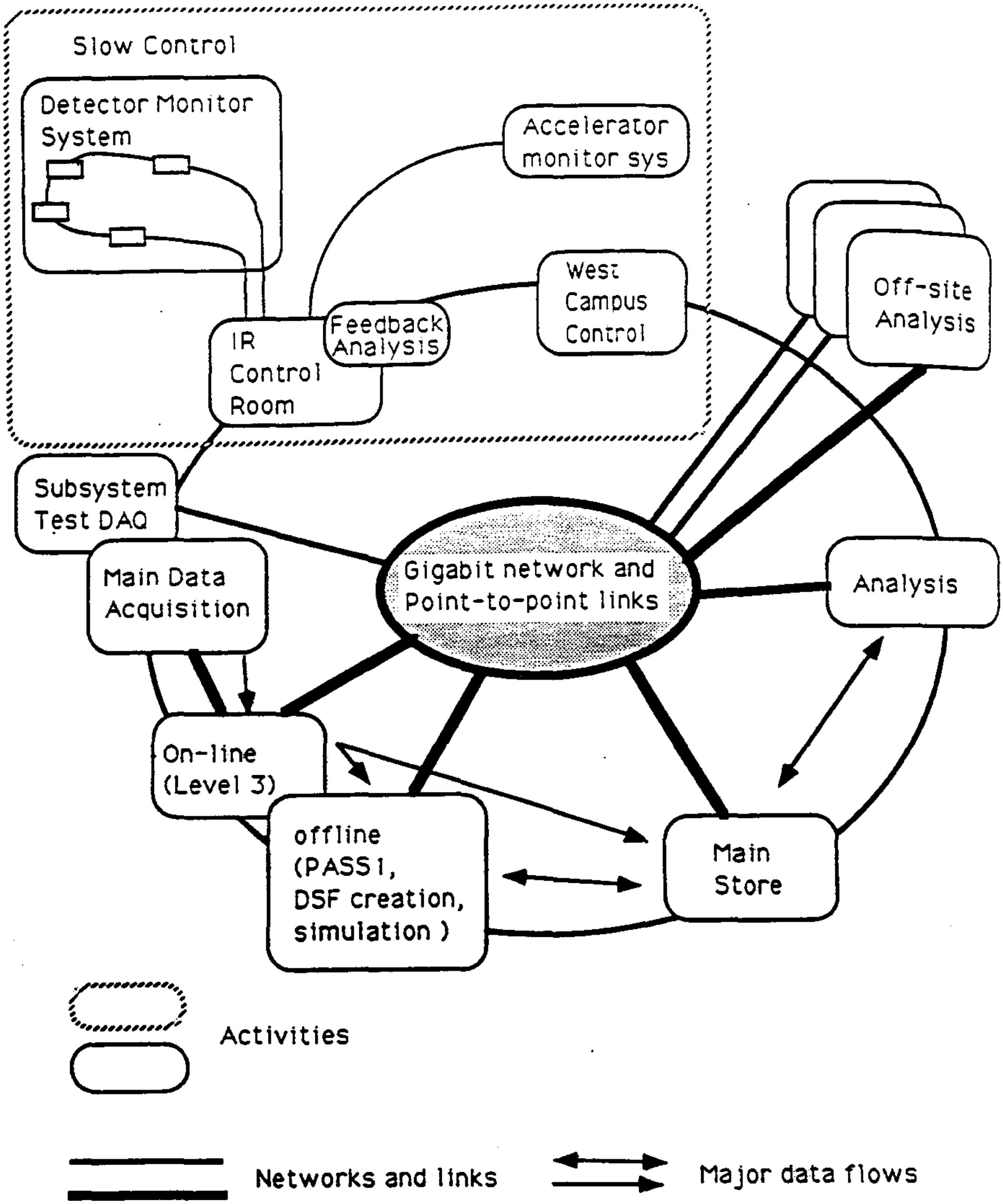

Figure 1 - Gem Computing System schematic

Data Flow

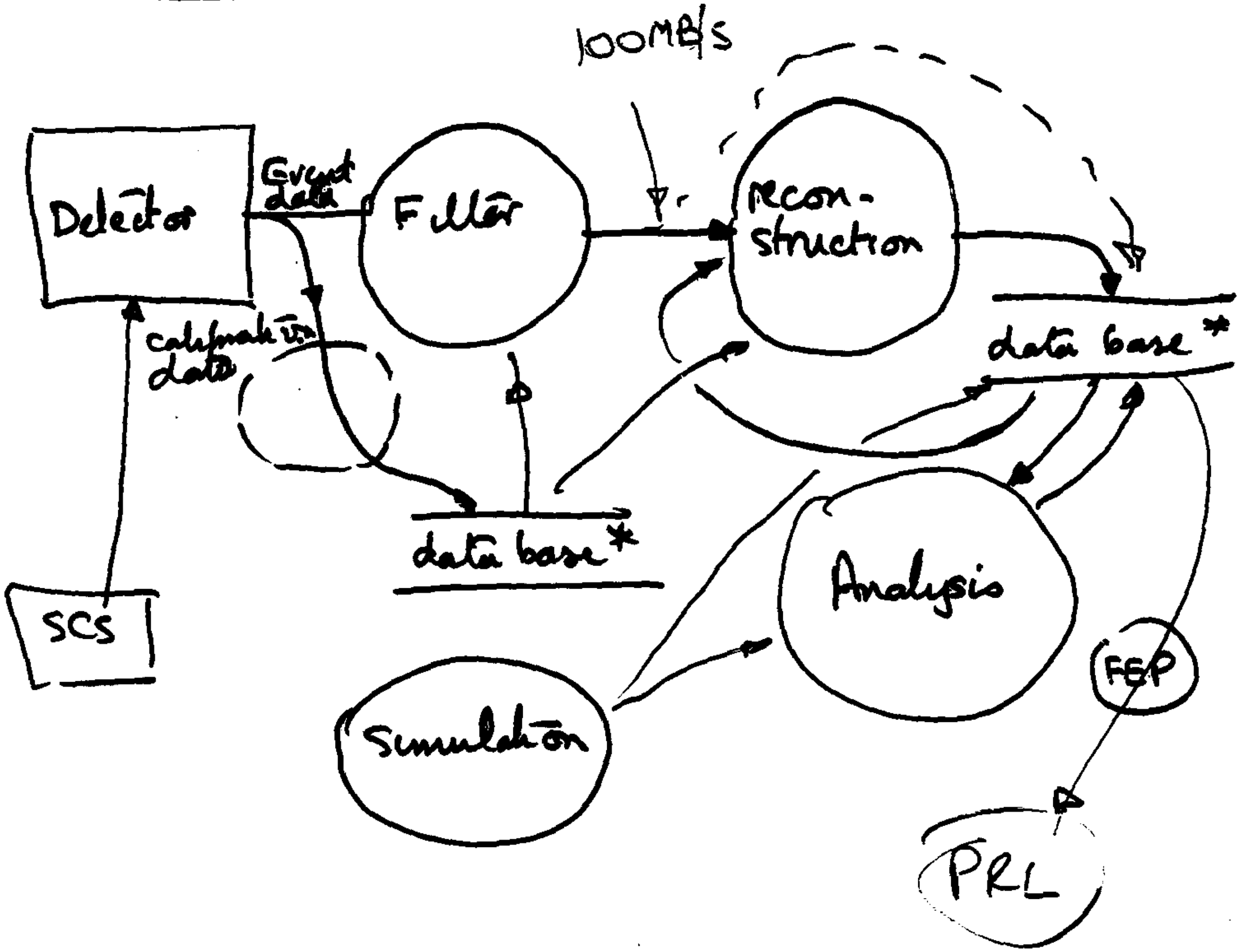
100MB/s
Detector
Event data
Filter
recon-
struction
calibration data
data base*
data base*
SCS
Analysis
Simulation
FEP
PRL

COMPUTING

Requirements Summary

Note that we have adopted the convention of Section 13, that the input capacity of a trigger level should be 10 times the desired output rate from the previous level. This permits variations in the rejection ratio of a given level. However, we desire to have the full capacity available at detector turn on, to allow the use of loose triggers. The expected rates are shown in Table 14-1. It is assumed that the input to PASS1bis is the output of PASS1, not Level 3.

Table 14-1 -- Trigger rates, event sizes and rate to storage

Stage	Input rate	Rejection factor	Output rate	Event size	Rate to store
Level 1	60 MHz	600 - 6,000	10-100 kHz	0.35 - 1 MB	NA
Level 2	10-100 kHz	30 - 300	0.3 - 3 kHz	0.35 - 1 MB	NA
Level 3	0.3 - 3 kHz	30	10 - 100 Hz	0.4 - 1.05 MB	4 - 105 MB/s
PASS1	10 - 100 Hz	1 - 2	5 - 100 Hz	1.4 - 2 MB	7 - 200 MB/s
PASS1bis	0 - 200 Hz	1	0 - 200 Hz	1.4 - 2 MB	0 - 400 MB/s

System	Input Rate Goal	Input Design requirement	Output rate goal
On-line (Level 3)	300 Hz @ 1 MB from Level 2	3 kHz @ 1 MB from Lvl 2 200kSSCUPS @ 67 SSCUP-s/event	10 Hz
Storage	10 Hz @ 1 MB from Level 3 10 Hz @ 2 MB from PASS1 10 Hz @ 2 MB from PASS1bis 10 Hz @ 2 MB from simulation 10 MB/s from analysis	600 MB/s: 100 MB/s from Level 3, 400 MB/s from Off-line, 100 MB/s from analysis, simulation	400 MB/s
Off-line	10 Hz @ 1 MB from Level 3 10 Hz @ 1 MB for PASS1bis from storage simulation, analysis, DSF creation @ 200,000 SSCUPs	100 Hz @ 1 MB from Lvl 3 for PASS1 @ 2100 SSCUP-s/event 100 Hz @ 1 MB for PASS1bis simulations Total: 600,000 SSCUPs	

Elements of Control System

- Processes
- Data bases
- User interfaces
- Workstations
- Processors
- Networks
- Storage Systems
- Hardware interfaces
- Monitor/control equipment
- CCTV
-

Requirements

- Meet standards (safety, data quality)
- Use standards
- Use software design standards/methods
- Reliability
  - Testing
  - Redundancy

Model

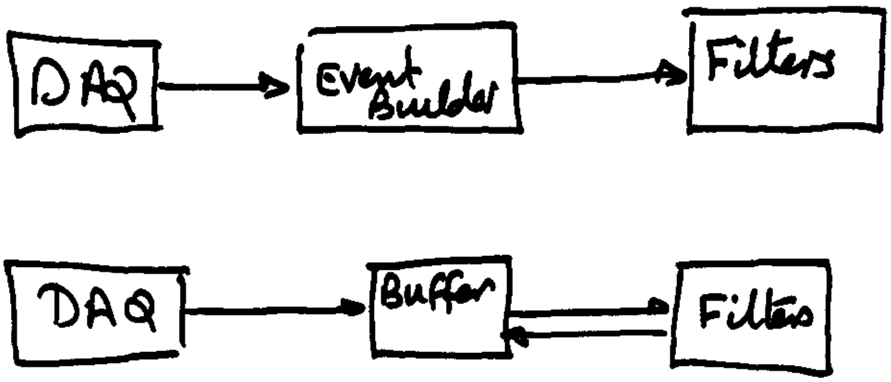

Event Filter

Reduce rate to level where long-term storage is
- techically practical
- risk of bias is acceptable

Elements

- Special purpose hardware (DSP)
- Special CPU's (transputers)
- General purpose CPUs
- Switches
- Networks
- Software

Reconstruction

- Software
  - Data structures
  - Data dictionary
  - Algorithms
  - Simulation
  - Calibration
  - Monitor data
- Hardware
  - CPU capacity needed is very large
    ($\approx 10^5$ VAX equivalents
    $\approx$ SSCUPs)
  - Storage system

Storage

Very High Performance

Software: manage ≈ 20,000 new files/day

manage ≈ 1 PB data/year

Allow rapid access, natural view of data

Hardware: up to 500 MB/s data in

up to 500 MB/s data out

Very Rapid access to some files (Freq. used)

automatic access to <u>all</u> data

Eg. Robots with 19mm tape

Disk arrays

Mass memory

Analysis

Provide physicists with tools: rapid access to all data, ability to relate data, ability to reprocess data

Software

Hardware

Workstations, networks

This will be a major distributed activity.

Data will be at SSCL

Need **excellent** network capability to other sites: In U.S.

Korea

China

F.S.U.

India

⋮

Simulation

- Assist in design of detector
- Provide understanding of data, by comparison

Input : Test beam data, other experiments ....

GEANT - based

Particle generators (PYTHIA, ISAJET, ...)

urrent Software:

Subsystems

- Central Tracker
- Calorimeter — EM
  - — HAD
  - — Barrel Axial Fiber (Tail catcher)
  - — Trigger
- Muon System
  - — Barrel
  - — End cap
  - — trigger

Global (at SSCL) — SIGEM

— gemfast

Simulation

Current Hardware:

- PDSF — at SSCL — 2,000 SSCUPs

  Fully utilized currently!

  Phase III ⟶ 4,000 SSCUPs

- Accessed by collaboration over networks – 80% GEM users outside

- Workstations at collaborating institutions
  – good network access useful for software exchange

Current organization

– Subsystems ⎤
– Physics/simulation group ⎥ overlap
– SSCL: global simulations ⎦

Natural place to contribute:
– Workstations
– People

Note: Unix is basic op. sys. used.

Global Simulations

SIGEM – Yu. Fisyak GEANT-based

- Full geometry (structure, detector elements)
- hits
- Baseline 1 complete (Sept. 92)
- Baseline 2 in process (slides)
- Neutron and γ fluxes
- Occupancies
- Pattern recognition, fitting
- Resolutions
- Interaction of subsystems

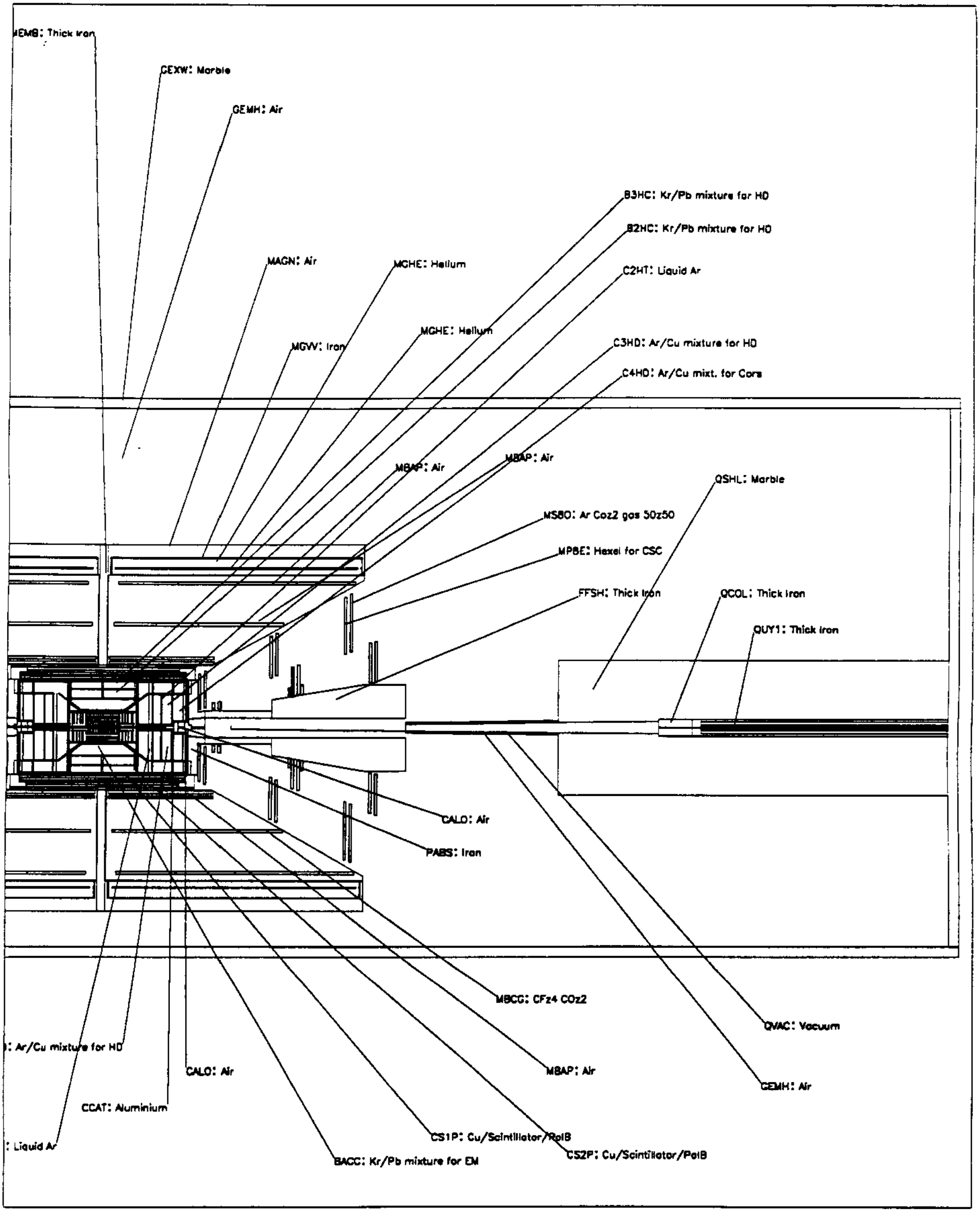
MEMB: Thick Iron
CEXW: Marble
GEMH: Air
B3HC: Kr/Pb mixture for HD
B2HC: Kr/Pb mixture for HD
MAGN: Air
MGHE: Helium
C2HT: Liquid Ar
MGHE: Helium
MGVV: Iron
C3HD: Ar/Cu mixture for HD
C4HD: Ar/Cu mixt. for Cors
MBAP: Air
MBAP: Air
QSHL: Marble
MSBO: Ar Coz2 gas 50z50
MPBE: Hexel for CSC
FFSH: Thick Iron
QCOL: Thick Iron
QUY1: Thick Iron
CALO: Air
PABS: Iron
MBCG: CFz4 COz2
QVAC: Vacuum
: Ar/Cu mixture for HD
CALO: Air
MBAP: Air
GEMH: Air
CCAT: Aluminium
: Liquid Ar
CS1P: Cu/Scintillator/PolB
CS2P: Cu/Scintillator/PolB
BACC: Kr/Pb mixture for EM

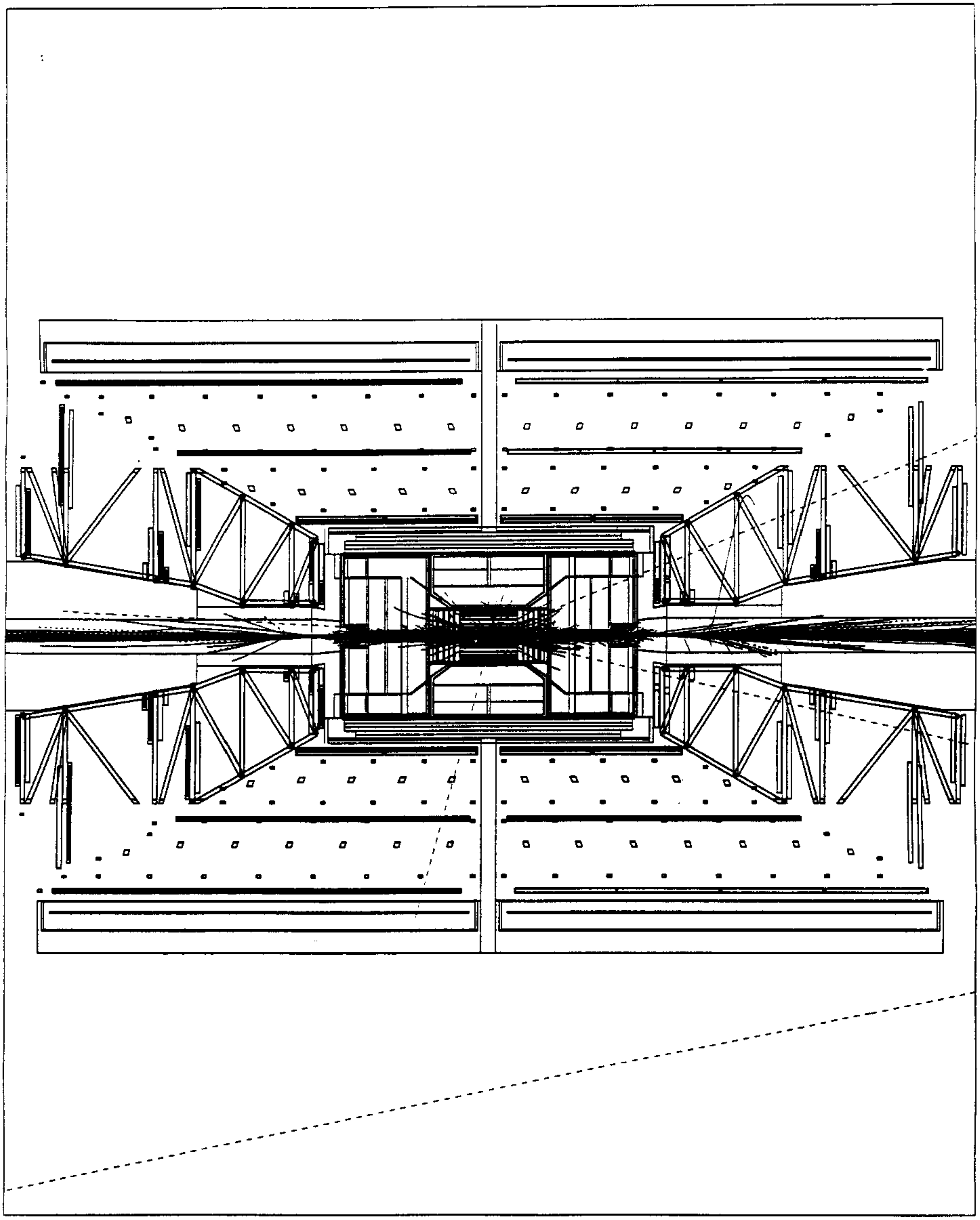

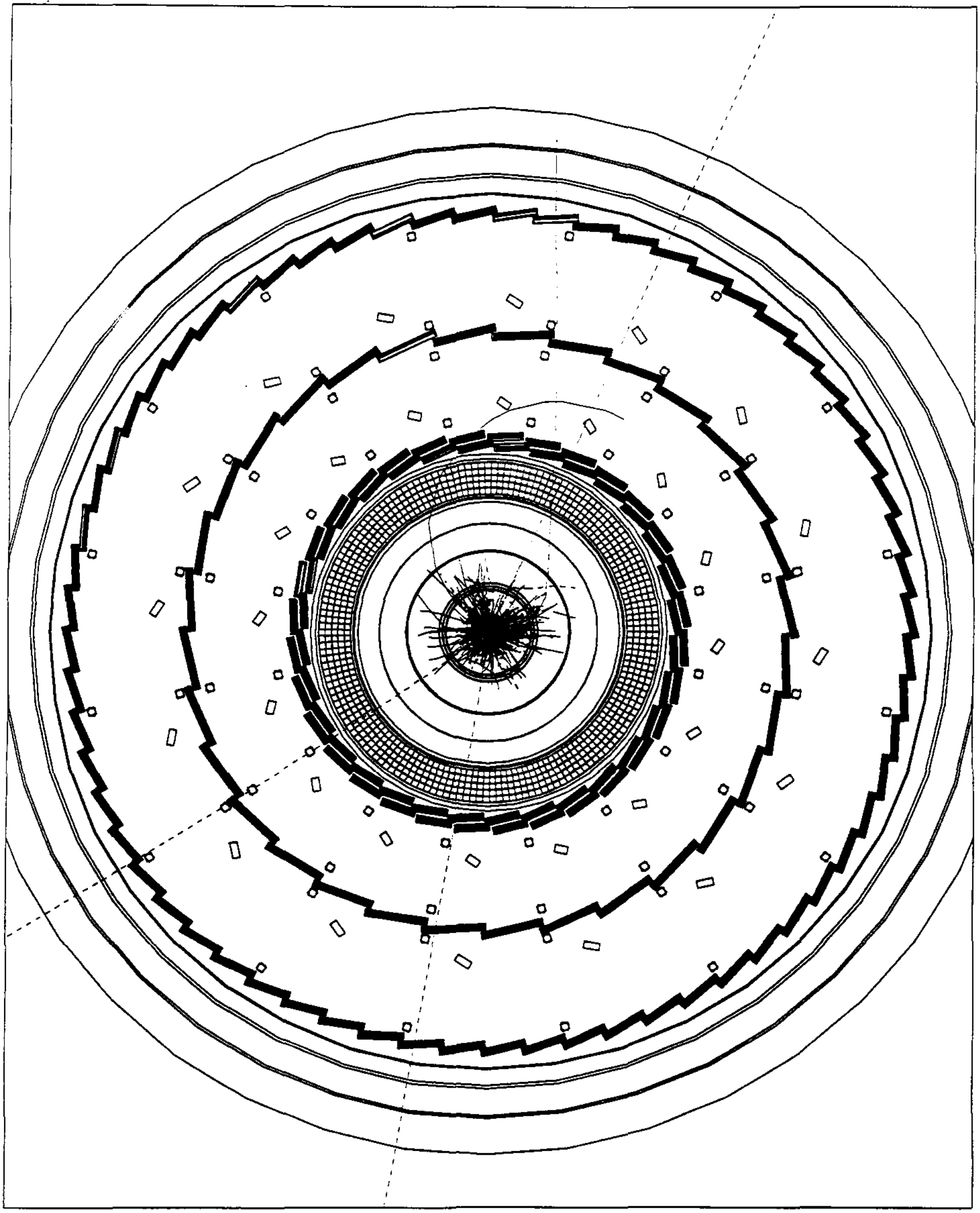

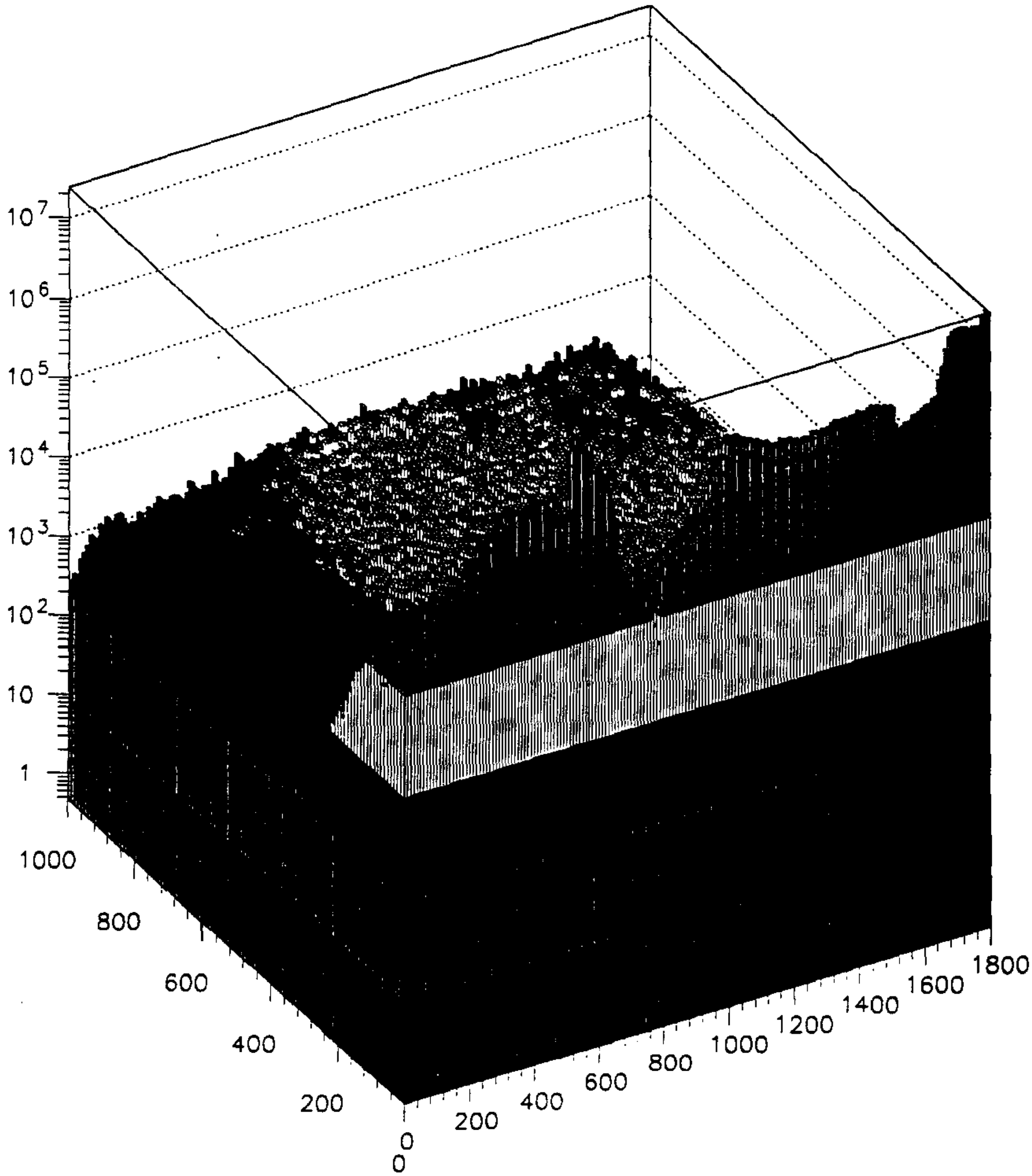

Neutron flux in $(cm^{-2}\ s^{-1})$ vs R and Z

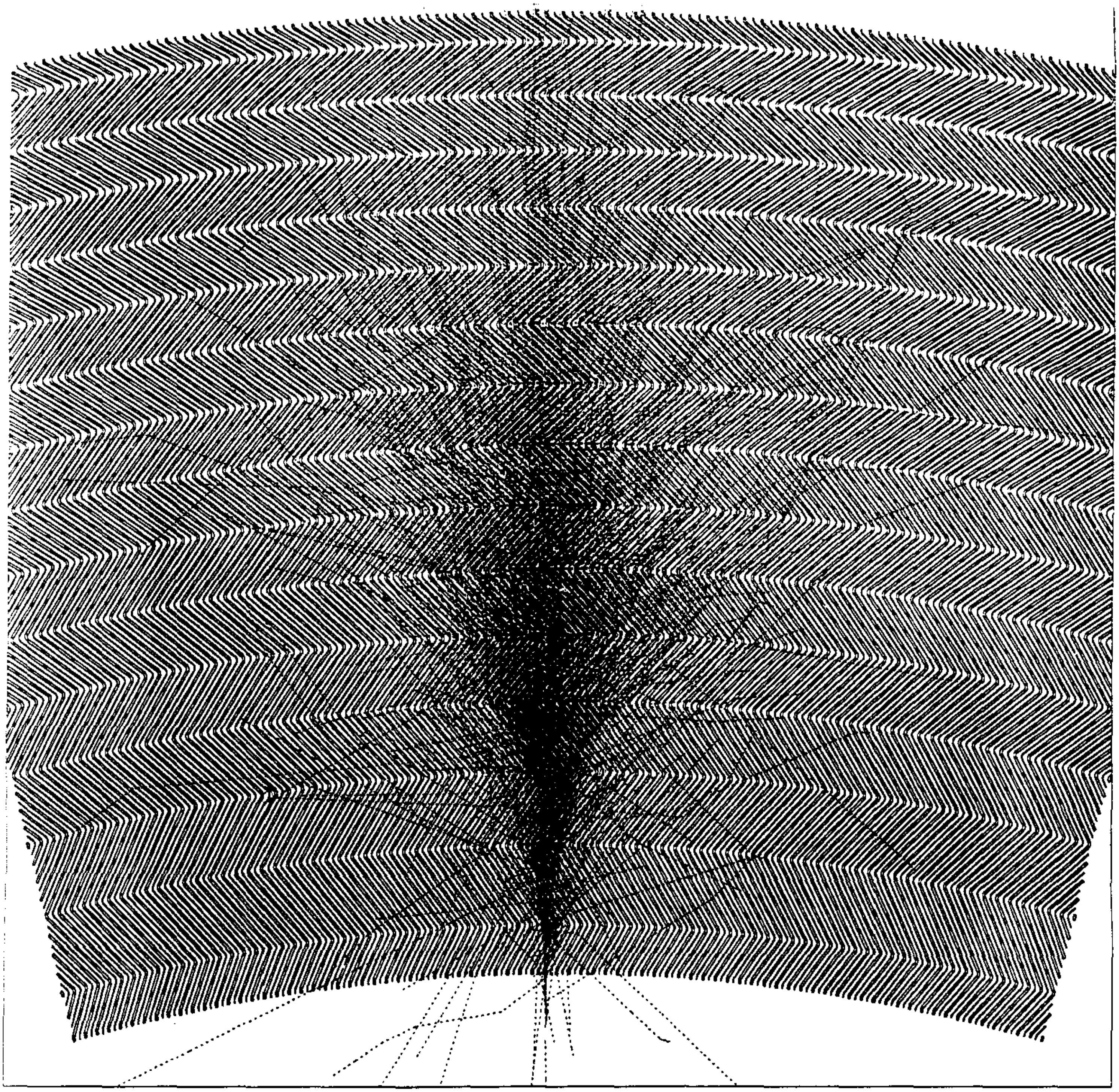

e

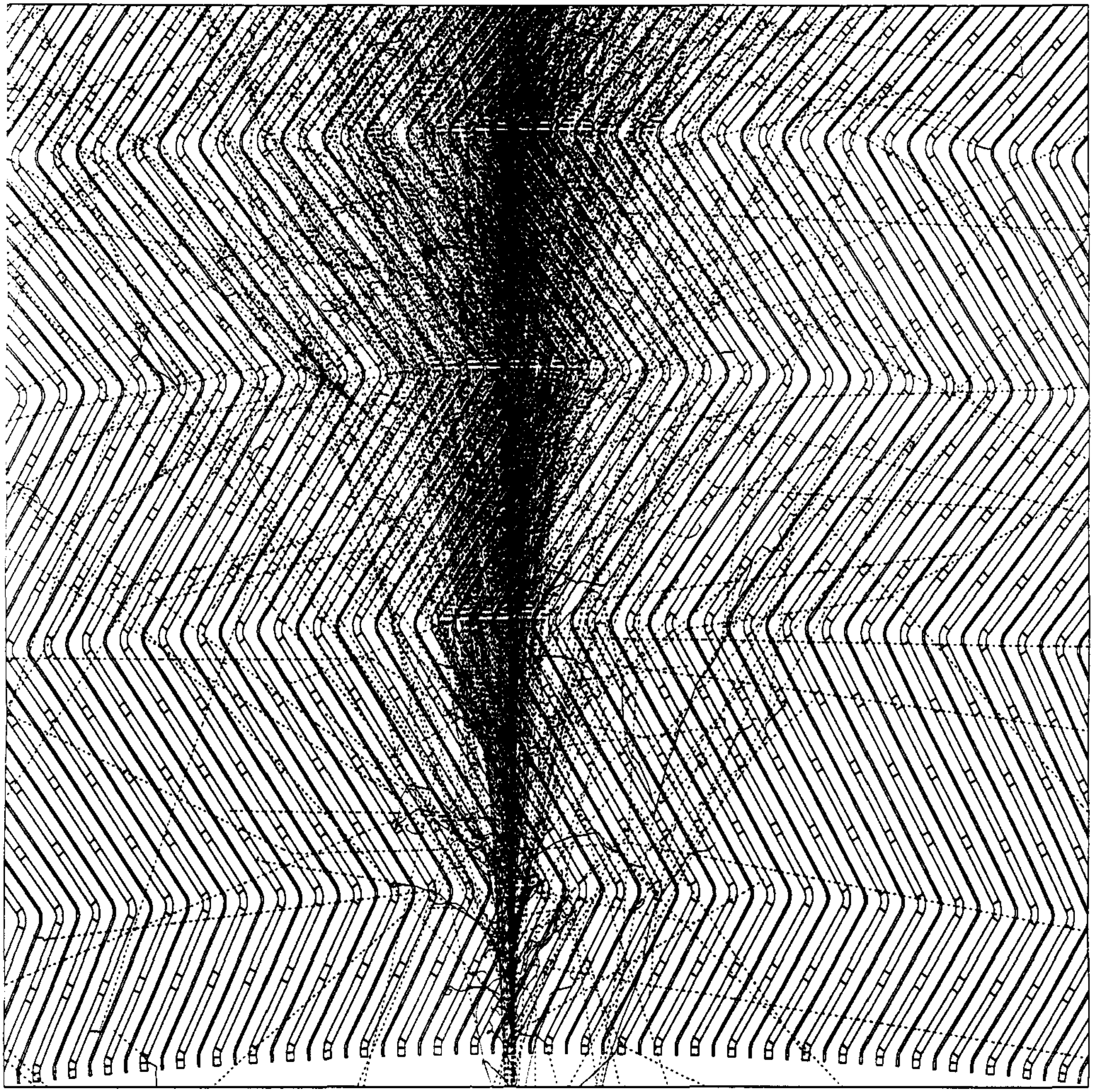

genfast

- Parameterized, simple geometric model

□ Central tracker (layers, discs for no. of hits)
    - momentum resolution (single track)
    - vertex resolution
    - materials
    - photon conversions
    - pattern recognition efficiency (underway)

□ calorimeter (segmentation in η, ϕ)
  - EM - resolution
    - multigamma rejection (π^0)
    - fluctuations in energy deposition (gflash)
  - HA - resolution
    - fluctuations (gflash)
  - Tail catcher
  - Forward Calorimeter
    - missing p_T

□ trigger
□ muon (contd)

genfast (contd)

- muons
  - acceptance
  - trigger efficiency
  - pattern recognition efficiency
  - momentum resolution (single track)

- pileup in calorimeters

genger

Flexible generator package

ISAJET, PYTHIA in same package (HERWIG..)

combine signal, minbias

simulate pile up

All under Unix approach.

gemfast

detector geometry

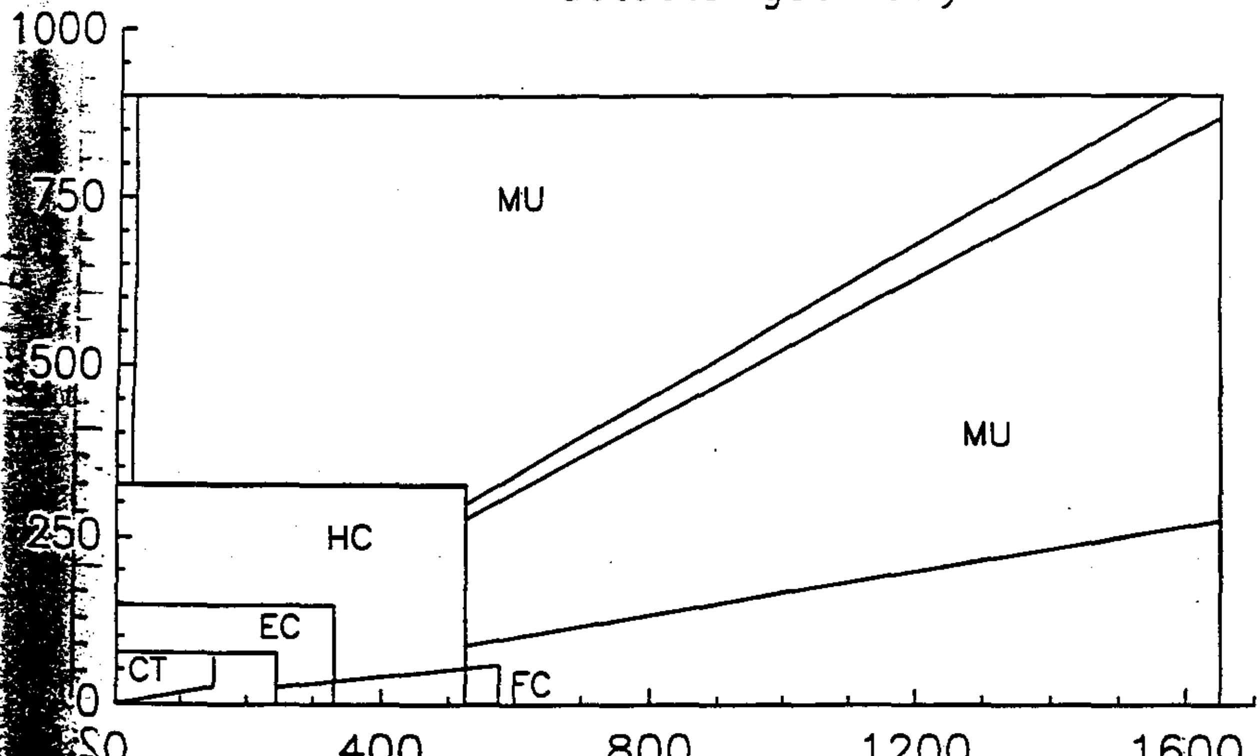

FIG. 3.2-1

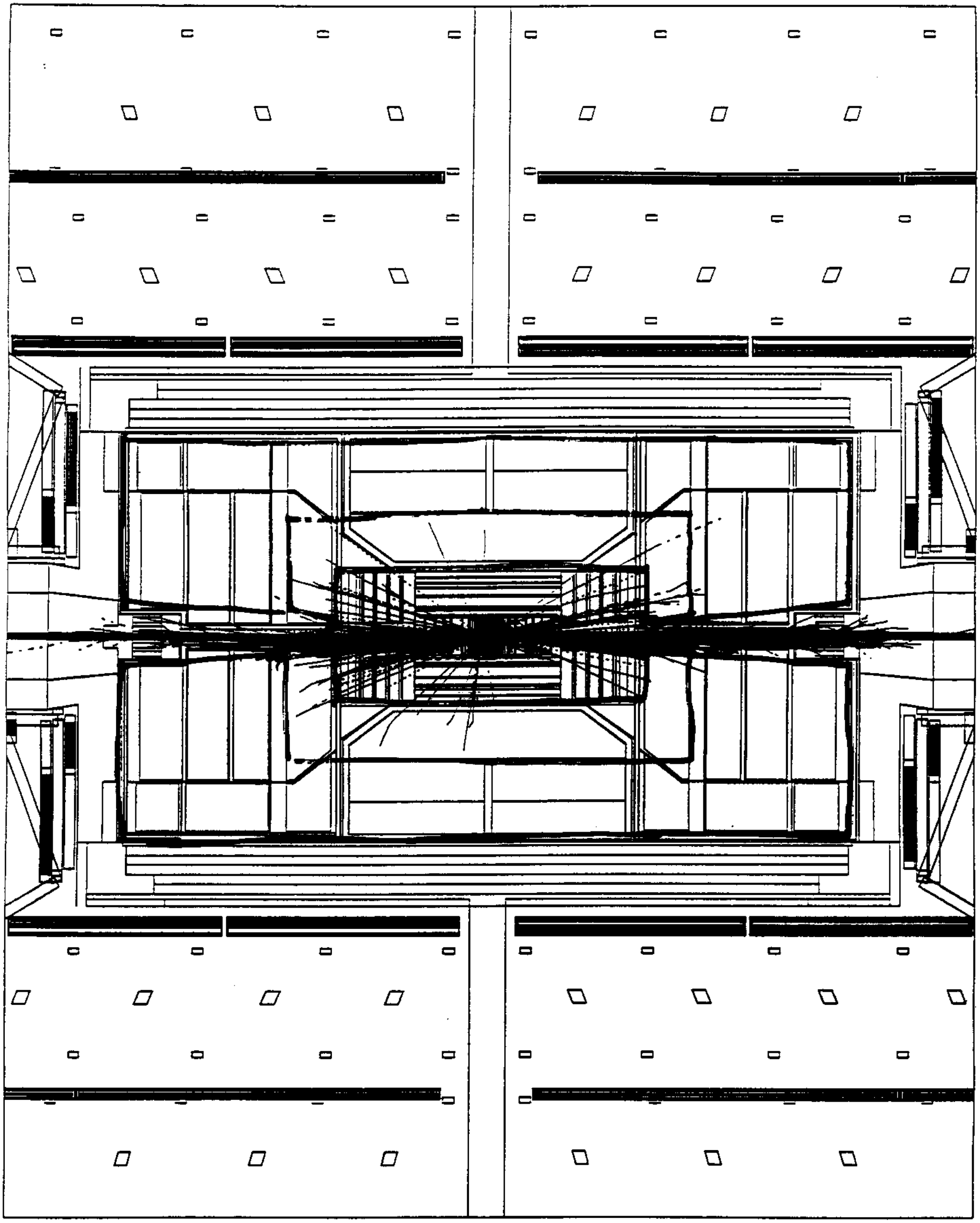

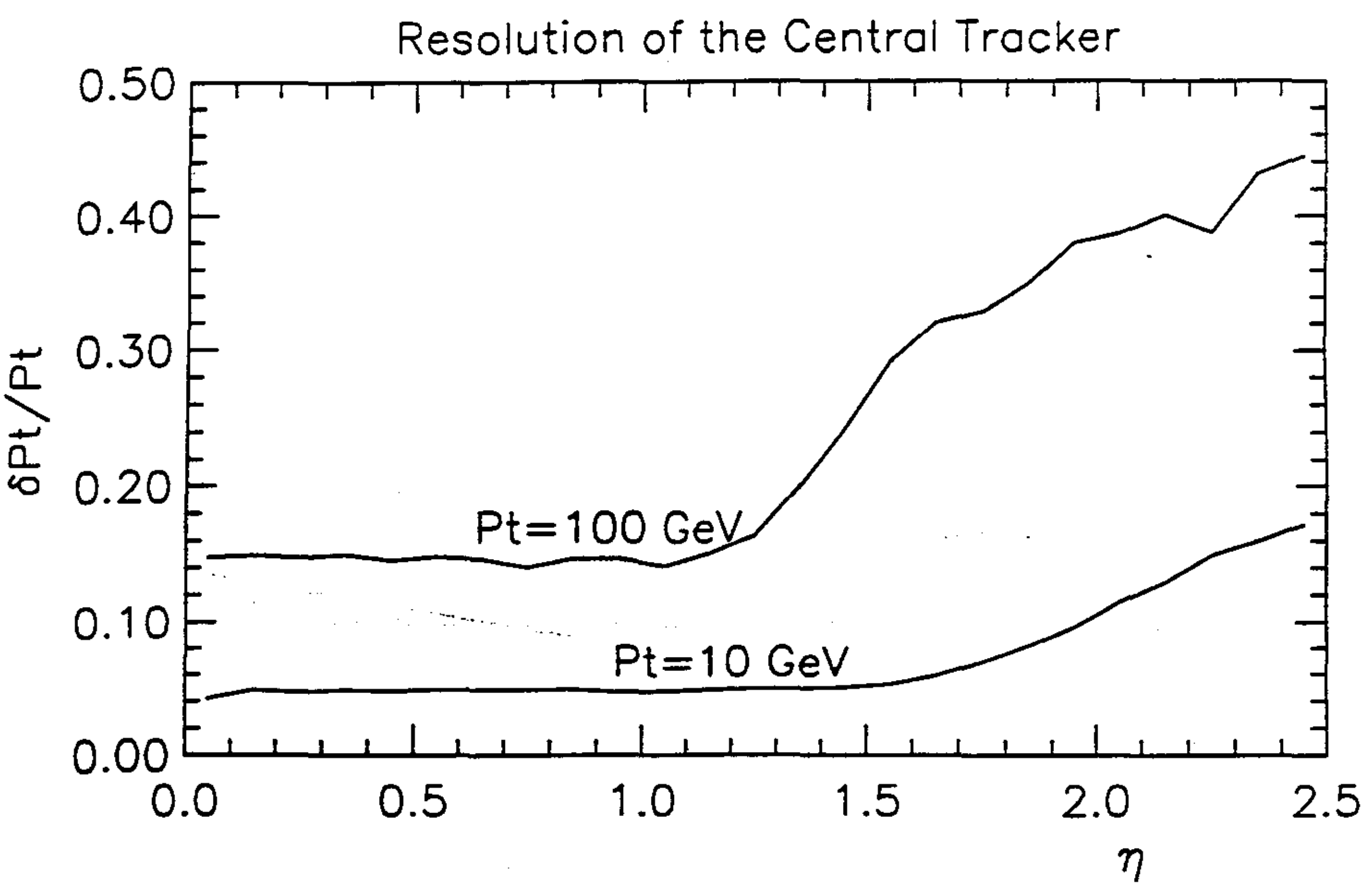

Resolution of the Central Tracker
0.50
0.40
0.30
0.20
0.10
0.00
δPt/Pt
Pt=100 GeV
Pt=10 GeV
0.0
0.5
1.0
1.5
2.0
2.5
η

FIG. 3.2-2

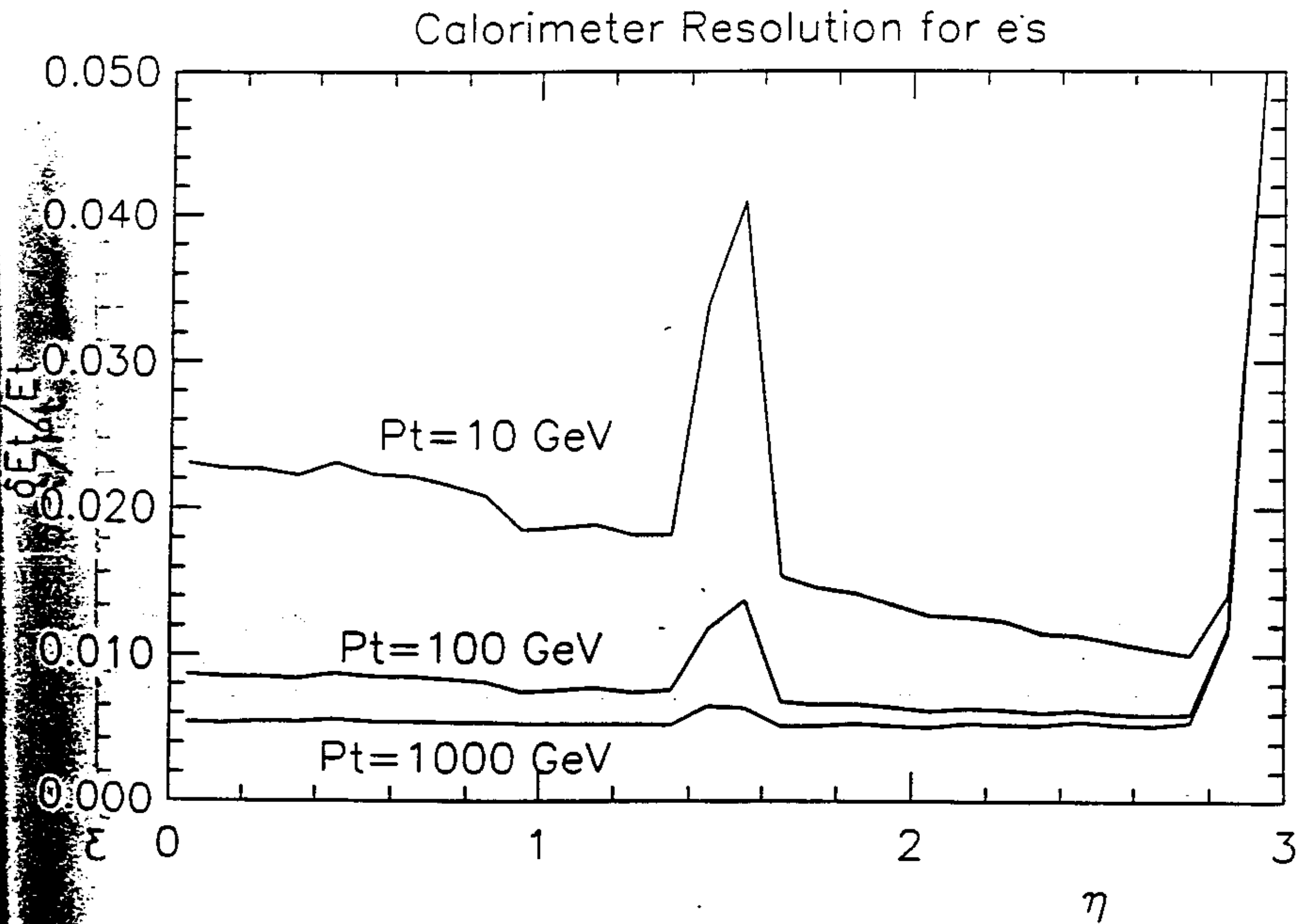

Calorimeter Resolution for e's
0.050
0.040
0.030
0.020
0.010
0.000
δEt/Et
Pt=10 GeV
Pt=100 GeV
Pt=1000 GeV
0
1
2
3
η

FIG. 3.2-3

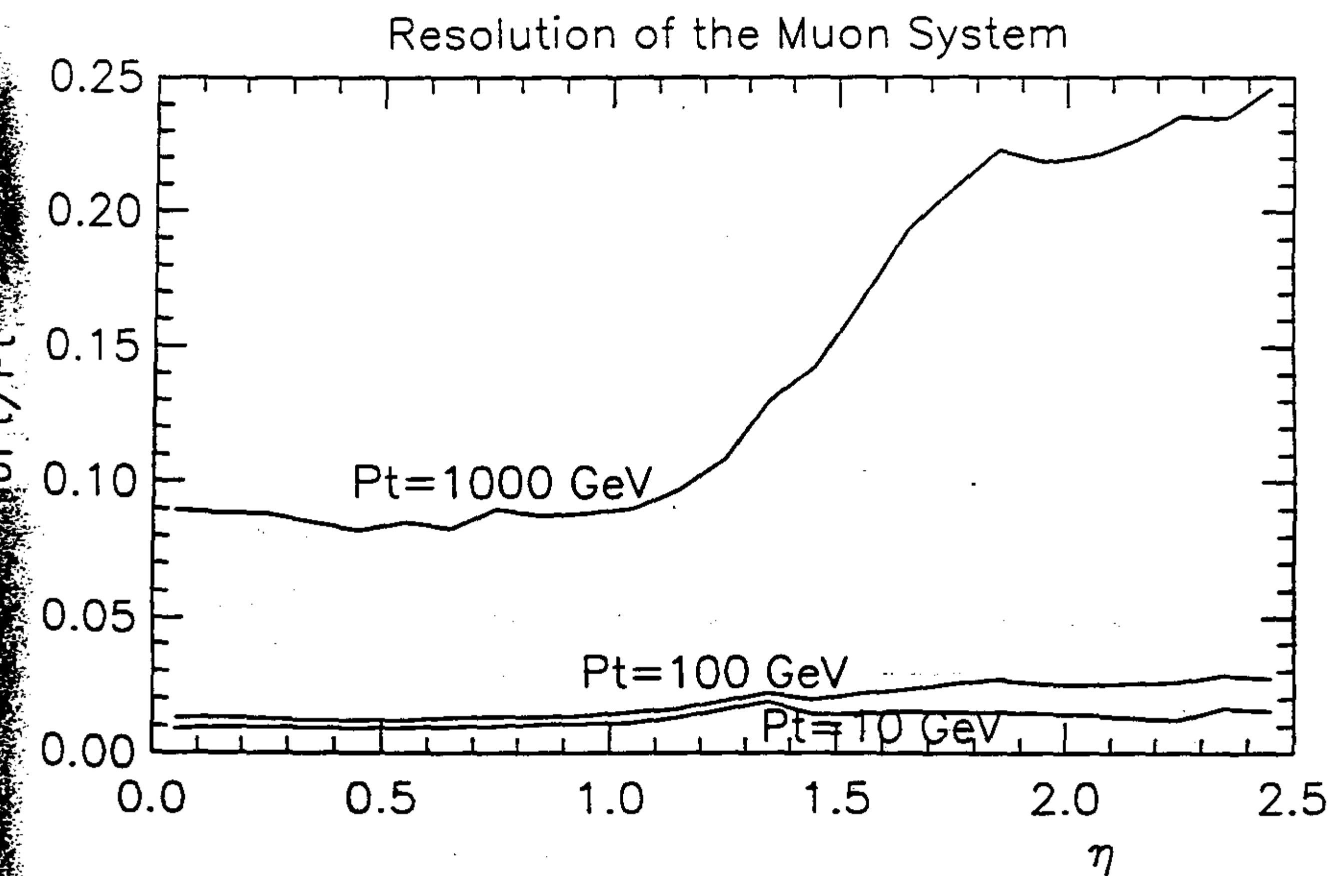

Resolution of the Muon System
δPt/Pt
0.25
0.20
0.15
0.10
0.05
0.00
0.0
0.5
1.0
1.5
2.0
2.5
η
Pt=1000 GeV
Pt=100 GeV
Pt=10 GeV

FIG. 3.2-6

Simulated Geometry of CSC in barrel muon

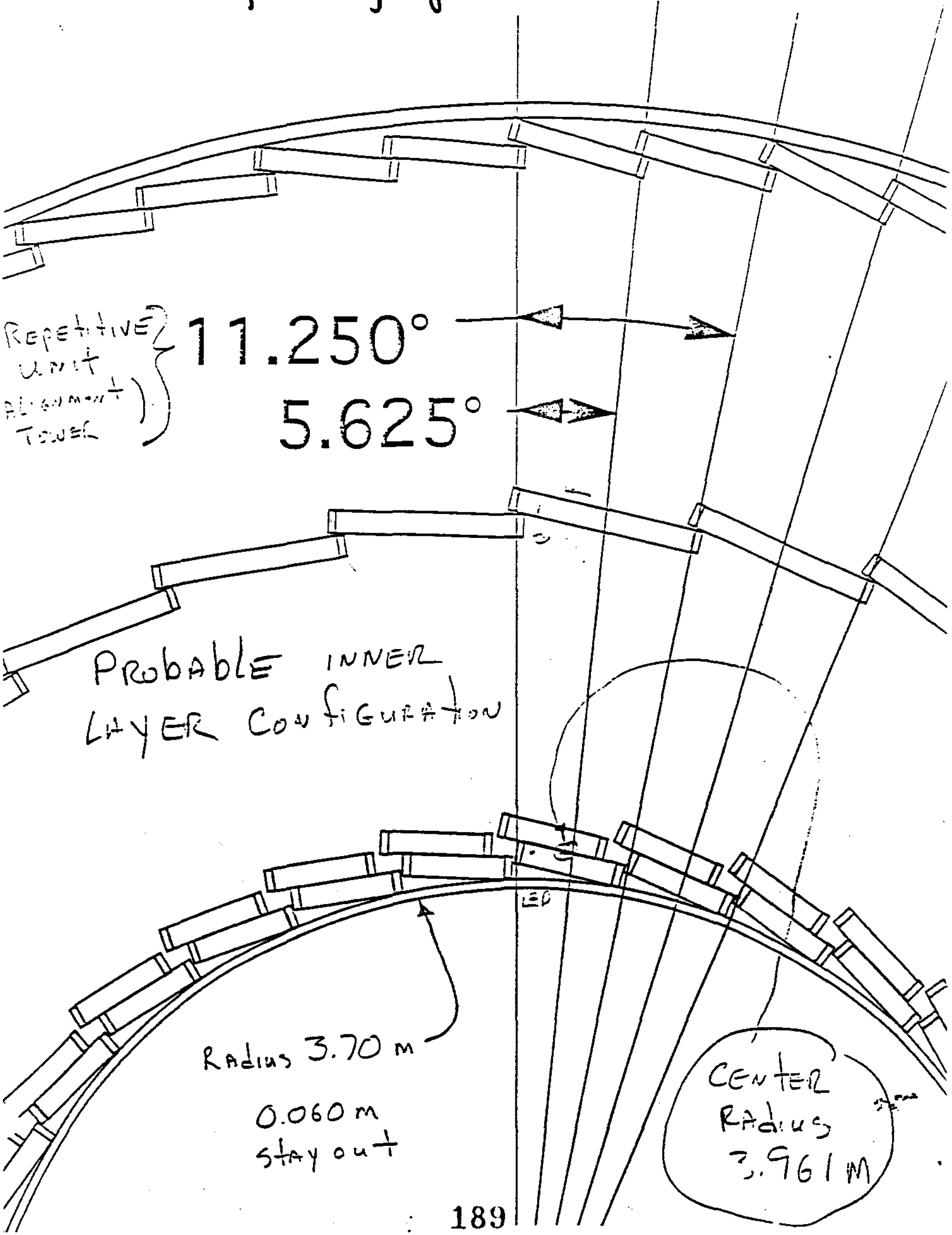

dsc

ORIGINS OF PARTICLES CAUSING HITS*

r- φ

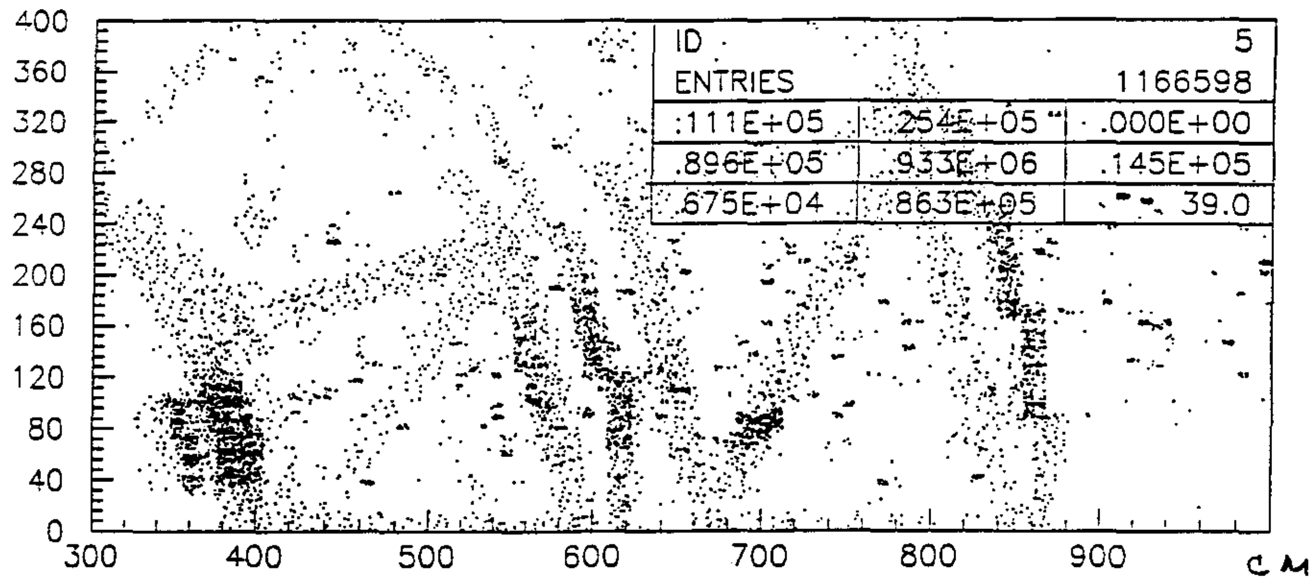

YY VS XX

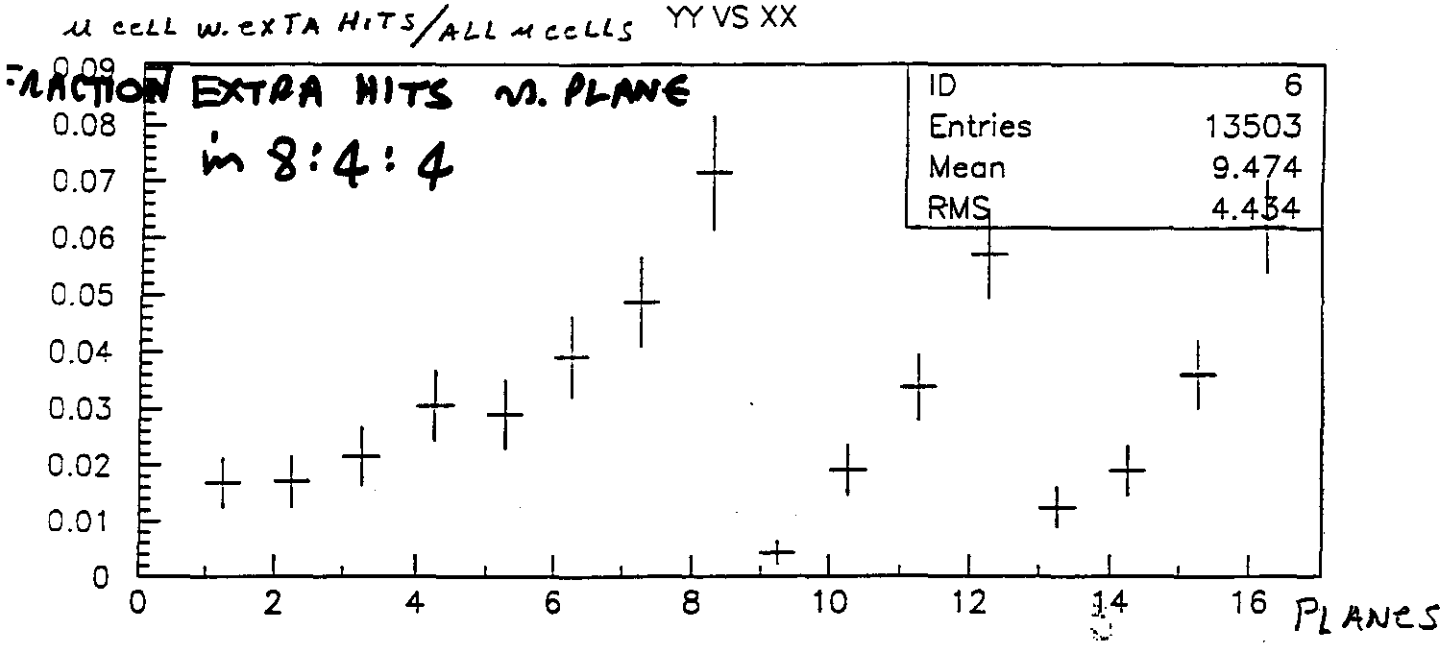

EXTRA HITS VS PLANE

* Illuminated with muons scanned over φ-θ cone.

GEM Calorimeter Simulation

Current Situation — many discrete simulation packages

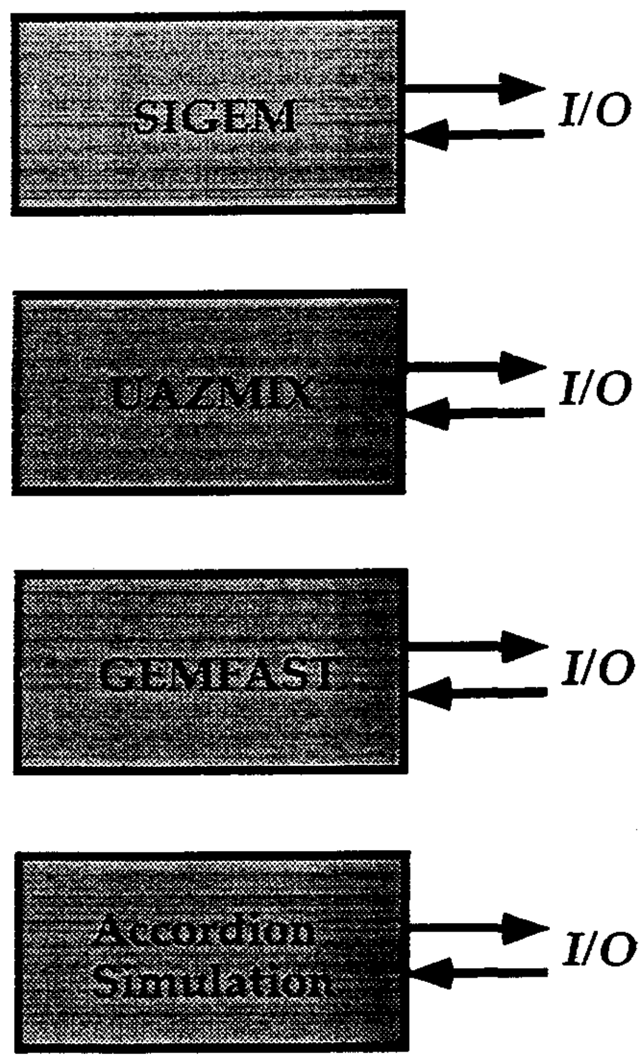

GEM Calorimeter Simulation

Integrated Solution

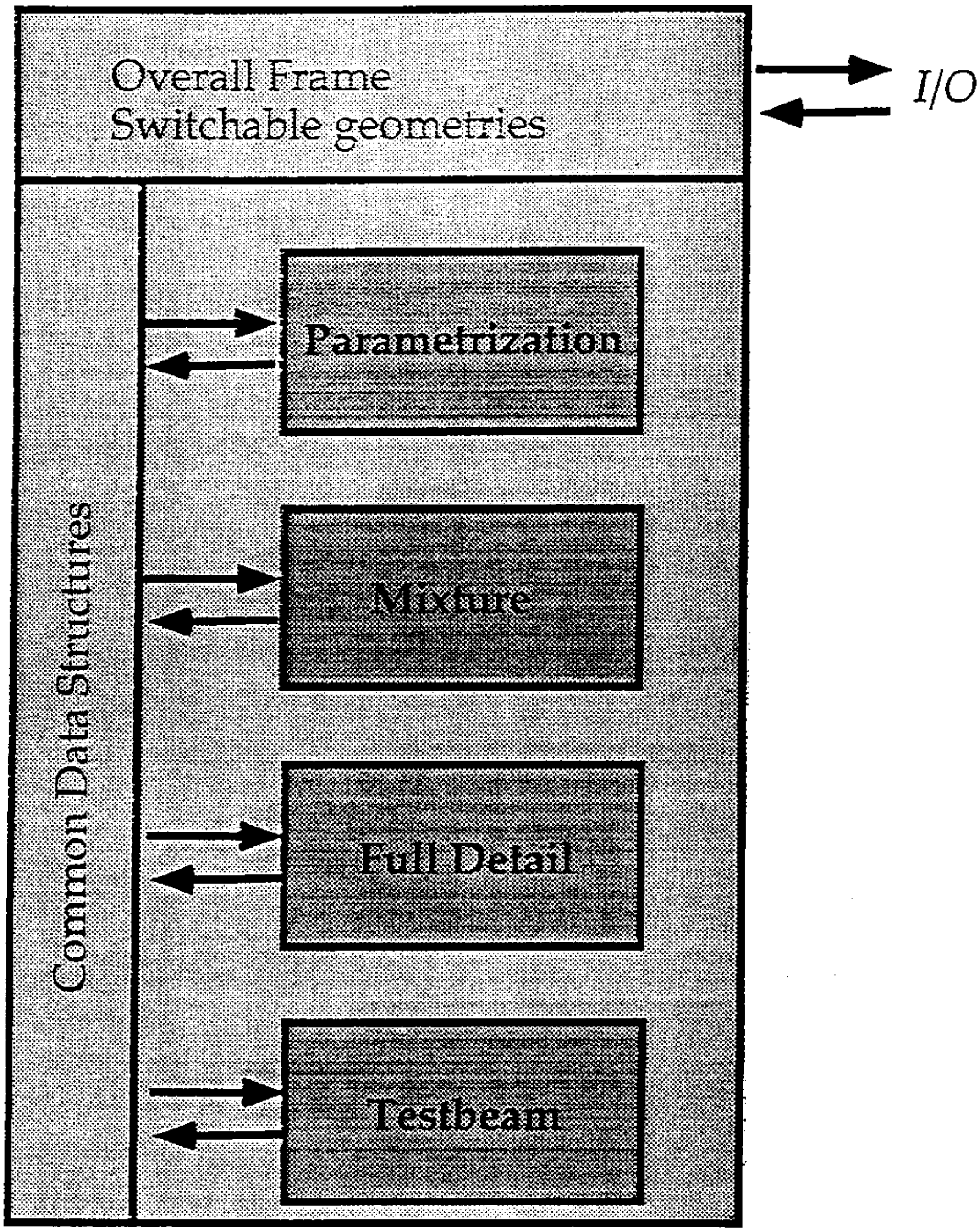

LIST OF CALORIMETER SIMULATION TASKS

'Full' means tasks that require a fully detailed level of simulation within GEANT, though not necessarily for the full GEM configuration. Full simulation geometries should be created for the accordion (basically done by Ma and Seman), and for the hadronic layers behind.

'Mixture' means tasks that can be performed with a 'mixtures' level of simulation (individual modules replaced by single materials) within GEANT, modelling of the full GEM detector being required.

EM:

1) Gamma resoloution as a function of eta. (Full)
   - a) Variable density of Pb. — Misha Leltchouk
   - b) Massless Gap. — Misha Leltchouk

2) Accordion structure. (Full)
   - a) geometry beta/delta — Michael Seman
   - b) Field effects. — Iuliu Stumer

2) Pointing resolution as a function of eta. (Full)
   - a) Granularity — Jean-Yves Hostachy
   - b) Longitudinal segmentation.

3) Gamma/jet rejection as a function of eta. (Mixture and Full)
   - a) Shower shape — Hong Ma
   - b) Fine theta granularity (strips) — Misha Leltchouk

Use of the first hadronic section to optimize the Isolation cut. Here we can see what the optimal transverse granularity is. This is both for isolated gammas and for electrons near the jet axis.

4) Optimization of Jet rejection.
   Using existing structure. — S.Vanyashin

5) Gamma resolution at very high energies. Use of the first hadronic section as a tail catcher. (Full)

6) Acceptance. (Mixture)
   How far in eta must be covered. eta=1.1 transition.

Integration Questions

A suggestion . . .

If we strive for the final answers to all our questions we run the risk of arguing all day and achieving nothing. It is better to aim for interim solutions, which may be ugly, but can be implemented now.

Data Structures

Data exchange within the simulation program:
Common blocks
I/O to file:
Zebra

Some issues:
How to handle segmentation
Do we store energies track-by-track or only integrated over the event?
What about pileup events?

Naming Conventions

Routine and variable names
MATE, TMED definitions
Rotation Matrix definitions

Hadronic sections:

1) Single particle resolution and linearity of liquid section (Full)
   --- what segmentation is needed?
   Washington, Rochester?
2) Single particle resolution and linearity of scintillator section (Full)
   --- how to unfold timing resolution?
   --- what is two track response?
   Oak Ridge
3) Single Particle and Jet resolution of combined system as a function of eta.
   (Mixture may be OK, may need full)
   --- Weighting schemes. Can weights be made independent of E, eta, particle type?
   --- jet-jet mass resolution, esp. impact of scintillator (Mixture)

4) Maybe need specialized e/pi simulation? Do we believe GEANT?
   GEANT 3.14 will predict liquid argon e/pi to 0.05.
   Krypton is untested.
   CALOR89 predicts e/pi to 0.03 in D0. Maybe we need to get Mississippi people (Brent Moore) involved here.

5) Missing E_T for the whole detector. (Gemfast, Mixture) Mike Shupe
   Here the emphasis is on the Dead material due to the cryostats, also cableways and the eta=1.5 and eta=3 transitions.

6) Missing E_T for the forward Cal. (Gemfast, Mixture) Mike Shupe
   Here the empahsis is on the Forward Cal performance and beam pipe.

7) Neutron problem of the forward cal. L. Waters/Nelson Desilva.
   C. Zeitnitz (Arizona) will help.

Muons

(list of questions from Peter Dingus)

1) Muon identification in liquid section
   --- is the noise low enough to see (80 MeV/cell) MIPs?

2) Muon identification/triggering in scintillator section

3) What level of multiple scattering do we get in the calorimeter?
   --- Cu vs Pb

4) Muon catastrophic energy loss:
   --- can the energy be recovered? How well does it need to be measured in the scintillator calorimeter? Do we really need time structure for isolated muons?
   --- is the muon ever confused with a jet punching through?

5) Is 12 λ really needed? Or is it better to curl up tracks in air?

Note: TDR date is now April 30, 1993

Integration Questions

A suggestion . . .

If we strive for the final answers to all our questions we run the risk of arguing all day and achieving nothing. It is better to aim for interim solutions, which may be ugly, but can be implemented now.

Data Structures

Data exchange within the simulation program:
Common blocks
I/O to file:
Zebra

Some issues:
How to handle segmentation
Do we store energies track-by-track or only integrated over the event?
What about pileup events?

Naming Conventions

Routine and variable names
MATE, TMED definitions
Rotation Matrix definitions

Conclusion

Many areas where there can be contributions to GEM through computing. We welcome your help!

Coordination: mcfarlan@sscvx1

Subsystems: see subsystem leaders

global simulation: mcfarlan@sscvx1

gemfast: T. Skwarnicki (tomasz@sscvx1)

gem software: I. Sheer (sheer@sapphire.gem.ssc.gov)

Physics/simulation: F.E. Paige (paige@sscvx1)
K. Lane (lane@buphyc.bu.edu)

Physics/Simulation/Computing

Frank Paige

SSC PHYSICS SIGNATURES

F.E. Paige, SSC Laboratory

Will concentrate on main goals of SSC and LHC physics program:

- Origin of electroweak symmetry breaking.
- Origin of masses.
- Search for new heavy particles.

Should not forget other possibilities:

- ☐ *B* physics using collider or external beams.
- ☐ Classical strong interactions.
- ☐ High mass diffractive physics.

Physics Prospects

Standard model (SM) is in agreement with almost all existing data, including:

Precise electroweak data from LEP;

QCD tests from UA1, UA2, CDF, etc.

Missing particles are t and H. Bounds:

$$m_t = 130 \pm 40\,\text{GeV}$$

$$m_H > 48\,\text{GeV}$$

Lattice Higgs calculations suggest

$$m_H \lesssim 650\,\text{GeV}$$

Should find t at Tevatron.

Might still find H at LEP-200.

Main problem with SM is to explain electroweak symmetry breaking and fermion masses. We know the scale:

$$v = 246\,\mathrm{GeV}$$

New physics at TeV scale is required.

No hint of anything new. Can parameterize by effect on W, Z:

$$\frac{\Pi_W\left(m_W^2\right) - \Pi_W(0)}{m_W^2} = \frac{\alpha\left(m_W^2\right)}{4\sin^2\theta_W(m_Z)} S$$

$$\frac{\Pi_W(0)}{m_W^2} - \frac{\Pi_Z(0)}{m_Z^2} = \alpha\left(m_Z^2\right) T$$

Find [Peskin, Takeuchi; ...; Marciano, Rosner]:

$$T = -0.06 \pm 0.23\,, \quad S = -2.2 \pm 1.3$$

Justification for studying 1 TeV scale remains strong. List of possibilities hardly changed since Snowmass 1984:

- Standard model Higgs boson.
- Multiple elementary Higgs bosons.
- Higgs $\Rightarrow$ $t\bar{t}$ bound state.
- Higgs $\Rightarrow$ new fermion bound state, e.g. technicolor.
- Supersymmetry.
- Composite fermions $\Rightarrow$ dynamical masses.

Other possible new particles:

- New quarks (including t).
- New W' and Z'.
- The unknown!

Of course much better understanding both of theories and of experimental signatures.

Basis of "physics benchmarks." Object is not to cover all physics but to find representative list to test detectors.

SSC could find (almost) all proposed physics at $10^{33}\,\mathrm{cm}^{-2}\mathrm{s}^{-1}$. LHC is competitive at $10^{34}\,\mathrm{cm}^{-2}\mathrm{s}^{-1}$ for most of it.

Top

Discovery likely at Tevatron, but detailed measurements will need SSC/LHC — LEP almost excluded.

Mass: Could be important — t may play unique dynamical role. Several methods:

(1) Measure σ.

Calculable to ~50% ⇒ determine m_t to ~10% *assuming* standard model. Note

$$\sigma \approx 10\,\mathrm{nb} \quad m_t = 140\,\mathrm{GeV}$$

so negligible statistical error.

(2) Reconstruct $W \to q\bar{q}'$ and Wb masses with single lepton trigger:

$$t + \bar{t} \to \ell^+ \nu b + q\bar{q}'\bar{b}$$

Example of jet spectroscopy. Several variations:

Tag b jets with vertex detector and reconstruct jet masses (SDC).

Tag b jet with nonisolated μ and reconstruct jets. (L*)

Require $p_{T,\ell} + p_{T,\mathrm{jet}} > 300\,\mathrm{GeV}$. Select highest jet with 2 other jets in $\Delta R = 1.0$ and reconstruct masses. (GEM)

Expect $\Delta M \sim$ few GeV, limited by systematics.

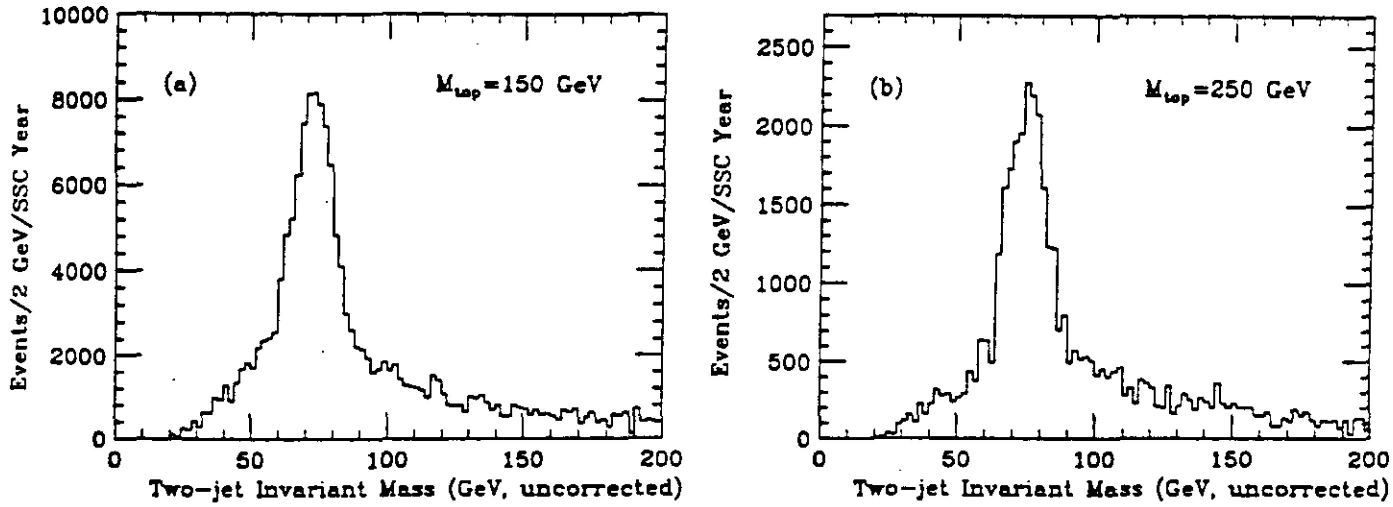

FIG. 3-47. The observed (uncorrected) two-jet invariant mass distribution using the cuts described in text for (a) $M_{top} = 150$ GeV and (b) 250 GeV.

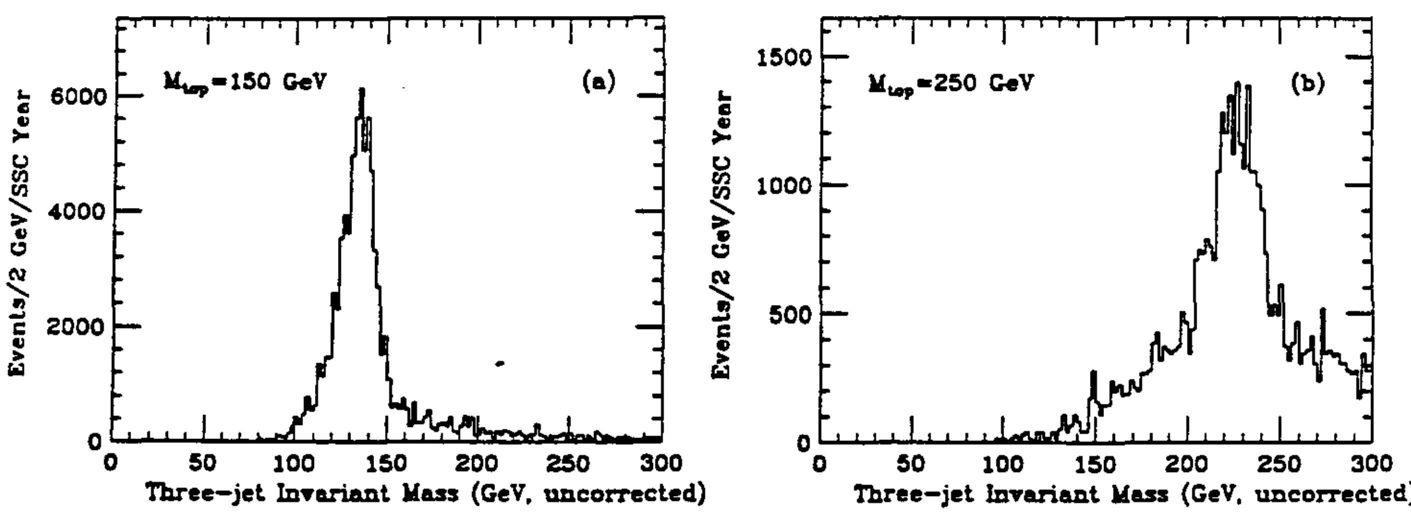

FIG. 3-48. The observed (uncorrected) three-jet invariant mass distribution for (a) $M_{top} = 150$ GeV and (b) $M_{top} = 250$ GeV.

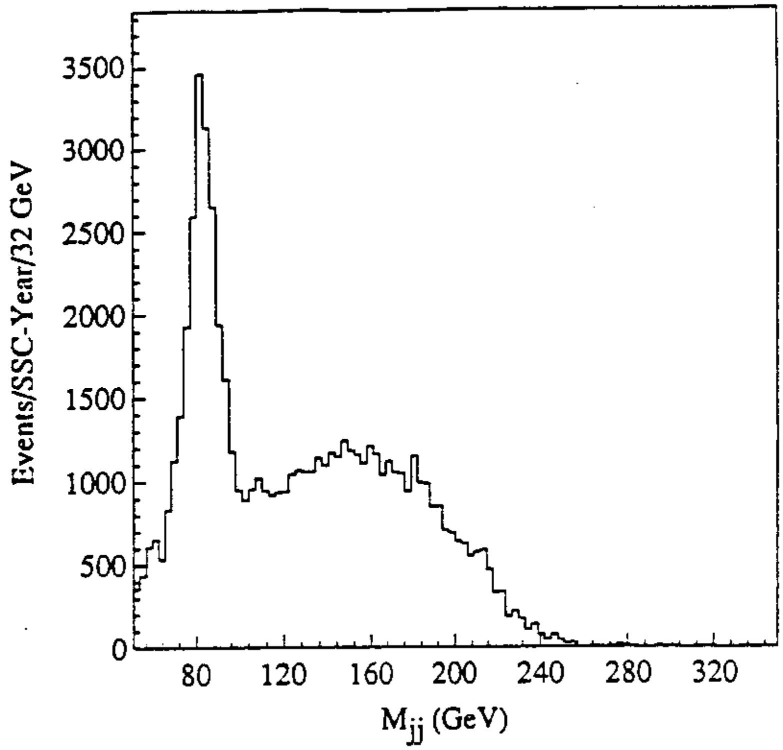

Figure 3.3-1 **Reconstructed $W^{\pm} \rightarrow jj$ mass distribution and background with high-p_T top selection**

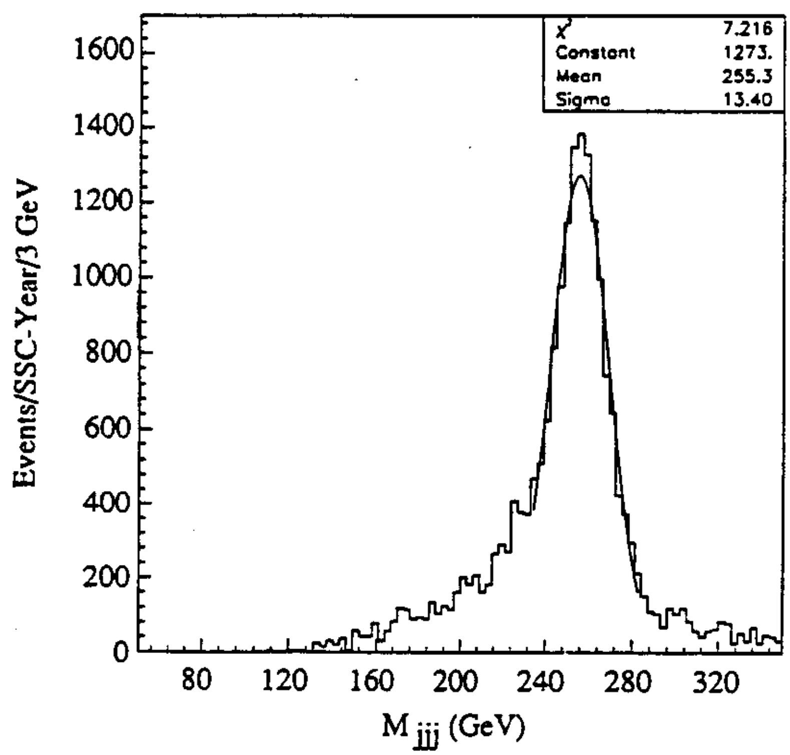

Figure 3.3-2 **Reconstructed $t \rightarrow jjj$ mass distribution and background with high-p_T top selection**

(3) Use high statistics to find mean of distribution, e.g.

$$M(\ell_1\ell_2): \quad t+\bar{t} \rightarrow \ell_1\nu b + \ell_2\nu\bar{b}$$

$$M(\ell_1 b): \quad t \rightarrow \ell_1\nu b$$

$$M(\ell_1\ell_3): \quad t \rightarrow \ell_1\nu b,\ b \rightarrow \ell_3 X.$$

Again limited by systematics. Could be modified by nonstandard decays.

Need several independent methods to check systematics. High statistics allows this.

Decays: No interesting decays in standard model. Verify $t \to Wb$: need b vertex and/or nonisolated μ.

If H^+ lighter than t, then expect substantial branching ratio for

$$t \to H^+ b, \quad H^+ \to \tau^+ \nu$$

Trigger on

$$\bar{t} \to \ell^- \bar{\nu} \bar{b}$$

and measure ratio of one-prong jets/leptons. τ misidentification seems small, but still systematics limited.

Possible that $H^+ \to c\bar{s}$ dominates. Can check ℓ branching ratio, study jet distributions, or reconstruct M_{jj}.

Dominant decay if allowed is

$$H^+ \to W^+ h^0, \quad h^0 \to b\bar{b}$$

Need to identify and measure b's.

Other possible nonstandard decays:

$$t \to Z^0 c$$

$$t \to \tilde{t}\tilde{\chi}_1^0$$

$$t \to W^+ s$$

Higgs

Standard Higgs is unnatural in presence of high mass scales.

Lattice analysis gives [Kuti, ...]

$$m_H \lesssim 650\,\mathrm{GeV}$$

Consistency with renormalization group up to GUT scale requires [Cabibbo, ...]

$$m_H \lesssim 200\,\mathrm{GeV}$$

LEP should cover $m_H < 80\,\mathrm{GeV}$.

Increased emphasis on light Higgs, particularly SUSY Higgs.

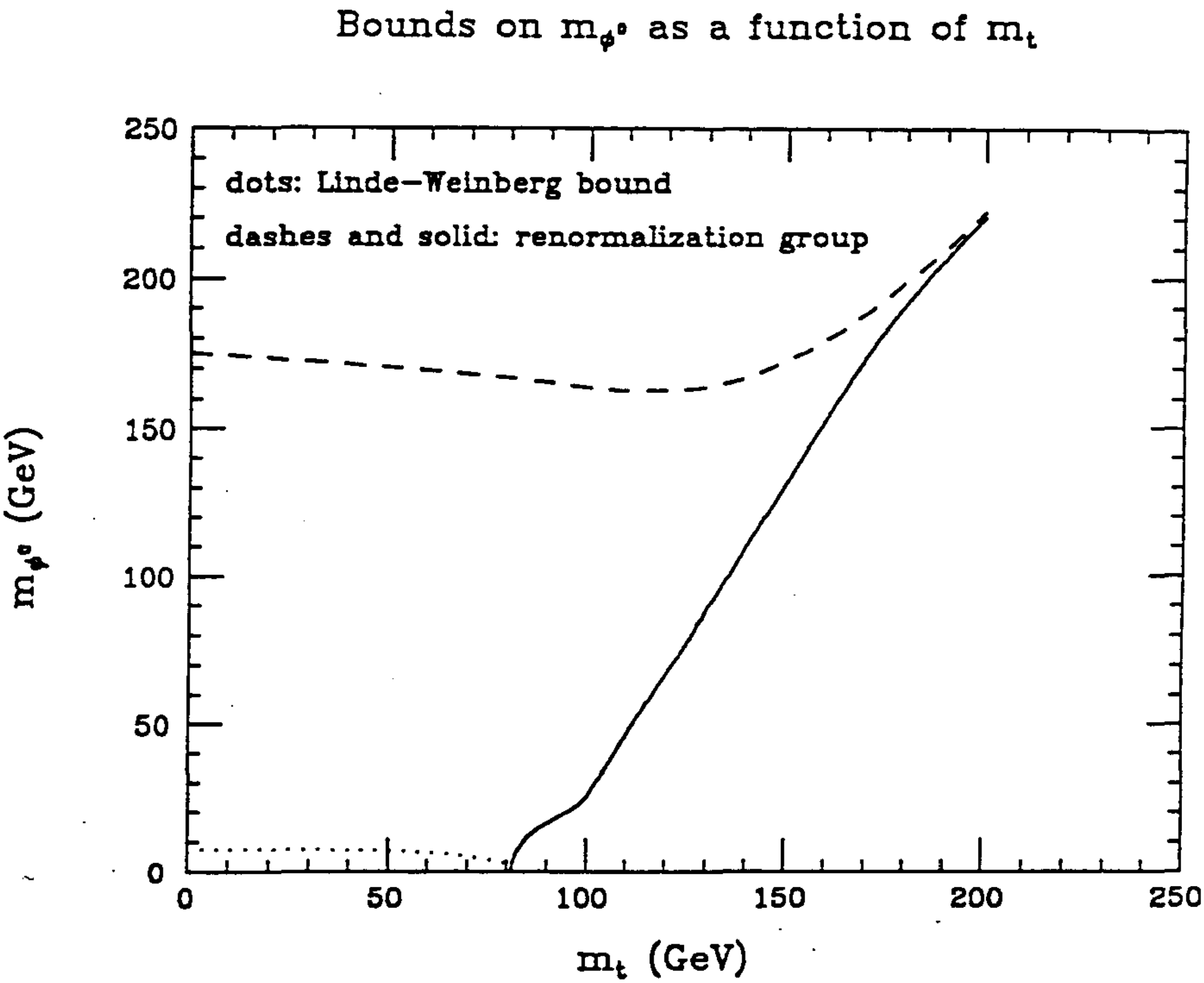

Figure 2.16 Upper and lower bounds on m_{ϕ^0} as a function of m_t, coming from the requirement of a perturbative theory at all energy scales from v to M_U. This figure is taken from ref. 76, where M_U is taken to be the grand unification scale $M_U \simeq 10^{16}$ GeV and $\sin^2\theta_W \simeq 0.2$. Three generations of quarks and leptons have been assumed.

Heavy Standard Higgs:

$H \to Z^0 Z^0 \to \ell^+\ell^-\ell^+\ell^-$: Beaten to death. Low statistics for $m_H \sim 800\,\mathrm{GeV}$.

If $\Delta M \sim \Gamma_Z$, then only known background is $Z^0 Z^0$ continuum.

$H \to Z^0 Z^0 \to \ell^+\ell^-\tau^+\tau^-$: Doubles 4ℓ rate. Can fit for τ momenta using $\vec{p}_{T,\,\mathrm{miss}}$ and m_Z.

Needs background study. Tracking? Vertex detector?

$H \to Z^0 Z^0 \to \ell^+\ell^-\nu\bar{\nu}$: Six times 4ℓ rate.

Large background from Z^0 + jets. Can reject with perfect detector covering $|\eta| \lesssim 5.5$.

Simulations suggest signal survives in realistic detectors covering $\eta \lesssim 5.5$.

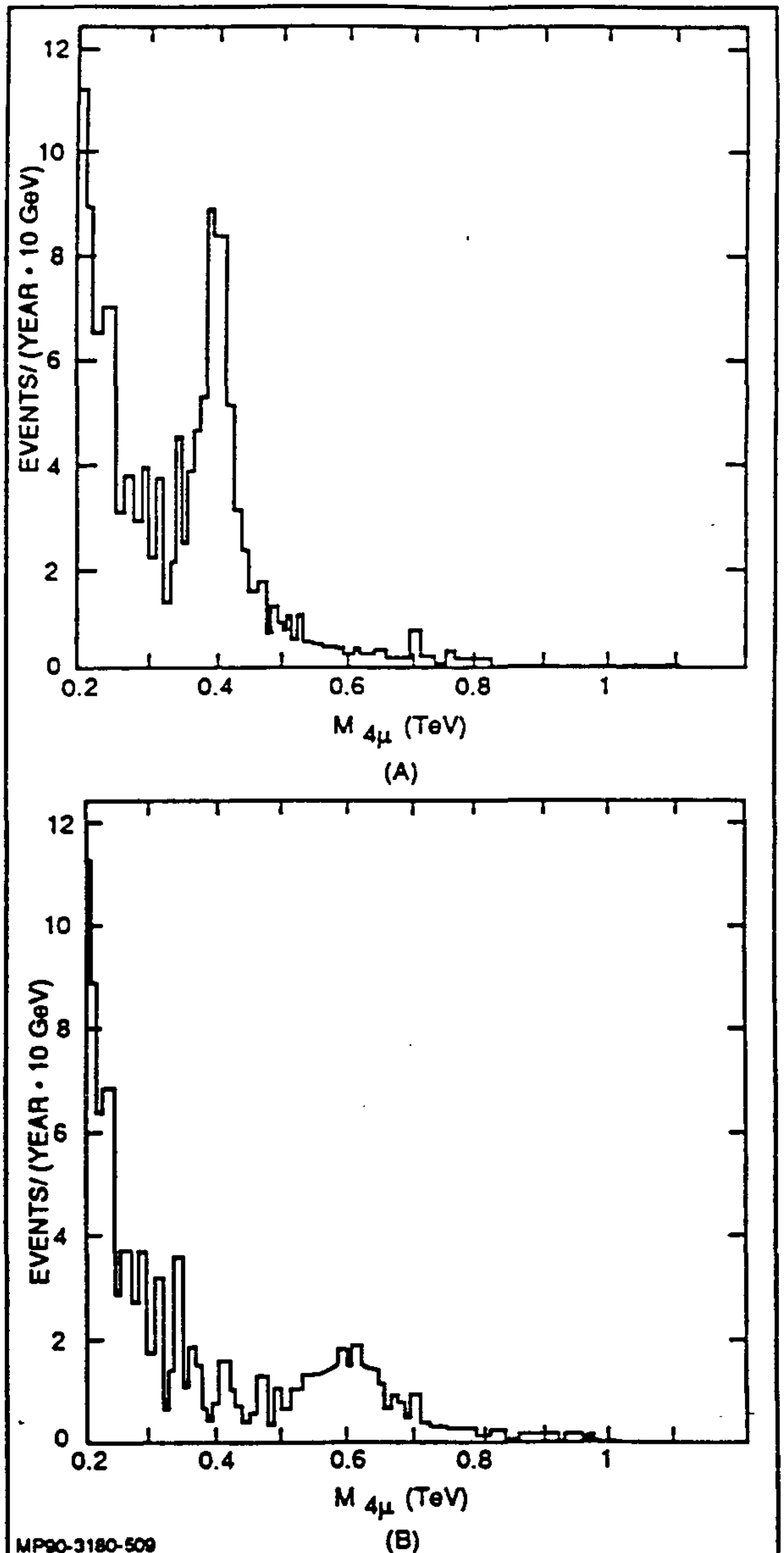

Fig. 6-4 Invariant Mass Spectra for $H \rightarrow Z^0Z^0 \rightarrow 4\mu$ for (A) 400 GeV (B) 600 GeV Higgs, Plus the Z^0Z^0 Continuum Background

$H \to Z^0 Z^0 \to \ell^+ \ell^- q\bar{q}$: Large background from $Z^0 + \text{jets}$. L* cuts for 800 GeV:

$p_{T,Z} > 240\,\text{GeV}$

2 jets in $\Delta\phi = \pm 50°$ from Z^0.

Finds 210/640 events.

E/T analysis found modest improvement by requiring jet with $p_T > 50\,\text{GeV}$ and $\eta > 3$.

Might add jet shape cuts and/or multiplicity cut.

$Z^0 \to q\bar{q}$ reconstruction important — useful in many channels. Width probably limited by clustering provided $\Delta\eta = \Delta\phi \sim 0.05$.

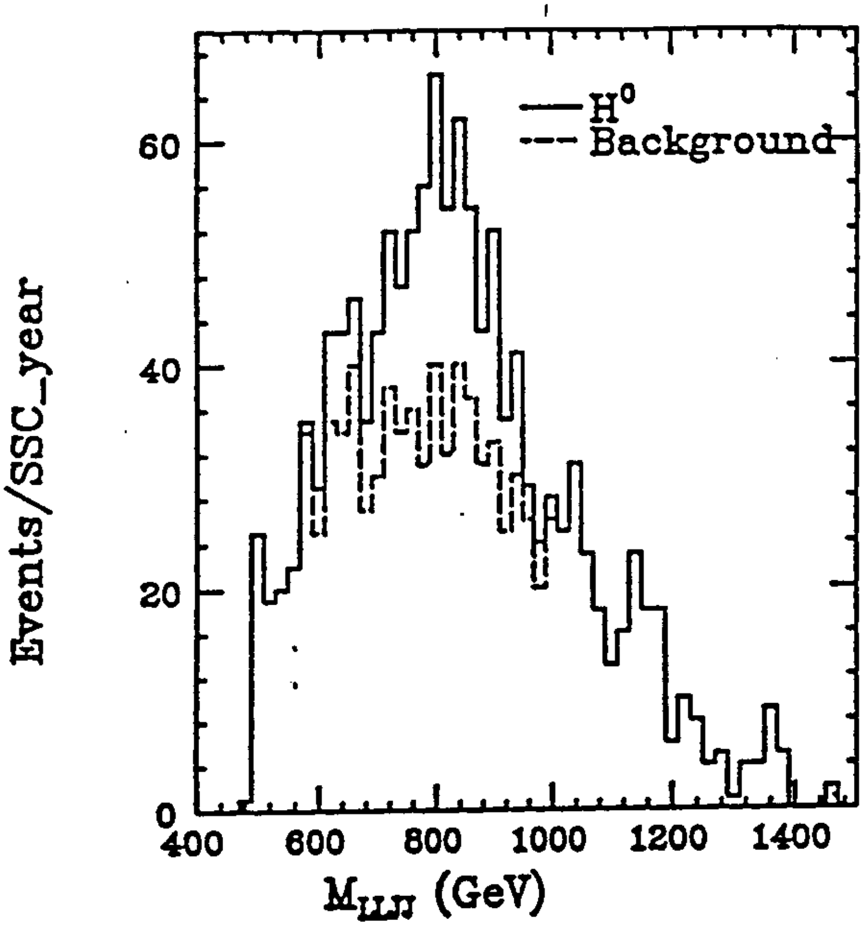

Figure 6: Reconstructed $H \to \ell^+\ell^- q\bar{q}$ mass. (L*)

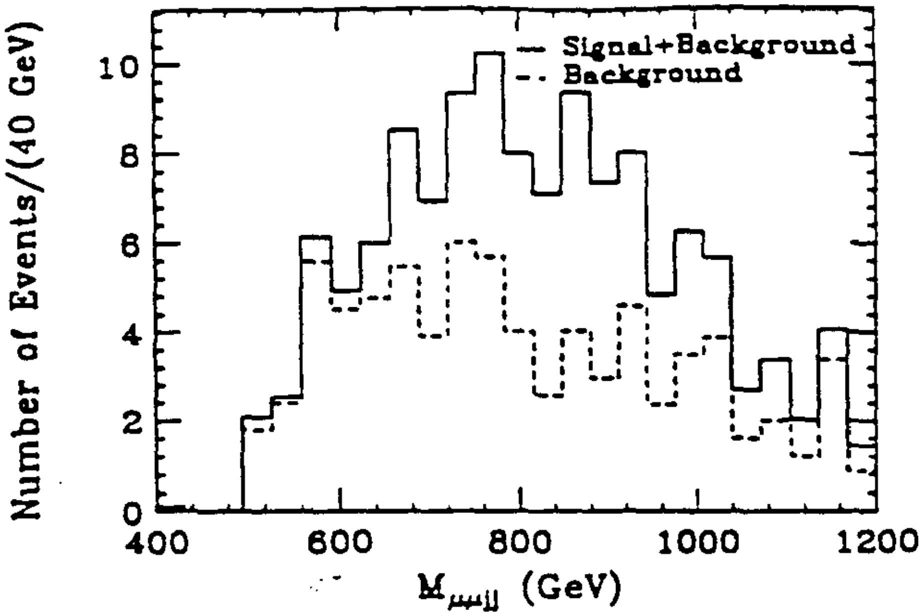

Figure 6-14 $M_{\mu\mu jj}$ *distribution of signal plus background (solid) and the background only (dash).*

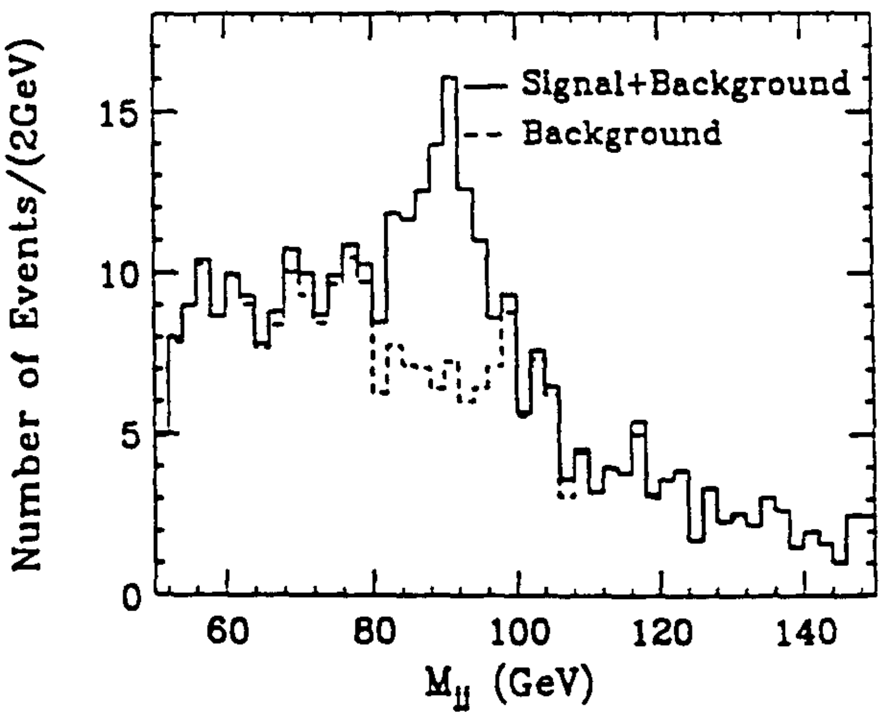

Figure 6-15 M_{jj} *distribution of signal plus background (solid) and background only (dash).*

Intermediate Mass $H \to ZZ^*$:

$H \to Z^0Z^{0*} \to \ell^+\ell^-\ell^+\ell^-$ has adequate branching ratio for $m_H \gtrsim 140\,\mathrm{GeV}$.

Must detect low-p_T leptons.

Backgrounds quite small. H is narrow, so resolution helps.

$H \to ZZ^*$ small for $2m_W < m_H < 2m_Z$. Might confirm with $H \to W^+W^- \to e^\pm\mu^\mp X$.

Must veto jets to reject $t\bar{t}$. Need more careful background study.

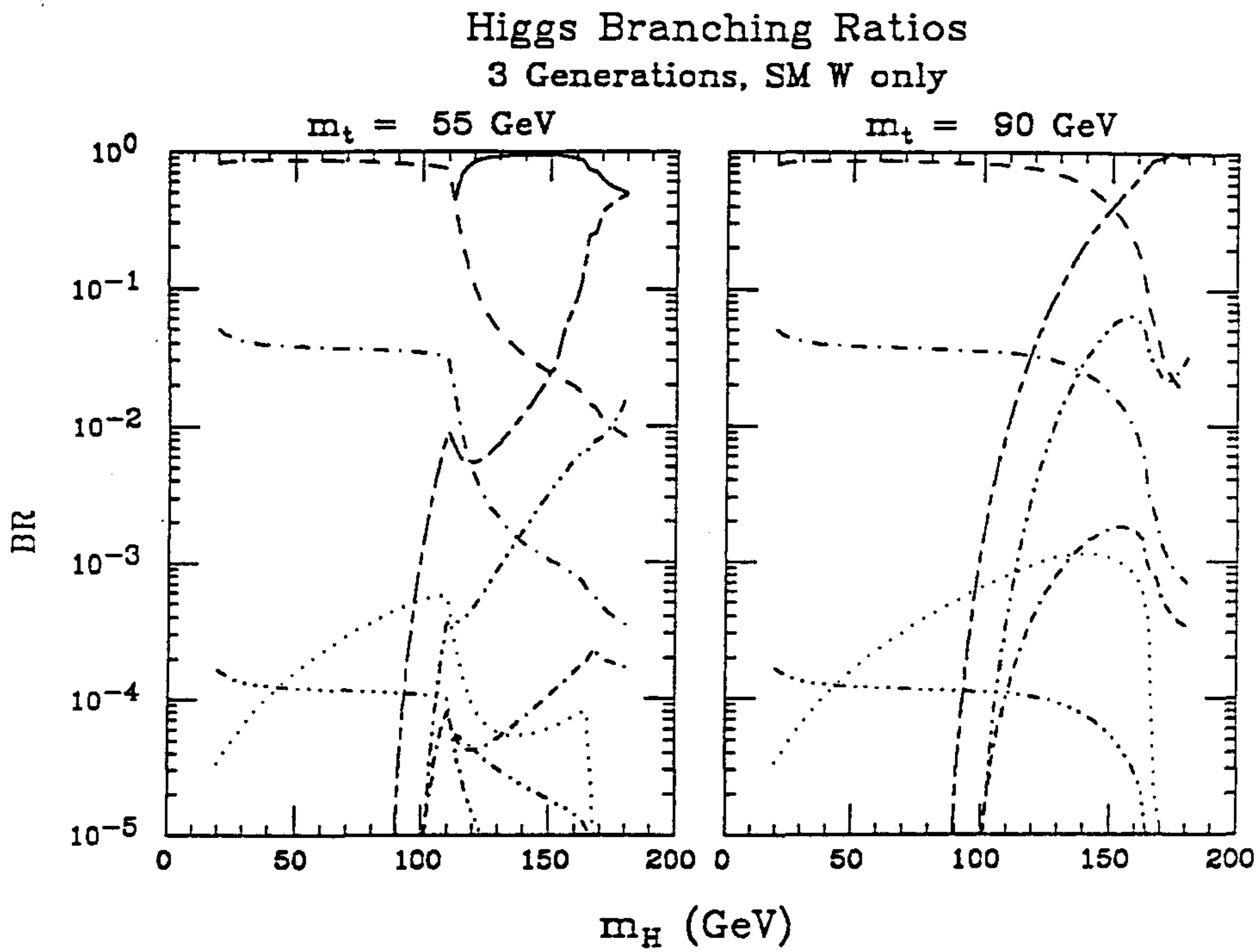

Figure 2.6 The branching ratios for ϕ^0 decay to a variety of channels. We consider $m_t = 55$ and 90 GeV. The curves for the various channels are: solid $= t\bar{t}$; dashes $= b\bar{b}$; dashdot $= \tau^+\tau^-$; longdash-shortdash $= WW$ or WW^* (with no W, W^* branching ratios included); dash-doubledot $= ZZ^*$ (no Z, Z^* branching ratios included); dots $= \gamma\gamma$; doubledash-dot $= Z\gamma$; dash-tripledot $= \Theta\gamma$ (Θ is the toponium bound state); and dash-quadrupledot $= \mu^+\mu^-$. Since the gg decays are not experimentally useful, they are not plotted.

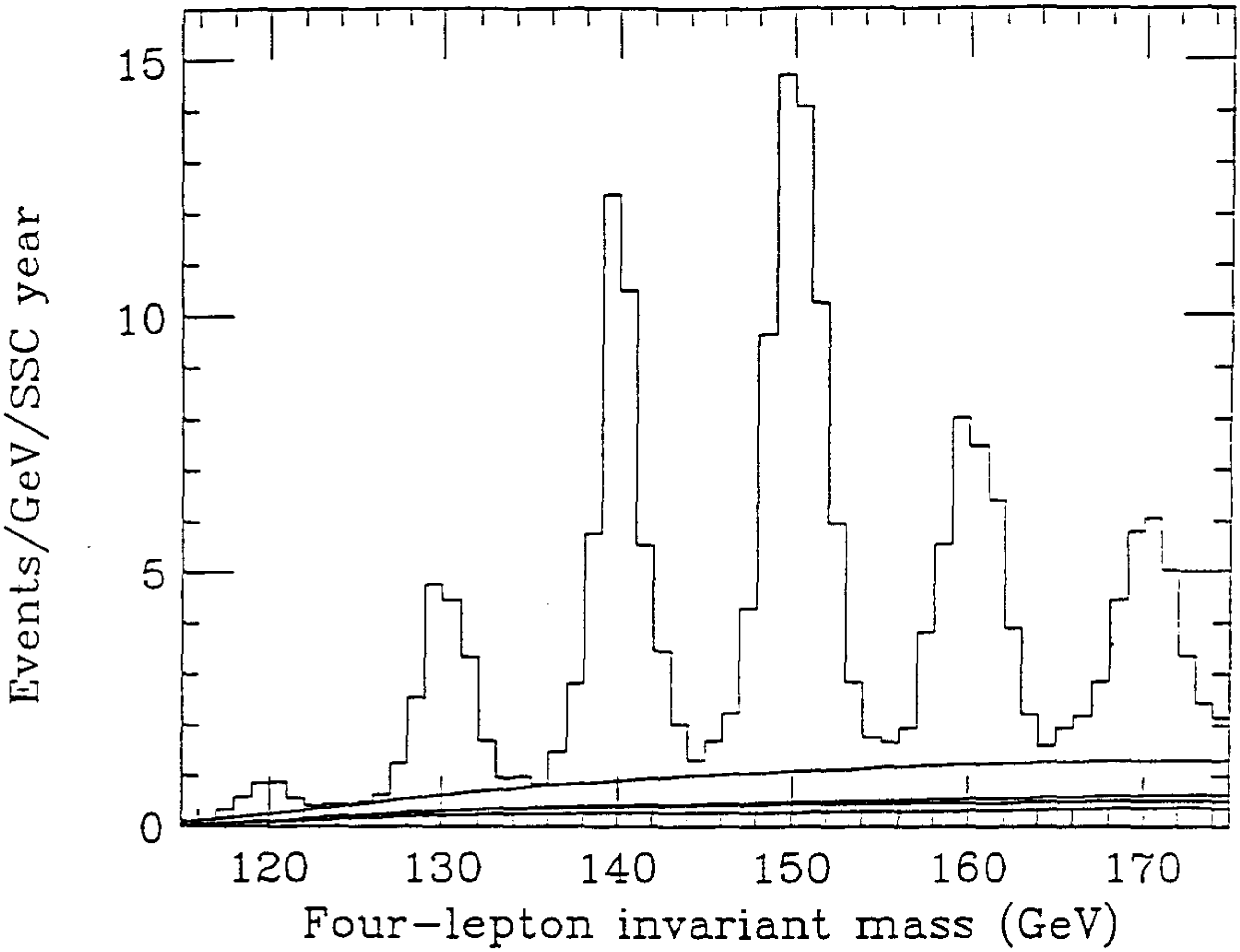

FIG. 3-18. The reconstructed Higgs mass for ZZ^* decaying to $4e$, 4μ, and $2e2\mu$ with $M_{\mathrm{Higgs}} =$ 120, 130, 140, 150, 160, and 170 GeV, including the expected backgrounds. The backgrounds curves are cumulative, and are (from lowest to highest): $q\overline{q} \to ZZ^*$, multiplied by 1.65 to account for $gg \to ZZ^*$, $Z + b\overline{b}$, $Z + t\overline{t}$, and $t\overline{t}$. The invariant mass has been calculated using calorimeter measurements for the electrons.

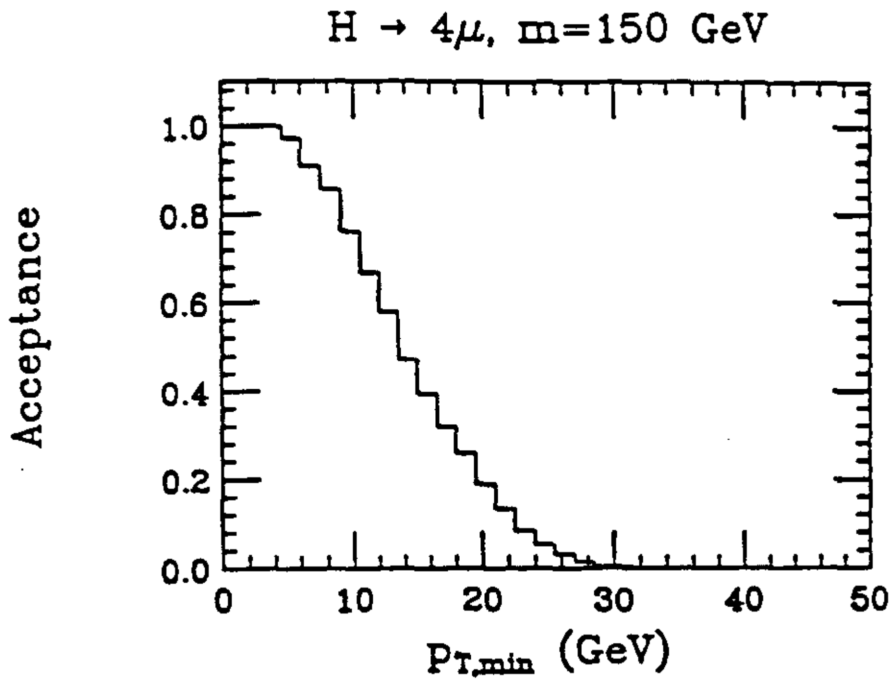

Figure 10: Minimum $p_{T,\ell}$ for $H \rightarrow Z^0 Z^{0*} \rightarrow \ell^+ \ell^- \ell^+ \ell^-$. (EMPACT)

Detailed simulations $\Rightarrow$ can reduce jet background below $\gamma\gamma$.

EAGLE generated jets (mainly gluons?) at $p_T > 40\,\text{GeV}$, $\eta = 0$. Used shower library for single particles:

- Homogenized calorimeter.
- Segmentation $\Delta\eta \times \Delta\phi = .02 \times .02$.

Cuts:

Isolation:

$$\text{EM: } E_T\,(.18 \times .18) - E_T\,(.10 \times .10) < 5\,\text{GeV}\,.$$

$$\text{HAD: } E_T\,(.18 \times .18) < 5\,\text{GeV}\,.$$

Shower shape.

Preradiator: factor of 5 for isolated π^0.

Find

$$\text{“}\gamma\text{”}/\text{jet} \approx 1/(3000 \times 5)$$

GEM analysis makes similar cuts.

Parameterize full simulations of shape and γ/π^0 rejections for LKr accordion with strips in first $3X_0$.

Strips also provide pointing to vertex.

Generate signal and backgrounds with PYTHIA. Most of γj and jj background comes from real γ radiation. Backgrounds after cuts:

	$\gamma\gamma$	γj	jj
Total	31 pb	19 pb	20 pb
γ	31 pb	17 pb	10 pb
π^0		2 pb	10 pb

Could reduce jj π^0 background more.

Probability of finding a correct Higgs Vertex

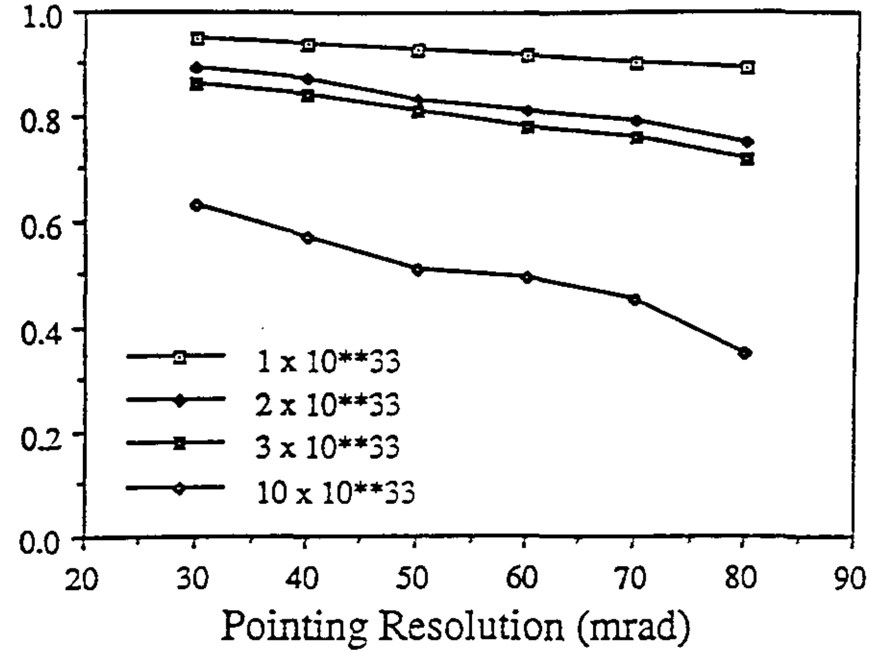

z resolution of wrongly chosen vertices (cm)

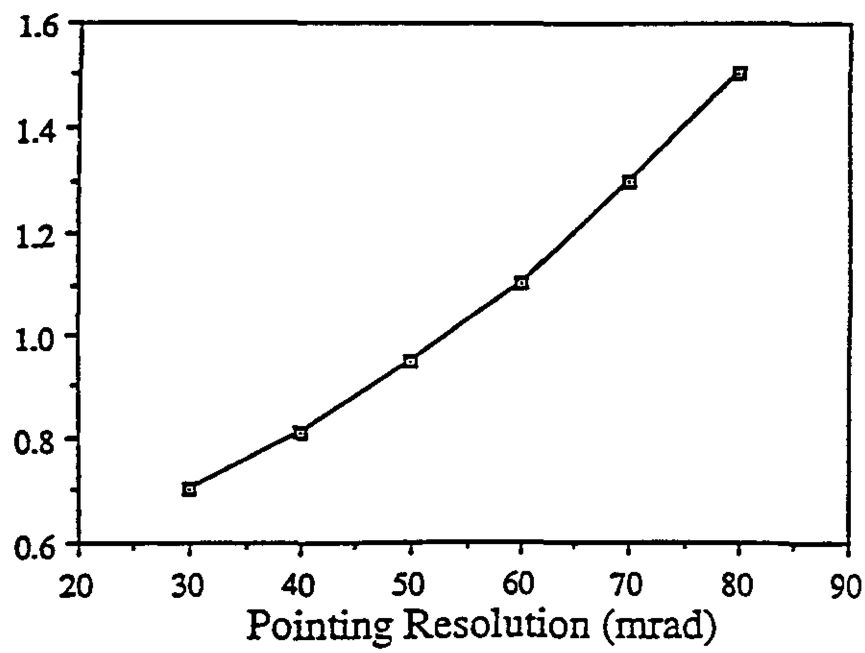

Real γ radiation is Monte Carlo approximation to higer order QCD. Gives $K \approx 1.9$.

Should not double count higher order QCD by including γ radiation and multiplying background by K factor.

PYTHIA gives reasonable agreement with isolated single γ at LEP, so use it.

Also include K factor for signal $\Rightarrow 4.2\sigma$ for $M_H = 80\,\text{GeV}$.

Better for higher masses.

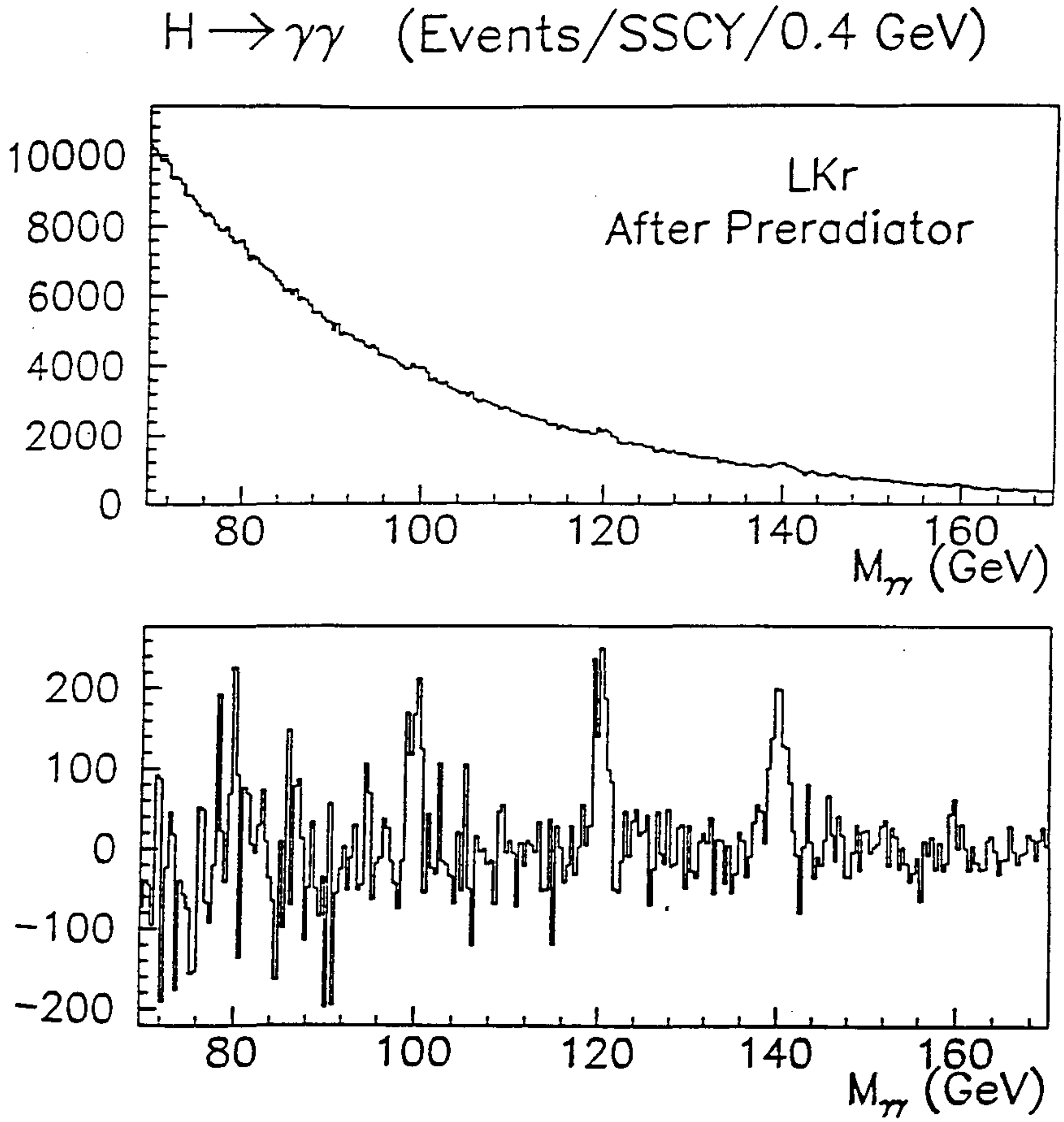
H→γγ (Events/SSCY/0.4 GeV)
LKr
After Preradiator
10000
8000
6000
4000
2000
0
80
100
120
140
160
M_γγ (GeV)
200
100
0
−100
−200
80
100
120
140
160
M_γγ (GeV)

Intermediate Mass $H \to \gamma\gamma$:

Need $\gamma\gamma$ mode for lighter masses, either inclusive or with $t\bar{t}$ or W.

Inclusive production by gg and WW fusion. QCD correction gives [Dawson; ...]

$$K \approx 1.5$$

Background from $q\bar{q}$, $gg \to \gamma\gamma$ requires

$$\frac{\Delta M}{M} < 1\%$$

Hence need

High resolution e.m. calorimeter.

Vertex position.

$\sim 10^{-4}$ γ/jet rejection.

Reject jets in trigger.

Require tight isolation cut to reject jets. Also use shower shape and/or preradiator.

Detailed simulations $\Rightarrow$ can reduce jet background below $\gamma\gamma$.

EAGLE generated jets (mainly gluons?) at $p_T > 40\,\mathrm{GeV}$, $\eta = 0$. Used shower library for single particles:

- Homogenized calorimeter.
- Segmentation $\Delta\eta \times \Delta\phi = .02 \times .02$.

Cuts:

$$E_{EM}(.06 \times .06) > 35\,\mathrm{GeV}$$

$$E_{HAD}(.18 \times .18) < 5\,\mathrm{GeV}$$

$$E_{EM}(.18 \times .18) - E_{EM}(.10 \times .10) < 5\,\mathrm{GeV}$$

Leaves mainly π^0 and multi-π^0.

Next use shape cut: require E_t weighted RMS size consistent with single shower. Then find

$$\text{“}\gamma\text{”}/\text{jet} \approx 1/3000$$

Mainly leaves single π^0's.

Finally use preradiator, which gains another factor of 5 for isolated π^0's.

But difficult even with just real $\gamma\gamma$ background. Significance S for $M_H = 80\,\text{GeV}$:

$\sqrt{s}$ (TeV)	EM Resolution	S
SSC	$2\%/\sqrt{E} \oplus 0.5\%$	4.6
SSC	$7.5\%/\sqrt{E} \oplus 0.5\%$	3.2
LHC	$10\%/\sqrt{E} \oplus 1.0\%$	2.5

Better at higher masses.

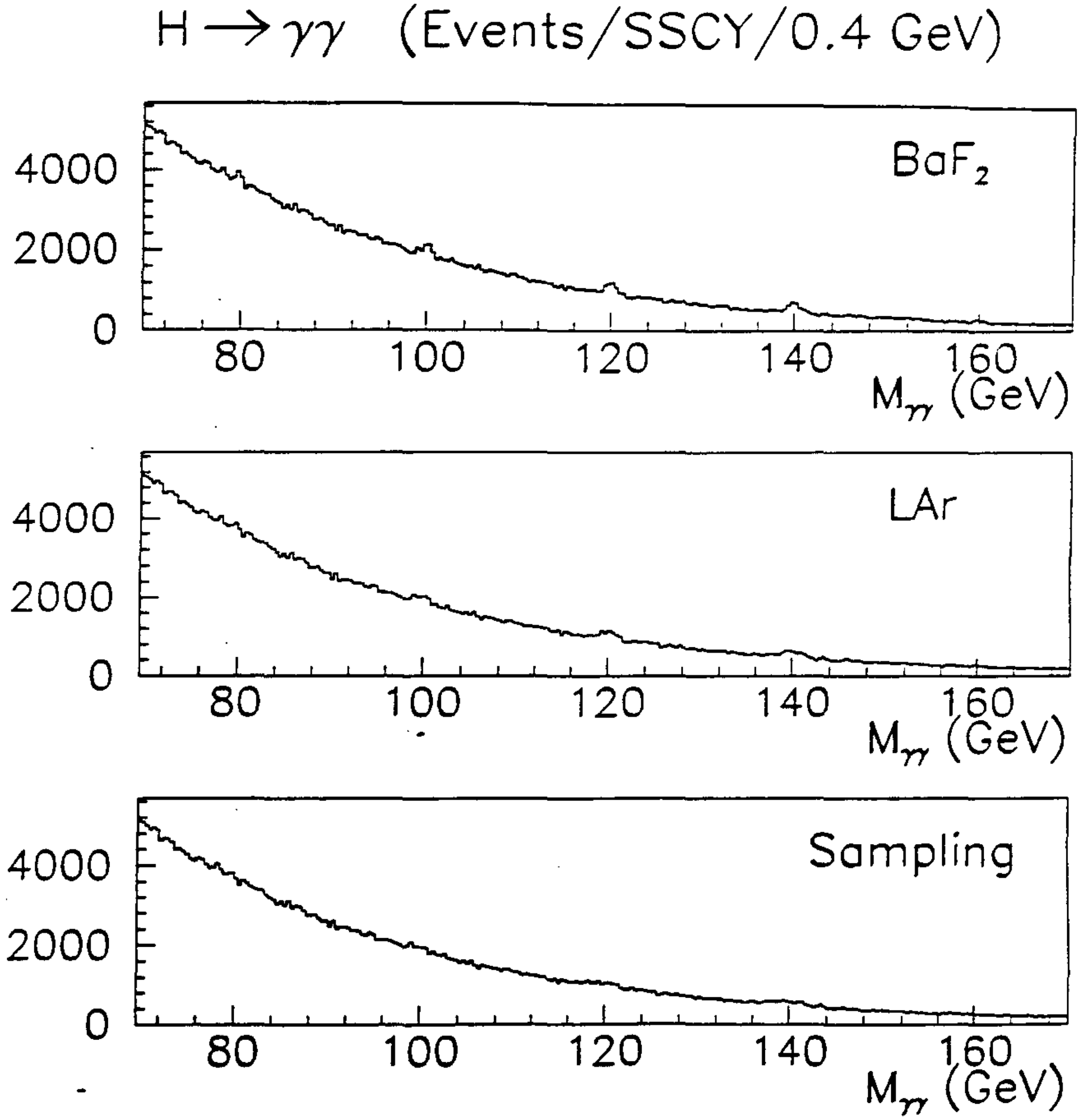

Figure 4: $\gamma\gamma$ invariant mass spectra obtained within 1 SSCY for Higgs signals of 80, 100, 120, 140 and 160 GeV superimposed on irreducible background are shown for three energy resolutions: $(2/\sqrt{E} \oplus 0.5)\%$ (BaF_2), $(7.5/\sqrt{E} \oplus 0.5)\%$ (LAr) and $(15/\sqrt{E} \oplus 1.0)\%$ (Sampling).

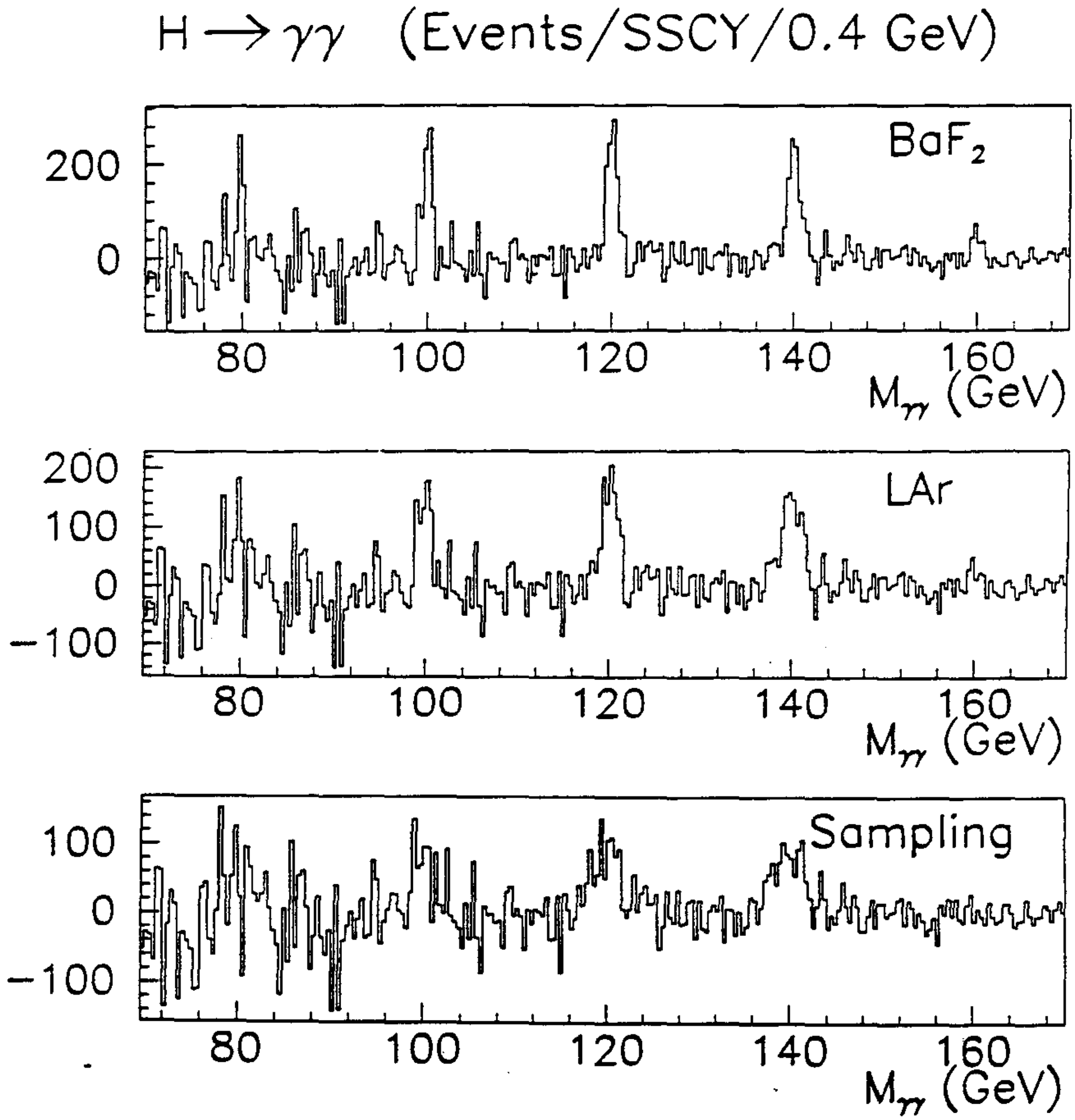

Figure 5: Background subtracted $\gamma\gamma$ invariant mass spectra obtained within 1 SSCY for Higgs signals of 80, 100, 120, 140 and 160 GeV are shown for three energy resolutions: $(2/\sqrt{E} \oplus 0.5)\%$ (BaF_2), $(7.5/\sqrt{E} \oplus 0.5)\%$ (LAr) and $(15/\sqrt{E} \oplus 1.0)\%$ (Sampling).

Associated Production:

Much better signal/background possible with lepton tag. [Kleiss, Kunszt, Stirling; Marciano, FP; Gunion]:

$$q\bar{q}' \to HW^{\pm} \to \gamma\gamma\ell^{\pm}\nu$$

$$gg \to Ht\bar{t} \to \gamma\gamma\ell\nu X$$

But only 50 events/yr before cuts at SSC.

$t\bar{t}H$ less important at LHC.

Backgrounds from $t\bar{t}\gamma\gamma$, $b\bar{b}\gamma\gamma$, $W\gamma\gamma$, etc., calculated with PAPAGENO.

Not negligible but seem OK. Are there more?

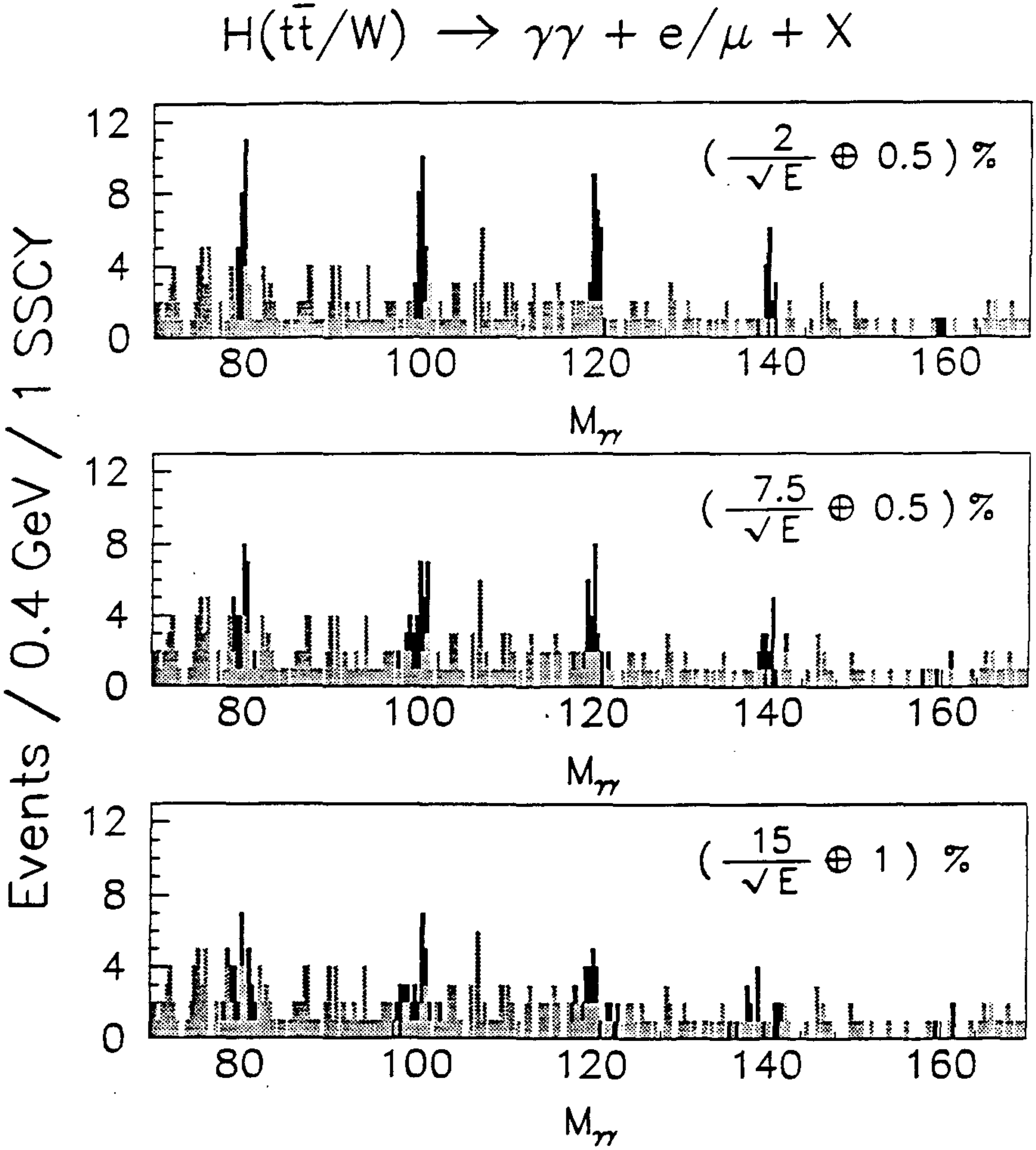

Figure 15: H($t\bar{t}$/W)→ $\ell\gamma\gamma$X signals of 80, 100, 120, 140 and 160 GeV (black area),superimposed on the sum of all backgrounds (gray area) are shown for three different energy resolutions: $(2/\sqrt{E} \oplus 0.5)\%$, $(7.5/\sqrt{E} \oplus 0.5)\%$ and $(15/\sqrt{E} \oplus 1.0)\%$.

Dominant background is $t\bar{t}$ ($\sigma = 16\,\text{nb}$, $m_t = 140\,\text{GeV}$). Generated 2.6M events with PYTHIA 5.5.

Large $t\bar{t}$ background with 2 EM clusters. Make cuts:

- $p_{T,\ell} > 20\,\text{GeV}$, $|\eta_\ell| < 2.5$
- $p_{T,\gamma} > 20\,\text{GeV}$, $|\eta_\gamma| < 2.5$
- Isolation cut:

$$\sum_{R=0.45} E_T - E_{T,\gamma} < 5\,\text{GeV} + 0.1 E_{T,\gamma}$$

- Shower shape cut.
- $p_{T,\gamma\gamma} > 40\,\text{GeV}$.

Then find good S/B, particularly with good EM resolution. [Zhu, Yamamoto]

Must use Poisson statistics to calculate significance. With good resolution, about 5σ in 1 yr for background to fluctuate to signal.

Probably easier to use higher luminosity than for inclusive mode.

Nonstandard Higgs:

Not very unlikely: SUSY provides only known natural framework for elementary scalars.

Generally more difficult than SM. Try to find at least one of h, H, A, H^+.

Use same ZZ and $\gamma\gamma$ modes as standard model plus $t \rightarrow H^+ b$. Still leaves gap in parameter space. [Kunszt, Zwirner]

Try to close gap with $H, A \rightarrow \tau^+\tau^-$. Larger signal than for SM. Can reconstruct mass from $p_{T,\mathrm{miss}}$ provided $p_{T,H} \sim m_H$.

But relevant region close to m_Z.

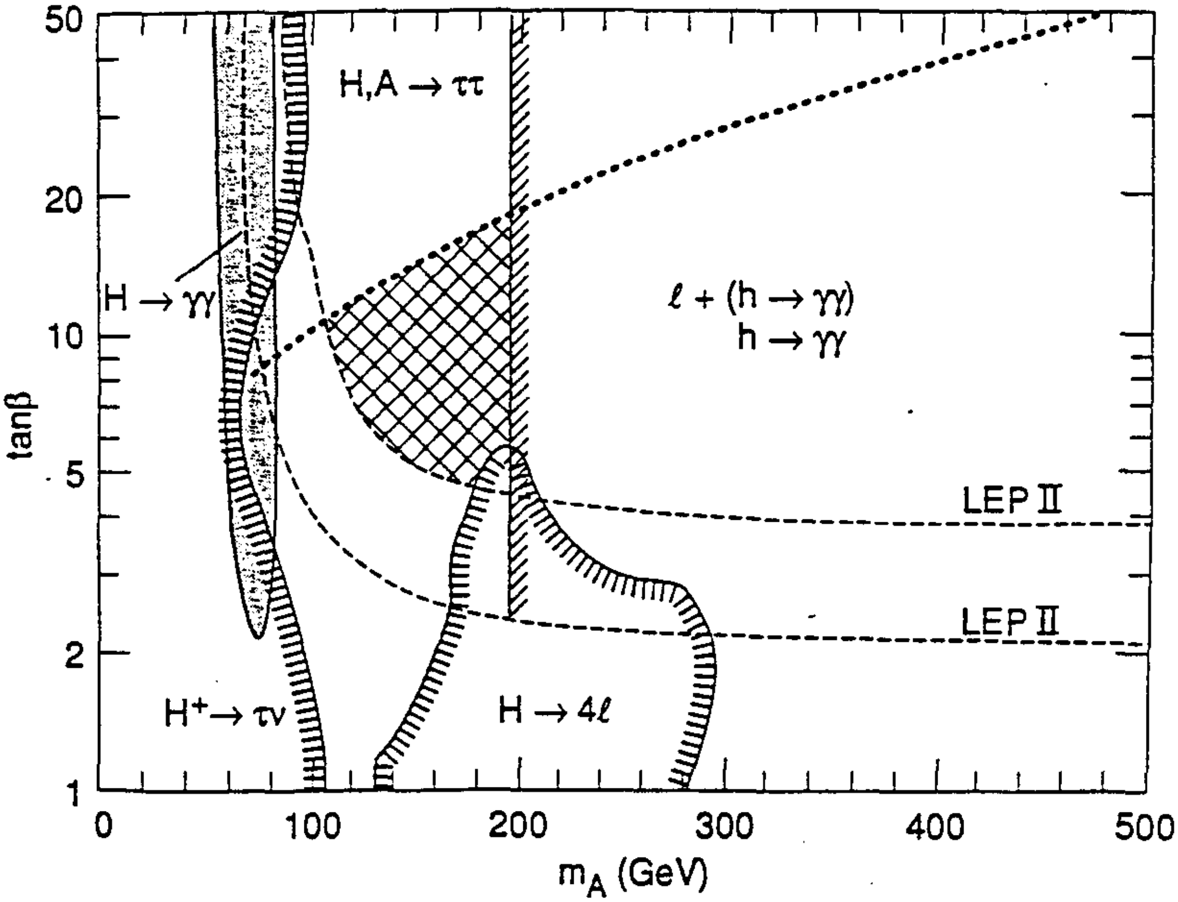

50
20
10
5
2
1
tanβ
0
100
200
300
400
500
m_A (GeV)
H,A → ττ
H → γγ
ℓ + (h → γγ)
h → γγ
LEP II
LEP II
H⁺→ τν
H → 4ℓ

Fig. 30

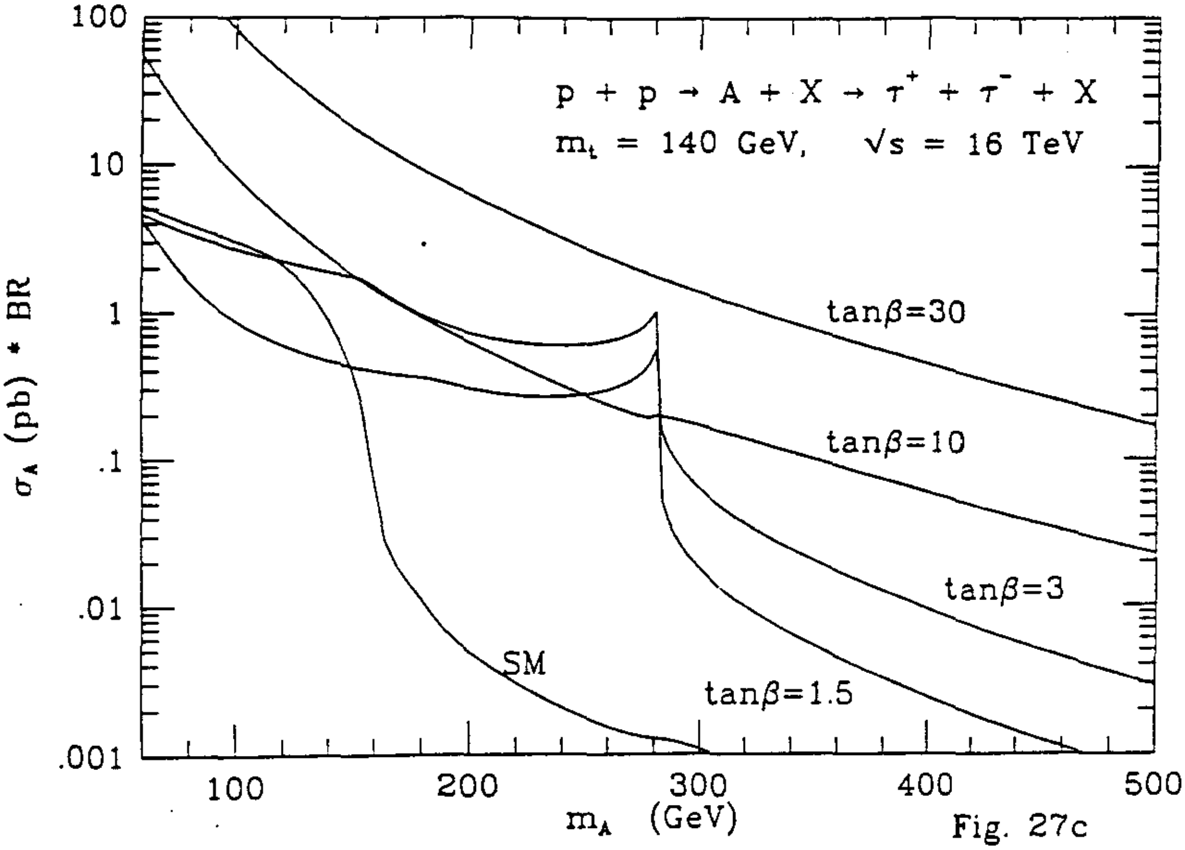

Fig. 27c

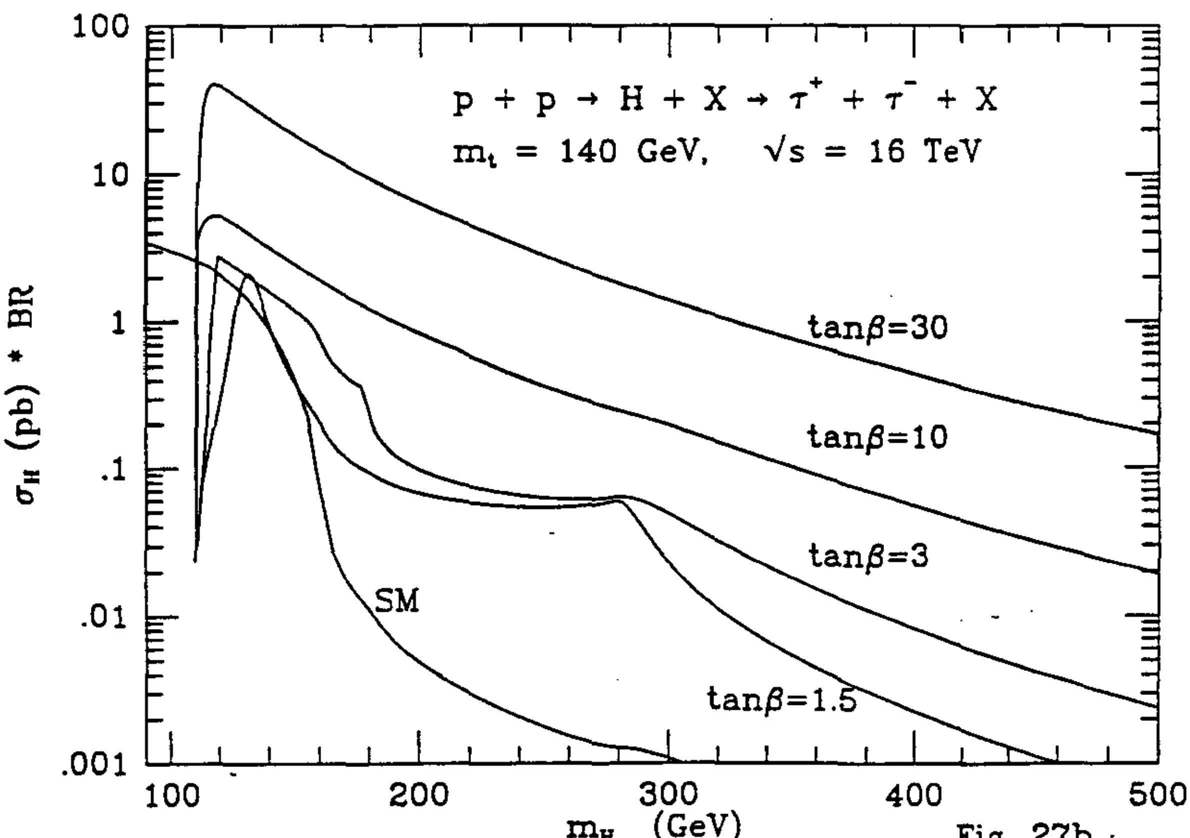

Fig. 27b

Technicolor

Walking technicolor has revived interest. [Holdom; Appelquist, Wijewardhana]

Minimal model hard — only WW physics. QCD-like spectrum at TeV scale.

$\rho^{\pm}_{TC} \to W^{\pm} Z^0$: Produced by WW fusion, W mixing. Expect $m = 1$–$2\,\mathrm{TeV} \Rightarrow \sigma$ tiny.

Leptonic decays: need $\mathcal{L} \sim 10^{34}$ with both e and μ.

Mixed decays: Hard — similar to standard Higgs. Similar methods might work for WW fusion contribution.

$\omega_{TC} \to Z^0\gamma$: Better signature. Need to identify single photon.

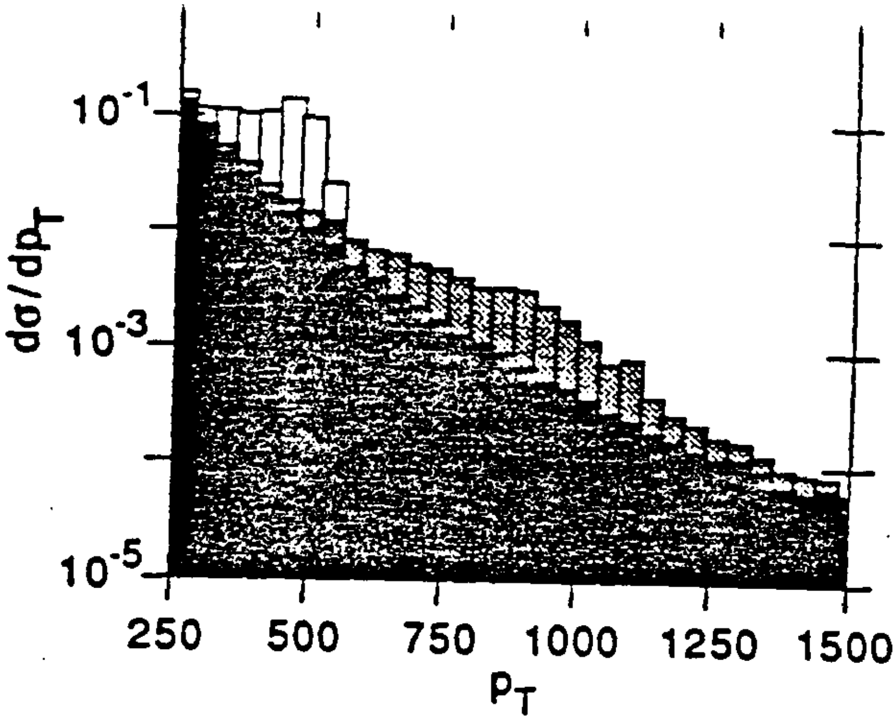

Fig. 4. The transverse momentum of the reconstructed Z, for the background and for the one and two TeV narrow-width techni-rhos of Table I, in fb/GeV.

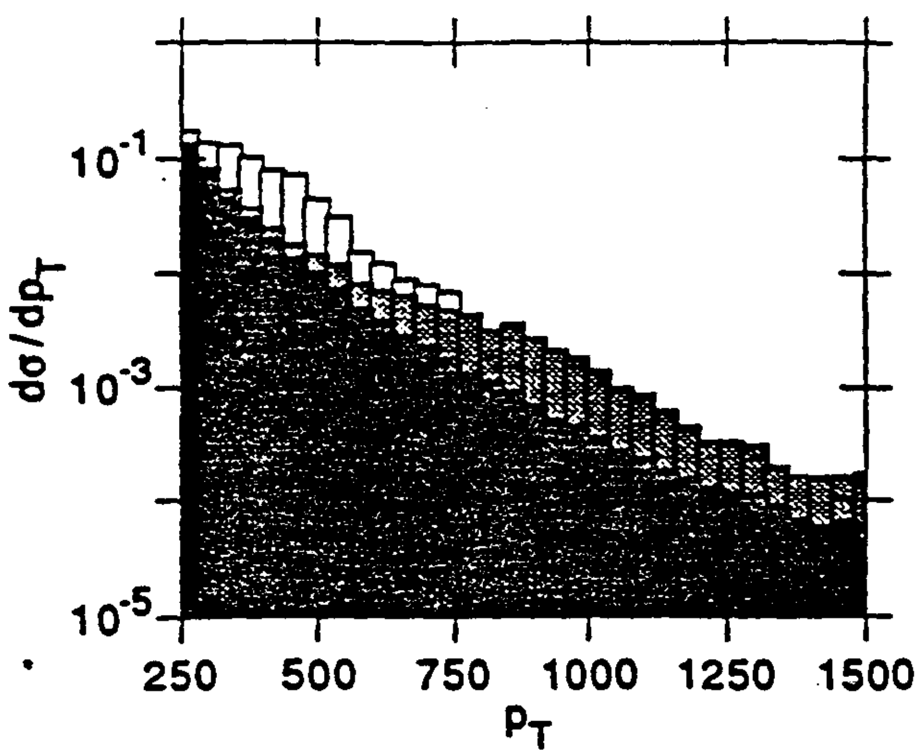

Fig. 5. The transverse momentum of the reconstructed Z, for the background and for the one and two TeV broad-width techni-rhos of Table I, in fb/GeV.

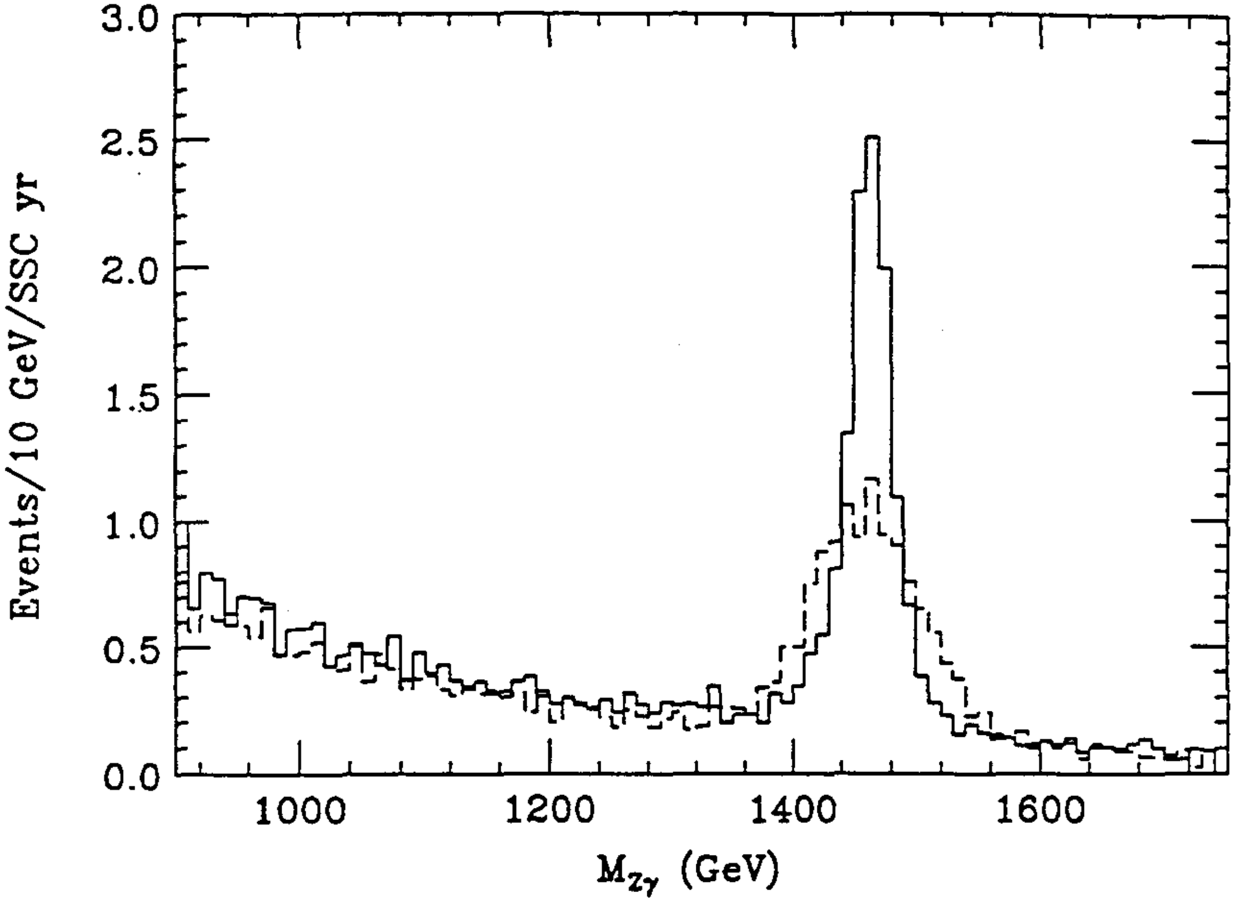

FIG. 33. The invariant mass of the final state system of a photon and an e^+e^- (solid histogram) or $\mu^+\mu^-$ pair (dashed histogram). The lepton pair is required to have mass $M_Z \pm 10$ GeV. The leptons have $|\eta| < 2.5$ and the photon has $|\eta| < 3.0$. The peak corresponds to the production and decay of the techniomega particle of mass 1.46 TeV[51].

Realistic models have much more structure. Typical ingredients:

- More technifermions, some with $SU(3)$ color.
- "Walking" couplings above Λ_{TC}. May change masses and decays.
- Perhaps multiple mass scales.
- Pseudo-Goldstone bosons.

Pseudo-Goldstone boson signatures:

$P_3 \to \tau b$: Pair produced with cross section 15% of quark of same mass.

Can reconstruct in principle: use $\vec{p}_{T,\text{miss}}$ to determine two sums of ν energies. Resolution? Is vertex detector needed?

Guess $P_3 \to \tau b$ dominates, with

$$\frac{\Gamma(\mu b)}{\Gamma(\tau b)} \sim \left(\frac{m_\mu}{m_\tau}\right)^2 \sin^2\theta.$$

Might use one μ decay.

$P_8 \to t\bar{t}$: Studied extensively for $m_t = 20\,\mathrm{GeV}$(!). Simplest model had $m = 240\,\mathrm{GeV}$.

Might also have *narrow* colored ρ^8_{TC} in some models, decaying into leptoquarks or jets. [Lane, Ramana]

Plausible example with complex signatures.

Minimal model has conserved R parity.

Requires two Higgs doublets, so

$$\tilde{\gamma},\ \tilde{Z},\ \tilde{h}^0,\ \tilde{H}^0 \Rightarrow \tilde{\chi}_i^0$$
$$\tilde{W}^\pm,\ \tilde{H}^\pm \Rightarrow \tilde{\chi}_i^\pm$$

Heavier $\tilde{\chi}$'s decay to lighter ones, eventually giving stable LSP $\tilde{\chi}_1^0$.

No evidence for SUSY. But can construct models consistent with all data, grand unification, limited fine tuning, ... [Ross, Roberts]

TABLE 1
Masses of the supersymmetric states for the two solutions (Z and X of fig. 4) with $\alpha_s(M_Z) = 0.118$, (Z) with $m_t = 160$ GeV, (X) with $m_t = 100$ GeV. Here $|\mu_0/m_0| = 1$ and $B_0 = A_0 = 0$

	Parameters	
$m_{1/2}$	140	230
m_0	190	120
μ_0	190	−120
m_t	160	100
$\tan\beta$	21	5
	Gauginos	
$\tilde{\gamma}$	57	83
$\tilde{Z}$; $\tilde{W}$	99; 99	120; 112
$\tilde{g}$	354	559
	Sleptons	
$\tilde{l}_L$	220	206
$\tilde{l}_R$	195	146
	Squarks	
$\tilde{u}_L, \tilde{c}_L; \tilde{d}_L, \tilde{s}_L$	365; 373	511; 517
$\tilde{u}^c_L, \tilde{c}^c_R$	359	495
$\tilde{d}^c_R, \tilde{s}^c_R, \tilde{b}_R$	358	491
$\tilde{t}_L; \tilde{b}_L$	325; 335	491; 497
$\tilde{t}^c_R$	273	452
	Higgs, Higgsinos	
H^0	91; 264	84; 221
$H^{\pm}$; A^0	276; 264	232; 218
$\tilde{H}^0$	205; 225	139; 226
$\tilde{H}^{\pm}$	229	228

The soft supersymmetry breaking contributions have been corrected by including electroweak symmetry breaking terms. The masses (which are in GeV units) of the two solutions represent the range of values of our predictions. The light Higgs does not have the quartic corrections included.

Concentrate on gluinos for pp. "Typical" 750 GeV gluino event:

$$g + g \to \tilde{g} + \tilde{g}$$

$$\begin{array}{ll} \tilde{g}_1 \to \tilde{\chi}^0_4 q\bar{q} & \tilde{g}_2 \to \tilde{\chi}^+_2 q\bar{q}' \\ \tilde{\chi}^0_4 \to \tilde{\chi}^+_1 W^- & \tilde{\chi}^+_2 \to \tilde{\chi}^0_2 W^+ \\ \tilde{\chi}^+_1 \to \tilde{\chi}^0_1 \ell^+ \nu & \tilde{\chi}^0_2 \to \tilde{\chi}^0_1 h^0 \end{array}$$

Many possible signatures.

Missing p_T: LSP $\tilde{\chi}^0_1$ escapes detector.

Physics backgrounds: ν from c, b, t quarks, $W^\pm$ and Z^0.

Also detector induced backgrounds for $\not{E}_T$. Most dangerous for small $\not{E}_T \Leftrightarrow$ small mass.

Previous studies included parameterized calorimeter resolution and segmentation, including transition regions. Effects are small.

Have now included forward calorimeter angular resolution.

Hadronic shower spreads in forward calorimeter over $\mathcal{O}(\lambda_I)$. Depends on fluctuations, so need GEANT.

Mixture level GEANT simulation done for GEM W/LAr forward calorimeter with small-gap tube readout. (Slightly non-projective geometry is included.)

Generated single $\pi^{\pm}$ showers with fixed E distributed uniformly over $3 < \eta < 7$. Then bin in η. Result is [Shupe]

$$\frac{\Delta p_T}{p_T} \approx 15\% \,.$$

Resolution appears Gaussian, but only limited statistics.

Constant $\Delta p_T/p_T$ for $\eta \lesssim 5$ implies $\Delta\theta$ resolution dominates.

Leakage dominates for $\eta \gtrsim 5$.

$\Delta E/E$ important only for very low p_T.

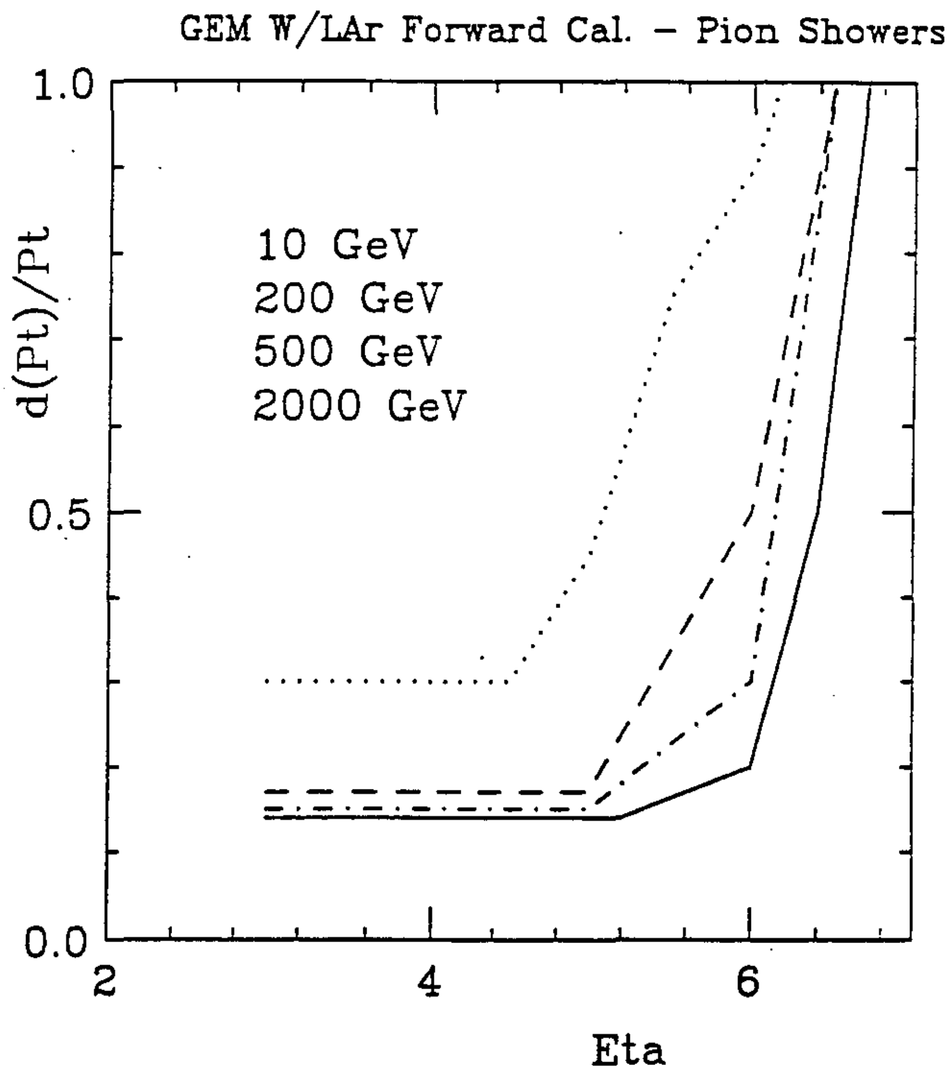

GEM W/LAr Forward Cal. - Pion Showers
1.0
0.5
0.0
d(Pt)/Pt
10 GeV
200 GeV
500 GeV
2000 GeV
2
4
6
Eta

300 GeV Gluino:

Expect most difficulty at low mass.

Generate $\tilde{g}\tilde{g}$ signal for one point in MSSM parameter space for detailed study:

$$m_{\tilde{g}} = 300\,\mathrm{GeV} \quad m_{\tilde{q}} = 600\,\mathrm{GeV}$$

$$\mu = -300\,\mathrm{GeV} \quad \tan\beta = 2$$

Use ISAJET with full cascade decays fed in.

Main sensitivity is to $m_{\tilde{g}}$.

Dominant SM physics background is from heavy quarks.

Dominant detector background is from mismeasured jets.

Generate 1.8M jets with $p_T > 50\,\text{GeV}$ with ISAJET.

Simulate all events with GEM FAST1 simulation, including forward calorimeter $\not{E}_T$ resolution plus central calorimeter with:

- Uniform $\Delta\eta = \Delta\phi = 0.32,\ 0.8$;
- Energy resolution

$$(\Delta E/E)_{EM} = 7.5\%/\sqrt{E} \oplus 0.5\%\,,$$
$$(\Delta E/E)_{HAD} = 60\%/\sqrt{E} \oplus 2\%\,.$$

- Fixed transverse and longitudinal profiles.
- Fluctuated shower start.
- No leakage from $\eta = 3$ edge.
- Electronic and pileup noise.

Comments:

All resolutions are Gaussian(!?).

Effect of $\eta = 3$ edge not included. Believed to be small compared to ν background.

[Forden]

Forward calorimeter parameterization does not describe energy deposition in calorimeter. Hence cannot study jets there.

Event selection:

- $\geq$4 jets, $p_T > 75\,\text{GeV}$.
- Sphericity $S_T > 0.2$, calculated from calorimeter with $E_{T,\,\text{cell}} > 0.5\,\text{GeV}$.

Then find $S/B \approx 2$.

Can improve by lepton veto. Veto μ with $p_T > 20\,\text{GeV}$ and $\eta < 2.5$.

Veto e with same kinematics plus match of energy in $R = 0.1$:

$$|E_{\text{tot}}\,(R = 0.1)\,/p - 1| < 0.1$$

Combines HAD/EM and EM/p cuts.

Then find $(S + B)/B \approx 5$.

Lepton veto not studied in detail, but not critical because of $t \to \tau X$ background.

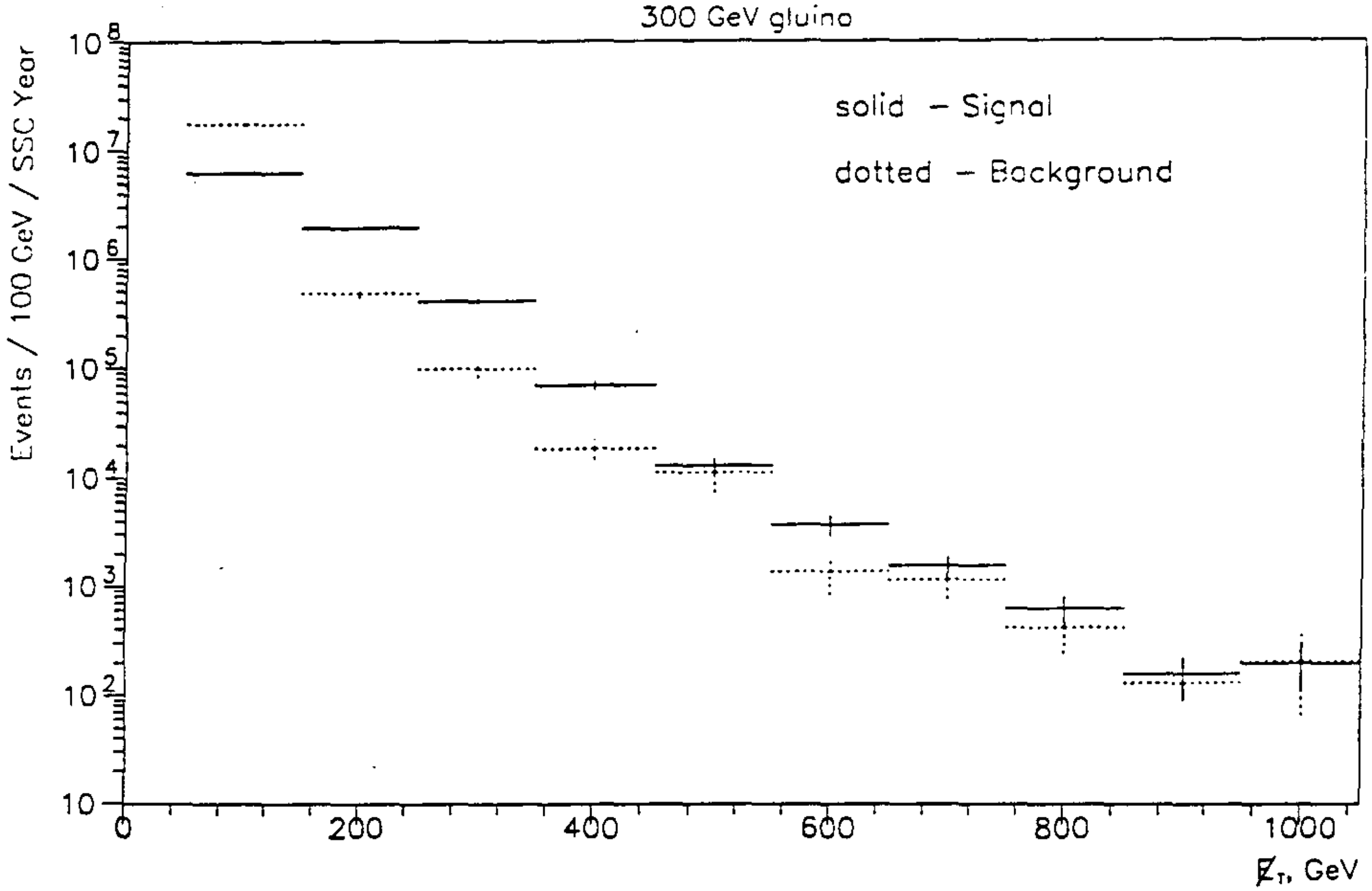
300 GeV gluino
solid – Signal
dotted – Background
Events / 100 GeV / SSC Year
Ɇ_T, GeV

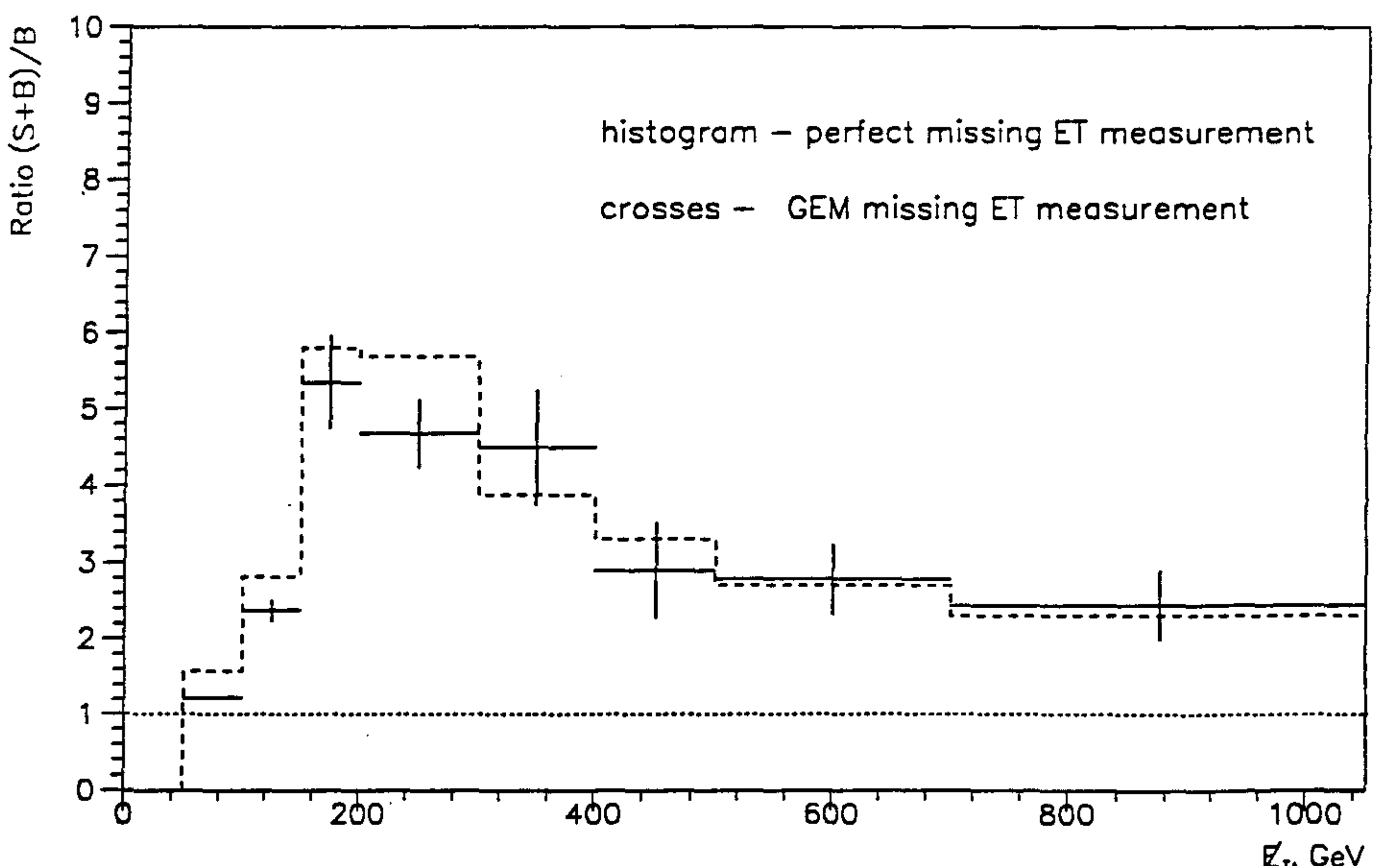
histogram – perfect missing ET measurement
crosses – GEM missing ET measurement
Ratio (S+B)/B
Ɇ_T, GeV

SM backgrounds can be measured. Determine $t\bar{t}$, W, and Z production from isolated leptons, b and c production from μ in jets.

Hence $\not{E}_T$ signal seems credible.

S/B after cuts comparable for real ν background and for detector provided

$$\frac{\Delta p_T}{p_T} \approx 15\%, \qquad \eta_{\max} \approx 5.5$$

Can be achieved.

Must next worry about non-Gaussian tails and cracks.

Multilepton signatures: $\tilde{g}$ is Majorana, so equal rate for $\ell^{\pm}\ell^{\pm}$ and $\ell^{+}\ell^{-}$.

Require [Baer, Tata, Woodside]

$$p_{T,\ell} > 20\,\text{GeV}\,, \quad \eta_\ell < 2.5$$
$$E_T < 5\,\text{GeV in } R < 0.3$$

Then backgrounds small:

Process	σ (pb)
$\tilde{g}\tilde{g}$ (300 GeV)	10
$\tilde{g}\tilde{g}$ (1000 GeV)	0.7
$t\bar{t}$	< 0.2
$Wt\bar{t}$	0.013
$W^{\pm}W^{\pm}$	0.12

Other backgrounds are smaller.

Also 3, 4, 5 lepton signatures.

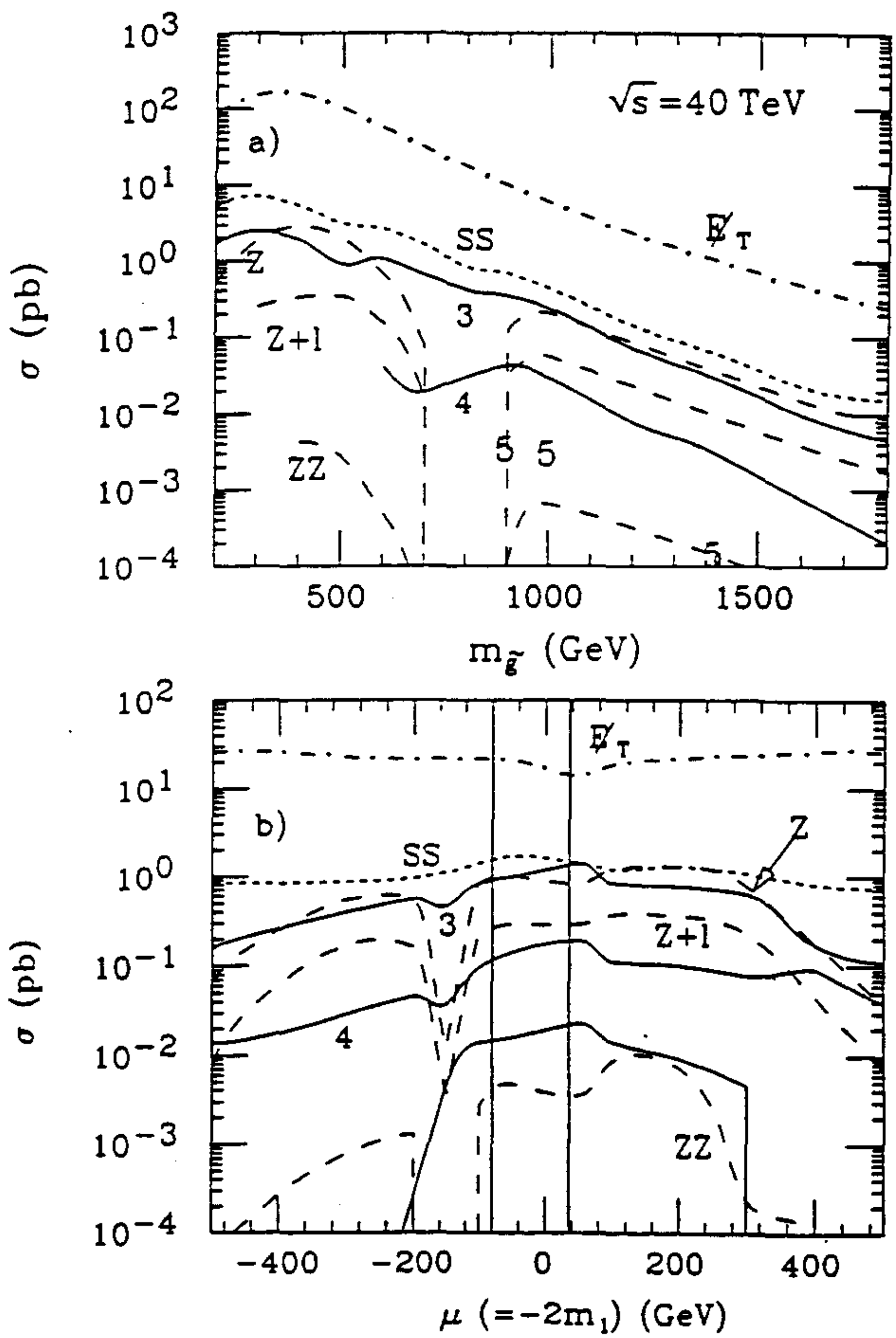

FIG. 2. Cross sections after cuts specified in Sec. II for the various event topologies discussed in the text, for $\sqrt{s}=40$ TeV. We plot (a) vs $m_{\tilde{g}}$ for $\mu=-150$ GeV, while (b) is vs μ for $m_{\tilde{g}}=750$ GeV. We take $m_{\tilde{q}}=2m_{\tilde{g}}$, $\tan\beta=2$, $m_t=140$ GeV, and $m_{H^+}=500$ GeV. The vertical bars in (b) correspond to a region excluded [19] by current LEP data.

Quark/Lepton Substructure

For $Q^2 \ll \Lambda^2$, dominant effect is new 4-fermion interaction:

$$\mathcal{L}_I = \frac{4\pi}{\Lambda^2}\,\bar{f}\Gamma f\,\bar{f}\Gamma f$$

between fermions sharing constituents.

For $q\bar{q} \to \mu^+\mu^-$ at $\mathcal{L} = 10^{34}\,\mathrm{cm}^{-2}\mathrm{s}^{-1}$, sensitive to $\Lambda \gg 20\,\mathrm{TeV}$.

Can also measure angular distributions (model dependent).

Similar effects in jet cross section.

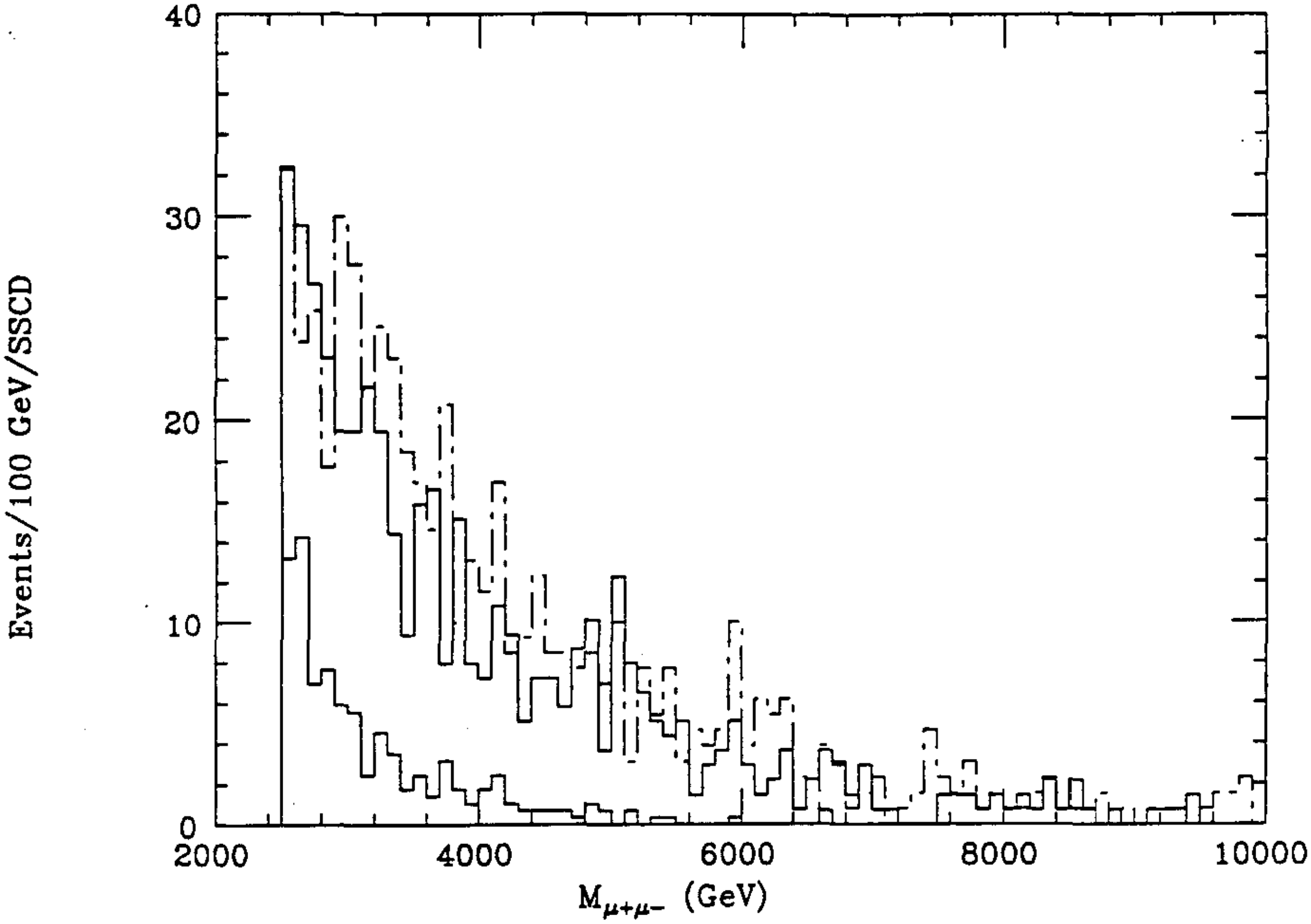

40
30
20
10
0
2000
4000
6000
8000
10000
Events/100 GeV/SSCD
$M_{\mu+\mu-}$ (GeV)

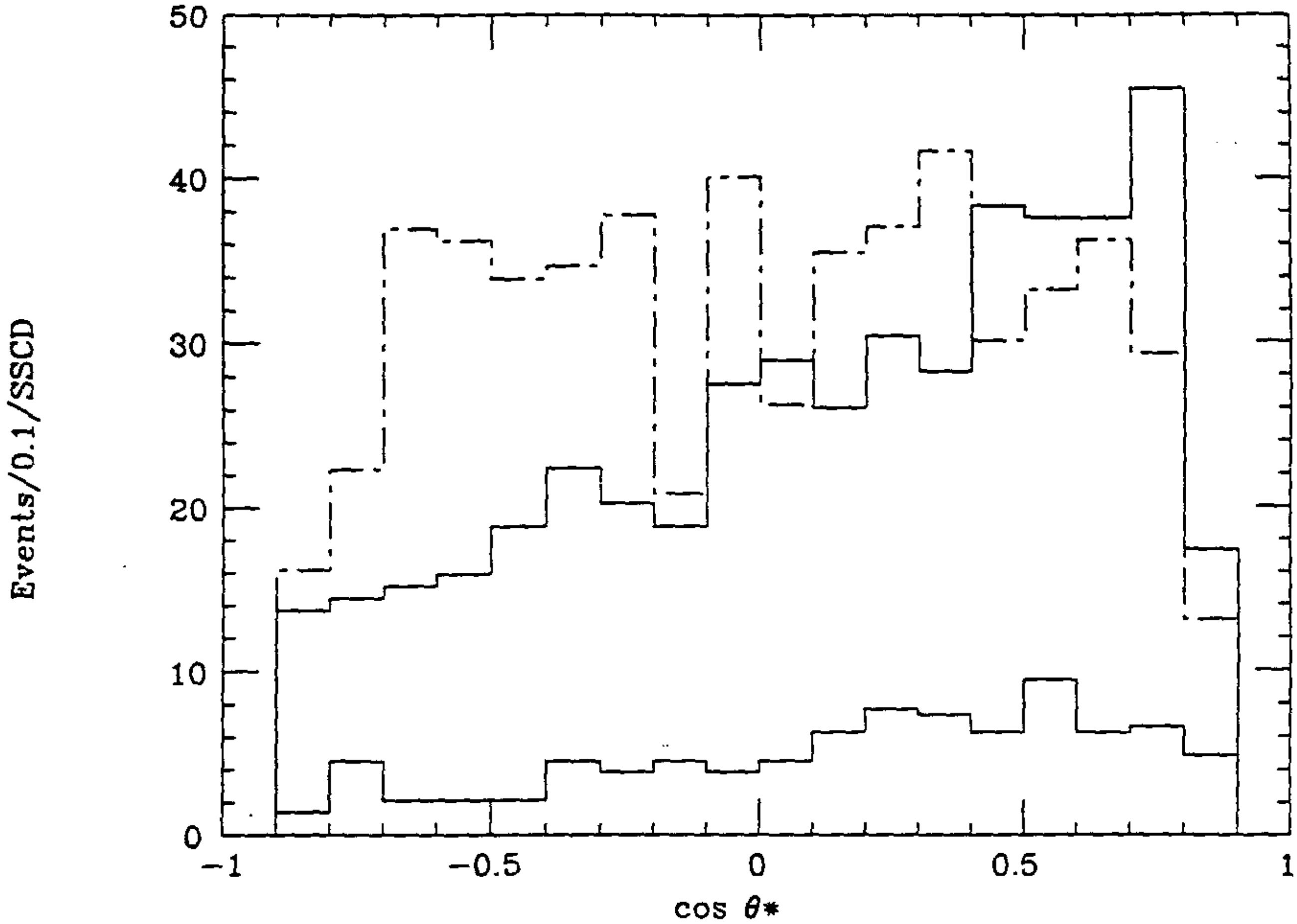
50
40
30
20
10
0
Events/0.1/SSCD
−1
−0.5
0
0.5
1
cos θ*

New W' and Z'

Cross sections are model dependent. For standard model couplings, get a few $Z' \to \ell^+\ell^-$ events for $m \sim 8\,\mathrm{TeV}$.

Can't miss them.

Does constrain e dynamic range and μ resolution.

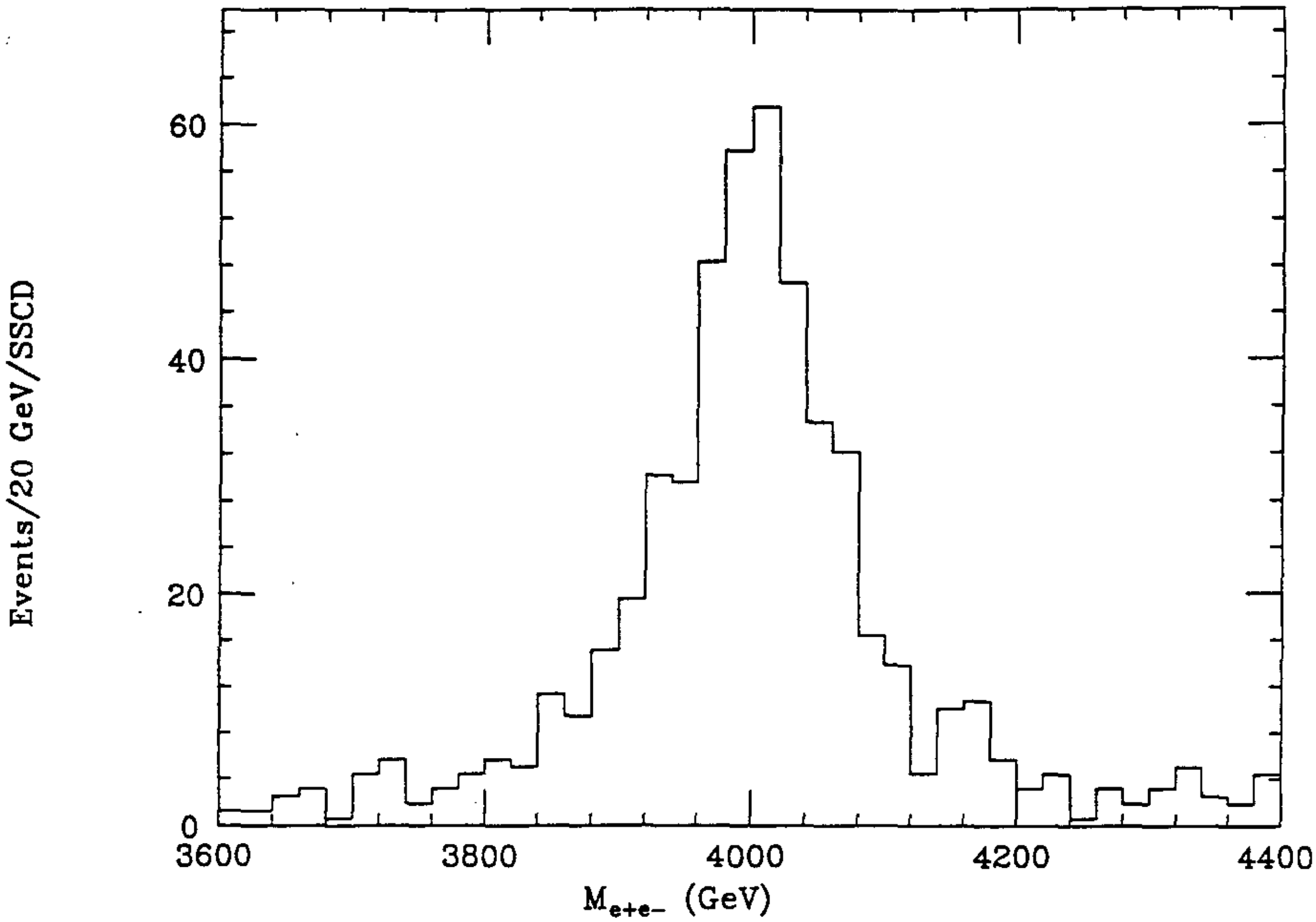
Events/20 GeV/SSCD
0
20
40
60
3600
3800
4000
4200
4400
M_{e+e-} (GeV)

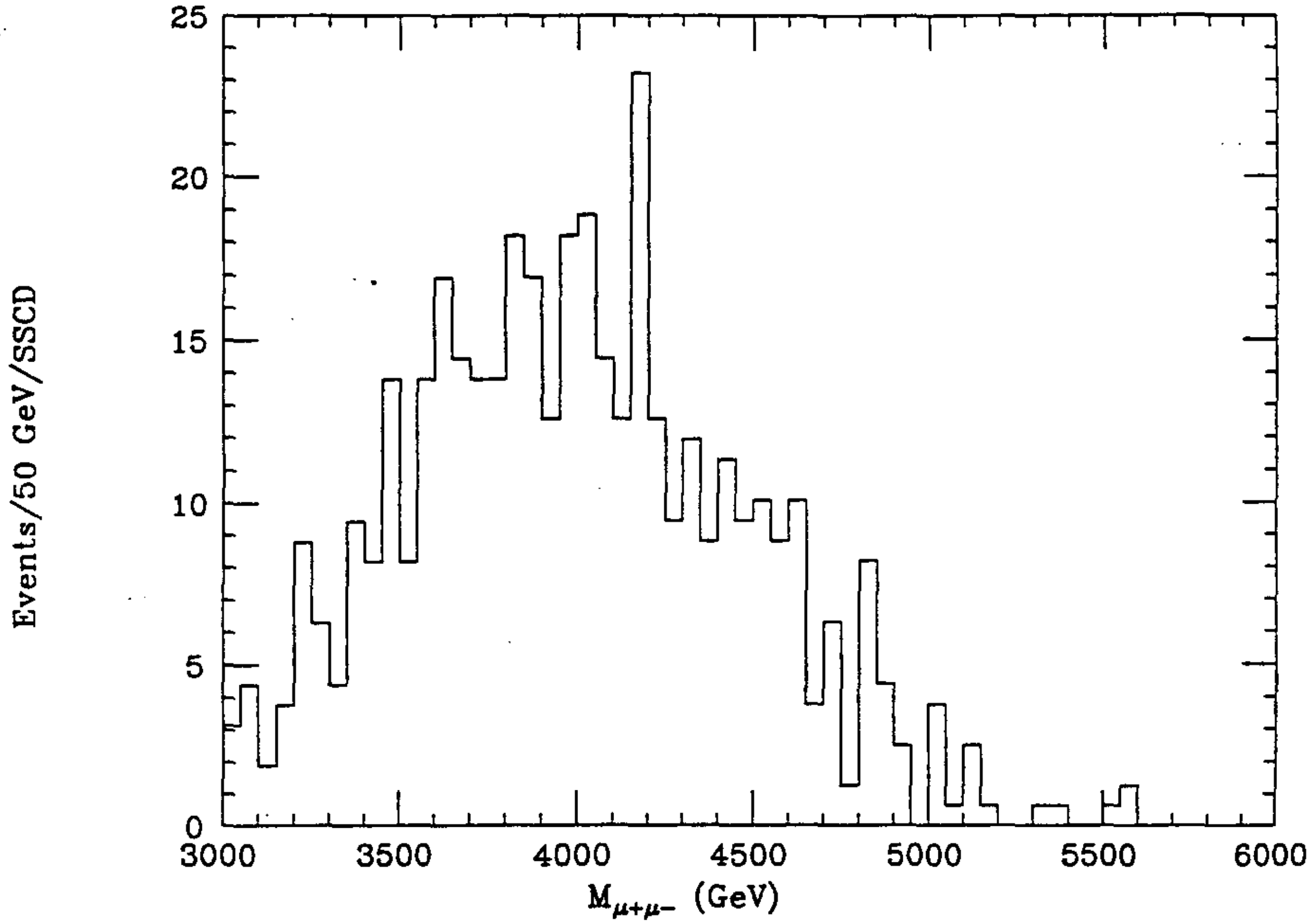

Events/50 GeV/SSCD
$M_{\mu+\mu-}$ (GeV)
0
5
10
15
20
25
3000
3500
4000
4500
5000
5500
6000

Conclusion

SSC/LHC will open up qualitatively new mass scale.

Expect to understand electroweak symmetry breaking at this scale. May also understand fermion masses.

Many physics possibilities. But we know that *any* new particle must decay into

Quanta of the standard model.

Invisible new particle $\Rightarrow$ missing energy.

Several different quanta may be involved, so need large 4π detectors.

Look forward to data instead of Monte Carlo!

Calorimetry + Discussion

Howard Gordon

GEM Liquid Calorimetry

I. Physics Requirements

Higgs search - **Energy resolution** $\frac{a}{\sqrt{E}} \oplus b(\oplus \frac{c}{E})$

- **γ Pointing** $\sim \frac{40mrad}{\sqrt{E}}$
- **π^0 rejection**
- **Depth (25 X_0), segmentation,...**

Z' **Dynamic Range: 10 MeV - few TeV**

Jets **Energy resolution - constant term**

Segmentation (<0.1)

Depth ~9 λ

η coverage - 5.5

Forward Jet Tagging

Muons **12 - 16 λ, sensitivity to MIP's and catastrophic energy loss**

Fast Liquid Ionization Fundamentals

EM Calorimeter - Based on Accordion

Hadron Calorimeter - Based on D0/SLD

Higgs search with EMPACT/TEXAS

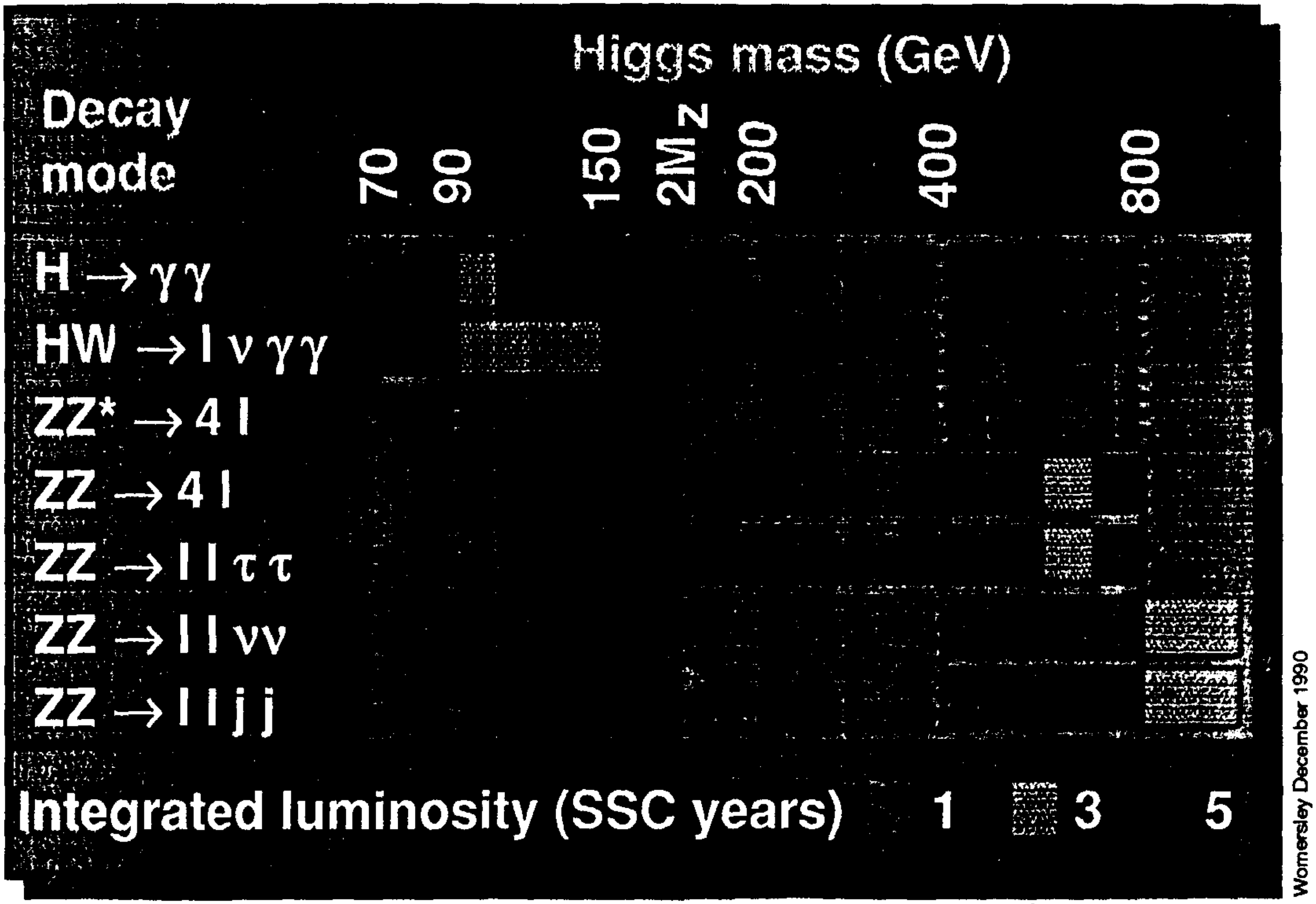

If there is a Higgs – we'll find it

– if there is something new, we'll discover it!

Mass Resolution (%)
H$\rightarrow \gamma\gamma$

$$\Delta E/E = (a/\sqrt{E} \oplus b)\%$$

a/b	2/0.5	5.5/0.5	5-7/0.5	7.5/0.5	8/1
80	0.43	0.63	0.66	0.79	1.0
90	0.41	0.60	0.62	0.74	1.1
100	0.41	0.59	0.61	0.73	0.97
120	0.39	0.55	0.57	0.67	0.93
140	0.39	0.55	0.55	0.66	0.93
150	0.41	0.55	0.57	0.65	0.93

Photon Direction Measurement

No CT, with Pointing

The most robust approach is to measure the photon direction by using **pointing** provided by longitudinally segmented calorimeter information, and determine the primary Higgs vertex by using beam constraint.

Assuming:

$$\delta\theta = c/\sqrt{E}\ mrad$$

the mass resolution (GeV) of 80 GeV Higgs($\rightarrow \gamma\gamma$) accepted in $|\eta| < 2.5$ is:

c (mrad)	0	30	40	50	60	80
a=2.0,b=0.5	0.34	0.40	0.43	0.47	0.51	0.60
a=5.5,b=0.5	0.52	0.56	0.59	0.62	0.66	0.74
a=7.5,b=0.5	0.66	0.68	0.70	0.73	0.76	0.85
a=15.,b=1.0	1.34	1.34	1.35	1.36	1.36	1.37

Works well for both SSC and LHC.

By using 3 longitudinal segments (3/6/16 X_0) and 6 θ strips in the first segment, the photon polar angle can be determined to c = 40 mrad for LKr EMC (H. Ma & M. Leitchouk, GEM Note), which degrades Higgs mass resolution by 14%.

Photon Direction Measurement

with both CT and Pointing

Combining pointing and vertices from CT: looking for the closest vertex to the z position reconstructed by pointing vectors.

Assuming:

$$\delta\theta = c/\sqrt{E}\ mrad$$

the probability of finding a correct Higgs vertex ($P_{correct}$) and the z resolution of wrongly chosen vertices (δz_{wrong}) are shown as function of luminosity ($\mathcal{L}$) in $10^{33}/s/cm^2$:

$\mathcal{L}$	c (mrad)	30	40	50	60	70	80
1	$P_{correct}$ (%)	95	94	93	92	90	89
2	$P_{correct}$ (%)	89	87	83	81	79	75
3	$P_{correct}$ (%)	86	84	81	78	76	72
10	$P_{correct}$ (%)	63	57	51	49	45	35
	δz_{wrong} (cm)	0.70	0.81	0.95	1.1	1.3	1.5

Works well for both SSC and LHC.

Background X-Section
H→ $\gamma\gamma$ Searches

	$\gamma\gamma$	γ-jet	2jets
$\hat{p}_t > 20$ GeV	280 pb	240 nb	2.0 mb
$E_T > 20$ GeV, $\lvert\eta\rvert < 2.5$	100 pb	80 nb	530 μb
$M_{\gamma\gamma} > 75$ GeV	42 pb	34 nb	240 μb
Rejection Needed		800	6×10^6
Final Background	31 pb	19 pb	20 pb
Single Photon	31 pb	17 pb	10 pb
Jet Background		2 pb	10 pb

Note, the Jet background may be reduced by optimizing kinematics cut, such as requiring high p_T on photon.

Significance of 80 GeV Higgs

	$\gamma\gamma$ Background	All Background
	3.7	2.8
1.5 k-Factor	5.6	4.2

Note, EHLQ set 1 structure function is used.

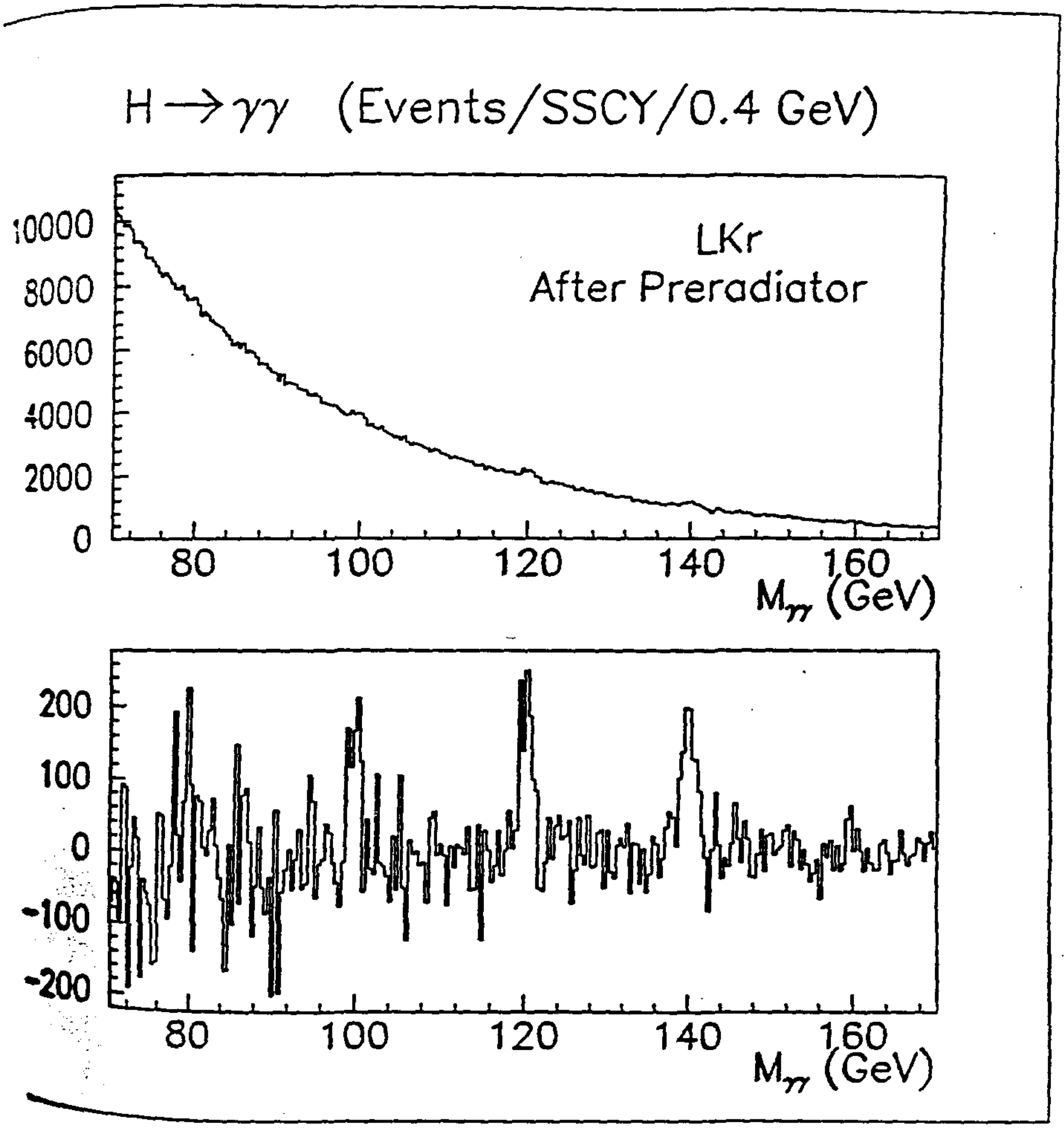

H → γγ (Events/SSCY/0.4 GeV)
10000
8000
6000
4000
2000
0
LKr
After Preradiator
80
100
120
140
160
M_γγ (GeV)
200
100
0
-100
-200
80
100
120
140
160
M_γγ (GeV)

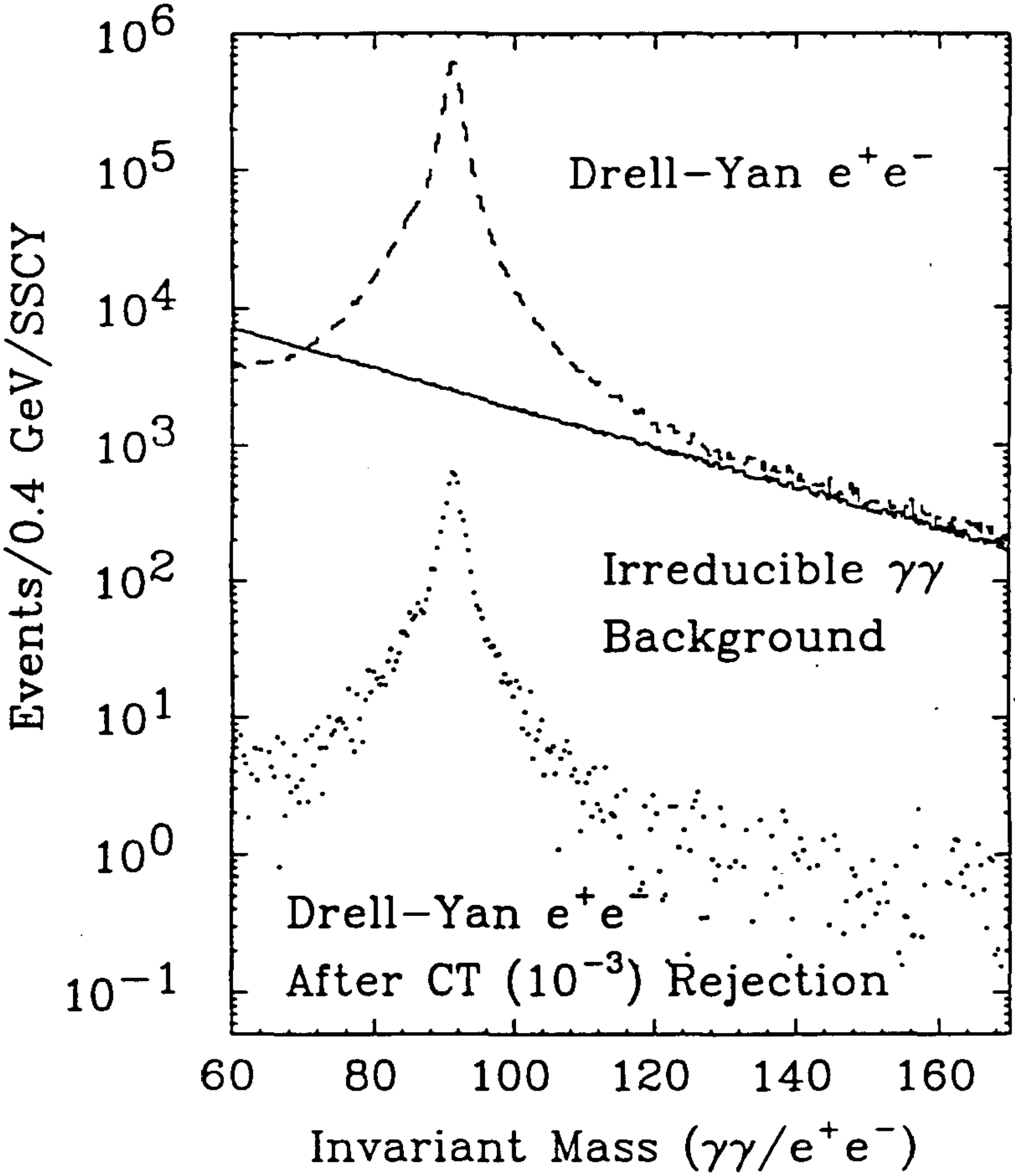

Figure 11: $\gamma\gamma$ and e^+e^- invariant mass distribution of Drell-Yan e^+e^- after event selection cut with no γ/e separation (dashed) is compared with irreducible $\gamma\gamma$ distributions (solid). Also shown in the figure is the Drell-Yan distribution, if 3% of electrons would misidentified as a photon.

Zhu

High Luminosity at SSC for H→ $\gamma\gamma$

- Comparing with LHC **in paper**, SSC has 10 times smaller designed luminosity, but 3 times higher x-section for both signal and background:

$$N_s/\sqrt{(N_b)} \Rightarrow LHC\ has\ \sqrt{3}\ \textbf{advantage}$$

- Detector must survive high luminosity; and
- Needs good photon identification:
  - Pointing;
  - π^0 rejection.
- Needs to work out trigger for H→ $\gamma\gamma$:
  - consequence of pile-up noise in trigger tower;
  - higher p_t cut to reduce level 1 rate: consequence at 80 GeV?

EM Electrode Structures

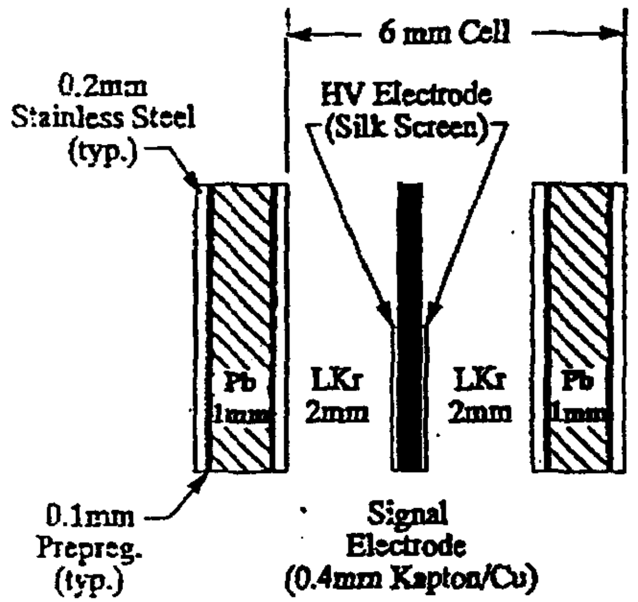

Barrel

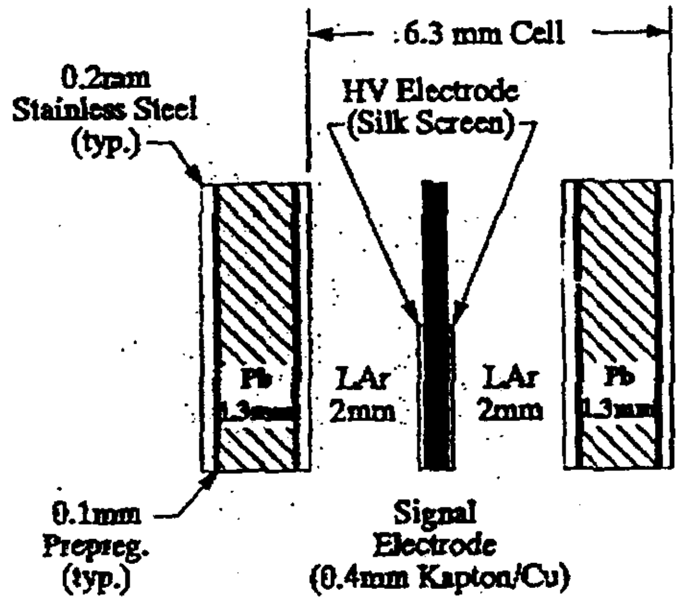

Endcap

	t_{Pb}	t_{ss}		
RD3	1.8	0.1 → 0.2	$10\%/\sqrt{E}$	Ar
AGS test	1.3	0.2	$6.7\%/\sqrt{E}$	Kr
GEM	0.96+?	0.2	$<6\%/\sqrt{E}$	Kr

LAr – Gap Variations and Calibration

Pulse width

single carrier:

$$i = \frac{q}{t_d} = q \cdot \frac{v}{d}$$

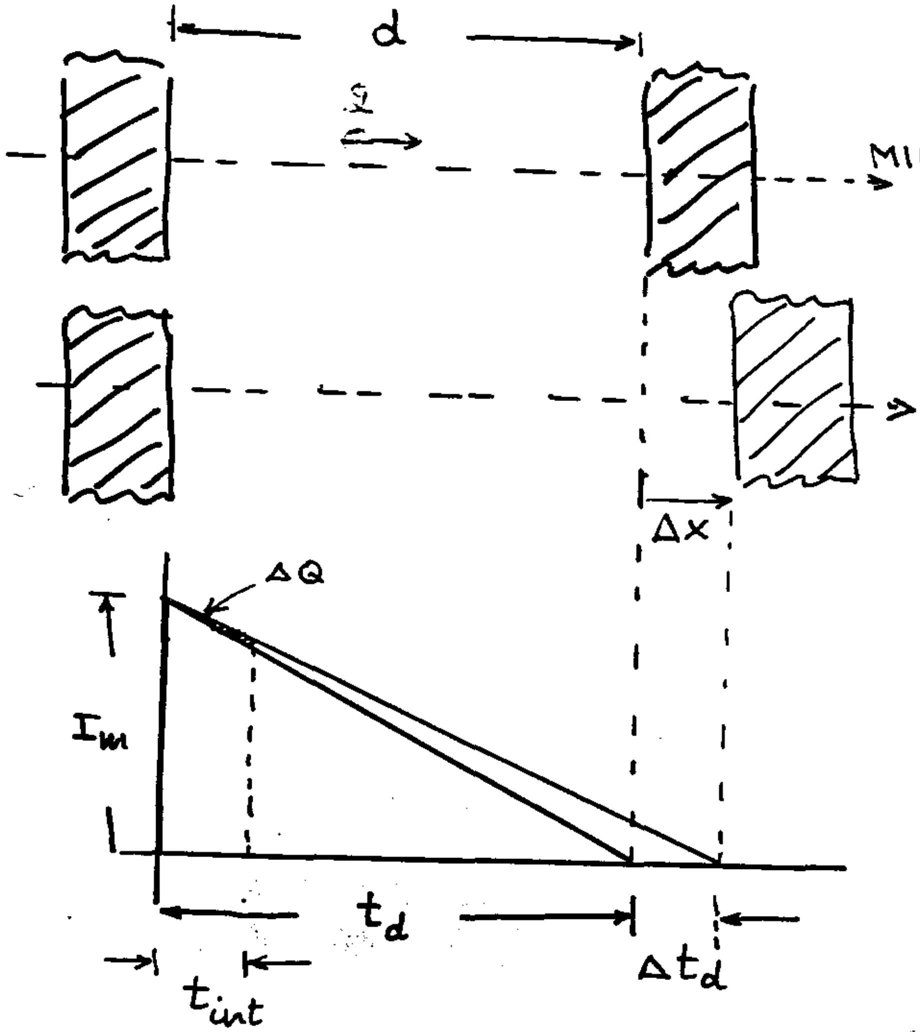

MIP responce:

$$I_m = e\,\frac{dn_e}{dx}\,\frac{d}{t_d}$$

$$= e\,\frac{dn_e}{dx}\,v_e$$

I_m is independent of d !

Long integration: $t_{int} > t_d$ $\qquad Q_s = \frac{1}{2} I_m t_d$

Short integration: $t_{int} \ll t_d$ $\qquad Q_s = I_m t_{int}\left(1 - \frac{1}{2}\frac{t_{int}}{t_d}\right)$

$$\frac{\Delta Q_s / I_m t_{int}}{\Delta t_d / t_d} = \frac{1}{2}\,\frac{t_{int}}{t_d} \approx \frac{1}{20} \quad \text{for} \quad d = 2\,\text{mm} \ (400\,\text{nsec}),\ t_{int} = 40\,\text{nsec}$$

∴ 20% gap variation results in 1% signal variation.

Calibration should be by I_m and not by $Q = \frac{1}{2} I_m t_d$!

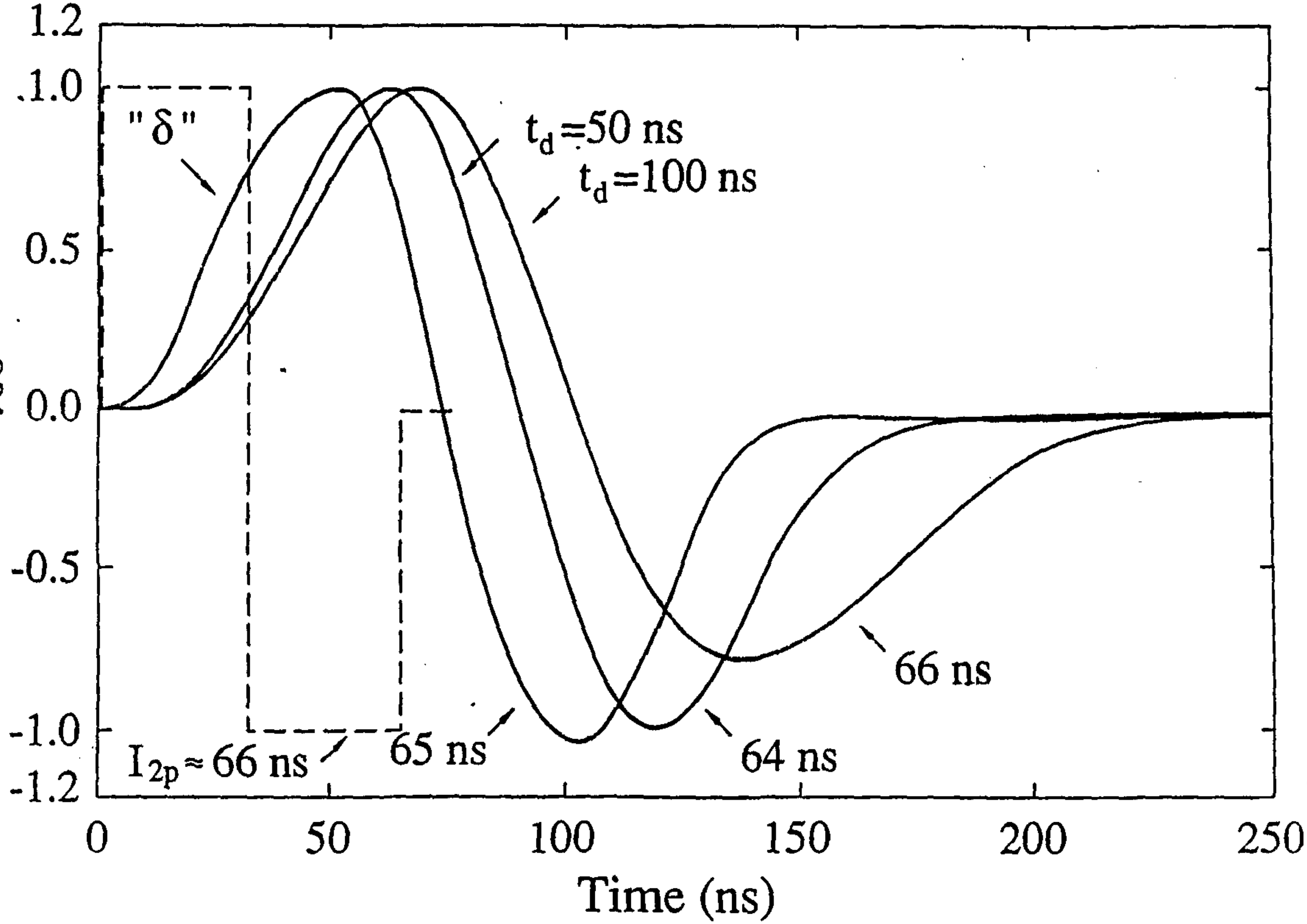
1.2
1.0
0.5
0.0
-0.5
-1.0
-1.2
0
50
100
150
200
250
Time (ns)
"δ"
t_d=50 ns
t_d=100 ns
I_2p ≈ 66 ns
65 ns
64 ns
66 ns

282

Calibration System and Preamplifier

Notes:
Dynamic Range 25MeV -- 2.5 TeV
(Em) 25 uV -- 2.5 V
Per Channel

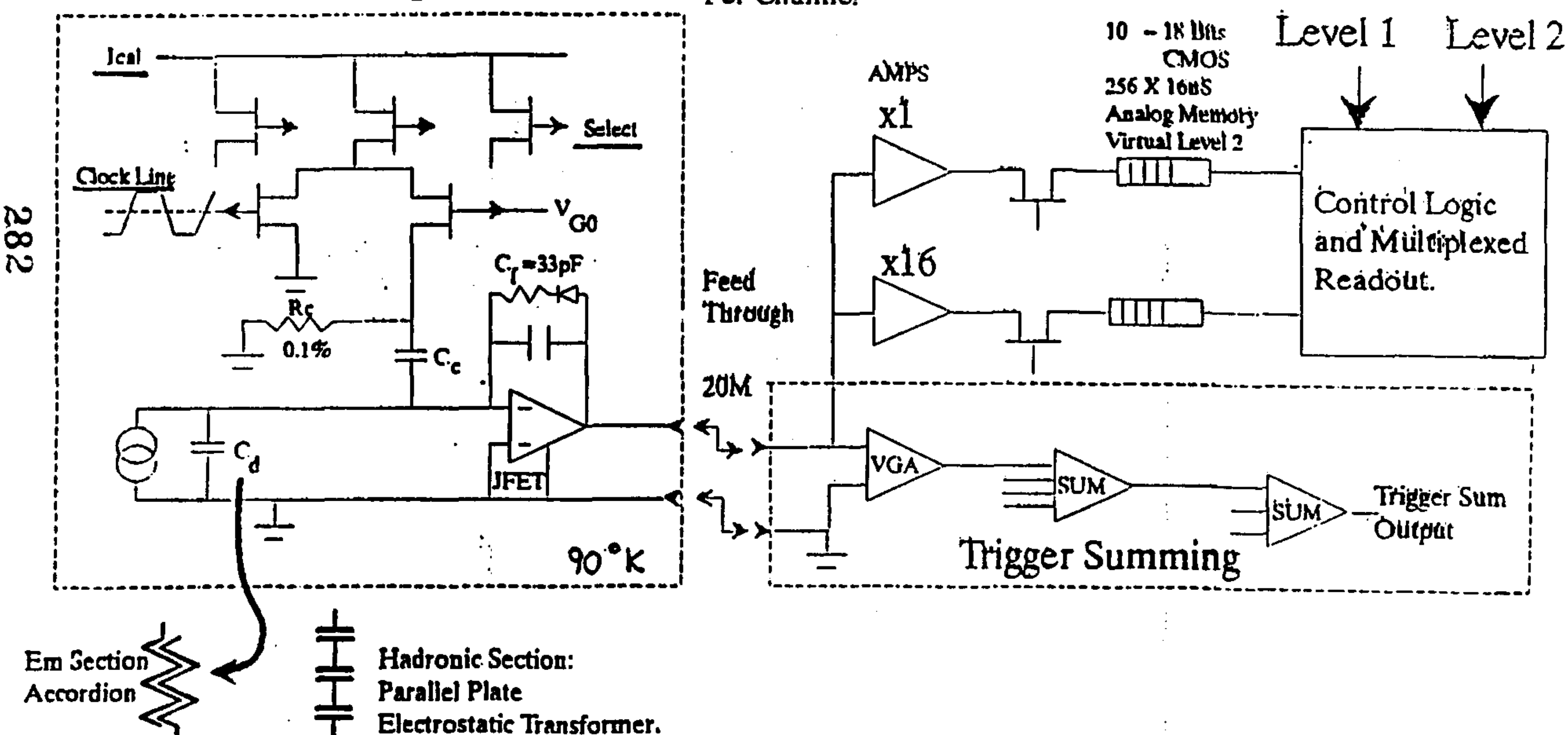

calibration

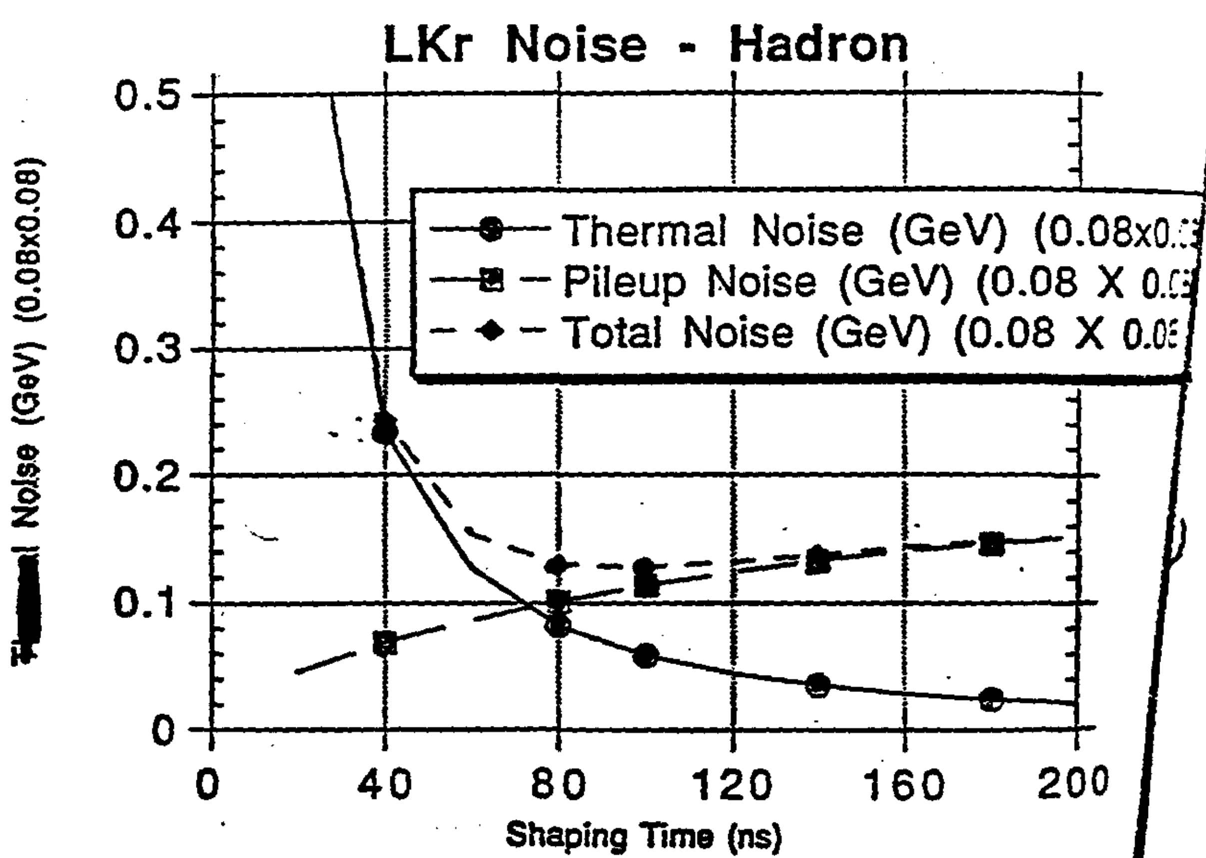
LKr Noise - Hadron
Thermal Noise (GeV) (0.08x0.
Pileup Noise (GeV) (0.08 X 0.
Total Noise (GeV) (0.08 X 0.
Noise (GeV) (0.08x0.08)
Shaping Time (ns)
0
0.1
0.2
0.3
0.4
0.5
40
80
120
160
200

Noise in Hadronic Tower (0.08X0.08) vs. Shaping Time

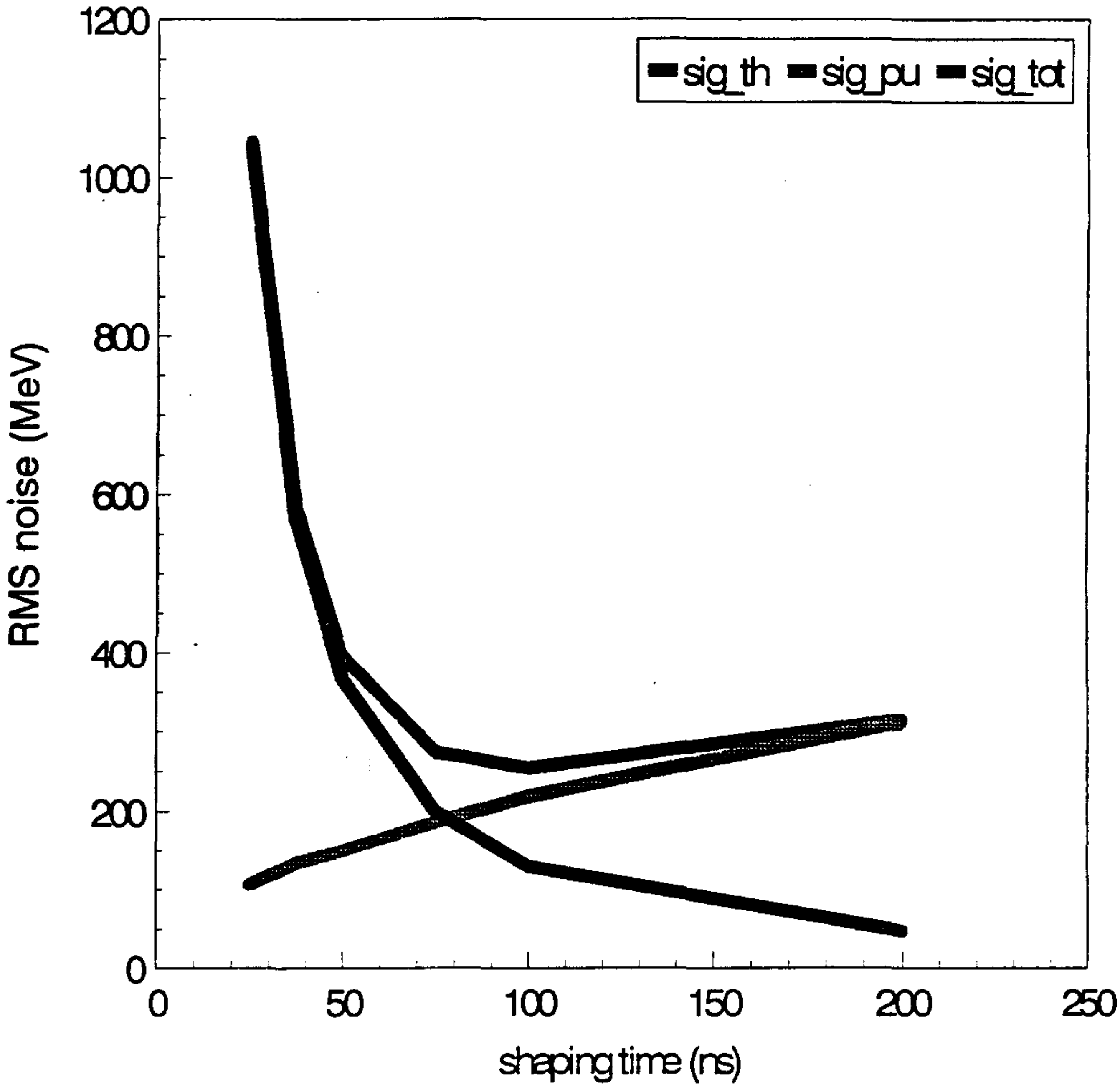

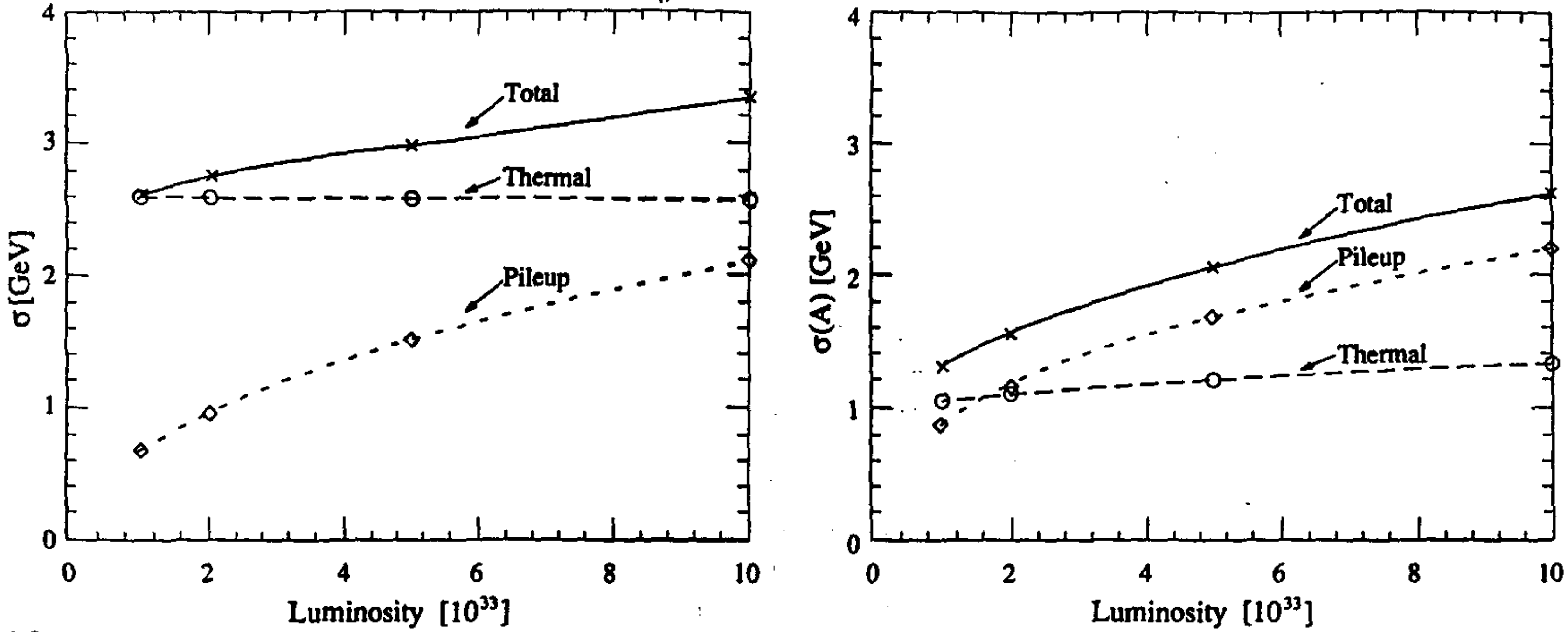

Figure 6.2.4: Illustration of the combination of pileup and thermal noise for 0.32×0.32 trigger towers (TOT deposition) using the method of adaptive filtering. (a) Noise contribution versus luminosity for individual samples from pileup and thermal sources for the particular case described in the text. (b) Value of sigma for the amplitude function obtained by linearly combining all samples with coefficients chosen (at each value of the luminosity) to minimize the noise. Note that for this case, with the use of adaptive filtering, the total noise increases by about a factor of two as the luminosity increases from 10^{33} to 10^{34}.

For Forward Calorimeter

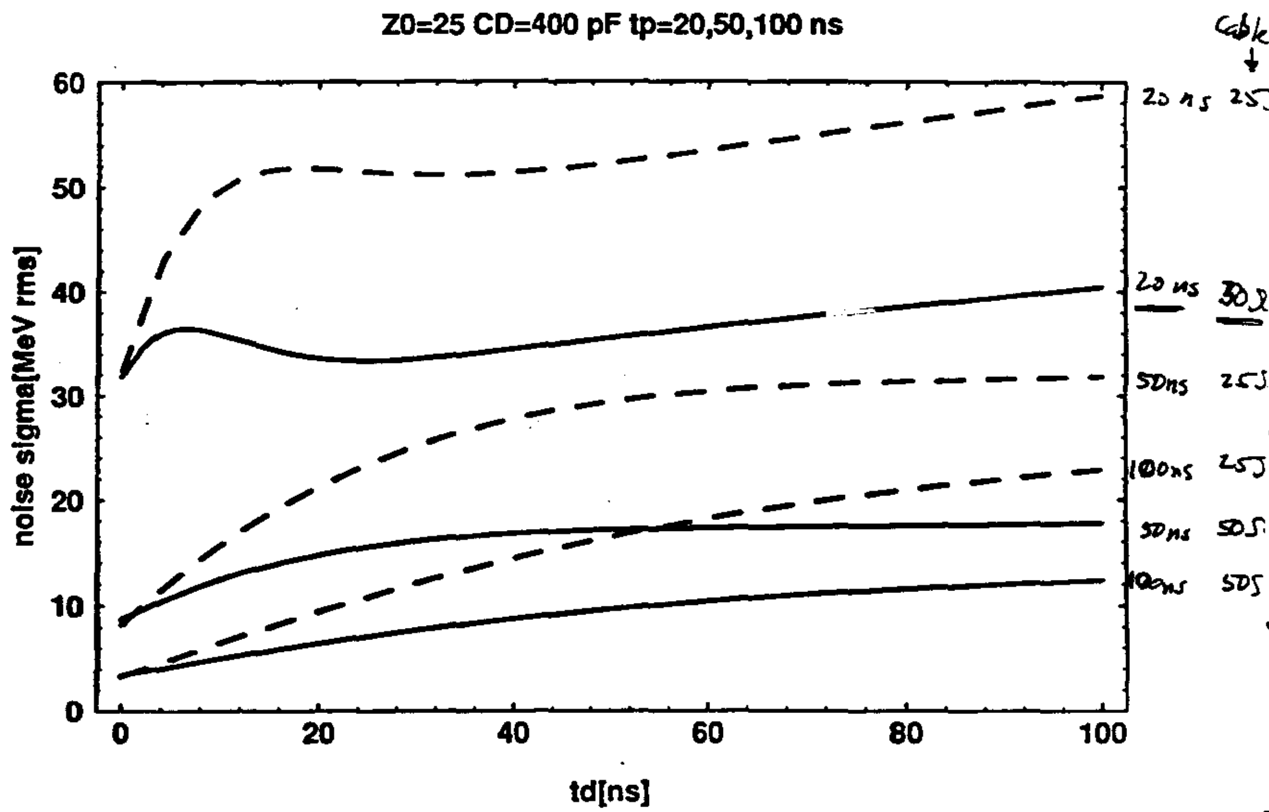

R. Chase et al., (Orsay, BNL, ...) preprint

.BNL

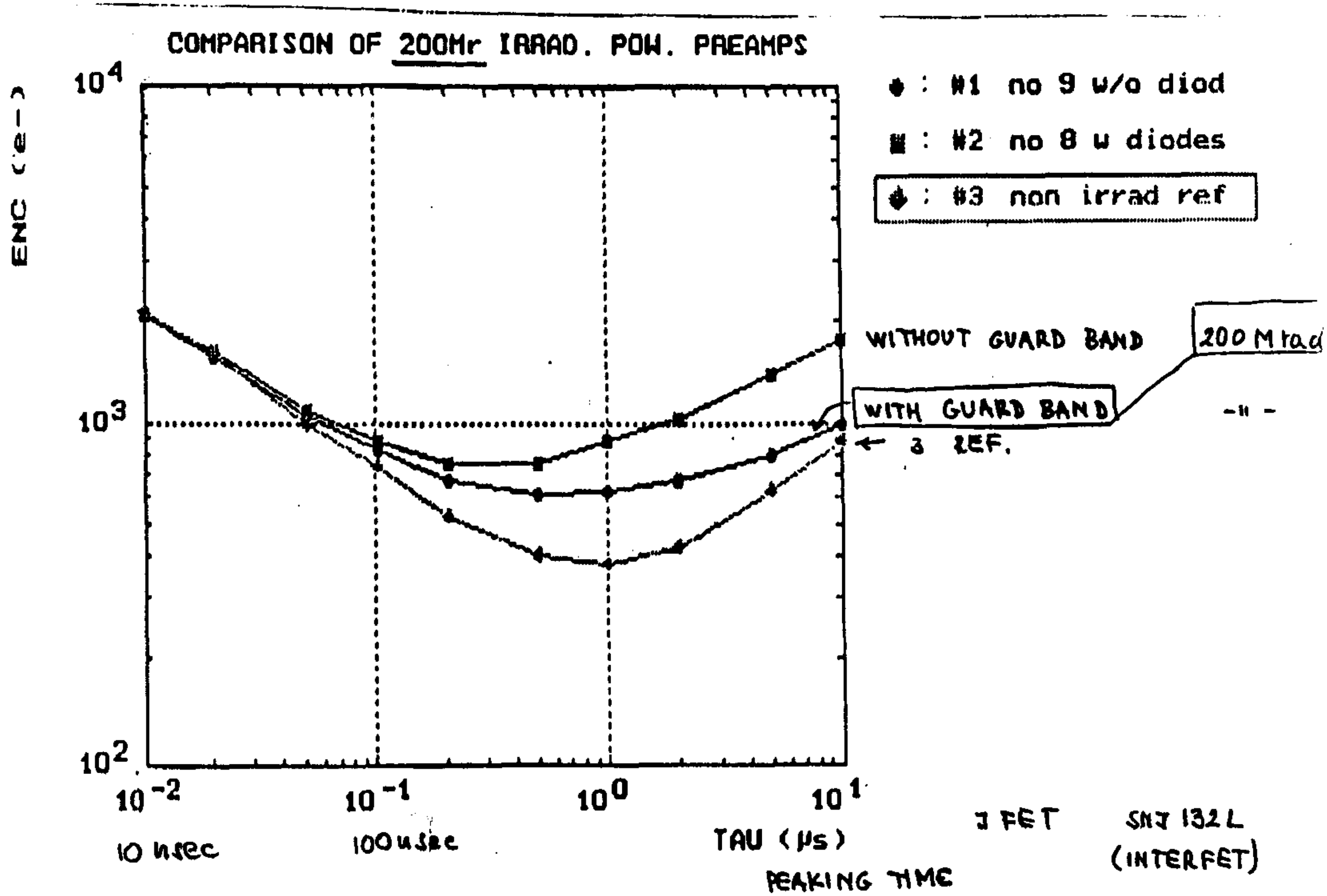

COMPARISON OF 200Mr IRRAD. POW. PREAMPS
ENC (e-)
10^4
10^3
10^2
10^-2
10^-1
10^0
10^1
10 nsec
100 nsec
TAU (μs)
PEAKING TIME
♦ : #1 no 9 w/o diod
■ : #2 no 8 w diodes
♦ : #3 non irrad ref
WITHOUT GUARD BAND
200 M rad
WITH GUARD BAND
-"-
← 3 REF.
J FET
SNJ 132 L
(INTERFET)

LAr Calibration

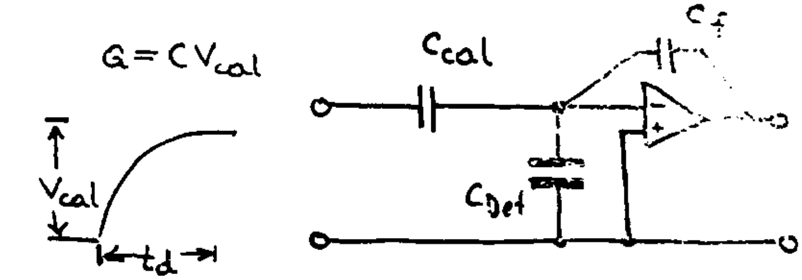

Conventional charge calibration

$$\frac{\delta C_{cal}}{C_{cal}} = 1-2\%$$

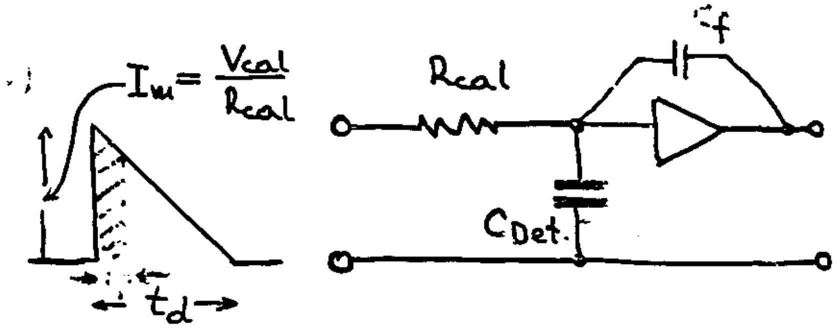

current calibration

$$\frac{\delta R_{cal}}{R_{cal}} = 0.1\%$$

- distribution of precisely controlled pulses needed

current calibration by local pulse generator

- dc current distributed
- 5% in c's results in 0.125% calibration

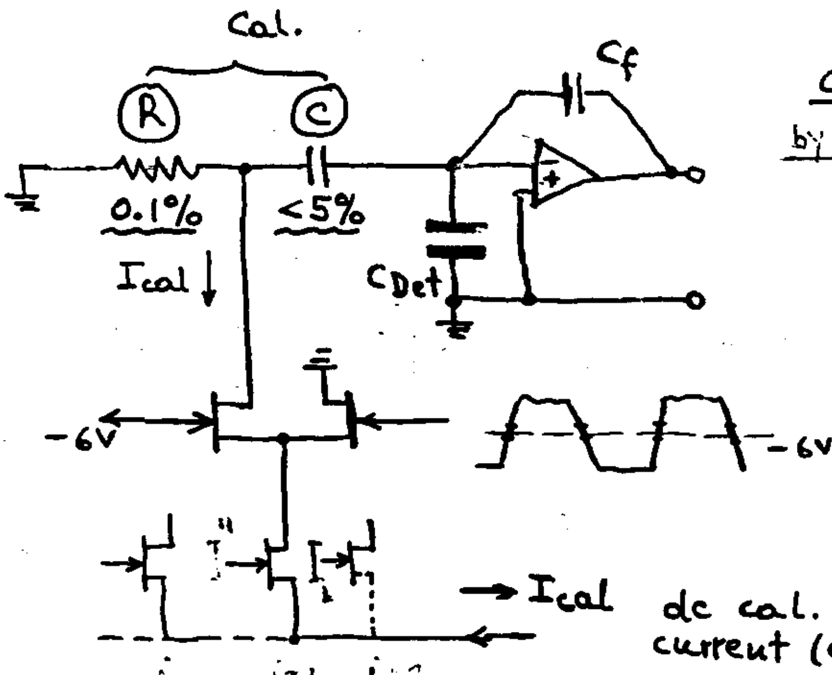

dc cal. current (0–2.5 mA)
100 MeV → 2 TeV

leakage pA after 850 M 100 pA ⇒ 0.1 MeV

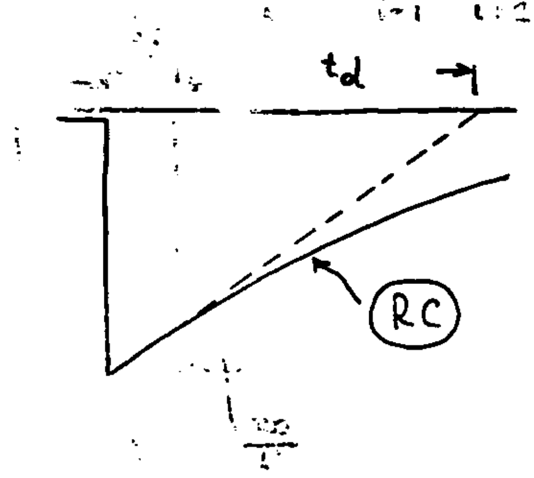

$$Q_{cal} = I_{cal}\, t_p \left(1 - \frac{1}{2}\frac{t_p}{t_d}\right)$$

$$\frac{\Delta G}{Q_{cal}} = \frac{1}{2}\frac{t_p}{t_d} \approx \frac{1}{40}$$

$$\frac{\delta Q_{cal}}{Q_{cal}} \approx \frac{1}{40}\left(\frac{\delta R}{R}, \frac{\delta C}{C}, \frac{\delta (RC)}{RC}\right)$$

Switch parameters (V_t, noise, etc.) do not influence calibration.

$I_{el} < 10^{-3}\, I_{cal}(min)$ after radiation.

LA Calibration - "IT" method

P Channel FET , t_m = 25 nsec

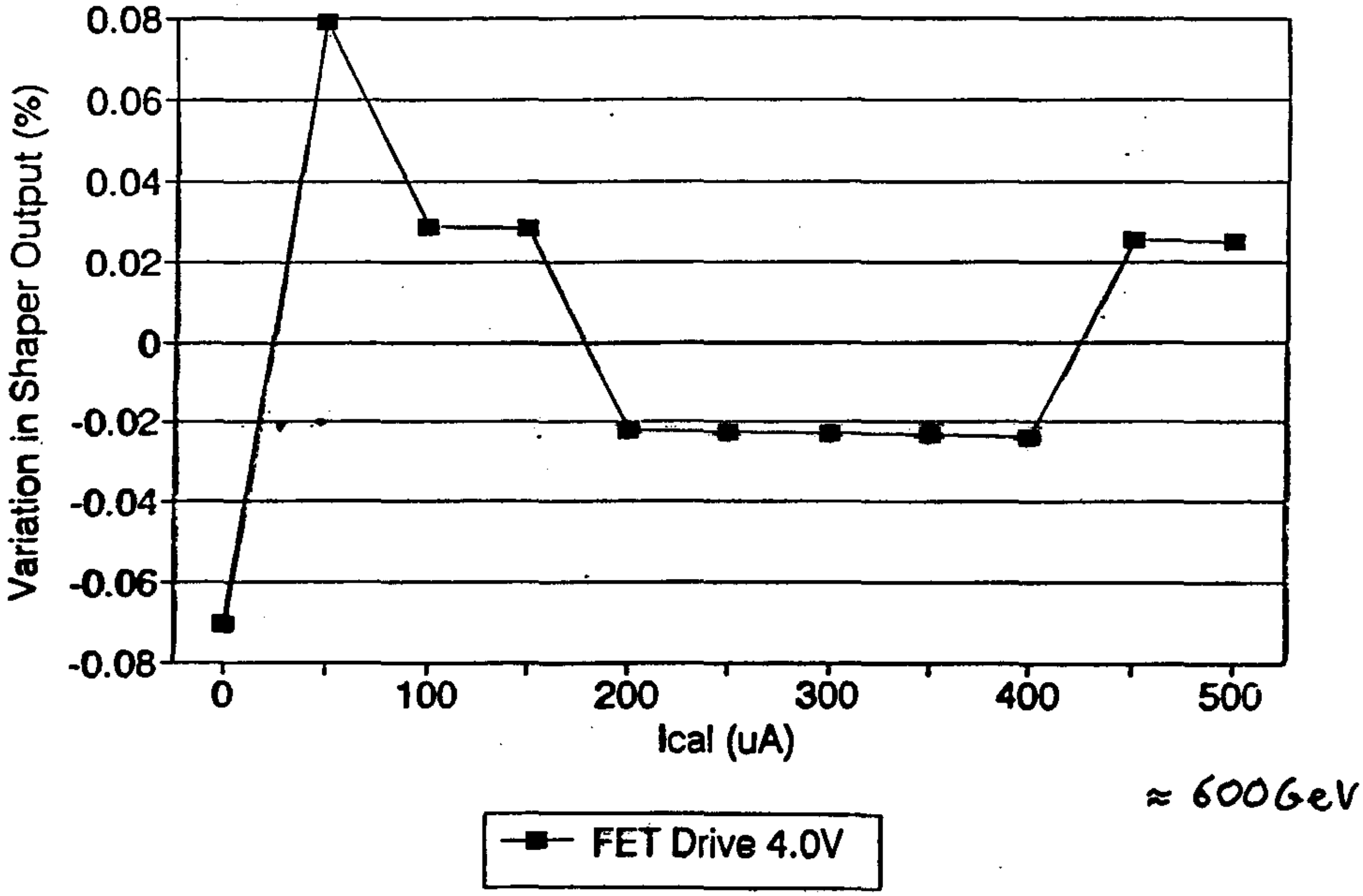

Fig. 5

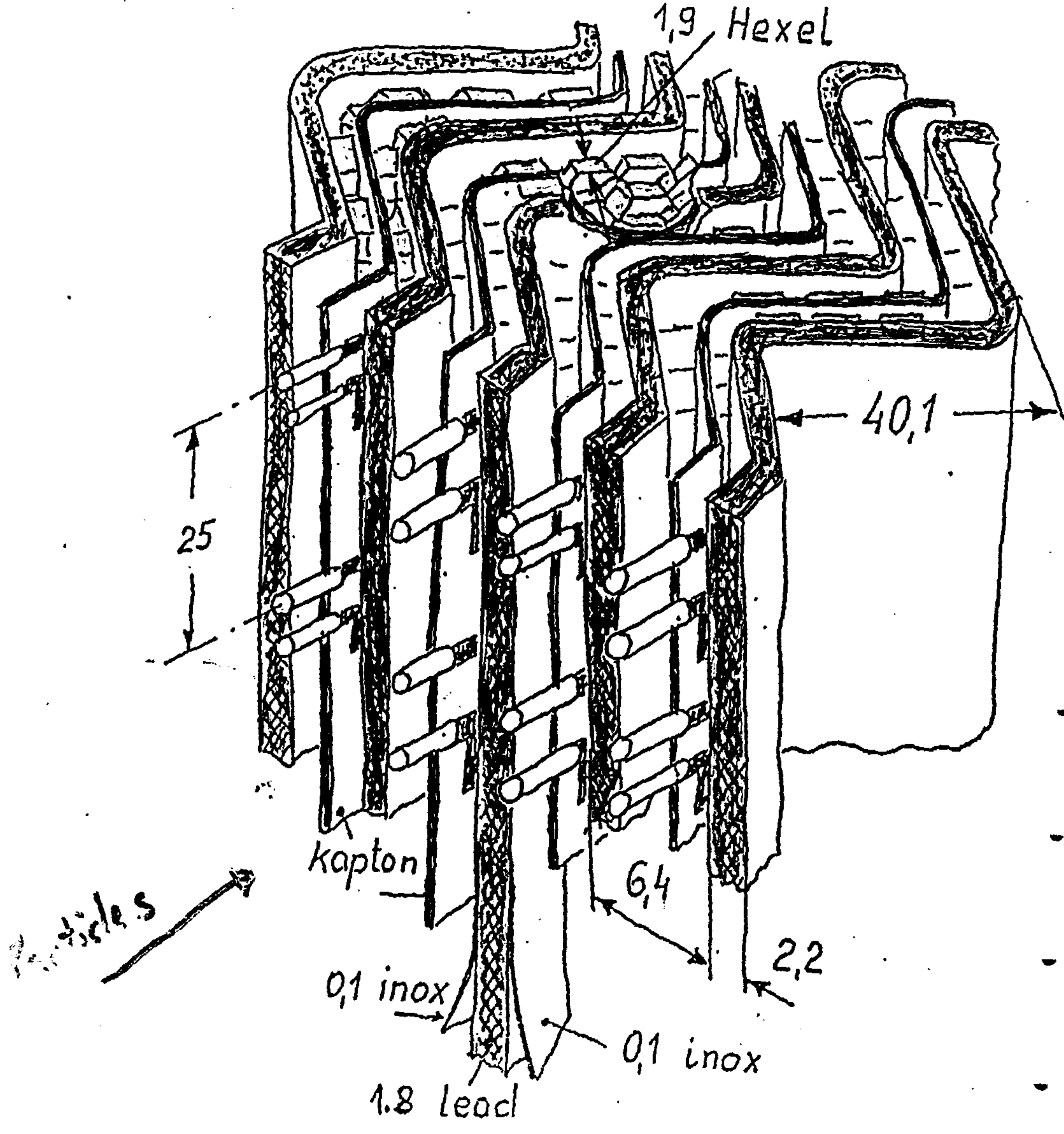

Fig 4 : "Artist's" view of prototype structure

Spatial resolution: along x
(ACCORDION FOLDS)

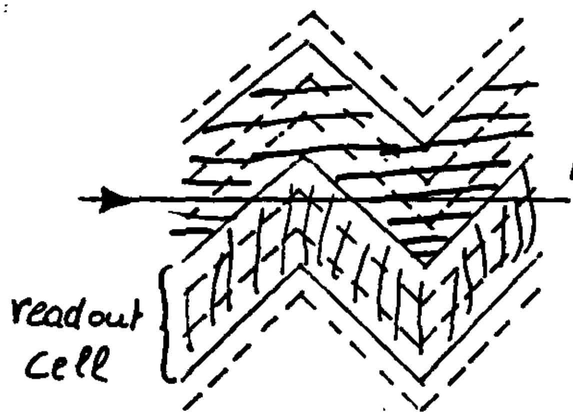

always 2 readout cells are involved

better energy sharing
⇕
better spatial resolution (σ_x)

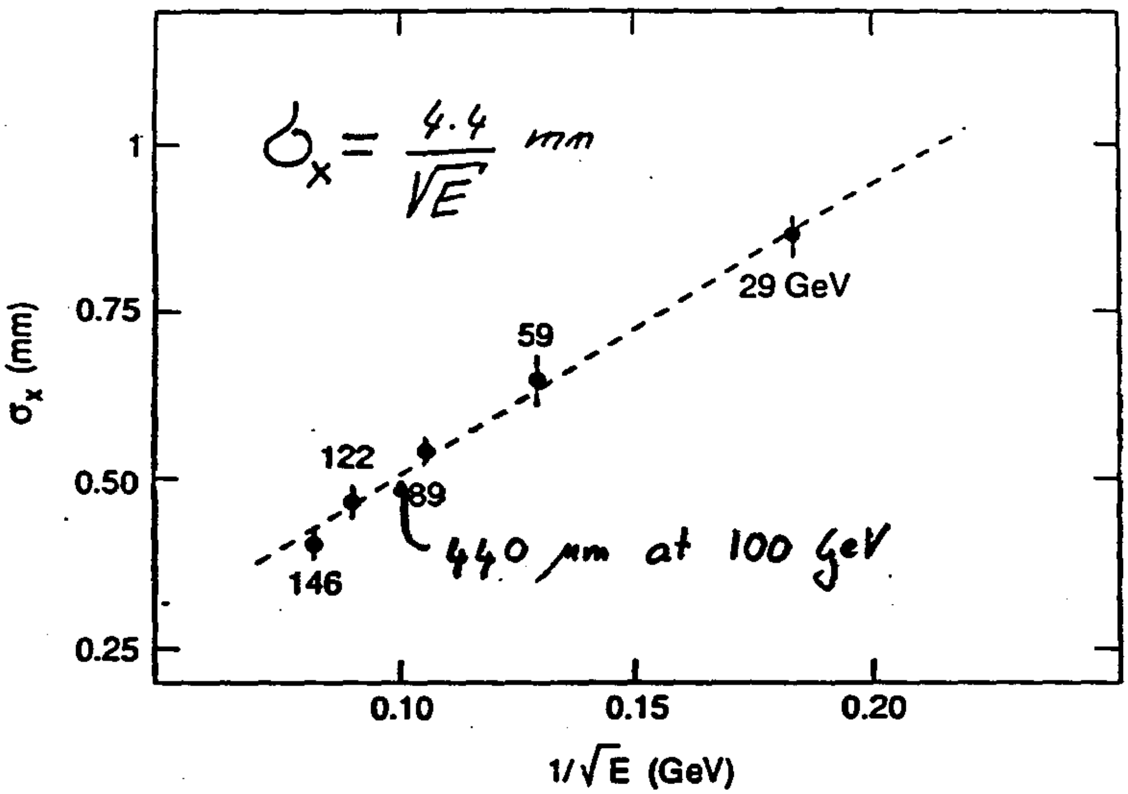

readout 100 ns

- ▲ same results with the fast shaping (20 ns)
- ▲ no bias $X_{Calor} = X_{Impact} \pm$ resolution
- ▲ in Y it behaves like a conventional pad detector $Y_{Calor} = f(Y_{Impact}) \pm$ resolution
- ▲ at 100 ns σ_x (muon) = 1.80 ± 0.05 mm

Angular resolution

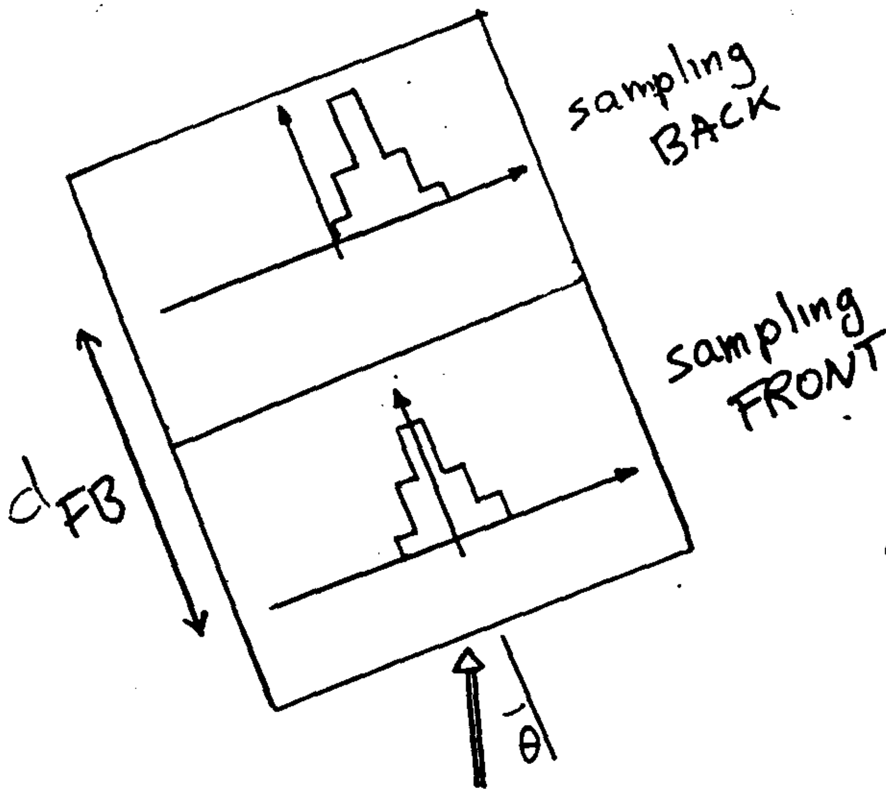

$$\theta = \frac{X_B - X_F}{d_{FB}}$$

- calibrated by rotating the calorimeter on a platform

- $\Delta\theta = 6.1$ mrad at 120 GeV
- same result with the fast readout
- not optimized longitudinal sampling $\rightarrow \Delta\theta$ dominated by Δx_B

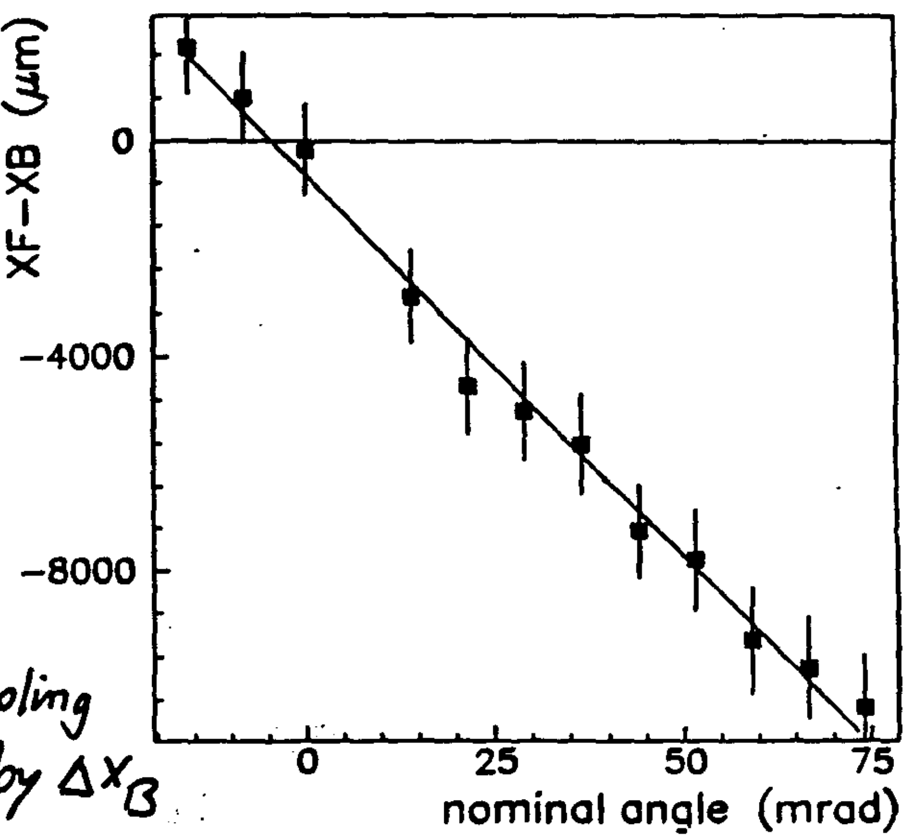

Liquid Krypton Calorimeter Test Results

O. Benary[9], S. Cannon[5], W. Cleland[7], I. Ferguson[2], C. Finley[5], A. Gordeev[6], H. Gordon[3], E. Kistenev[3], P. Kroon[3], M. Leltchouk[5], D. Lissauer[3], H. Ma[3], D. Makowiecki[3], A. Maslennikov[4], S. McCorkle[3], D. Onoprienko[6], A. Onuchin[4], Y. Oren[9], V. Panin[4], J. Parsons[5], J. Rabel[7], V. Radeka[3], L. Rogers[3], D. Rahm[3], S. Rescia[3], J. Rutherfoord[2], M. Seman[5], M. Smith[3], J. Sondericker III[3], R. Steiner[1], D. Stephani[3], E. Stern[7], I. Stumer[3], H. Takai[3], H. Themann[8], Y. Tikhonov[4]

1. Adelphi University, Garden City, NY 11530
2. University of Arizona, Tucson, AZ 85721
3. Brookhaven National Laboratory, Upton, NY 11973
4. Budker Institute for Nuclear Physics, Novosibirsk, Russia
5. Columbia University, New York, NY 15633
6. Oak Ridge National Laboratory, Oak Ridge, TN 37831
7. University of Pittsburgh, Pittsburgh, PA 15260
8. SUNY at Stony Brook, Stony Brook, NY 11794
9. Tel-Aviv University, Tel-Aviv, Israel

Experimental Setup

0.2 mm SS
1.3 mm Pb
0.2 mm SS

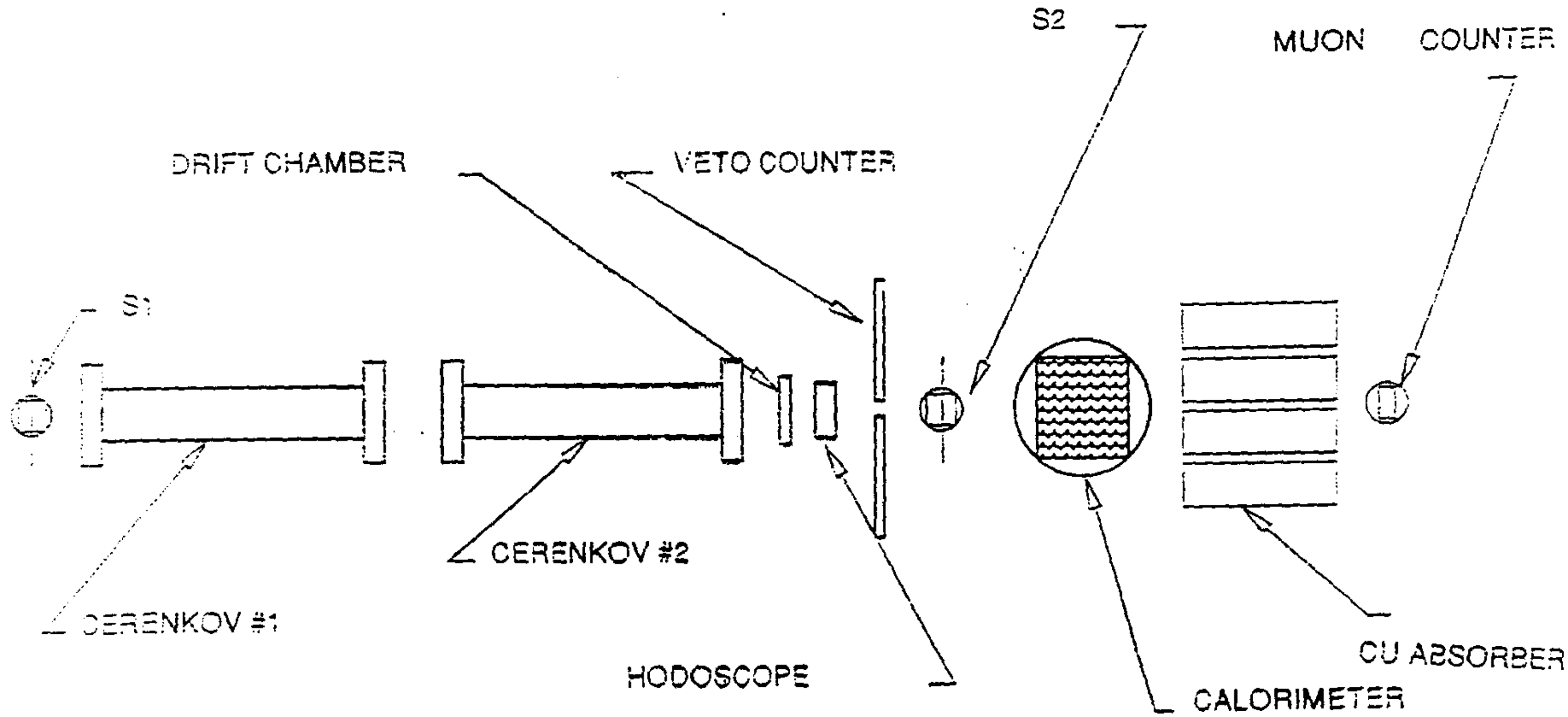

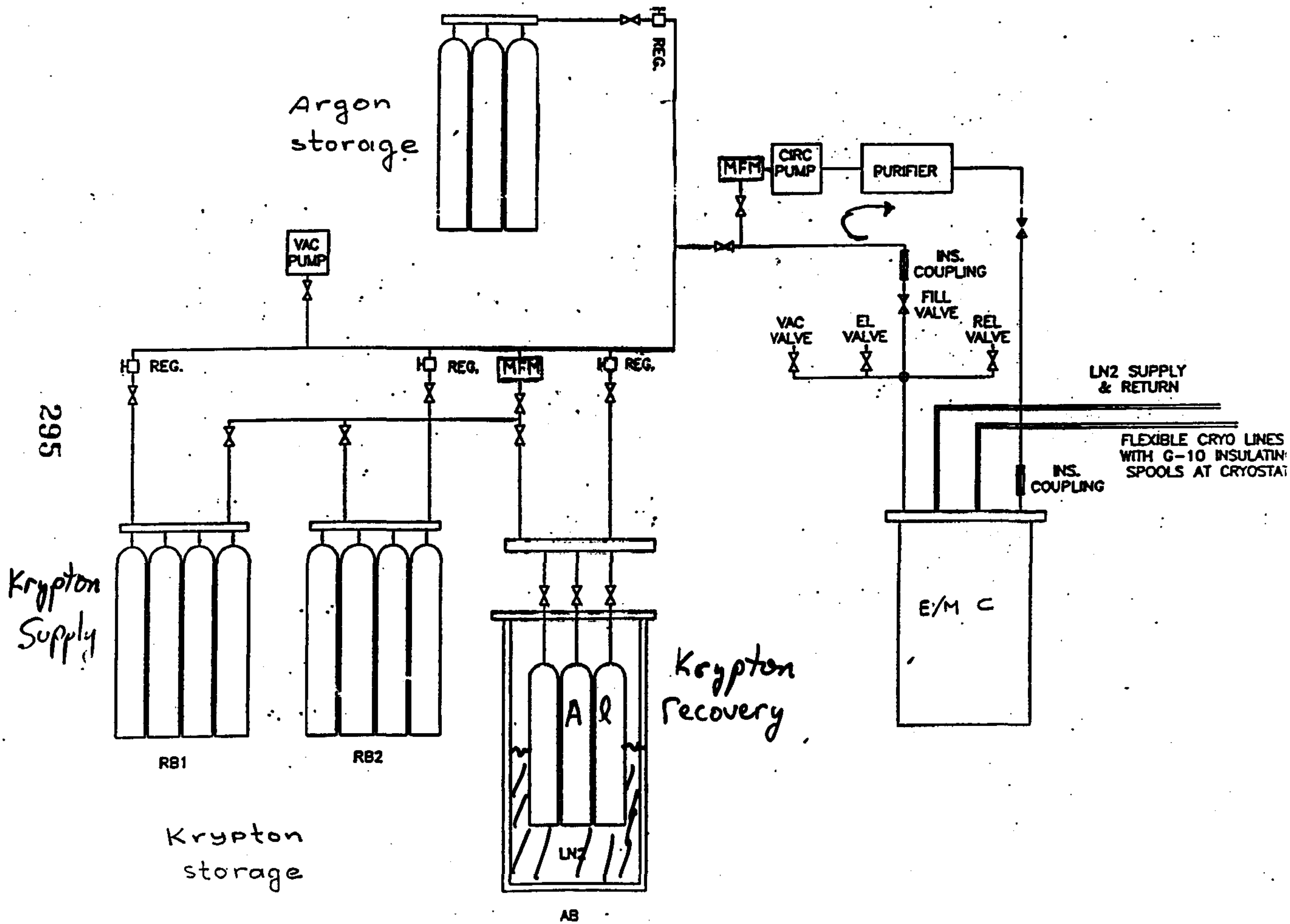

Argon storage
REG.
MFM
CIRC PUMP
PURIFIER
VAC PUMP
INS. COUPLING
FILL VALVE
VAC VALVE
EL VALVE
REL VALVE
REG.
REG.
MFM
REG.
LN2 SUPPLY & RETURN
FLEXIBLE CRYO LINES WITH G-10 INSULATIN SPOOLS AT CRYOSTAT
INS. COUPLING
Krypton Supply
E/M C
A l
Krypton recovery
RB1
RB2
LN2
Krypton storage
AB

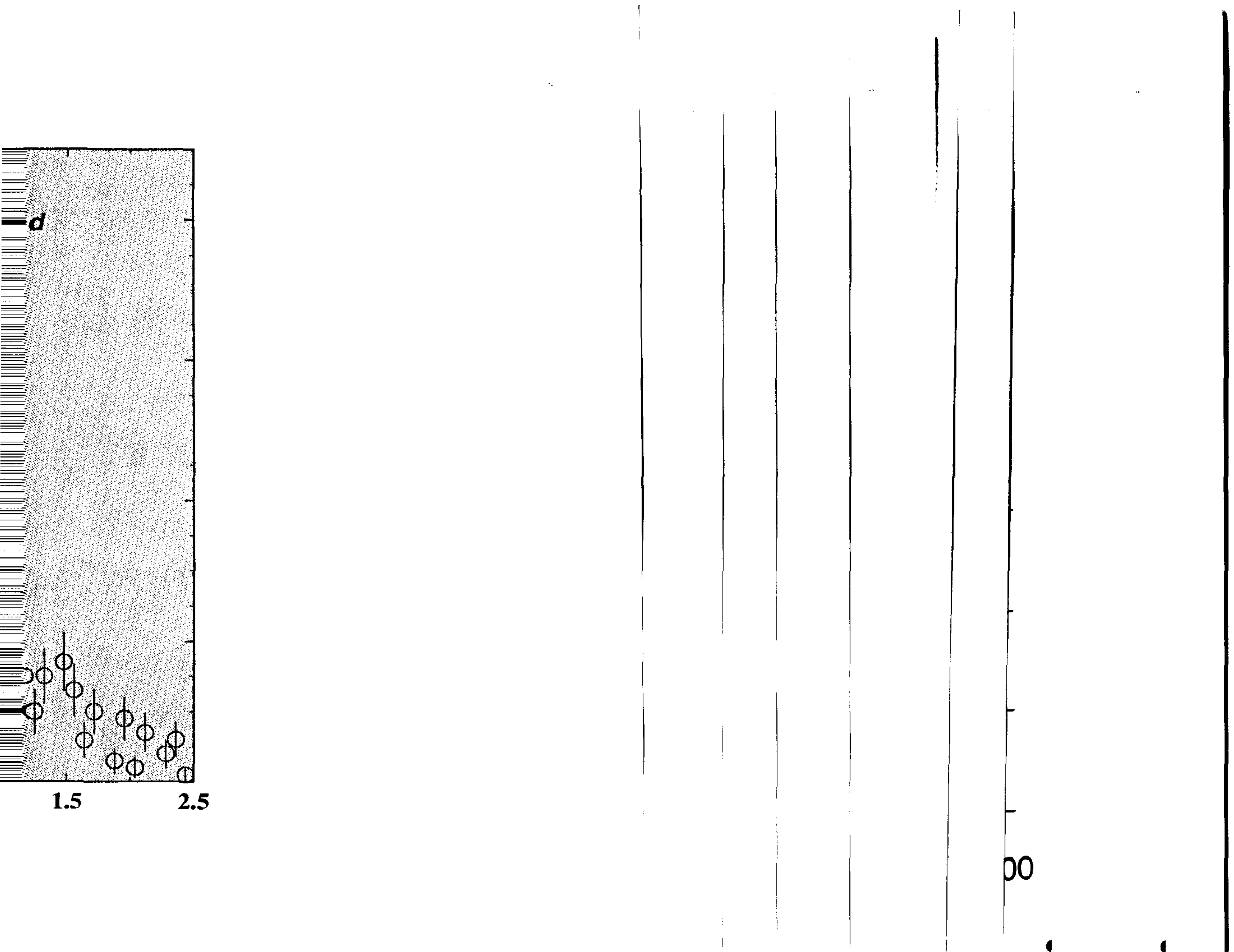

d
1.5
2.5

LKr Timing Resolution

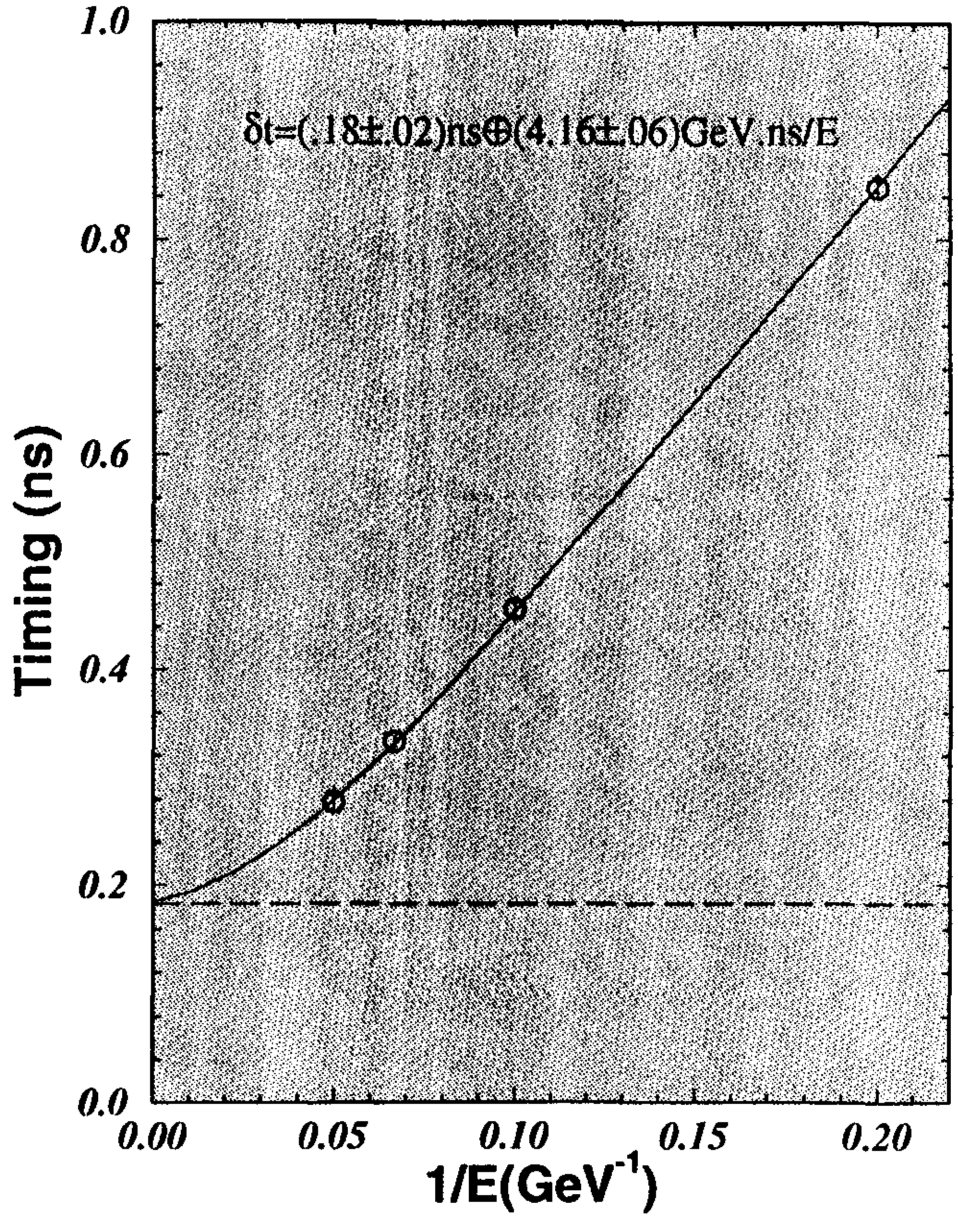

GEM DETECTOR PARAMETERS
BASELINE 2

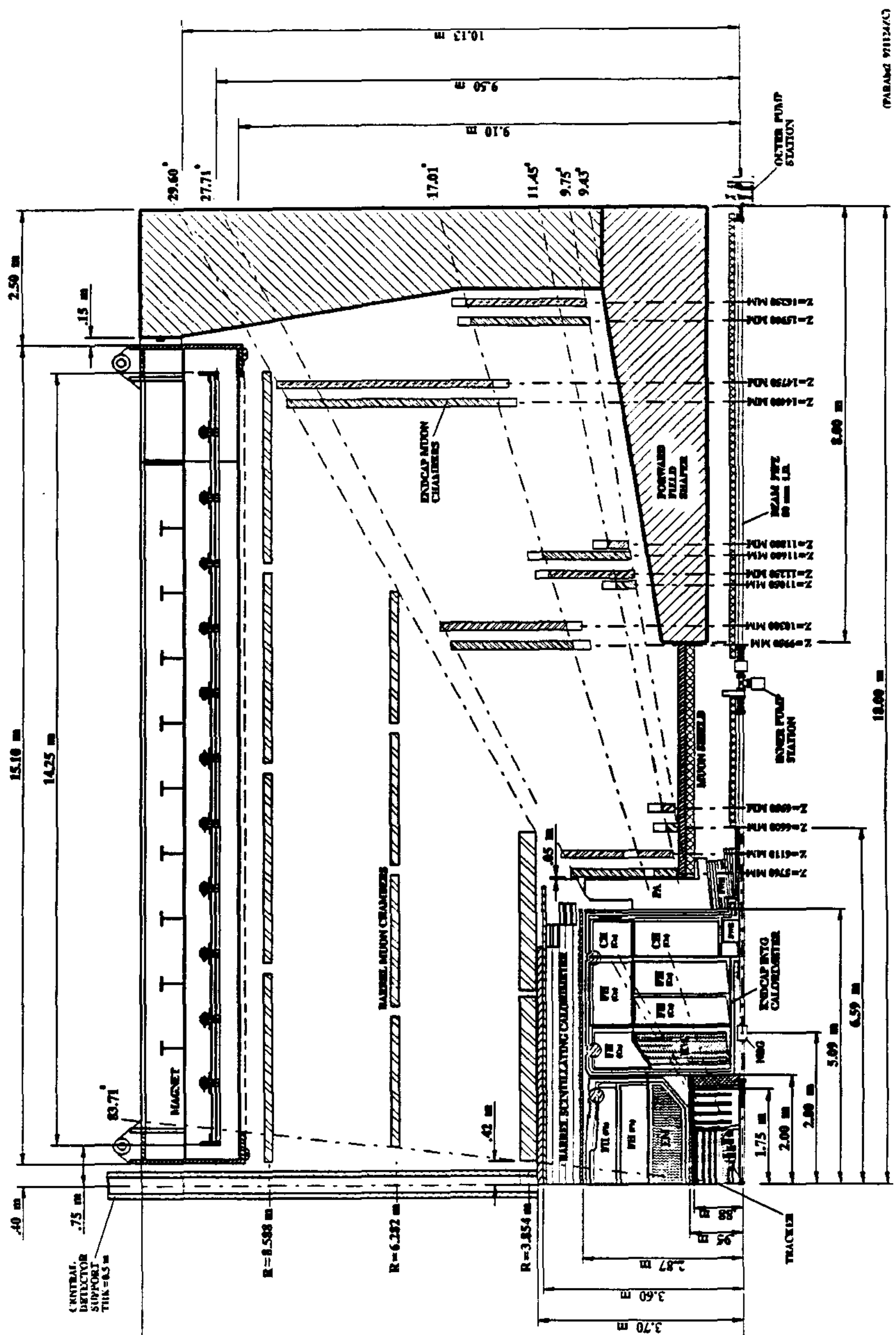

GEM Calorimeter

	Weight	Volume
Barrel Calorimeter	= 433 Mg	24135 L. LKr
2 Endcap Total	= 759 Mg	38475 L. LAr
Scint. Fiber & St. St.	= 1229 Mg	
2 Endcap PA Total	= 232 Mg	
2 FWH Total	= 30 Mg	
	2683 Mg	

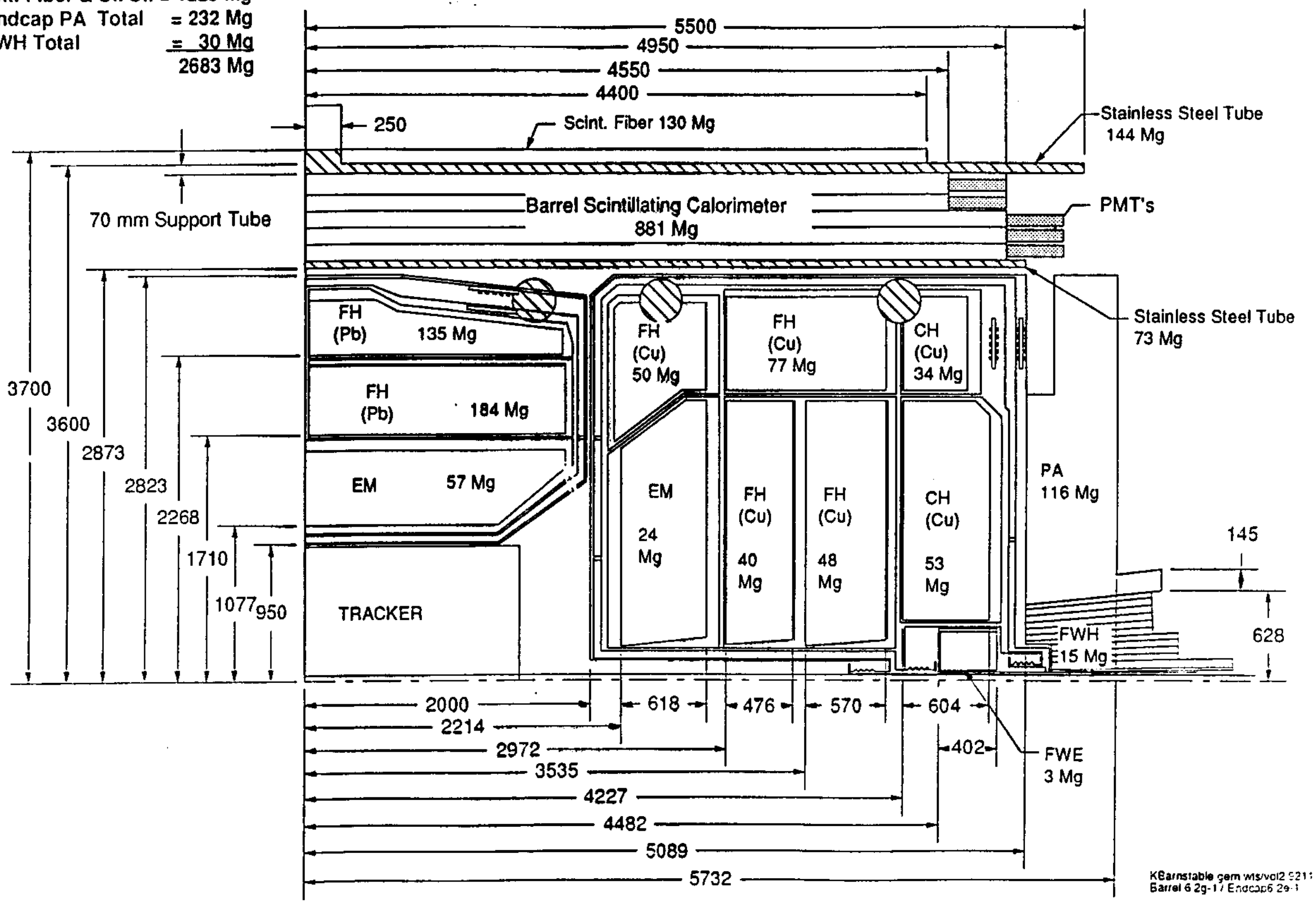

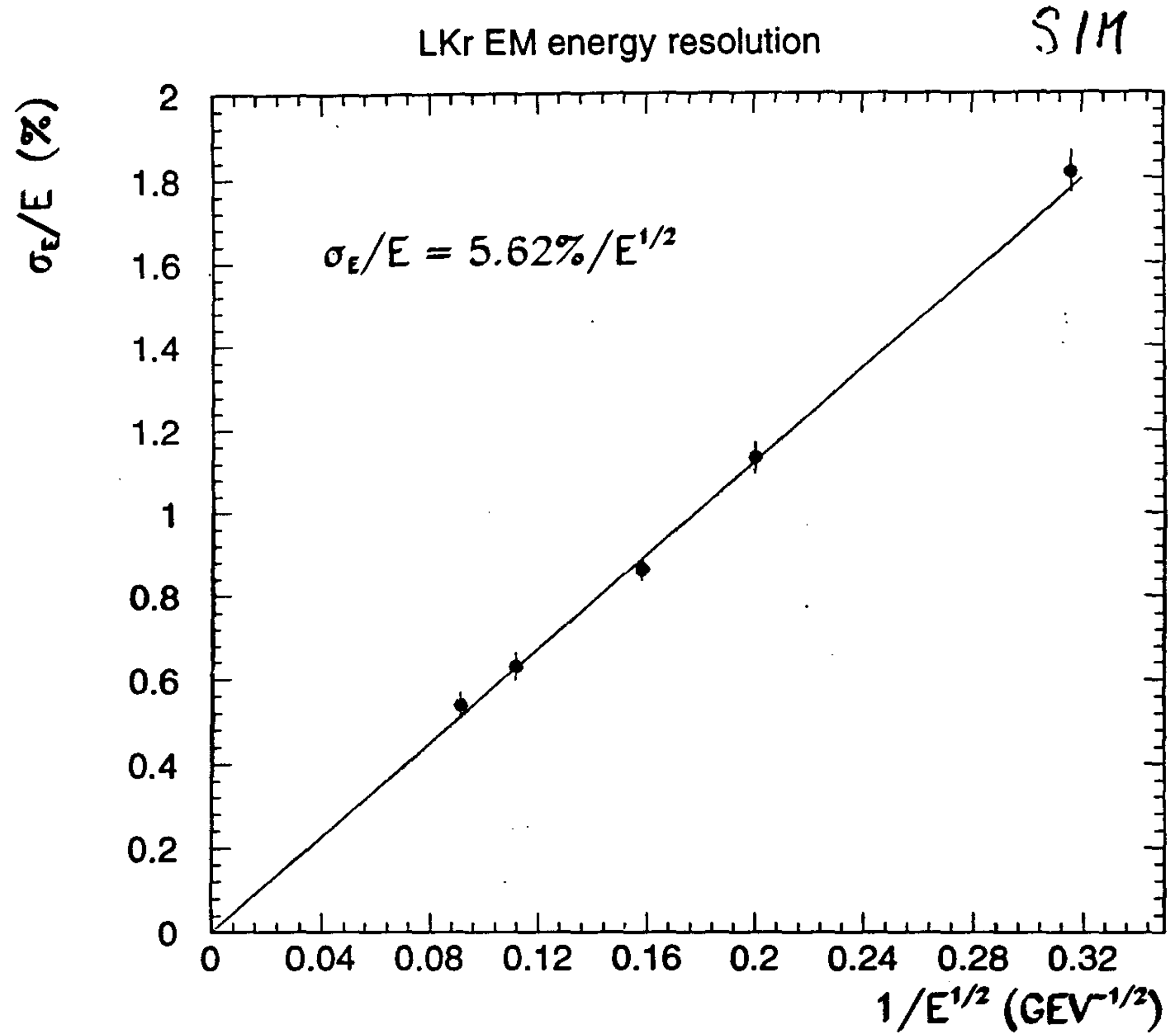

LKr EM energy resolution
SIM
σ_E/E (%)
$\sigma_E/E = 5.62\%/E^{1/2}$
2
1.8
1.6
1.4
1.2
1
0.8
0.6
0.4
0.2
0
0
0.04
0.08
0.12
0.16
0.2
0.24
0.28
0.32
$1/E^{1/2}$ ($GEV^{-1/2}$)

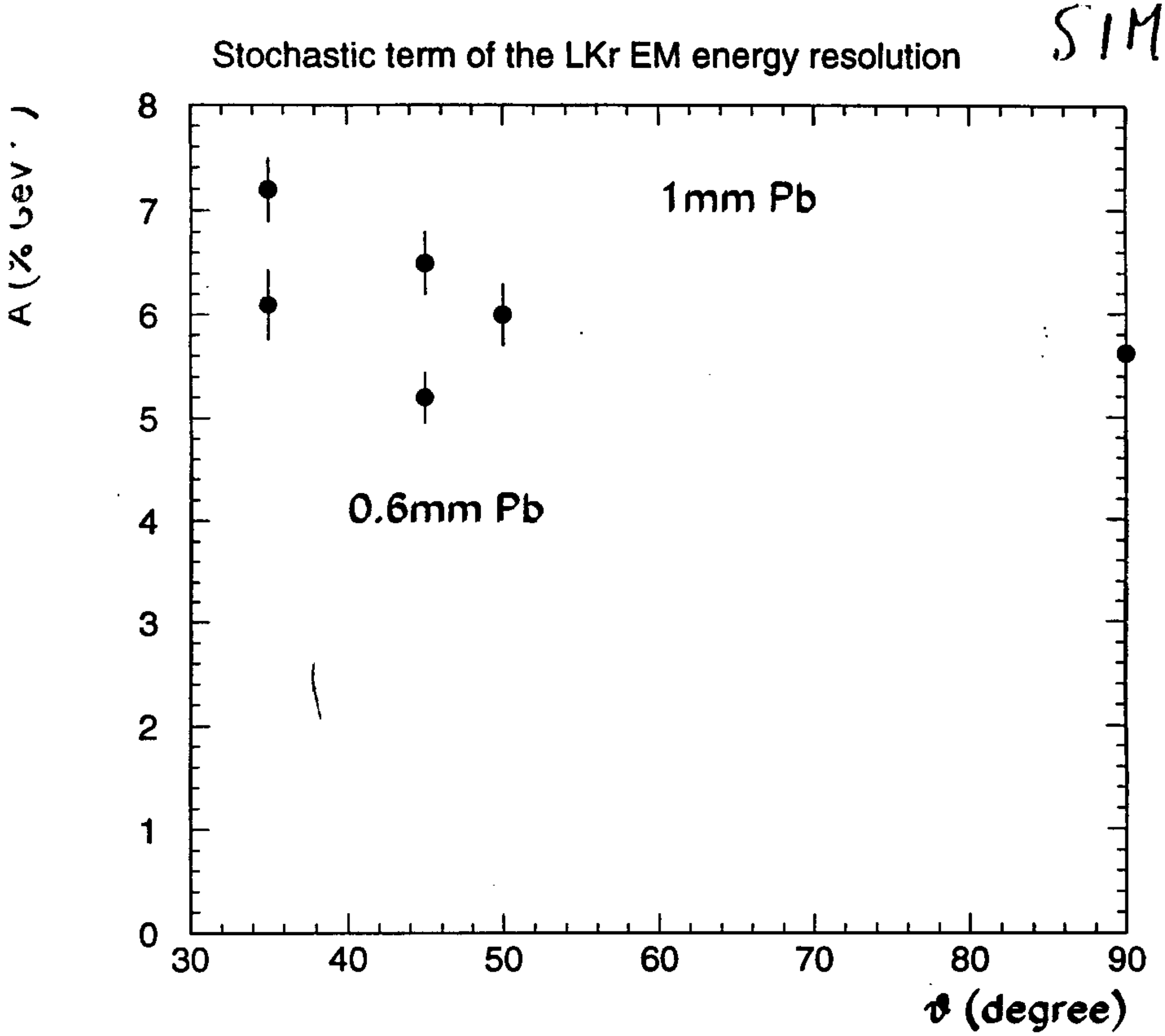
SIM
Stochastic term of the LKr EM energy resolution
A (% GeV
1mm Pb
0.6mm Pb
ϑ (degree)
0
1
2
3
4
5
6
7
8
30
40
50
60
70
80
90

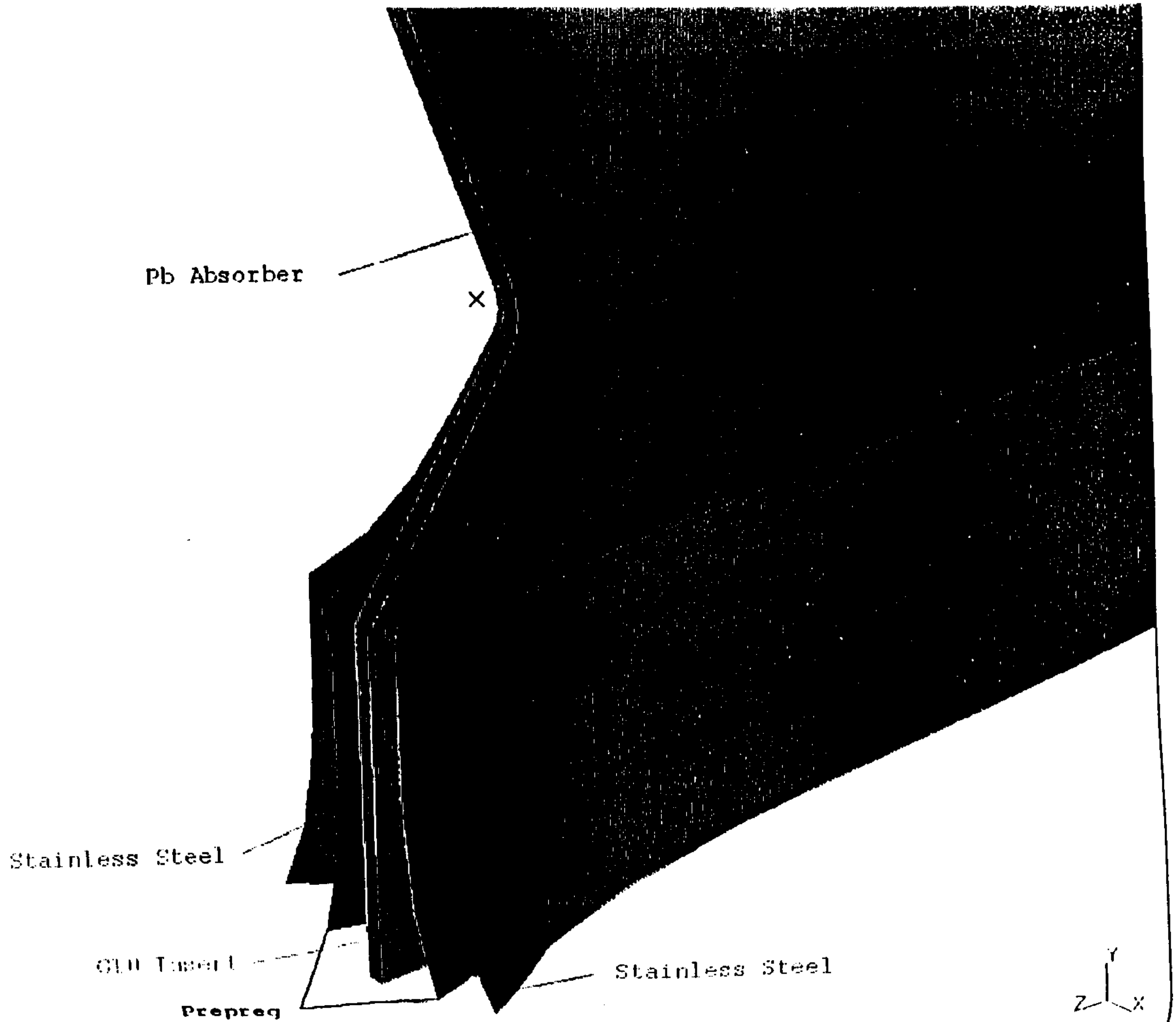
Pb Absorber
Stainless Steel
G10 Insert
Prepreg
Stainless Steel
Y
Z
X

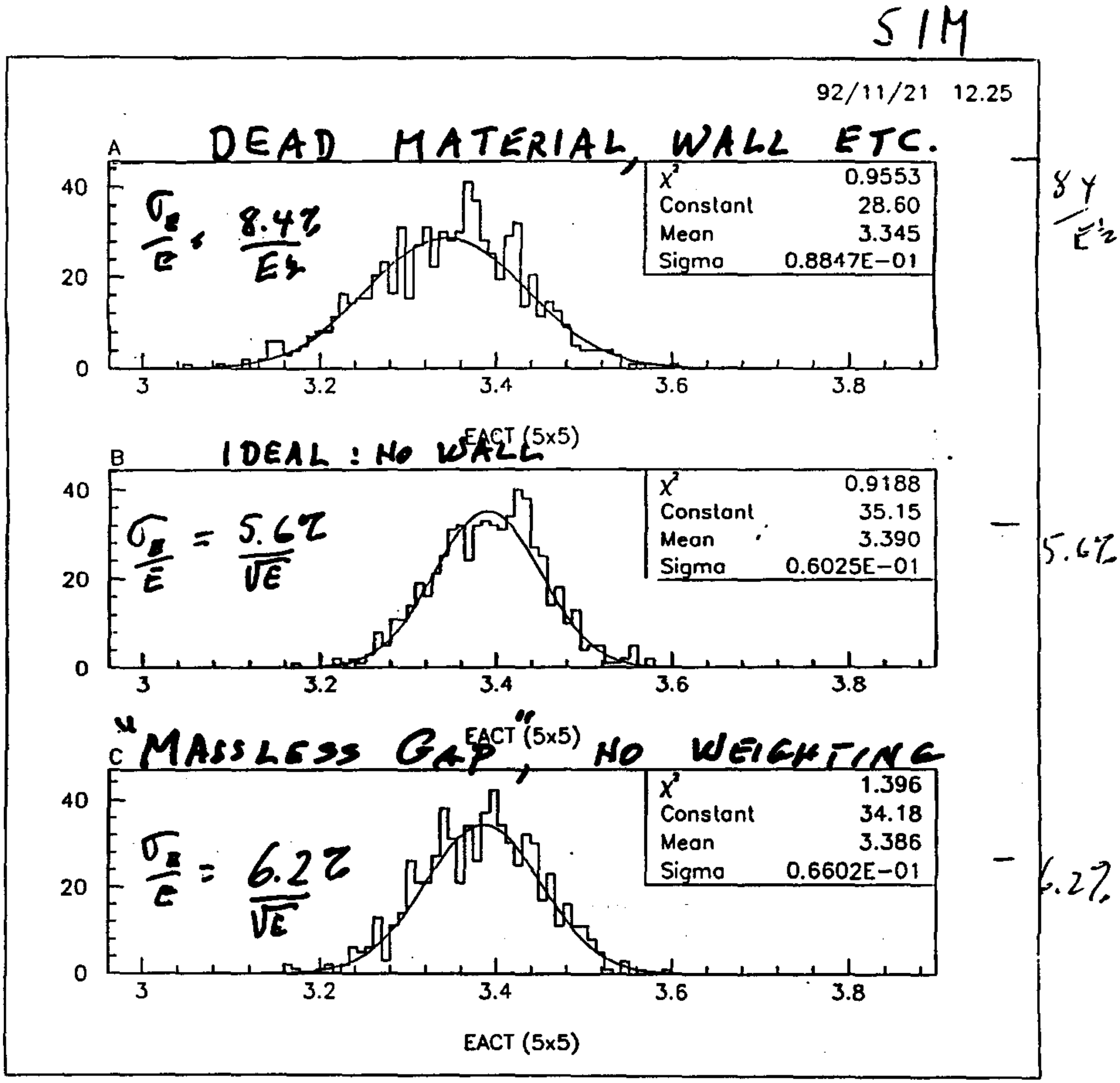

Figure 2: Energy in active medium for 10 GeV photons at $\vartheta = 45°$,
upper: with dead material but no massless gap;
middle: without dead material;
lower: with dead material and massless gap.

GEM.

EM Accordion Segmentation

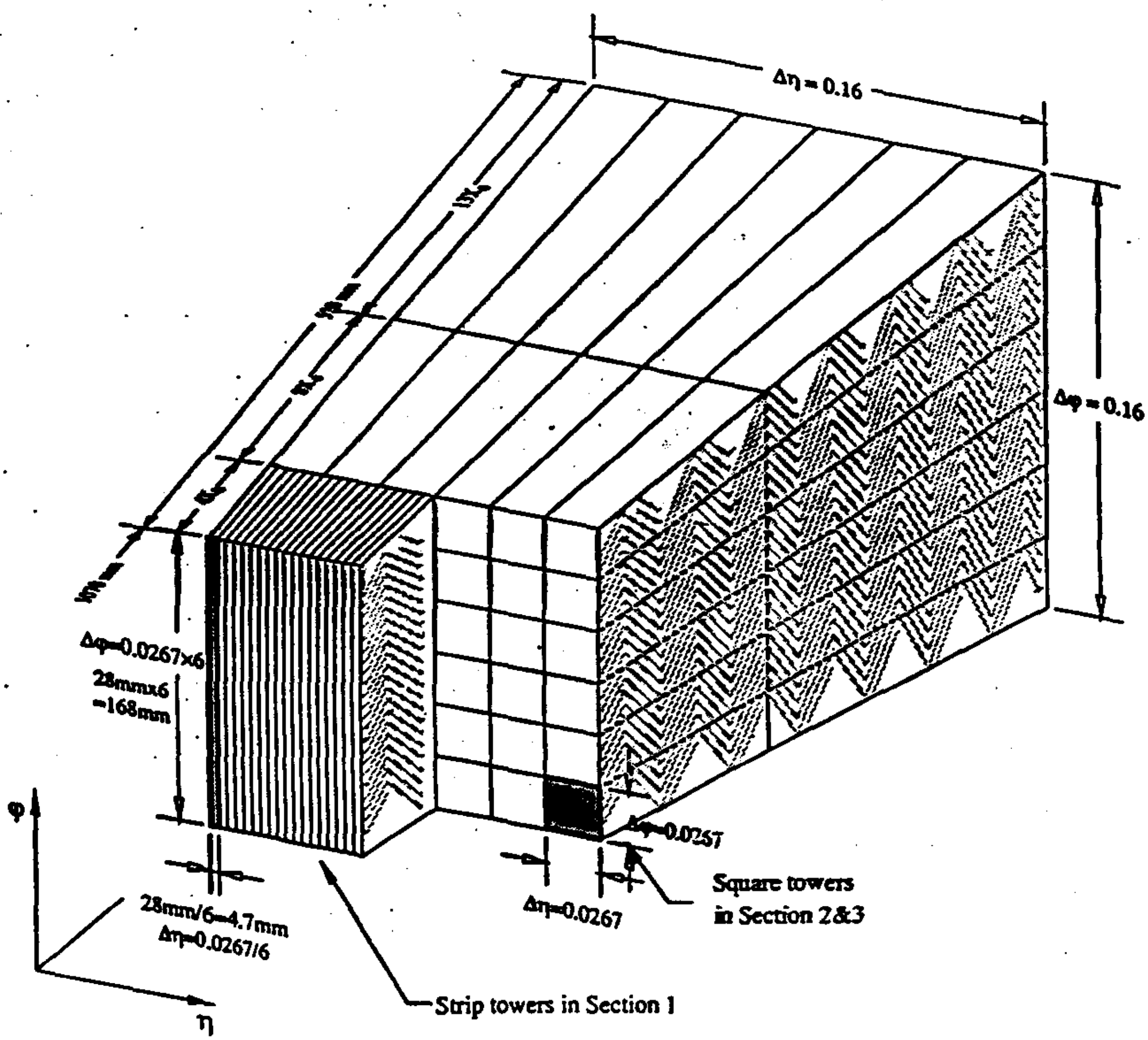

EM Accordion Electrodes
1st Section ($4X_0$), $\Delta\eta$ Strips

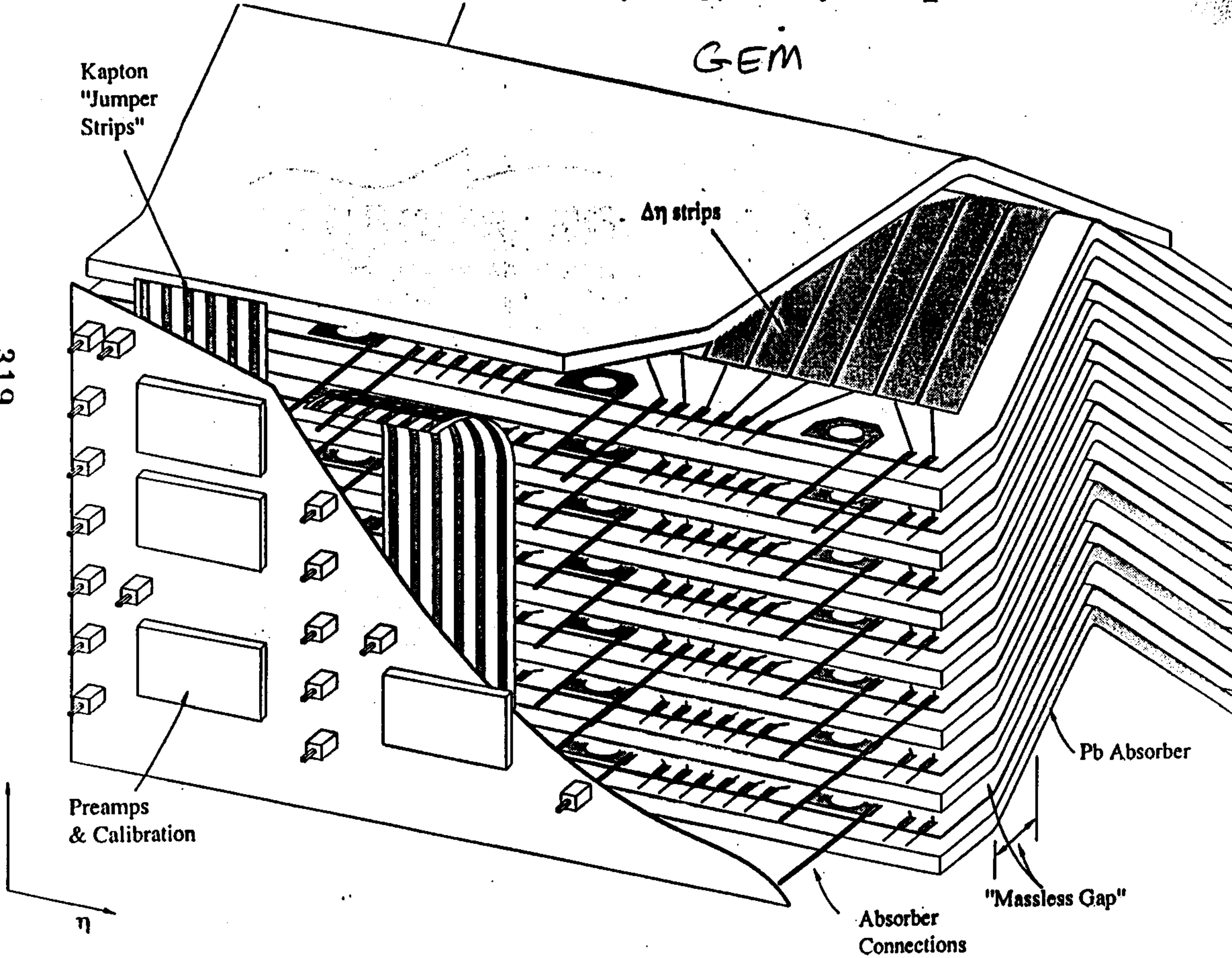

Likelihood Function

$$F = \log(SYM \times ASYM \times W2 \times W3)$$

E1 = Energy in the highest energy strip — center;

E3 = Energy sum in 3 strips around the center;

E_{right} = energy sum in 3 strips right to the center;

E_{left} = energy sum in 3 strips left to the center;

$SYM = (E_{right} + E_{left})/E3$

$ASYM = |E_{right} - E_{left}|/E1$

W2 = distance between the center and the second highset energy strip, in unit of strip numbers;

W3 = distance between the center and the third highset energy strip, in unit of strip numbers.

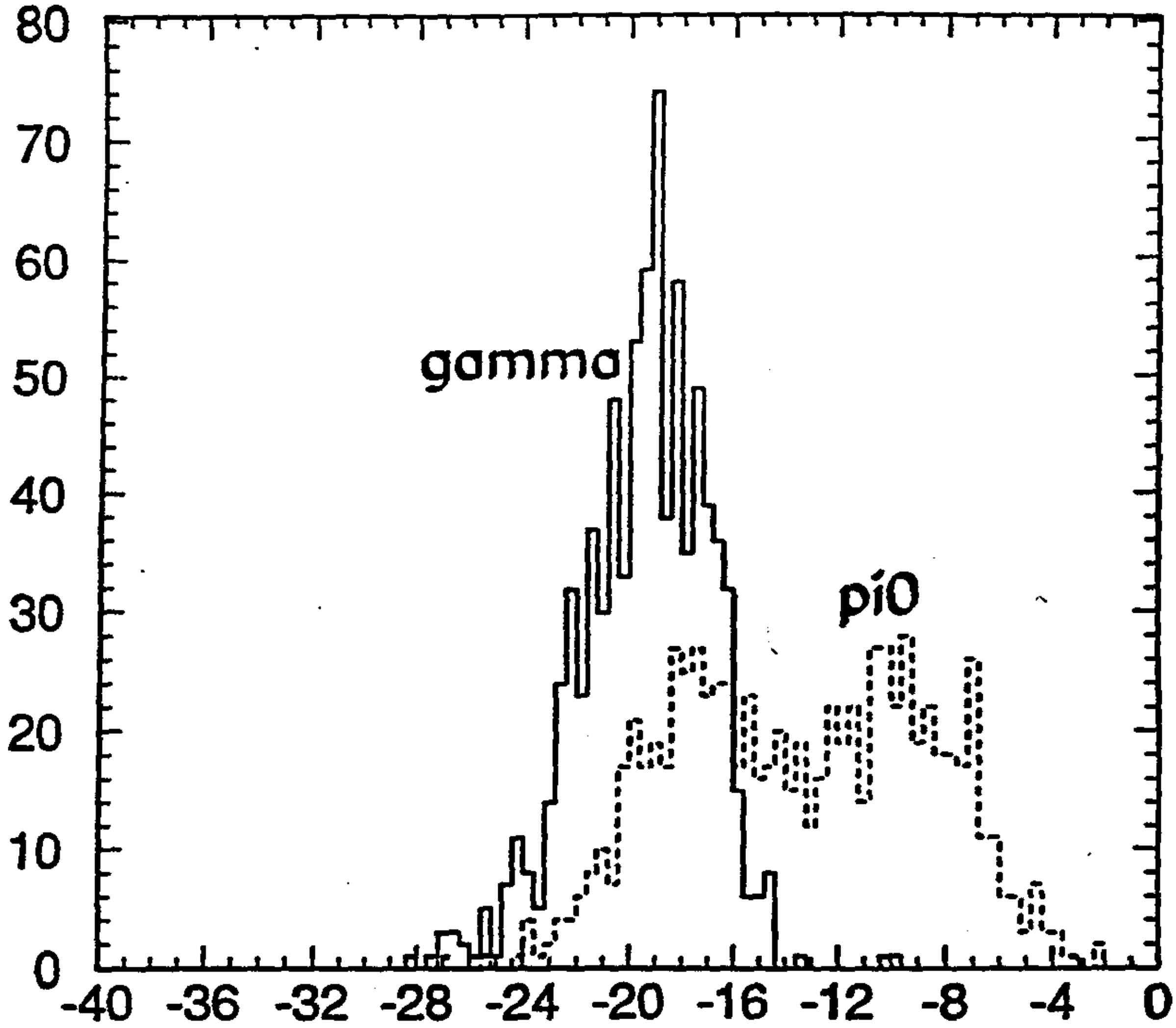

Figure 9: Separation of single photons and single π^0 of 25 GeV using strips.

Ma, Leltchouk

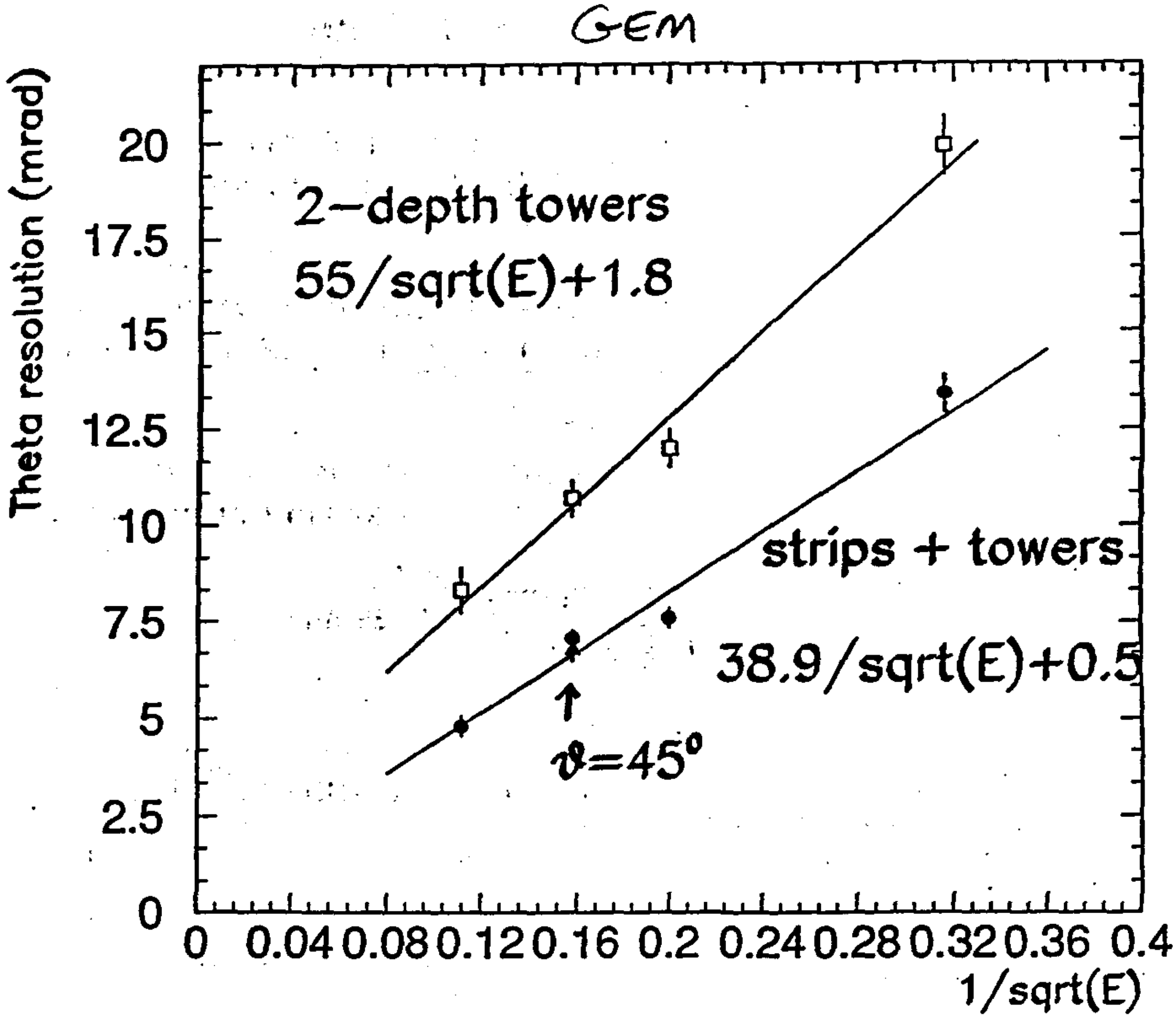

Figure 3: Angular resolution of tower and strip configuration.

GEM Mary Leltchouk

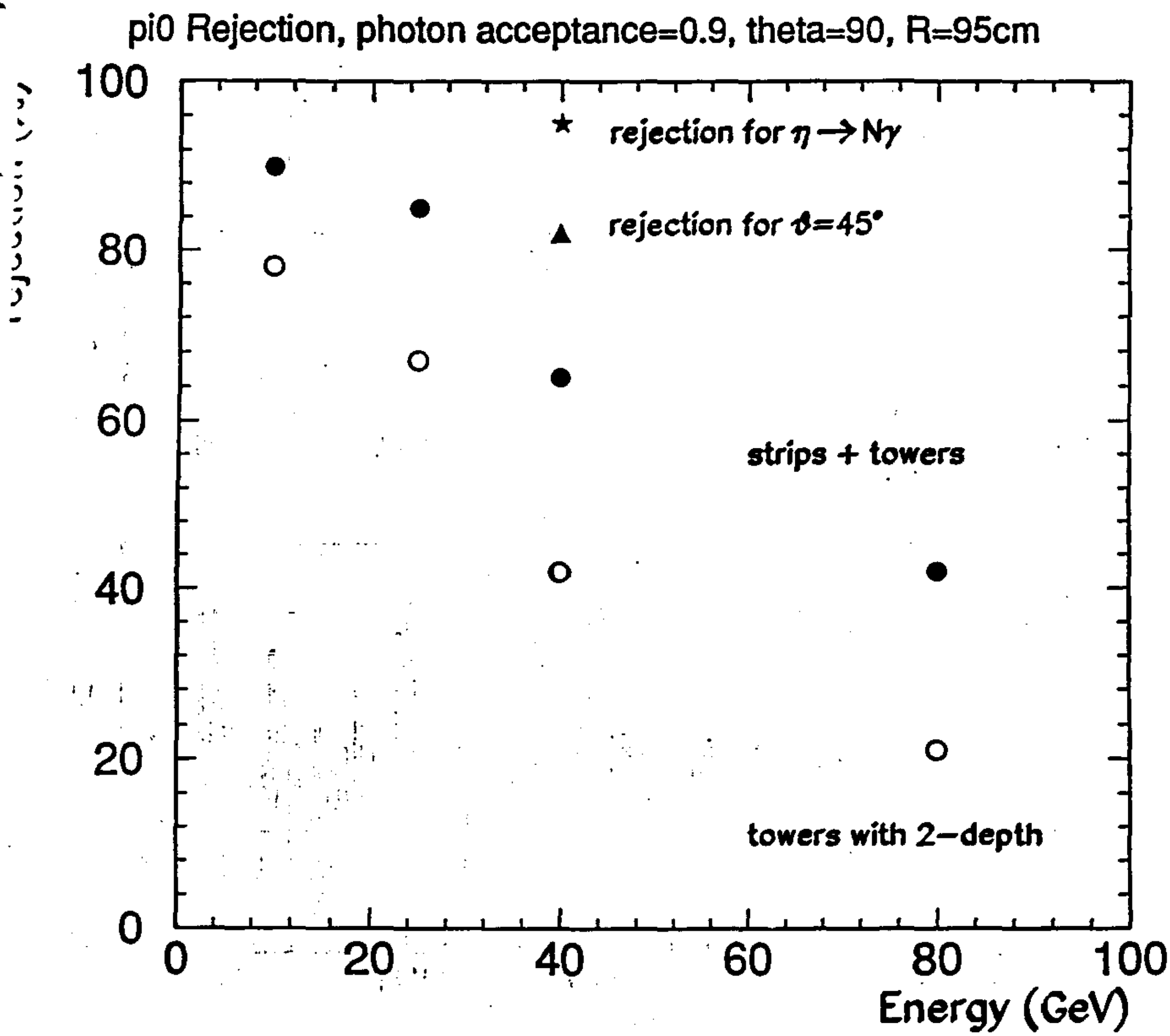

Figure 6: π^0 rejection rate as a function of energy

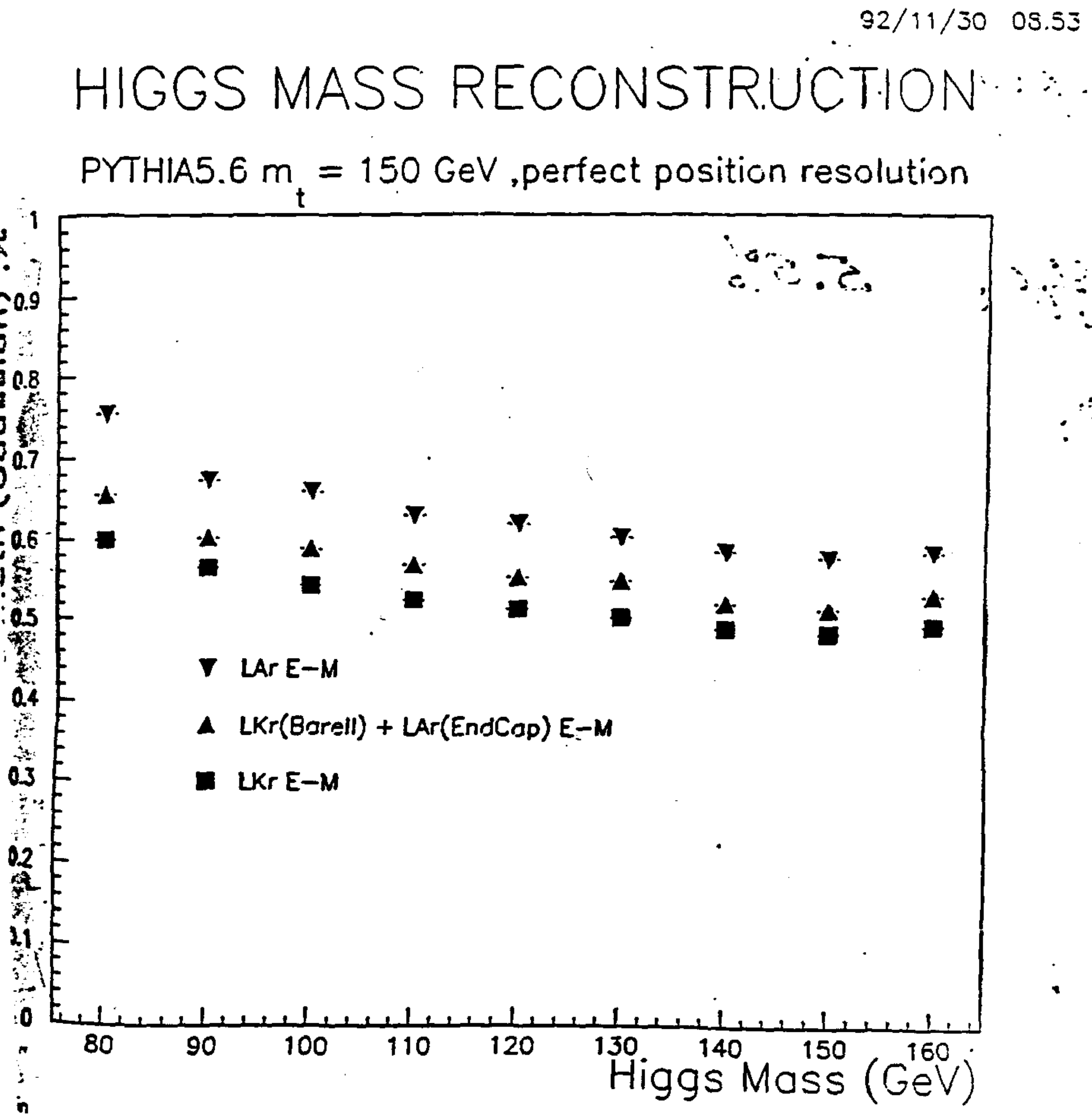
92/11/30 08.53
HIGGS MASS RECONSTRUCTION
PYTHIA5.6 m_t = 150 GeV ,perfect position resolution
LAr E–M
LKr(Barell) + LAr(EndCap) E–M
LKr E–M
0
0.1
0.2
0.3
0.4
0.5
0.6
0.7
0.8
0.9
1
80
90
100
110
120
130
140
150
160
Higgs Mass (GeV)

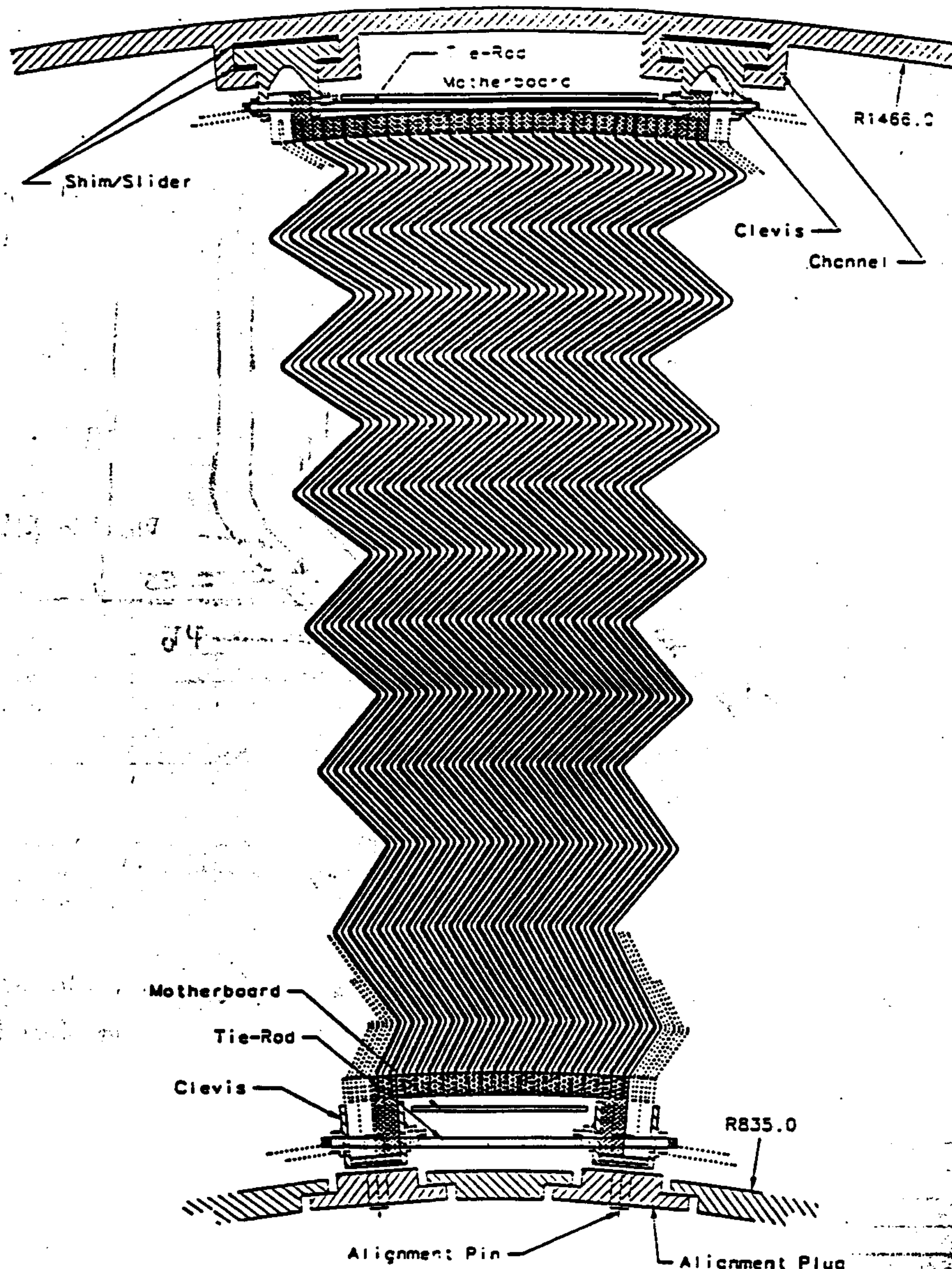

Figure 1-3a. Typical Module Lay-up in Section

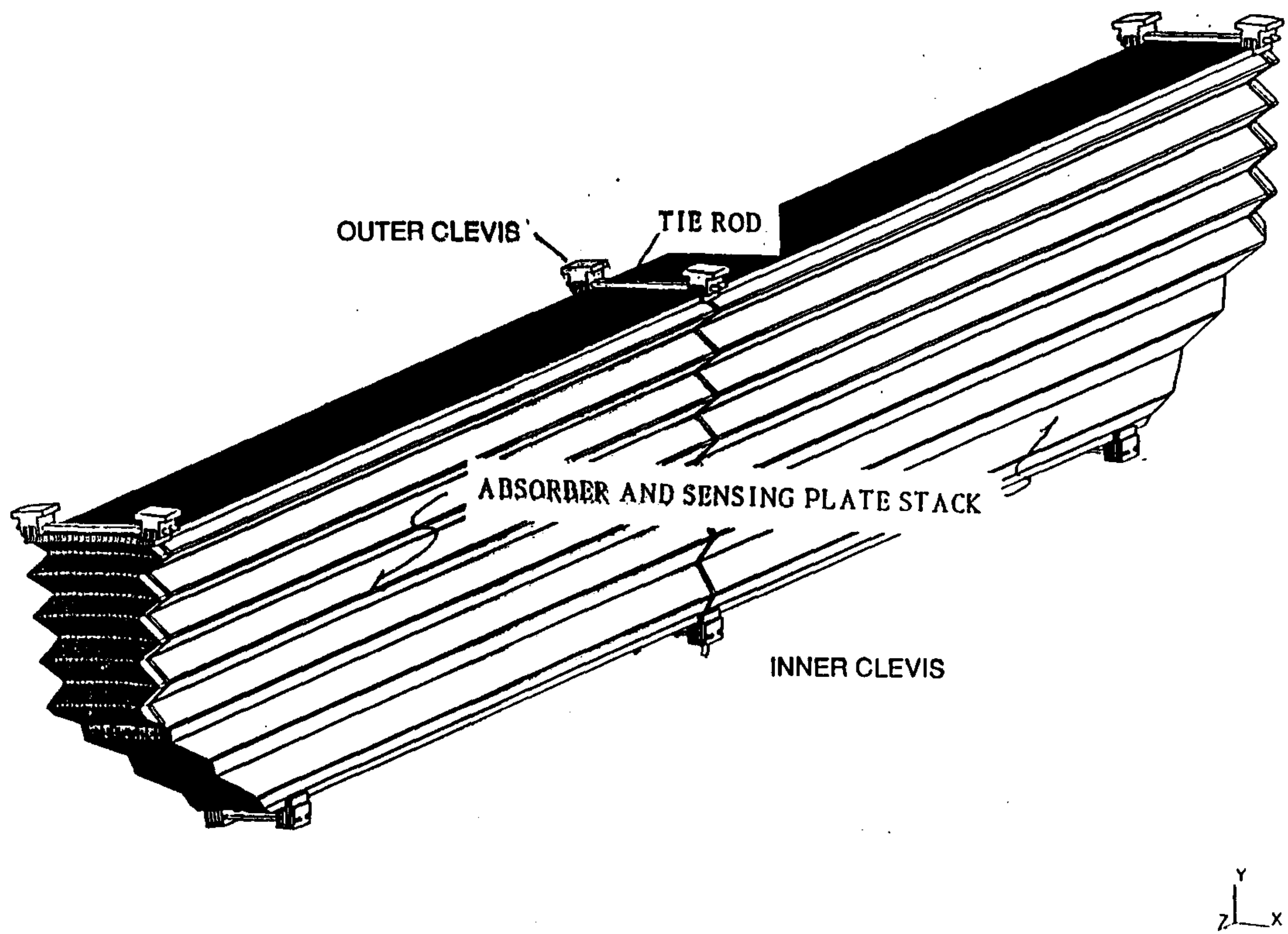

Figure 1-1 Barrel EM Module Assembly

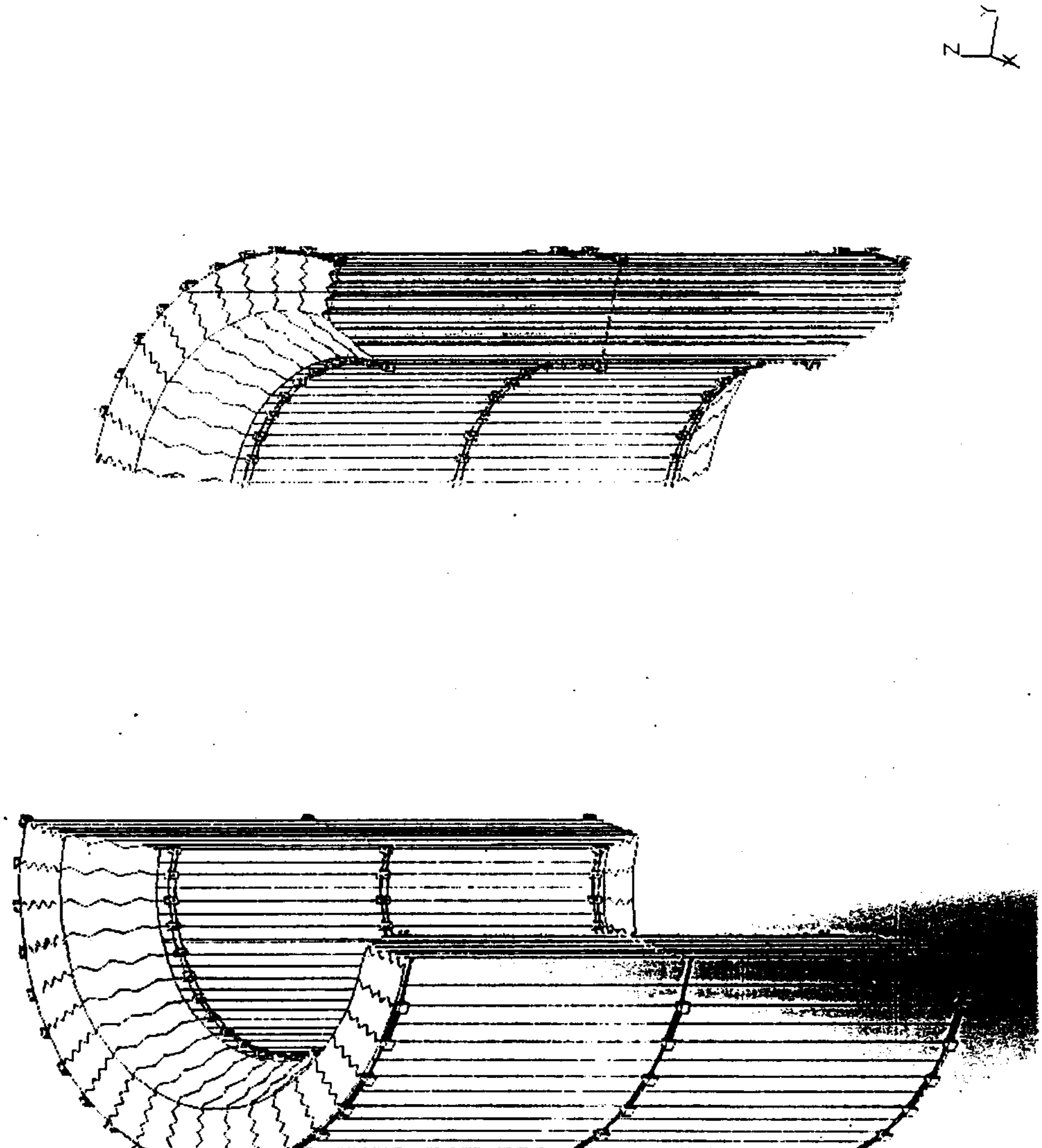

Y
Z
X

EM BARREL MODULE with Electronics and Cables

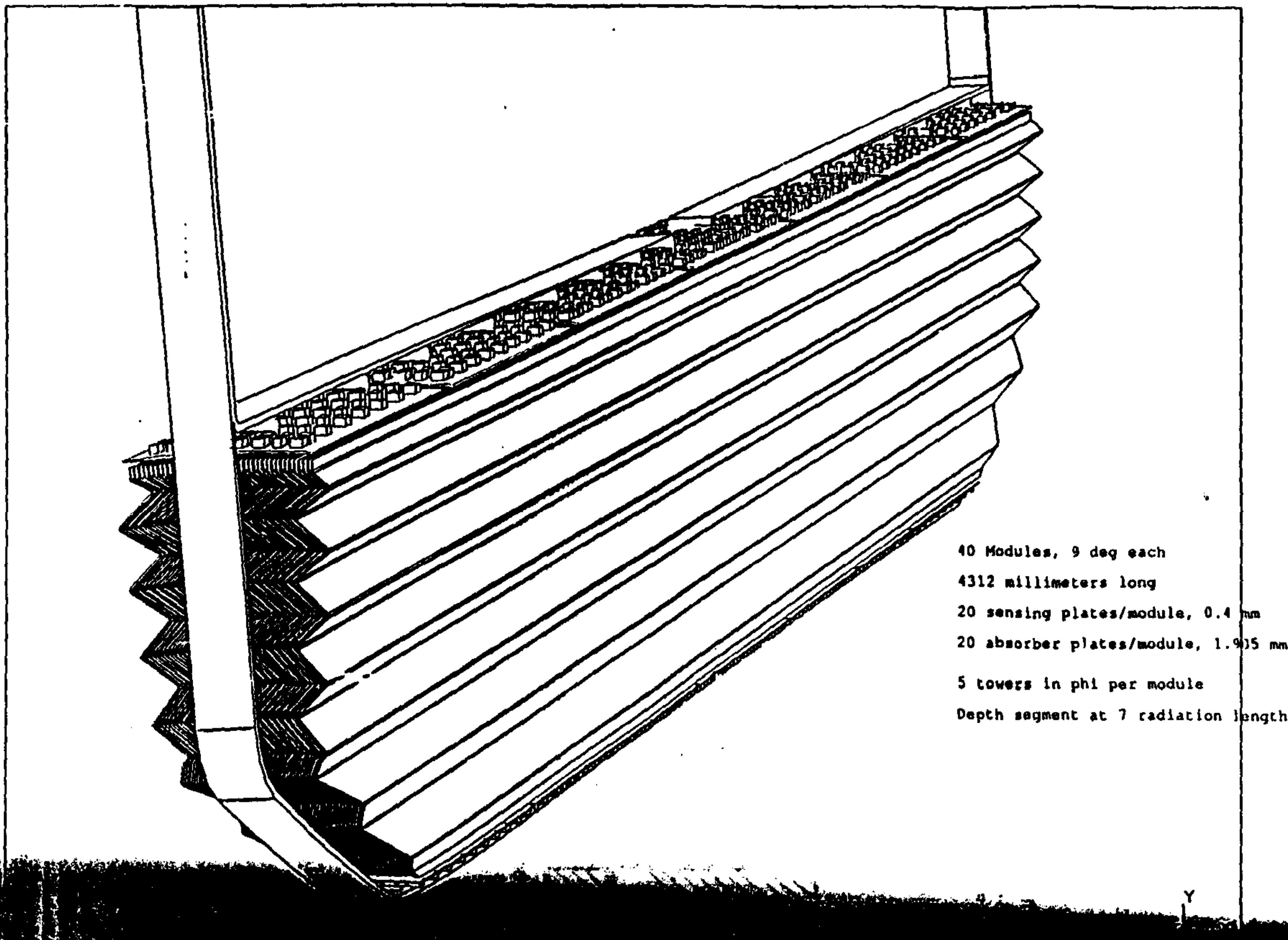

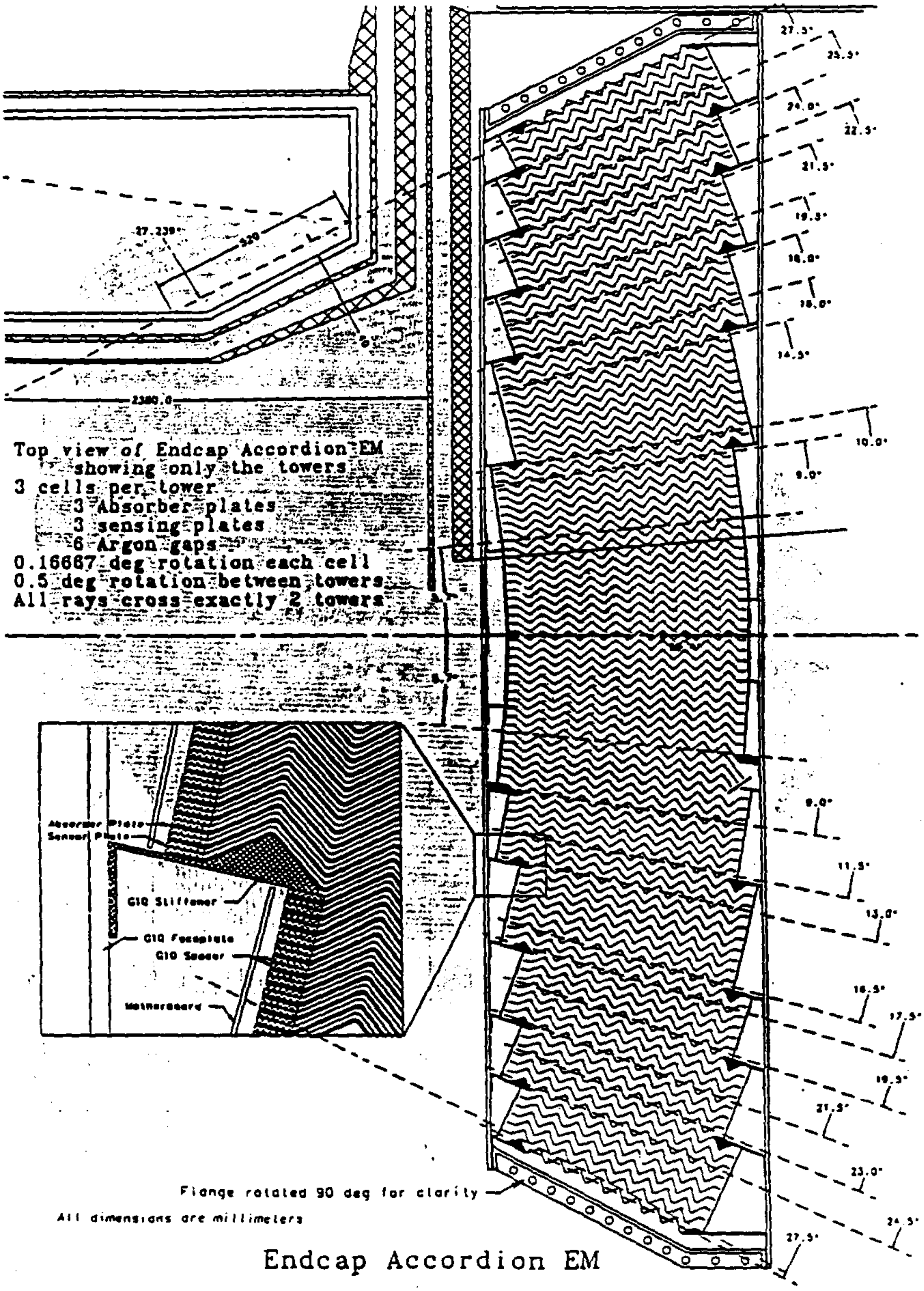

Endcap Accordion EM

Figure 5

Endcap EM Module

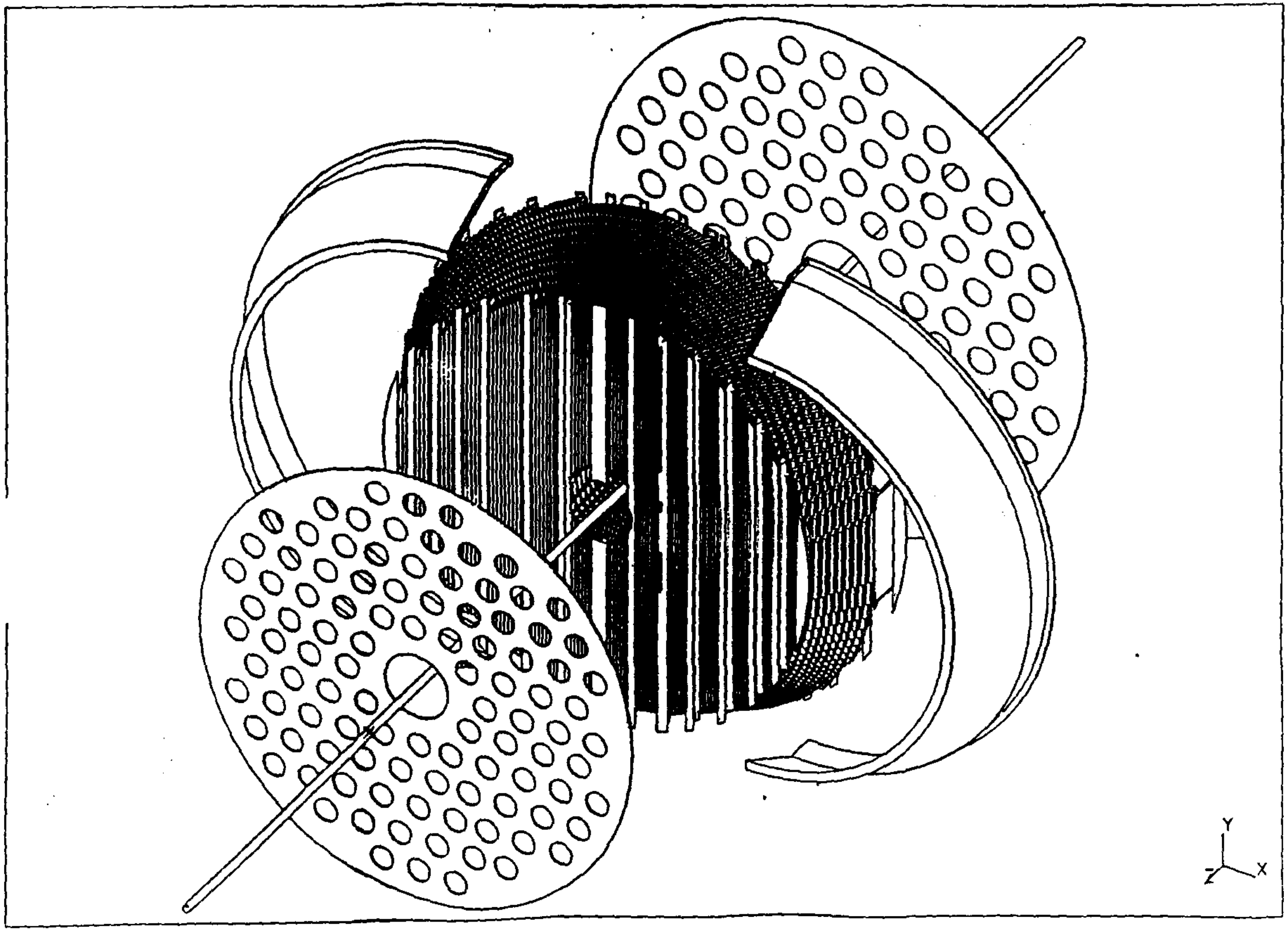

Feedthrough Flange
(9 deg. Sector)

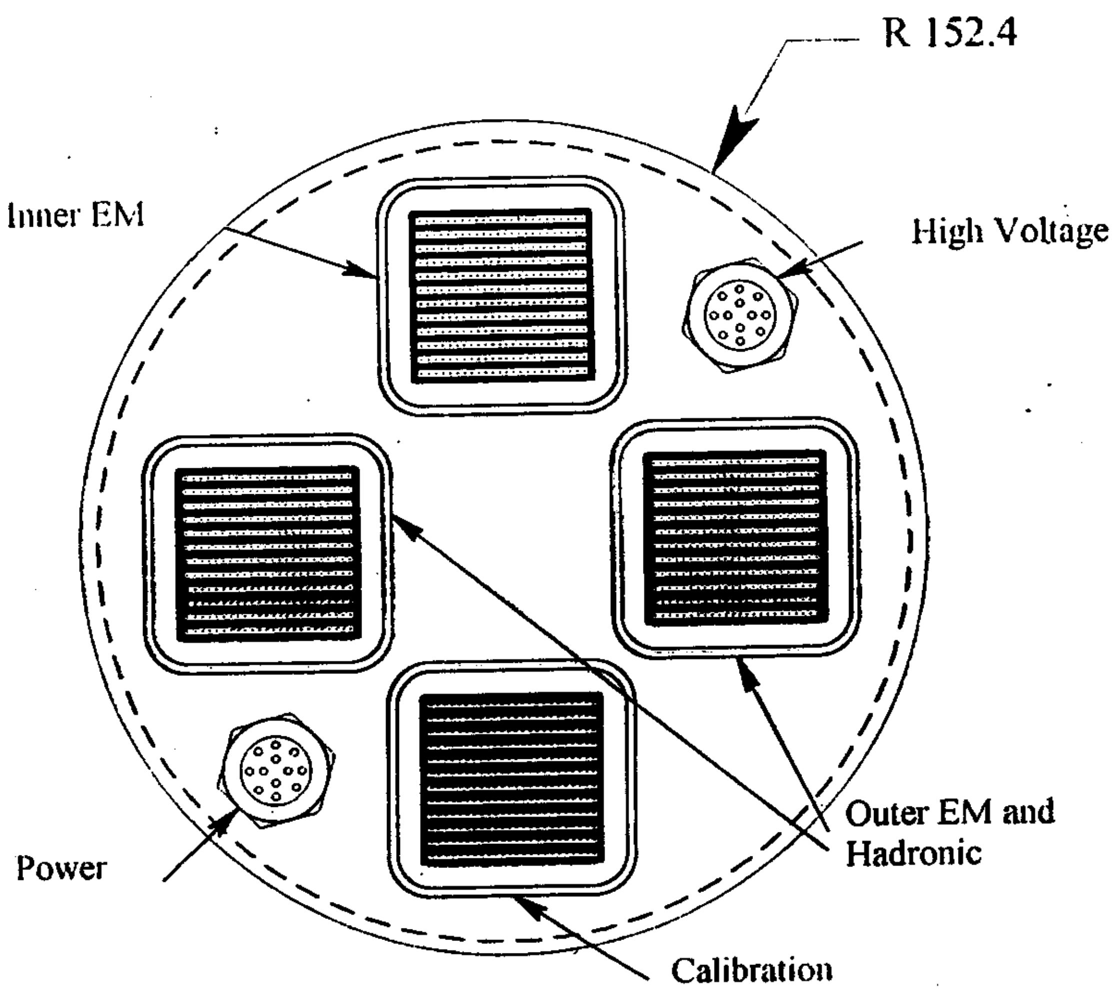

DSM

e # 2

0.08 x 0.08

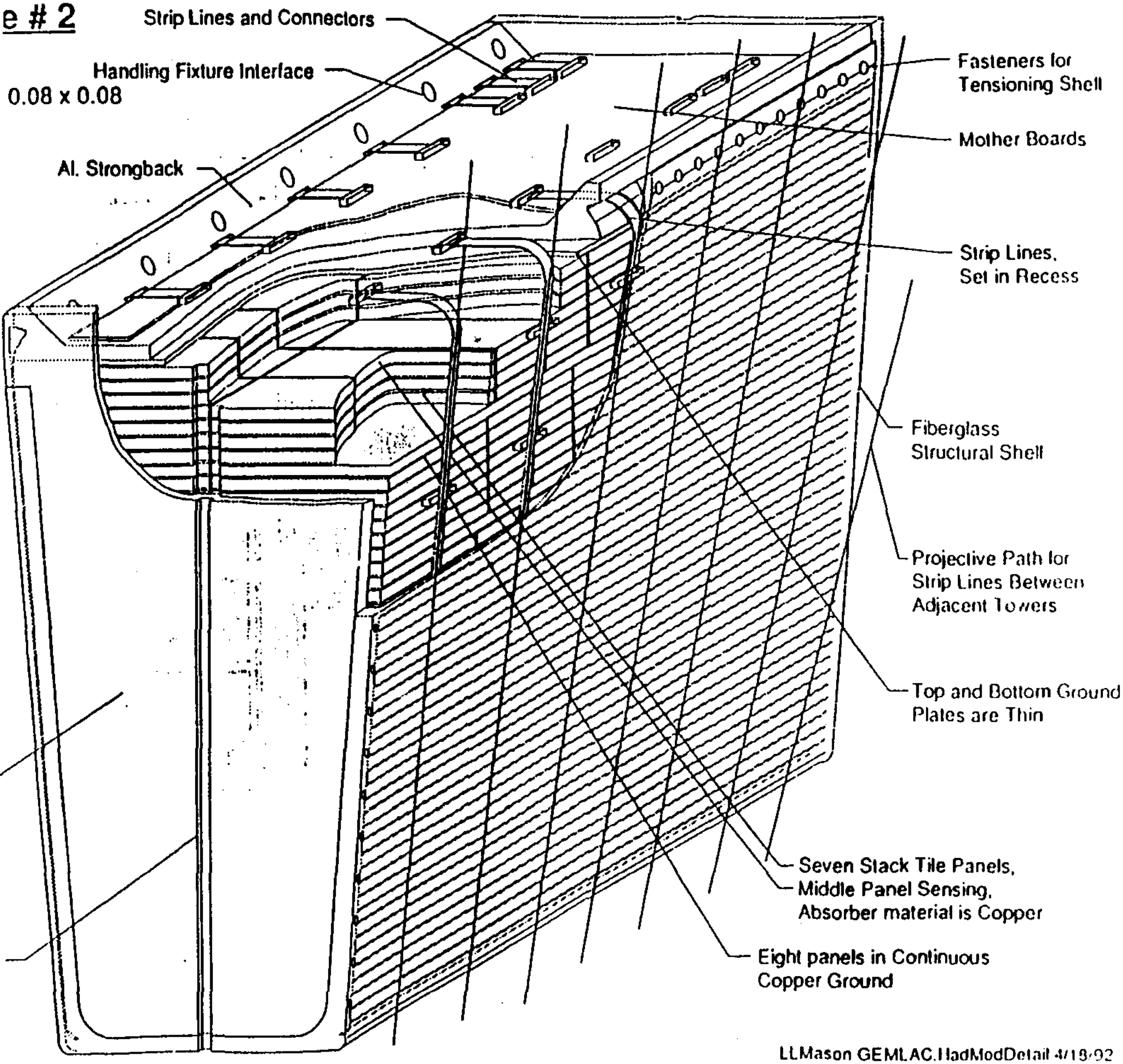
Strip Lines and Connectors
Handling Fixture Interface
Al. Strongback
Fasteners for
Tensioning Shell
Mother Boards
Strip Lines,
Set in Recess
Fiberglass
Structural Shell
Projective Path for
Strip Lines Between
Adjacent Towers
Top and Bottom Ground
Plates are Thin
Seven Stack Tile Panels,
Middle Panel Sensing,
Absorber material is Copper
Eight panels in Continuous
Copper Ground
LLMason GEMLAC.HadModDetail 4/18/92

Fine Hadronic Module Absorber Plate (Section 1)

Absorber Plate Layup

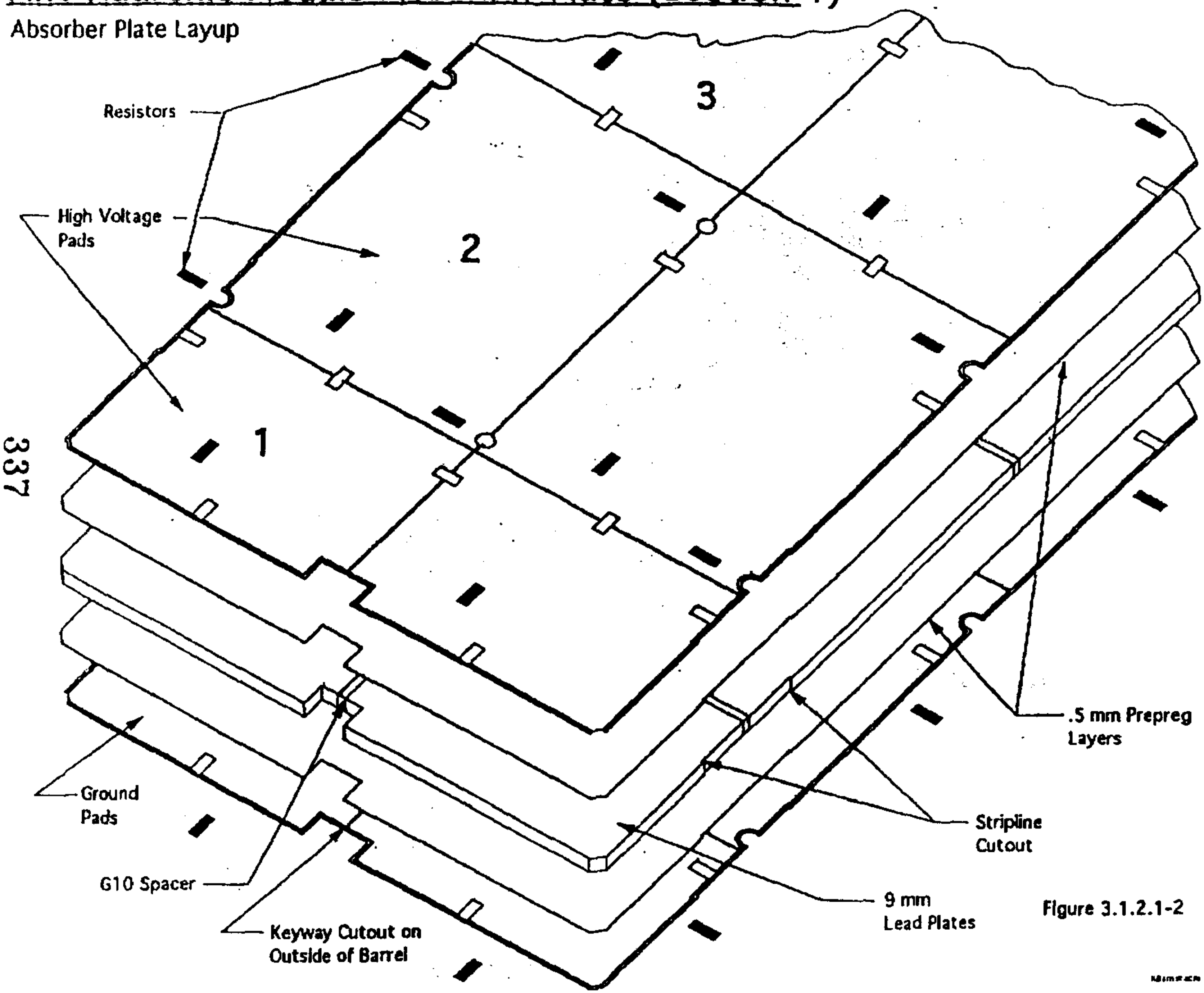

Figure 3.1.2.1-2

Top View Hadronic Module

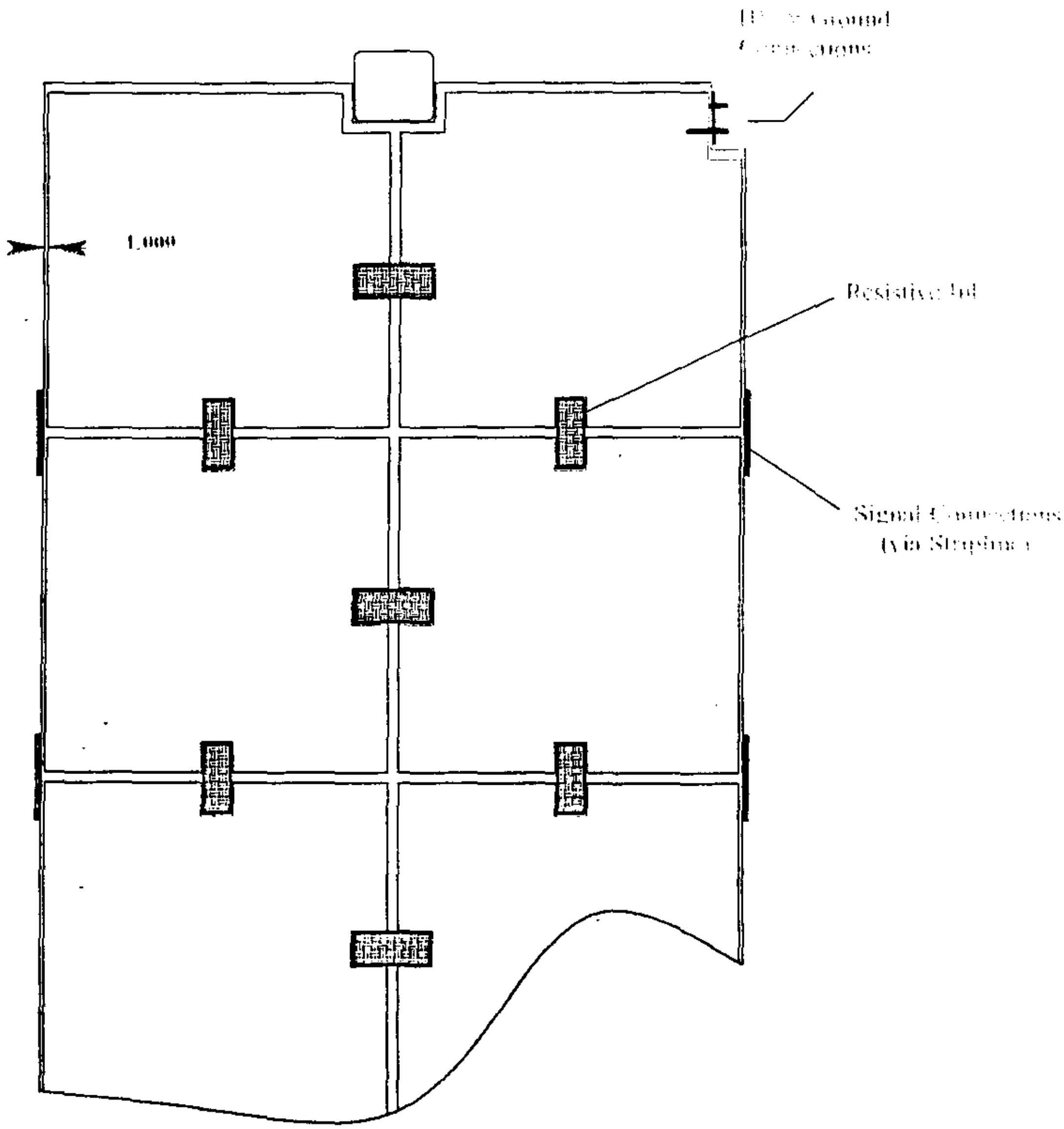

Conceptual Drawing

DSM

Conceptual Drawing

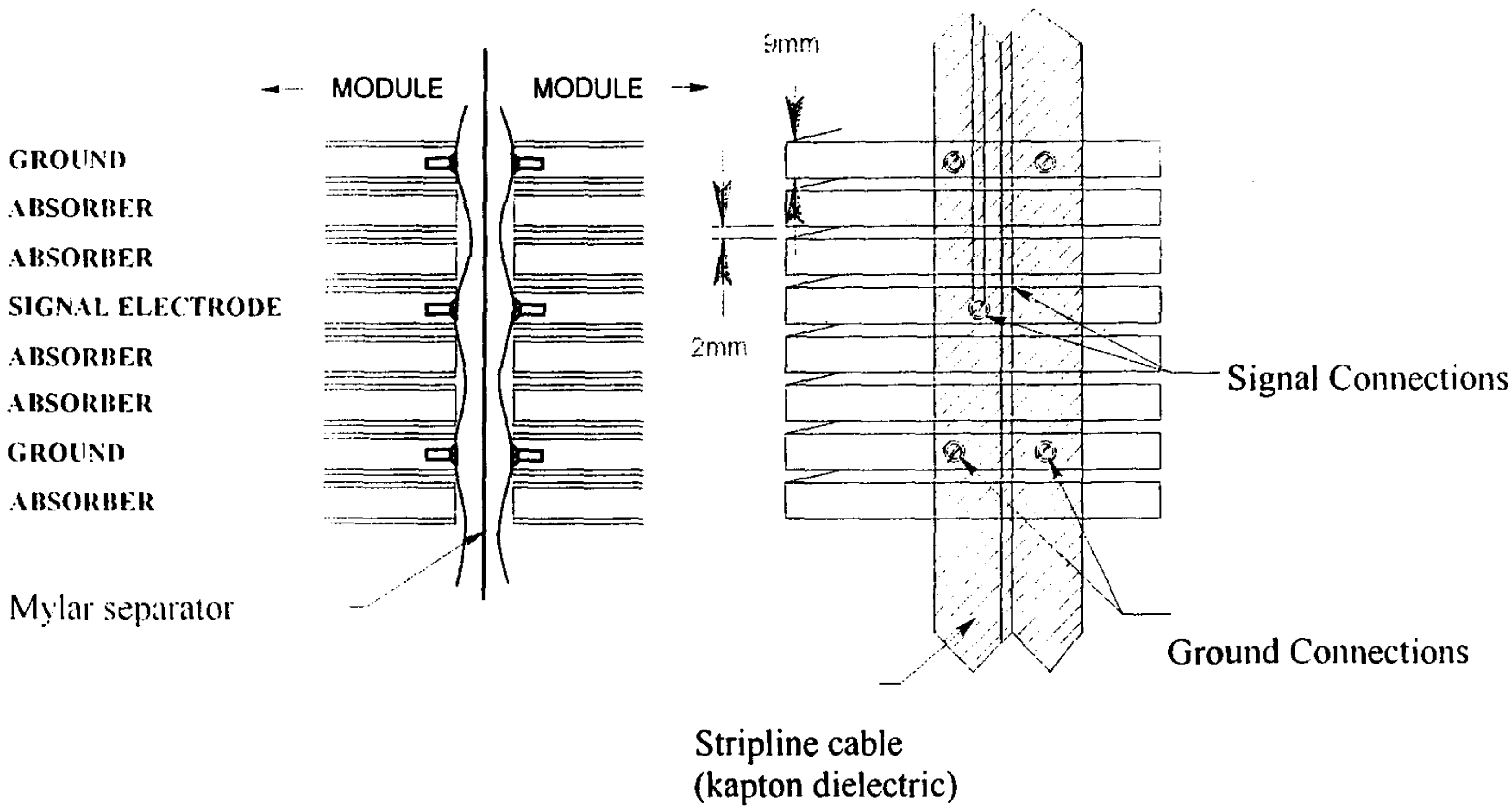

Signal Connections Hadronic Module

DSM

H. G...

Compensation

Why do we need it?

Compositeness? - Not too important as long as calorimeter is calibrated at "high" energies - G. Forden, AZPH-TH-91-9
also see M. Della Negra, Capri '91, p. 331.

Dijet Mass? - Jet algorithm, confusion with underlying event, magnetic field, and pileup at high L are more important than resolution.

Missing E_T ? η coverage more important - Capri

But e/h should not be too large.

We have not measured a mixed Kr/Pb-Kr/Cu calorimeter. We need to study what is the best absorber. What are the facts:

1992 AGS Tests:

	Pb/LAr 15 GeV Data	Pb/LAr MC	Pb/LKr 15 GeV Data	Pb/LKr MC
e/μ	0.752	0.768	0.895	0.835

1991 AGS Tests: Pb/LAr

e/π: (10 GeV) 1.18+0.04
(20 GeV) 1.17+0.03

NA34 Helios Data ...DU/LAr, H1 Pb/LAr, Cu/LAr - without weighting

All much less than 1.3....

How does the data scale with energy:

Groom: $$e/\pi = \frac{1}{1+(h/e-1)E^{m-1}}$$

Wigmans: $$e/\pi(E) = \frac{e/h}{1+(e/h-1)0.11\ \ln E}$$

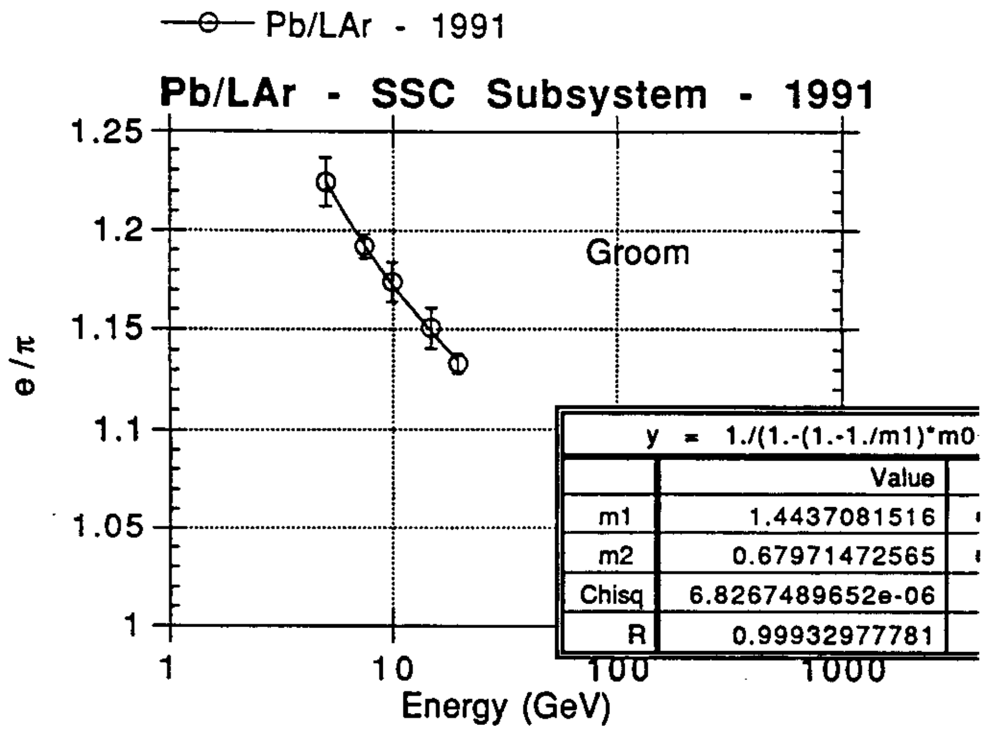
Pb/LAr - 1991
Pb/LAr - SSC Subsystem - 1991
1.25
1.2
1.15
1.1
1.05
1
e/π
Groom
y = 1./(1.-(1.-1./m1)*m0
Value
m1 1.4437081516
m2 0.67971472565
Chisq 6.8267489652e-06
R 0.99932977781
1
10
100
1000
Energy (GeV)

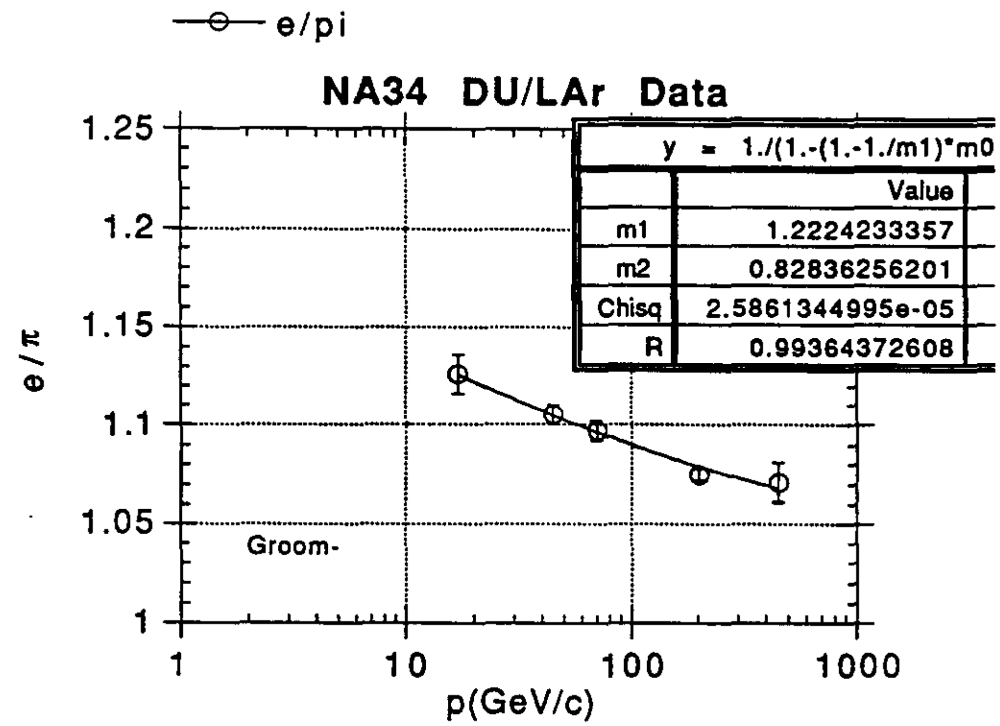

e/pi
NA34 DU/LAr Data
y = 1./(1.-(1.-1./m1)*m0
Value
m1
1.2224233357
m2
0.82836256201
Chisq
2.5861344995e-05
R
0.99364372608
1.25
1.2
1.15
1.1
1.05
1
e/π
Groom-
1
10
100
1000
p(GeV/c)

Take Groom:

	e/h	m
Pb/LAr	1.45(.05)	0.67(.03)
D0(DU)	1.37(.15)	0.56(.09)
NA34	1.25(.04)	0.81(.03)
H1	1.95(.26)	0.64(.04) but

look at the data...

How to relate e/π to resolution?

Groom: $\frac{\Delta E}{E} = \frac{A(E)}{\sqrt{E}} \oplus (0.171 - 0.01 \cdot \ln E(GeV))(1 - h/e)$

(Capri, p. 376) cf. Wigmans 21%*(1-h/e)

The best data is from NA34: at 450 GeV;

$\sigma_E/E=0.026$ (not much room for a constant term)

Groom predicts 0.022! Data can not determine the energy dependence of the constant term...

We can try to use GEANT to predict e/π for Cu/Kr - we know from D0 and 1991 AGS tests that GEANT is high in e/h by ~0.15.

	Pb/LAr	Pb/LKr	Cu/LAr	Cu/LKr
e/π	1.30	1.42	1.41	1.69

Pre-Atlas studies CAL-TR-037 M. Nessi et al. (1991) Pb/LAr accordion + Pb or Fe Hadronic section. Generate 30, 80, 150 GeV Jets

Pb: $\frac{\sigma}{E}(\%) = \frac{63 \pm 4}{\sqrt{E}} + (1.6 \pm 0.4)$

Fe: $\frac{\sigma}{E}(\%) = \frac{62 \pm 5}{\sqrt{E}} + (2.5 \pm 0.5)$

Weighting ala H1

H1-simulation (Singapore, 1990)

$37\% / \sqrt{E} \leq \sigma / \sqrt{E} \leq 43\% / \sqrt{E}$

Fit 8 parameters R = 0.7

RD3 – P. Battaglia, L. Cossi, L. Perini
10/17/92
Accordion + Fe/L Ar
Pythia Jets 20-300 GeV

GEANT 3.15+ FLUKA

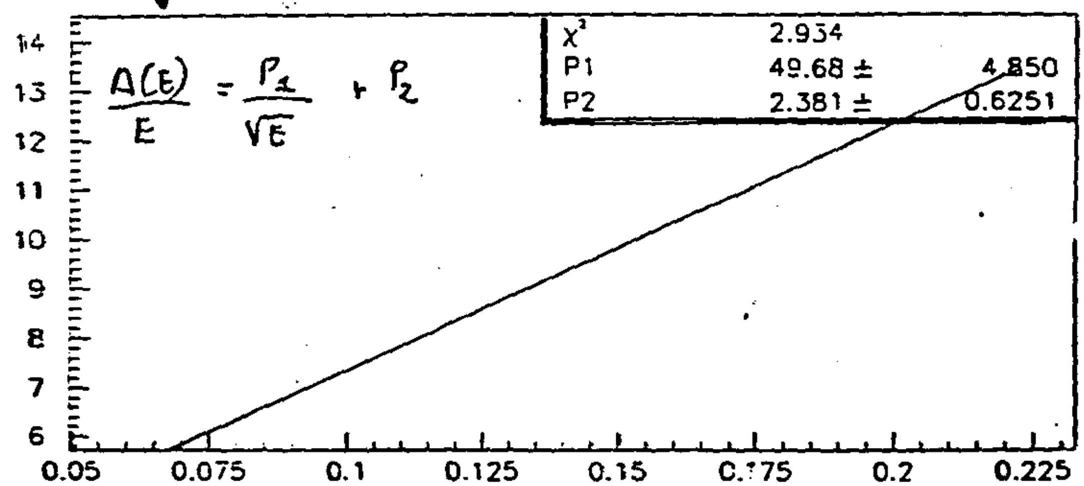

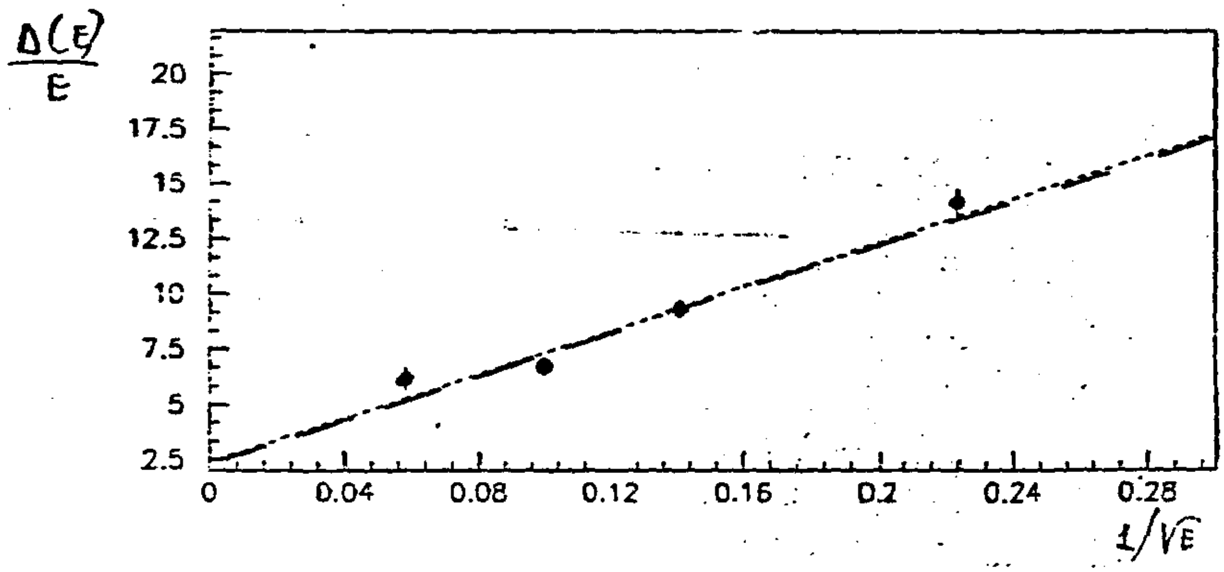

$$\frac{50 \pm 5\%}{\sqrt{E}} \oplus 2.4 \pm 0.6\%$$

8 parameters – 1 for each longitudinal division but NOT energy dependent

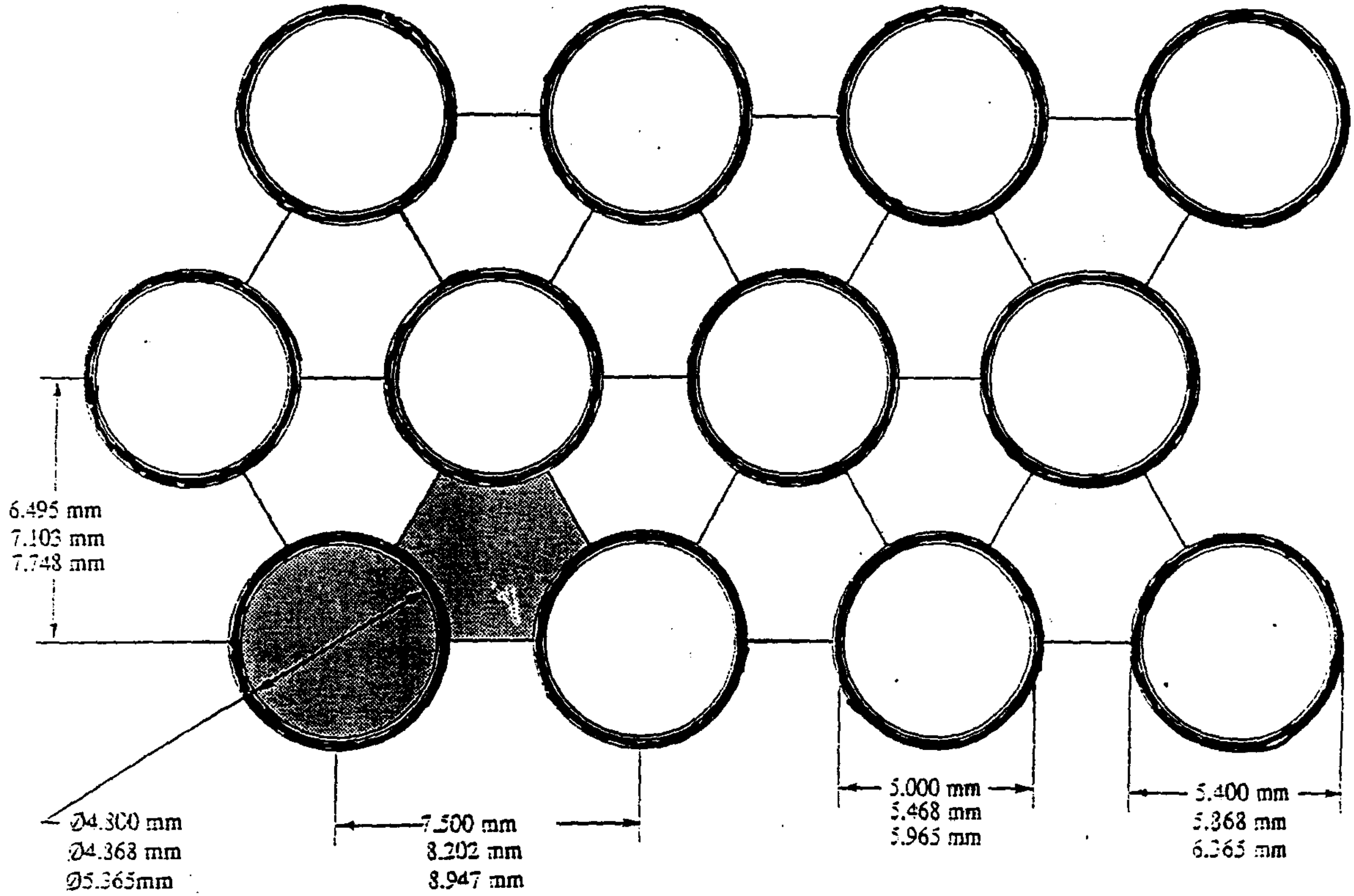

FCAL MODULE - TUNGSTEN ARRAGEMENT

LAR MODULE-DEFORM

SM CHAE

GEM Calorimeter Piping Plan

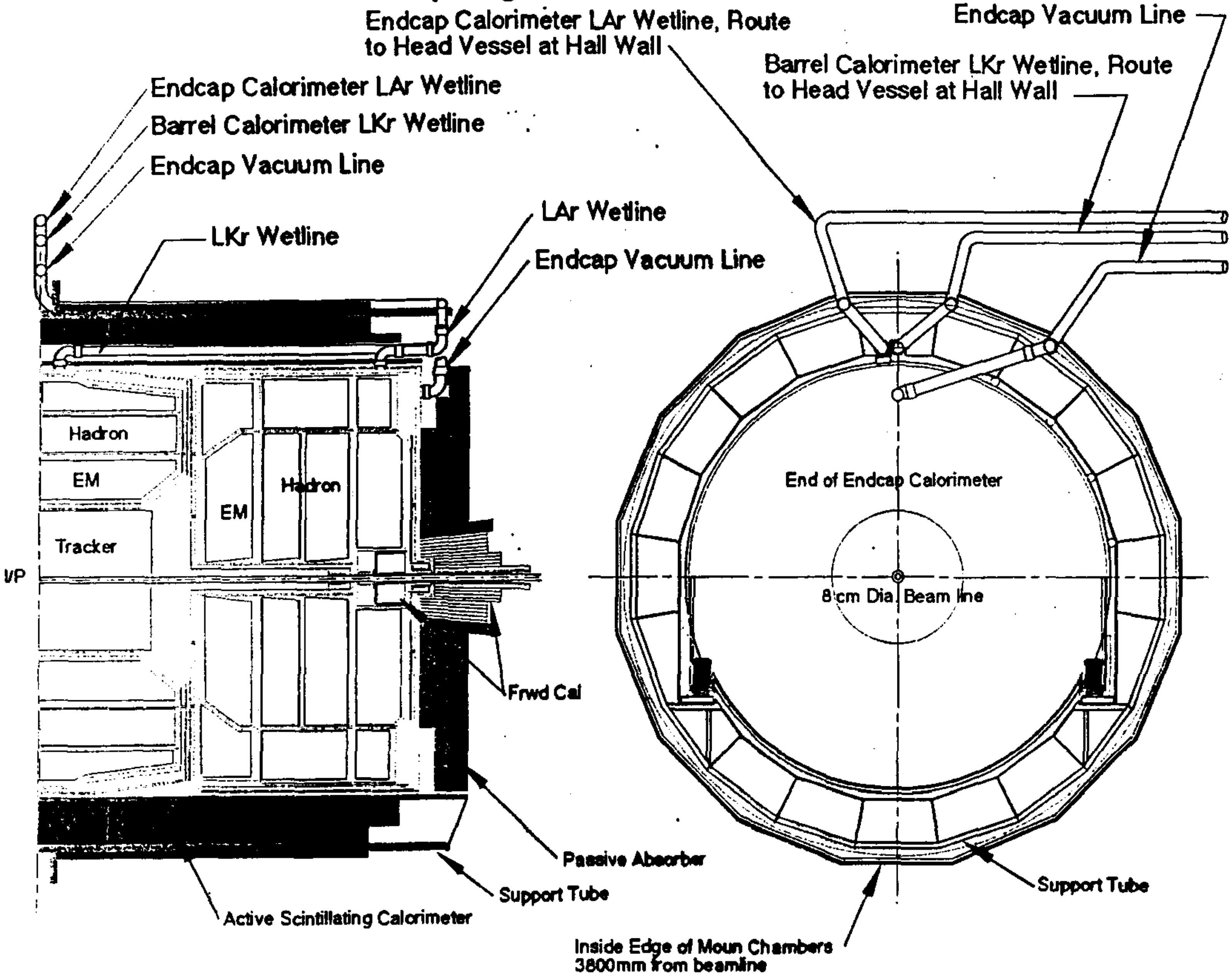

Half Section - GEM Calorimeter

End View - Gem Calorimeter

LLMason:Calorimeter Piping:11/16/92

FNAL Schedule

- Collider Run 1(a) —> Mid-1993 [25 pb^{-1}]
- Linac Upgrade —> Late-1993
- Collider Run 1(b) —> Late-1994 [75 pb^{-1}]
- SSC Test Beam Run —> Mid-1995
- MI Shutdown —> Late-1995
- Fixed Target Run —> Late-1996

Fermilab Draft Long-Range Schedule
November 1992

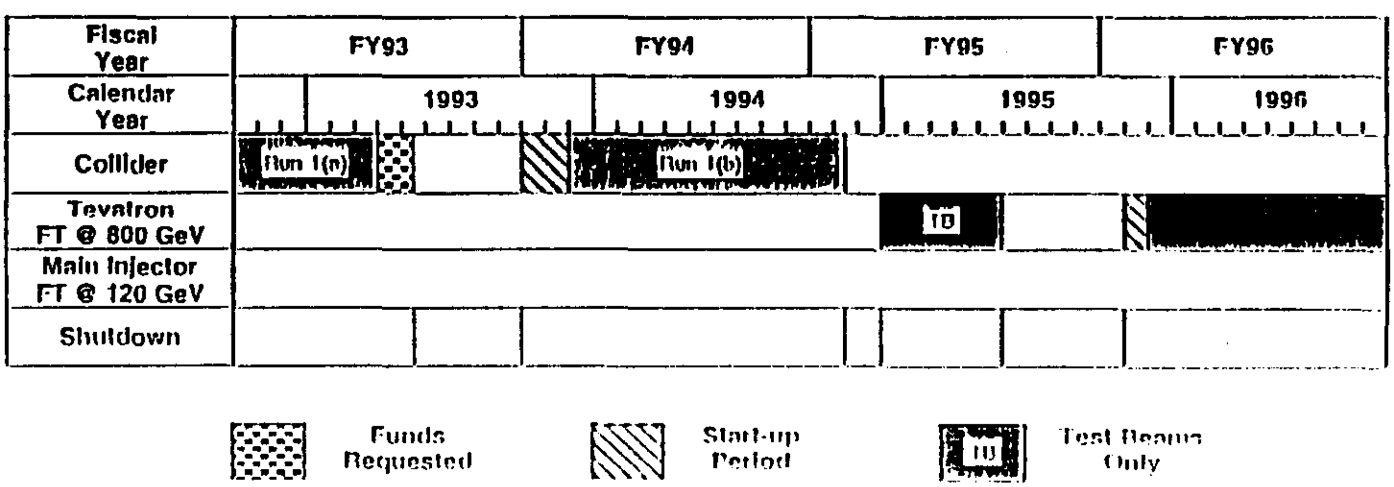

MWEST at FNAL

- **Layout for GEM Calorimeter Studies**

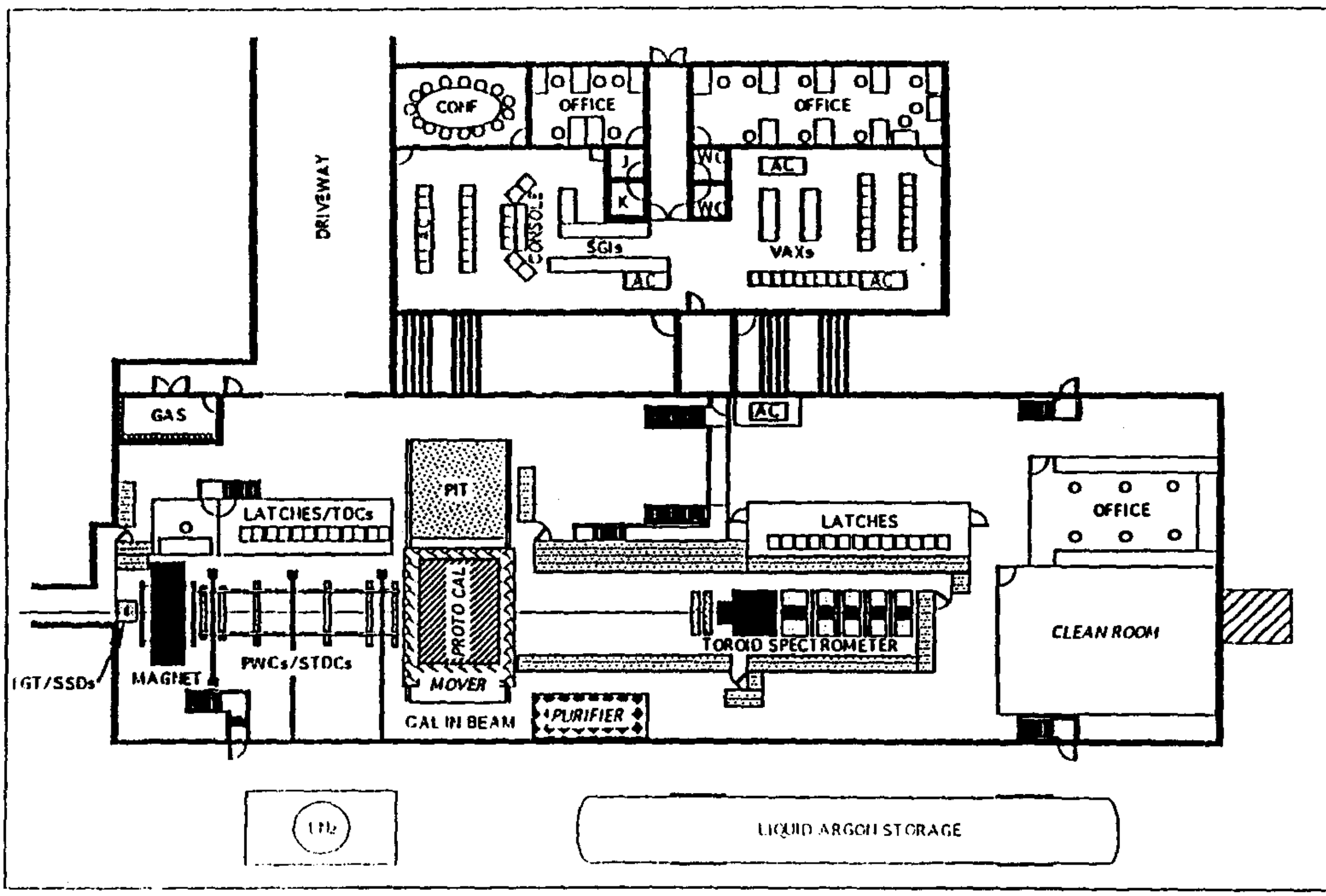

For Schematic Purposes Only - Not Drawn to Scale

2 m. dia dewar with 4 m long module in place.

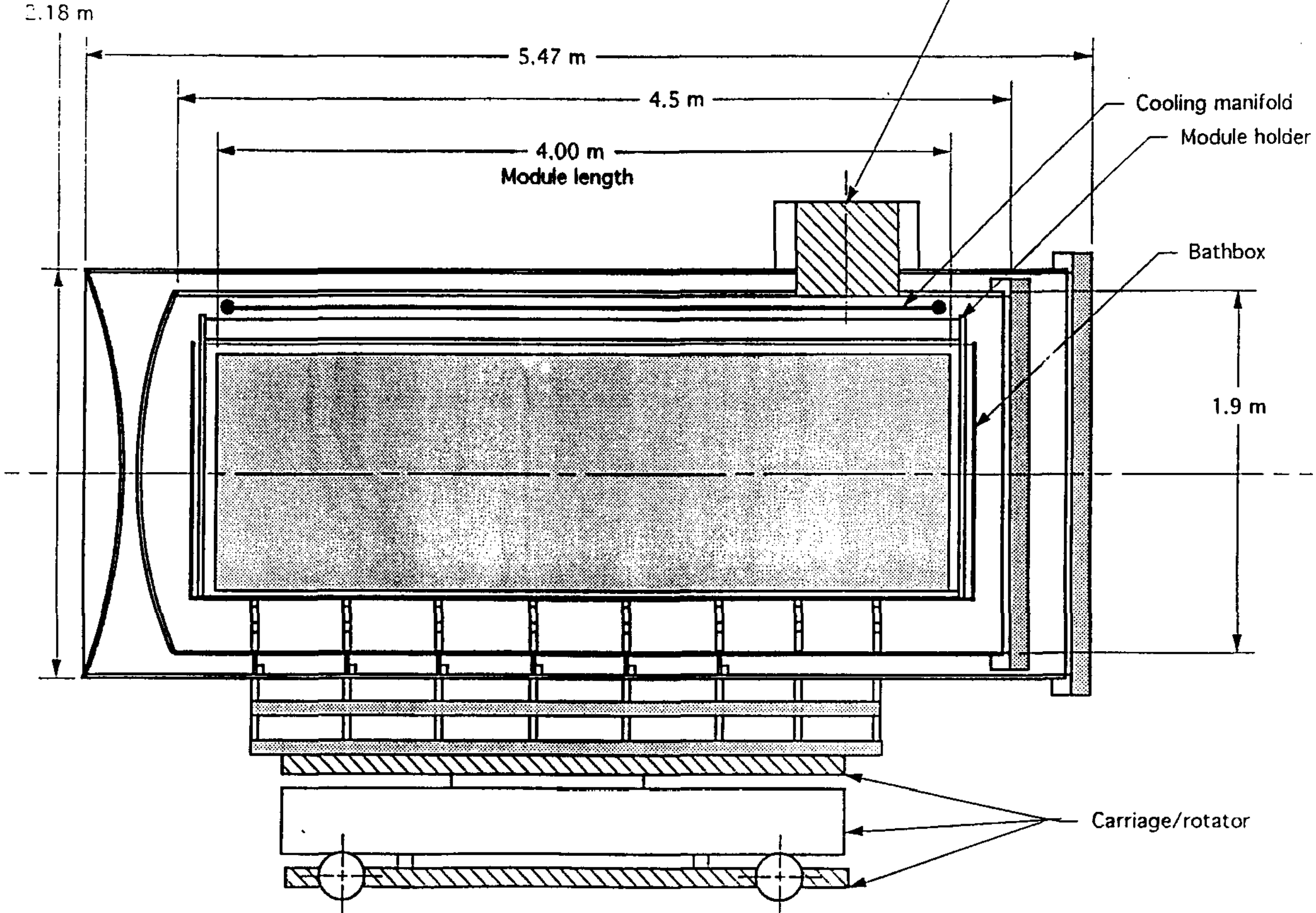

University of Washington
11/17/92

New 2 m. dewar with
2.65 m downstream
radius.

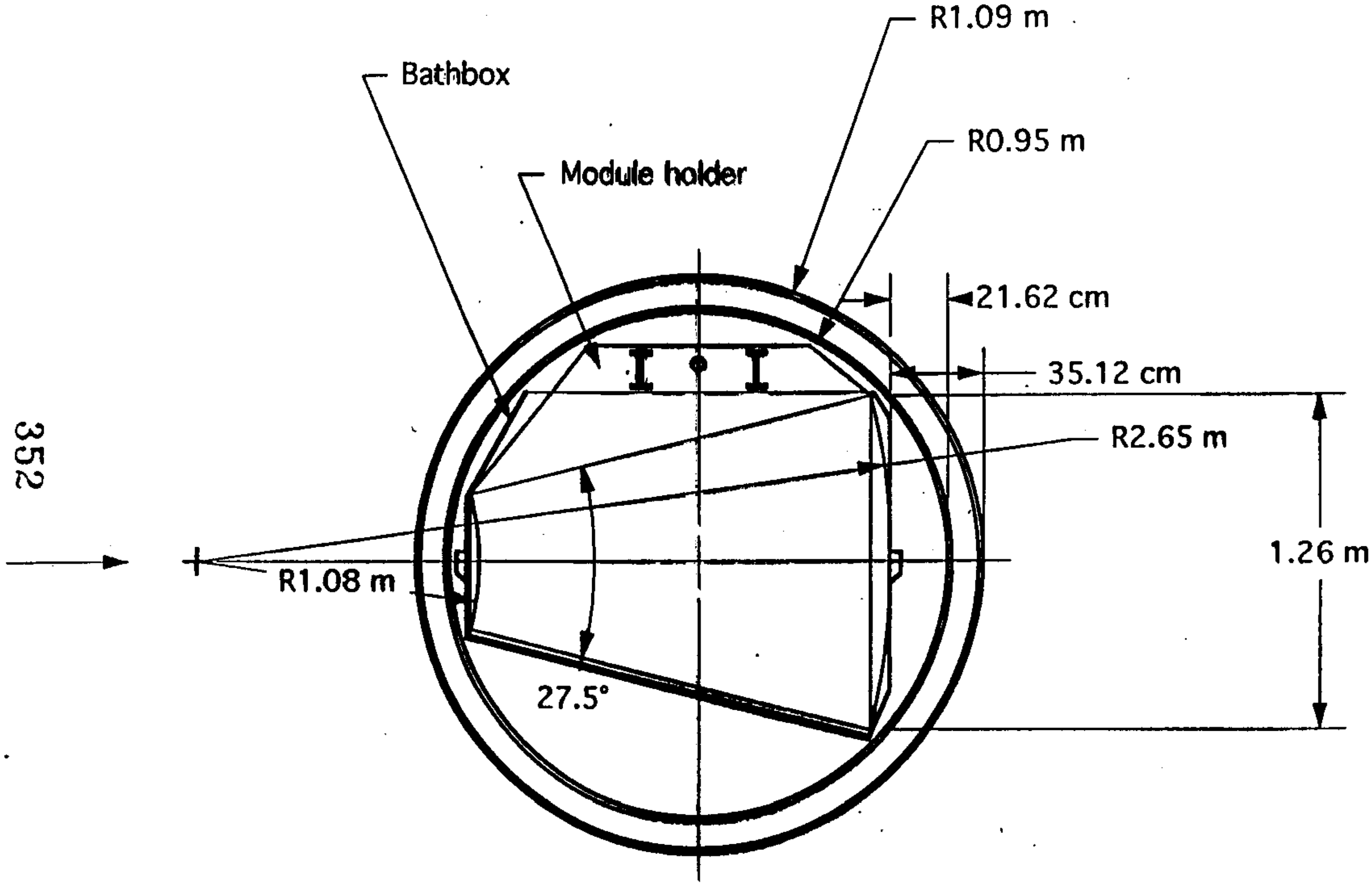

University of Washington
11/17/92

GEM CALORIMETER SCHEDULE.

1993-	9/93- Preliminary Design Completed.
	9/93- Begin Final Design
1994-	3/94- Final Design Completed.
	4/94- Tooling for Final Production
	9/94- Test production of components.
1995-	1/95- Component production
	6/95- Mini Module Assembly.
1996-	1/96- Preparation of Assembly Area at the SSC
	3/96- Barrel Assembly.
	7/96- Endcap Assembly.
1997-	
	7/97 Instalation in the Experimental HAll
1998-	1/98 Electronic Tests, Calibration Runs.
1999-	3/99 Close The detector.
	10/99 Ready for physics.